THE UNIVERSITY OF SOUTHAMPTON

NITRATE AS A SIGNAL IN *ARABIDOPSIS*

Sarah Jane Cookson

Doctor of Philosophy Thesis

School of Biological Sciences

January 2002

UNIVERSITY OF SOUTHAMPTON

ABSTRACT

FACULTY OF SCIENCE
SCHOOL OF BIOLOGICAL SCIENCES

DOCTOR OF PHILOSOPHY

NITRATE AS A SIGNAL IN *ARABIDOPSIS*

BY SARAH JANE COOKSON

This thesis describes an investigation of nitrate signalling in *Arabidopsis thaliana* leaf cells. The expression and activity of nitrate transporters and assimilatory enzymes are under complex regulation by mechanisms that are not yet fully understood. Experiments were designed to investigate the relationships between cytosolic ion activity changes and the regulation of nitrate transporters and assimilatory enzymes.

Two different approaches were used. Firstly, cytosolic ion activity changes were measured under light-dark transitions, treatments known to affect the regulation of nitrate transporters and assimilatory enzymes. These changes were initially studied using ion-selective microelectrodes. Light-dark transitions were shown to cause changes in mean cytosolic nitrate activity in mesophyll cells. Dark treatment caused an increase in mean cytosolic nitrate activity, light treatment a decrease. Plants without functional nitrate reductase (NR) did not show such changes and a higher mean level of cytosolic nitrate activity was observed compared with wild type, suggesting that NR activity has a role in cytosolic nitrate activity changes. These results are consistent with a signalling role for cytosolic nitrate activity in the regulation of nitrate transporters and assimilatory enzymes. The role of NR in influencing cytosolic pH was investigated using pH-selective microelectrodes. The microelectrode measurements were extremely difficult and time consuming so as an alternative pH-indicator dyes were tested but were not distributed in the cytosol of mesophyll cells.

The second approach involved the use of nitrate-inducible luciferase reporter plants. A photomultiplier tube/fibre optic cable system was developed and used to quantify luminescence from these plants. A low-light imaging camera was also used. Both systems showed that the reporter plants provided were unsuitable for the study of nitrate-induction. Alternative nitrate-inducible reporter plants were produced, which were shown to be nitrate-inducible and suitable for nitrate-induction studies.

The results presented provide supporting evidence for the hypothesis that NR-dependent changes in cytosolic nitrate activity may function as signals in *Arabidopsis* mesophyll cells.

LIST OF CONTENTS

LIST OF FIGURES

LIST OF TABLES

ACKNOWLEDGEMENTS

I would like to thank Dr Tony Miller for his supervision and advice throughout this work. I would also like to thank Dr Lorraine E. Williams at the University of Southampton for her assistance and support.

The assistance and encouragement of past and present members of the Plant Electrophysiology Group at IACR-Rothamsted are gratefully acknowledged: David Carden, Nick Cryer, Gordon Forbes, Janice Proud, Jacqui Sheridan, Sue Smith (who also kindly proof-read this thesis), David Walker, Darren Wells, and Jing-Jiang Zhou.

This work was funded by European Union grant BIO4-CT97-2231. I would like to express my gratitude to the various members of the consortium for their support, particularly Prof. Caboche of INRA-Versailles for providing the luciferase reporter plants.

I would like to thank Dr. Sancha Salguiero for teaching me molecular biology. Also thanks to Dr. Isabelle Carre for her kind assistance, advice and use of the CCD camera at the University of Warwick and Dr. Alan Entwistle for the use of the confocal microscope at the Ludwig Institute of Cancer Research.

Finally, I wish to thank all my family and friends for their support, patience and understanding, especially my parents for proof reading and my father for writing a computer program to rescue 9 months of corrupted data.

LIST OF ABBREVIATIONS

3D	3-dimensional
ADP	Adenine di-phosphate
AGPase	ADP glucose pyrophosphorylase
AM	Acetoxymethyl esters
AMP	Adenine mono-phosphate
ATP	Adenine tri-phosphate
B	Blue
BIN	Binary
CaMV	Cauliflower mosaic virus
CCD	Charged coupled device
CF	5-carboxyfluorescein
CFDA-AM	5-carboxyfluorescein diacetate AM ester
CLSM	Confocal laser scanning microscopy
DCDMS	Dimethyldichlorosilane
DNA	Deoxyribonucleic acid
DMSO	Dimethyl sulfoxide
EDTA	Ethylenediaminetetraacetic acid
EMF	Electromotive force
FAD	Flavin adenine dinucleotide
FW	Fresh weight
G	Green
GFP	Green fluorescent protein
GOGAT	Glutamate synthase or glutamate-2-oxoglutarate aminotransferase
GS	Glutamine synthetase
GTP	Guanine tri-phosphate
GUS	β-glucuronidase
HATS	High affinity transport systems
HEPES	N-[2-hydroxyethyl]piperazine-N'-[2-ethanesulfonic] acid

ICDH	Isocitrate dehydrogenase
ISE	Ion-selective microelectrode
KHP	Potassium hydrogen phthalate
K_m	Michaelis-Menten constant
LATS	Low affinity transport system
LB	Luria-Bertani
MADS	MCM1, agamous, deficiens, and serum response factor
MES	2-[-N-morpholino]ethanesulfonic acid
MoCo	Molybdenum-pterin cofactor
MOPS	2-[-N-morpholino]propanesulfonic acid
MS	Murashige and Skoog
MTTDA.NO_3	Methyl-tridodecylammonium nitrate
NADH	β-nicotinamide adenine dinucleotide
NADP	β-nicotinamide adenine dinucleotide phosphate
NiR	Nitrite reductase
NMR	Nuclear magnetic resonance
NR	Nitrate reductase
NR^-	NR deficient mutants
PCR	Polymerase chain reaction
PEP	Phospho*enol*pyruvate
PEPcase	Phospho*enol*pyruvate carboxylase
pH	Negative $\log_{10}[H^+]$
Pi	Inorganic phosphate
$PK_{I, -II, -III}$	NR protein kinase I, II and III
pNO_3	Negative $\log_{10}$ (NO_3^- activity)
PTFOC	Photomultiplier tube/fibre optic cable
PVC	Polyvinylchloride
R	Red
SPS	Sucrose phosphate synthase
T_1, T_2	Transformation generation 1 or 2
TAE	Tris-EDTA
TAPS	N-tris[hydroxymethyl]methyl-3-amino propanesulfonic acid
T-DNA	Transfer DNA

THF	Tetrahydrofuran
Ti	Tumour inducing
Tris	Tris(hydroxymethyl)aminomethane
YEB	Yeast extract-beef
ZMP	5-amino-4-imidazolecarboxamide-ribotide

1 INTRODUCTION

The idea that nitrate is a signal was first proposed by Trewavas (1983) who compared the response of plants to nitrate to their response to hormones. Changes in nitrate or hormone concentration and tissue sensitivity produce changes in a whole range of developmental processes in plants, many of which involve interactions with the external environment. The analogy drawn between nitrate and hormones was justified by Trewavas on the basis of nitrate's localised origin (root), its ability to convey information from the root to the shoot and its ability to affect developmental processes.

This chapter describes and discusses nitrate signalling in plants. It includes a brief overview of general signalling systems, nitrate uptake and assimilation, and the regulation of nitrate assimilation. Evidence for the role of nitrate as a signal to regulate metabolism and development is presented. The interactions between carbon and nitrogen metabolism are also described. Methods of studying cytosolic nitrate activity are compared with particular reference to electrophysiological techniques. Experimental subjects and systems are discussed and the scientific basis of the experimental work presented.

1.1 Signalling

All living organisms are continuously bombarded with complex information to which they must respond (e.g. changes in light, mineral nutrition, water status, gravity, temperature, wounding, pathogens). But as plants are generally unable to move in response to stimuli they have evolved complex signal transduction pathways to construct responses that maximise survival in a given environment. Environmental changes are sensed by unknown mechanisms initiating signalling events. Signalling events involve the transfer of information from one site to another, either within a cell or between different cells. The response of individual plants to a stimulus depends upon many factors such as developmental age, previous experiences and internal

clocks (reviewed by Trewavas, 2000). The response may take a physiological, biochemical, or morphological form. In addition to signals originating from outside the plant, internal signals are translocated within the plant in the circulatory system of xylem and phloem. The ability of plants to react and alter their growth in response to environmental cues is termed developmental plasticity (Trewavas, 2000). The mechanisms for sensing a stimulus and constructing a response are termed signal transduction pathways. In plant cells, signal transduction pathways often include two principal elements, cytosolic ion signals and reversible protein phosphorylation (see Figure 1.1, reviewed by numerous authors e.g.Trewavas, 2000).

1.1.1 Cytosolic ion activity signals

Changes in cytosolic free calcium concentration and pH are common secondary messengers (signals) in plant cells and are elicited by numerous stimuli e.g. light, temperature change, pathogen attack, osmotic stress (reviewed by Kurkdjian and Guern, 1989; Bush, 1995; Pandey *et al.,* 2000).

Plant cells maintain resting cytosolic concentrations of free calcium ions at 100 to 200 nM, with considerable stores within the vacuole, endoplasmic reticulum and cell wall. When a cell receives an appropriate signal, channels on membranes surrounding one of more of these stores of free calcium open and cytosolic free calcium increases. The increase in free calcium is localised due to the low diffusibility of calcium ions within the cytoplasm. Signal specificity is produced by differences in the extent, location, duration, and oscillation pattern of the calcium signal (e.g. McAinsh *et al.*, 1995). Calcium-binding proteins (such as calmodulin) respond to increases in cytosolic free calcium by changing their structure and action; these proteins are then activated and interact with specific regions of target proteins (reviewed by Pandey *et al.*, 2000). It is thought that signals are terminated by the activity of transporters in the plasma membrane, tonoplast and endoplasmic reticulum that restore resting cytosolic free calcium concentrations (reviewed by Geisler *et al.*, 2000).

In a similar fashion to cytosolic free calcium the pH of the cytosol is maintained at relatively constant values (approximately pH 7.2) with high proton concentrations in the vacuole and apoplast (pH 4.0 to 6.5) (reviewed by Kurkdjian and Guern, 1989). After perturbation of cytosolic pH by an environmental stimulus (e.g.

changes in light and temperature) it is restored by the proton buffering capacity of the cytosol and proton transporters on the tonoplast and plasma membranes (Kurkdjian and Guern, 1989).

In summary, both cytosolic free calcium and proton concentration have the following characteristics in common.

1. homeostatic control of cytosolic ion concentration
2. considerable gradients across membranes surrounding the cytosol
3. mechanisms and buffers to rapidly restore resting cytosolic ion concentration
4. change in response to environmental stimuli

Changes in cytosolic free calcium and pH interact, often occuring simultaneously in response to environmental stimuli for example during light-dark transitions (Pallaghy and Lüttge, 1970; Miller and Sanders, 1987). Additionally, experimental acidification of the cytosol has been shown to increase free calcium concentration (Felle, 1988).

1.1.2 Reversible protein phosphorylation

Reversible protein phosphorylation is recognised as a common and important mechanism for the regulation of a wide range of cellular processes (reviewed by Trewavas, 2000). Proteins affected include membrane channels and pumps, metabolic enzymes and cytoskeletal proteins. The enzymes that catalyse the phosphorylation process are called protein kinases. Protein kinases transfer the terminal phosphoryl group from Mg-ATP or Mg-GTP to specific serine, threonine or tyrosine residues in a target protein, changing its shape and function. The enzymes that catalyse the reverse reaction (dephosphorylation) are called phosphatases. These enzymes hydrolyse phospho-ester linkage(s) and as a result the protein reverts to its original conformation. Changes in cytosolic free calcium affect some protein kinases, which may be calcium-dependent or calmodulin-like and modify their activities following calcium binding (Pandey *et al.*, 2000).

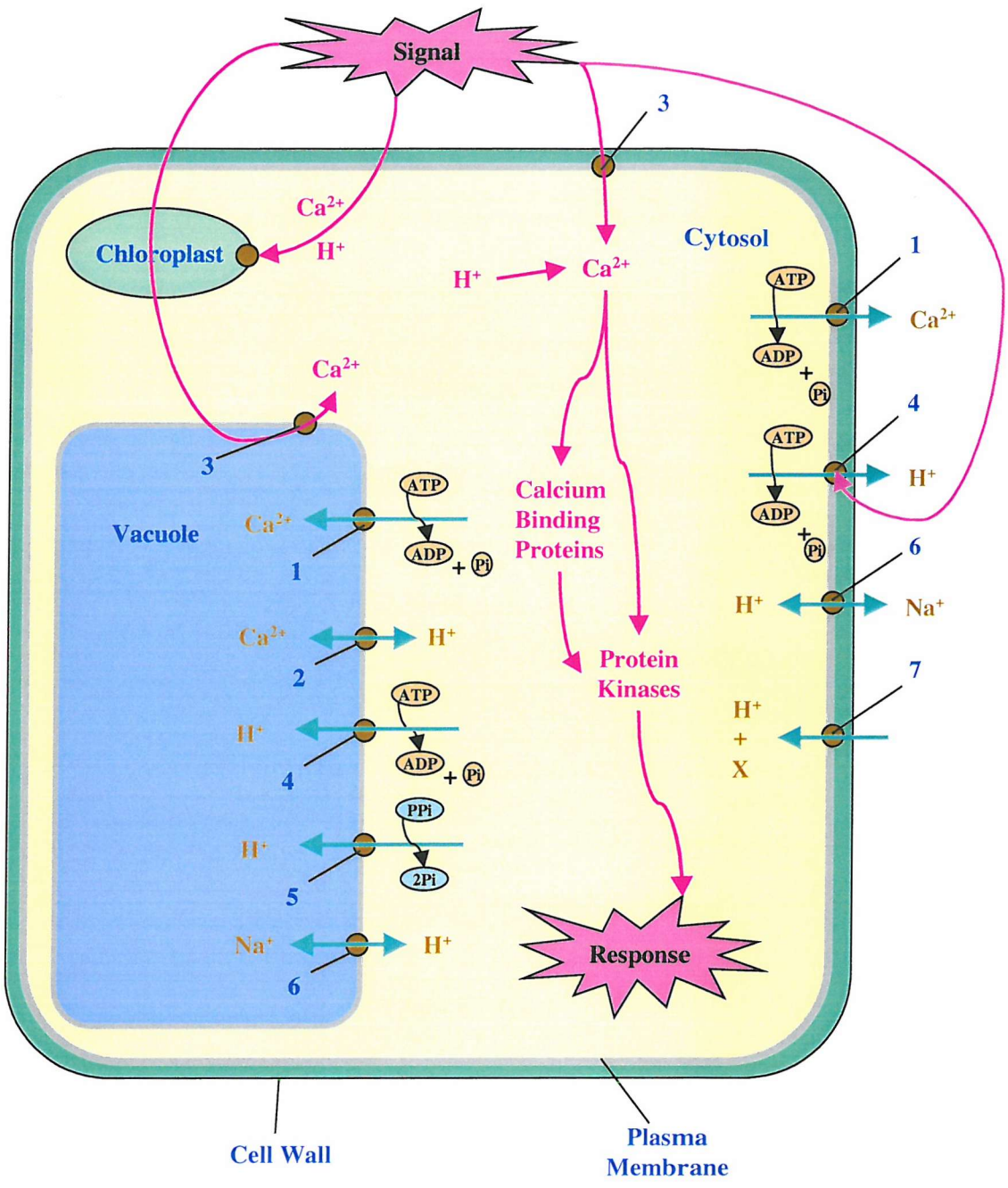

Figure 1.1 Schematic diagram summarising the basic elements of the major signalling transduction pathways of plant cells, cytosolic ion (Ca^{2+} and H^+) activity changes and protein kinases. For simplicity the endoplasmic reticulum is not shown.

Key: known steps involved in signalling cascades in pink, steps involved in terminating the response in turquoise. Transporters shown: 1. Ca^{2+}-ATPase, 2. Ca^{2+}/H^+ antiporter, 3. calcium channel, 4. H^+-ATPase, 5. H^+-pyrophosphatase, 6. Na^+/H^+ antiporter, 7. H^+/X symporter where X includes NO_3^-, K^+, $H_2PO_4^-$, SO_4^{2-}, amino acids, peptides, sucrose and hexoses.

1.2 Nitrate

This section gives a brief description of the availability of nitrogen to plants and then focuses on the uptake and assimilation of nitrate as a nitrogen source.

1.2.1 Nitrogen availability

Nitrogen availability was reviewed by Marschner (1995). Plants require higher quantities of nitrogen than that of any other mineral nutrient. In most environments the lack of nitrogen limits plant growth more frequently than the deficiency of any other mineral nutrient. Nitrogen is a constituent of proteins, nucleic acids and many other important cellular components. It is available in the soil in a variety of forms including ammonium, nitrate, amino acids, soluble peptides and complex, insoluble, nitrogen-containing compounds. Plants differ in their preferred nitrogen supply; however nitrate absorbed via the roots is the major source of nitrogen for the vast majority of plants. Once inside the plant, nitrogen is transported across the tonoplast to the vacuole, effluxed out of the cell, assimilated or transported to other cells of the plant via the vascular tissue.

1.2.2 Nitrate uptake

Recent reviews on nitrate uptake are given in Crawford and Glass (1998), Daniel-Vedele *et al.* (1998), Forde and Clarkson (1999), Forde (2000), Williams and Miller (2001). Net uptake is the balance between influx and efflux. Nitrate is actively transported across the plasma membranes of epidermal and cortical cells of roots. This transport requires energy input from the cell over almost the whole range of concentrations encountered in the soil (Zhen *et al.,* 1991; Glass *et al.,* 1992; Miller and Smith, 1996). It is generally accepted that the uptake of a nitrate ion is coupled with the movement of two protons down an energy gradient and is therefore dependent on ATP supply (McClure *et al.,* 1990; Meharg and Blatt, 1995; Miller and Smith, 1996). Figure 1.2 is a schematic diagram that shows nitrate uptake and the associated proton-pumping ATPase (H^+-ATPase) that maintains the electrochemical gradient to drive it. Hydropathy plots suggest that generally nitrate transporters

contain 12 putative membrane-spanning domains consisting of two groups of 6 segments separated by a hydrophilic region of many charged amino acids (Forde, 2000).

Physiological studies have shown the presence of both high and low affinity nitrate uptake systems operating at different external nitrate concentrations (Aslam *et al.*, 1992; Glass and Siddiqi, 1995). There are believed to be two high affinity transport systems (HATS) taking up nitrate at low concentration (generally below 0.5 mM with low transport capacity) and one low affinity transport system (LATS) that transports nitrate at high concentrations (generally above 0.5 mM with high transport capacity) (Glass and Siddiqi, 1995). Numerous nitrate transporters have been cloned from a variety of species (Crawford and Glass, 1998; Daniel-Vedele *et al.*, 1998; Forde and Clarkson, 1999; Forde, 2000; Williams and Miller, 2001). Those of the LATS have been given the name *NRT1* and those of the HATS have been given the name *NRT2*. Until recently it was generally thought that these two systems were in distinct gene families. Some doubt has been thrown on this by the observation that the *Arabidopsis* low affinity nitrate transporter, *AtNRT1.1*, also functions in the high affinity range (Liu *et al.*, 1999).

The *NRT1* and *NRT2* transporter genes are nitrate inducible and regulated by feedback from nitrogen metabolites in many plant species (Touraine *et al.*, 2001). Nitrate transporters are also diurnally regulated undergoing marked changes in transcript levels (and corresponding nitrate influx) during day/night cycles. Sucrose supply in the dark rapidly increases the transcript levels (Lejay *et al.*, 1999). These observations support the hypothesis of co-ordination between nitrate uptake and carbon metabolites of photosynthesis (Touraine *et al.*, 2001). Efflux systems have been less studied; however it is known that efflux is protein-mediated, passive, saturable and selective for nitrate (Grouzis *et al.*, 1997). Nitrate efflux is under a degree of regulation, induced by nitrate (Aslam *et al.*, 1996) and it is also proportional to whole tissue nitrate concentrations (Teyker *et al.*, 1988; van der Leij *et al.*, 1998). Net nitrate uptake is regulated by whole-plant demand via shoot derived signals transported in the phloem to the roots (Imsande and Touraine, 1994; Touraine *et al.*, 2001).

1.2.3 Nitrate assimilation

Nitrate is reduced and incorporated into cells by a number of enzymes (illustrated in Figure 1.2 and reviewed by Crawford *et al.*, 2000). Nitrate ions are initially reduced to nitrite ions, via the enzyme **N**itrate **R**eductase (**NR**). Nitrite ions are then reduced to ammonium ions via the enzyme **N**itr**i**te **R**eductase (**NiR**). Ammonium is then added to carbon skeletons to produce glutamine via the GS/GOGAT cycle. Glutamine can then be transformed into alternative biologically useful molecules such as other amino acids and proteins.

1.2.3.1 Nitrate reductase (NR)

NR is a complex, cytosolic enzyme made up of two identical subunits catalysing the transfer of two electrons from NAD(P)H to a nitrate ion via several redox centres composed of three prosthetic groups: flavin adenine dinucleotide (FAD), heme (cytochrome 557) and a molybdenum-pterin cofactor (MoCo) (Solomonson and Barber, 1990). There are various forms of NR in plants; the most common form and that found in *Arabidopsis* is NADH-specific NR (Wilkinson and Crawford, 1993).

1.2.3.2 Nitrite reductase (NiR)

NiR is a nuclear encoded enzyme that is transported into the stroma of chloroplasts in green tissue and into the plastids of roots, leaving behind a 30 amino acid transit sequence (Wray, 1989). The enzyme has two redox centres, a siroheme and an iron-sulfur centre, and catalyses the transfer of 6 electrons from reduced ferredoxin or a ferredoxin-like electron carrier to nitrite.

1.2.3.3 GS/GOGAT

The GS/GOGAT cycle comprises the enzymes glutamine synthetase (GS) and glutamate synthase (glutamate-2-oxoglutarate aminotransferase or GOGAT) (Temple *et al.*, 1998). GS catalyses the ATP-dependent amination (adding $-NH_2$) of glutamate to produce glutamine and GOGAT catalyses the transfer of an amide group from glutamine to 2-oxoglutarate to produce 2 molecules of glutamate.

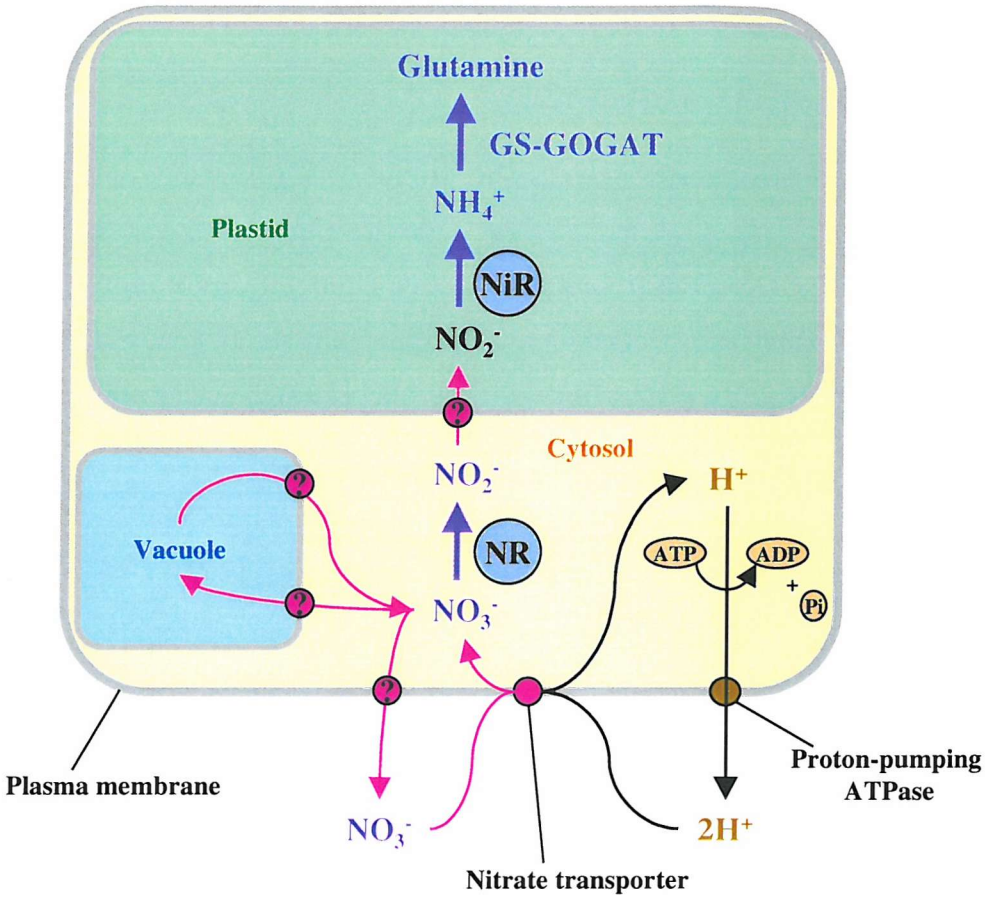

Figure 1.2 Schematic diagram of nitrate uptake and assimilation by plant cells.

Key: nitrate reductase, NR, nitrite reductase, NiR, glutamine synthetase, GS, glutamate-2-oxoglutarate aminotransferase, GOGAT (drawn from Crawford *et al.*, 2000).

1.3 Regulation of nitrate assimilation

The regulation of nitrate assimilation has been the focus of extensive study and has been reviewed by a number of authors, including Crawford, 1995; Daniel-Vedele and Caboche 1996; Kaiser *et al.,* 1999; Meyer and Stitt, 2001. Nitrate is the primary signal although other signals also influence the regulation of nitrate assimilation, e.g. light, sucrose, circadian rhythms and the end products of assimilation (Rothstein and Sivasankar, 1999). An overview of the regulation of the initial steps of nitrate assimilation is given below.

1.3.1 Transcriptional regulation of NR

NR is induced by its own substrate, nitrate (first reported by Tang and Wu, 1957). This induction is fast (within minutes) and requires very low concentrations (<10 μM) (Crawford, 1995). Light is required for optimal expression of NR. In etiolated plants this is mediated via phytochrome (Melzer *et al.,* 1989), and in green tissue via photosynthetic carbon fixation and sucrose (Cheng *et al.,* 1992). NR transcript levels show diurnal variation, increasing during the night to a maximum in the early morning (Galangau *et al.,* 1988; Bowsher *et al.,* 1991; Deng *et al.,* 1991). These diurnal changes are lost and transcripts remain consistently high in plants without functional NR (Cheng *et al.,* 1989; Pouteaut *et al.,* 1989). Deng *et al.* (1991) suggested that the circadian rhythms were due to inhibition by assimilation products, particularly glutamine, which fluctuates in an opposing manner to NR mRNA. This is further supported by the observation that supplying plants with glutamine or asparagine decreases nitrate uptake and NR transcription (Vincentz *et al.,* 1993; Sivasanker *et al.,* 1997). The picture is further complicated by the differential expression of the two NR genes in *Arabidopsis* (Cheng *et al.*, 1991; Yu *et al.,* 1998).

1.3.2 Post-transcriptional regulation of NR

Some degree of nitrate reduction control is facilitated by the short-lived nature of NR (Li and Oaks, 1993). However, studies have provided examples of extractable NR activity not matching NR protein or rate of nitrate reduction *in vivo,* indicating that other regulatory mechanisms may modulate NR activity (Lillo, 1994). NR activity responds rapidly and reversibly to changing environmental conditions, such as light/dark transitions, carbon dioxide removal and anoxia (Kaiser and Förster, 1989; Kaiser and Brendle-Behnisch, 1991; Glaab and Kaiser, 1993). The requirement for rapid post-transcriptional modulation of NR was thought to be due to the necessity to prevent the accumulation of toxic nitrite (Kaiser and Huber, 1994). However, recent work by Kaiser *et al.* (2000) has shown that NR reduction rates are frequently limited by cytosolic NADH concentrations. They suggested that the complex regulatory mechanism(s) to regulate NR activity could function to prevent the excessive accumulation of cytosolic NADH.

Kaiser and Spill (1991) suggested that NR activity modulation was linked to ATP levels, based upon *in vitro* experiments applying adenine nucleotides to crude

NR extracts and *in vivo* experiments manipulating adenine nucleotide concentrations with mannose feeding. This enzyme modulation has been ascribed to reversible protein phosphorylation. Evidence for the direct role of phosphorylation was provided by inhibitors of phosphatases preventing *in vivo* activation of NR by anoxia (Glaab and Kaiser, 1993) and confirmed as phosphorylation by using ^{32}P-labelled inorganic phosphate (Huber *et al.*, 1992). Additional evidence was provided by the discovery of an NR regulatory phosphorylation site, a serine residue on the hinge 1 region separating the MoCo and heme domains (Douglas *et al.*, 1995; Bachmann *et al*, 1996; Su *et al.*, 1996). Phosphorylation alone is not sufficient to inactivate NR. An additional 'NR inhibitor protein' and the presence of divalent cations (calcium or magnesium) are required (Bachmann *et al.*, 1995; Glaab and Kaiser, 1995; Kaiser and Brendle-Behnisch, 1991; MacKintosh *et al.*, 1995). The inhibitor protein was identified as a dimer of '14-3-3' proteins (Bachmann *et al.*, 1996; Moorhead *et al.*, 1996). 14-3-3 proteins were first known as abundant brain proteins and since then have been identified as a highly conserved protein family involved in many signalling systems in plant, fungal and mammalian cells (MacKintosh and Meek, 2001). The only site on NR identified as interacting with 14-3-3 proteins was around the phosphorylation site (Moorhead *et al.*, 1996; MacKintosh, 1998).

Leaf extracts contain several protein kinases that can phosphorylate NR (Douglas *et al.*, 1997). In spinach leaves there are at least 3 kinases (PK_I, $-_{II}$ and $-_{III}$) of differing dependence on calcium. PK_I is dependent or largely stimulated by calcium depending on extraction conditions. PK_{II} is dependent and PK_{III} is independent (Douglas *et al.*, 1997). There is evidence that PK_I and $-_{III}$ are also modified by phosphorylation (Douglas *et al.*, 1997), indicating the considerable complexity of cascades mediating the regulation of nitrate assimilation in response to environmental stimuli. The extent to which these three kinases contribute to NR phosphorylation *in vivo* is unknown.

NR is dephosphorylated by a type 2A protein phosphatase (MacKintosh, 1992). Type 2A protein phosphatases are involved in a myriad of signalling pathways in plants as well as animals (Smith and Walker, 1996). The phosphatase undergoes a rapid conversion at the onset of illumination, from an existing dimer to a trimer by the addition of an up-regulating subunit contributing to the activation of NR (MacKintosh, 1992). NR is also activated/dephosphorylated by a magnesium-dependent phosphatase *in vitro*. The activity of this enzyme is much lower than that

of the type 2A protein phosphatase. The physiological role of the magnesium-dependent phosphatase remains unknown (Kaiser *et al.*, 1999). Figure 1.3 shows a schematic summary of the activation/inactivation of NR by phosphorylation and 14-3-3 proteins.

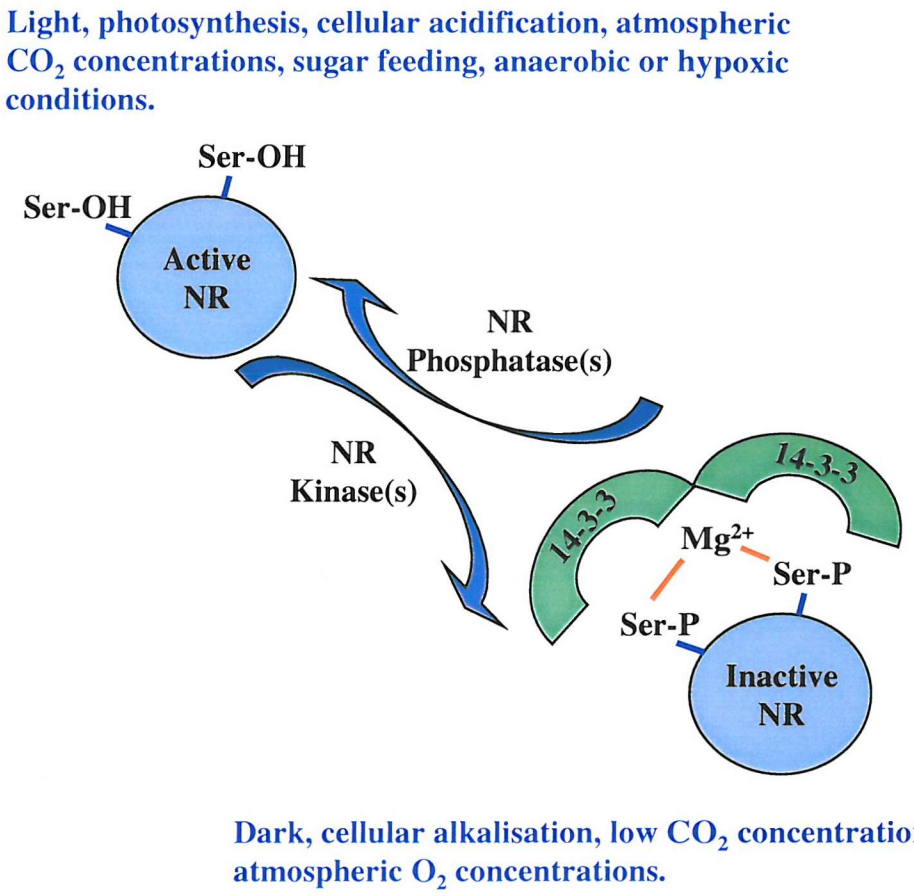

Figure 1.3 Schematic diagram of the environmental post-transcriptional regulation of nitrate reductase.

Key: nitrate reductase, NR, dephosphorylated serine residues, Ser-OH, phosphorylated serine residues, Ser-P (drawn from Kaiser *et al.*, 1999).

Changes in the phosphorylation status of NR increase its sensitivity to external or internal stimuli. Regulation of NR kinases and phosphatases may occur by changes in protein levels and modulation of existing proteins. When plants are grown in conditions known to reduce NR expression to almost zero, the amounts of the NR kinases, phosphatases and NR inhibitory 14-3-3 proteins appear to be normal (Glaab

and Kaiser, 1996). This suggests that the regulation of NR kinases, phosphatases and NR inhibitory 14-3-3 proteins may occur independently of NR.

1.3.3 Possible signals associated with the activation and inactivation of NR

1.3.3.1 Adenine nucleotides

The effect on NR activity of treatments such as anoxia or the administration of mannose has been ascribed to a decrease in ATP and an increase in AMP. Initially this was believed to directly affect NR kinases (Bachmann *et al.*, 1995; Huber and Kaiser, 1996). Conditions in which NR activity is known to change (such as anoxia or light/dark transitions) are not or not sufficiently accompanied by changes in concentrations of adenine nucleotides (Stitt *et al.*, 1982; Glaab and Kaiser, 1993). The estimated minimum cytosolic ATP concentrations under anoxia are 200-400 μM (Kaiser *et al.*, 1999) and the K_m (ATP) for NR kinase(s) is 10 μM (Bachmann *et al.*, 1995). Hence even under extreme ATP depleting conditions, NR protein kinase(s) activity should not be limited by cytosolic ATP concentrations. AMP and its analogue ZMP may act directly on NR at high concentrations (Huber and Kaiser, 1996). NR phosphatases have also been suggested as targets of adenine nucleotide signals; there is some evidence of activation *in vitro* (Huber and Kaiser, 1996). However, there is also evidence to indicate an interaction between AMP and 14-3-3 proteins (Athwal *et al.*, 1998).

1.3.3.2 Cytosolic pH

The plasma membrane H^+-ATPases have much lower affinities for ATP than NR kinases. These H^+-ATPases would be expected to respond first to a drop in cytosolic ATP and hence possibly trigger a cytosolic pH change (Hendrich *et al.*, 1986; 1989). Tissue acidification by weak acids causes activation of NR, and tissue alkalisation by bases causes inactivation presumably by causing changes in cytosolic pH (Kaiser and Brendle-Behnisch, 1995). The conditions in which NR activity and adenine nucleotides are known to change, e.g. mannose feeding and anoxia, also cause cytosolic acidification (St Gees *et al.*, 1991; Ricard *et al.*, 1994; Bligny *et al.*, 1997). Kaiser *et al.* (1999) proposed a mechanism for pH regulation of NR. They suggested that NR kinase activity drops to a greater extent below pH 7.0 than the activity of NR phosphatases, thereby promoting dephosphorylation and activation of NR.

1.3.3.3 Sugar phosphates

Sugar phosphates are possible signals associated with light/dark changes. In leaves, cytosolic sugar phosphates increase upon illumination (Gerhardt *et al.*, 1987) and sugar phosphates inhibit NR kinases (Bachmann *et al.*, 1995). Therefore, high cytosolic sugar phosphates may promote the activation of NR.

1.3.3.4 Cytosolic free calcium

Cytosolic free calcium triggers many signalling pathways in animal and plant cells. The existence of at least one calcium-dependent NR kinase (Bachmann *et al.*, 1995; Douglas *et al.*, 1997) and nitrate induction of a calcium transporter gene (Wang *et al.*, 2000) suggest a role for cytosolic free calcium in nitrate signalling. This has been further supported by the observation of light induced decreases in cytosolic free calcium (Miller and Sanders, 1987). Light induced increase in NR activity could be due to a decrease in calcium-dependent NR kinase(s) activity. The application of ammonia causes an influx of free calcium across the plasma membrane (Plieth *et al.*, 2000), possibly increasing calcium dependent NR kinase(s) activity and altering NR activity. This result is consistent with the hypothesis that cytosolic free calcium has a role in the regulation of NR activity.

1.3.4 NR turnover

The exact mechanism for controlling NR degradation is unknown; however there is evidence that the phosphorylation status of NR affects the susceptibility of the protein to proteolysis (Weiner and Kaiser, 1999).

1.3.5 Transcriptional regulation of NiR

Overall, NiR and NR are similarly transcriptionally regulated. One NiR gene has been identified in *Arabidopsis* (Tanaka *et al.*, 1994). The *Arabidopsis* NiR gene is strongly induced by nitrate; in fact the genes that are most nitrate inducible are those associated with nitrite reduction (Wang *et al.*, 2000). Wang *et al.* (2000) suggested that this is probably due to the requirement to prevent the accumulation of toxic nitrite. NiR induction in response to light is mediated by a phytochrome (Neininger *et*

al., 1992; Seith *et al.*, 1994). The degree of dependence on nitrate and light for NiR induction has been reported to vary considerably between different species. It has been shown that transcript levels are determined by different factors: solely by phytochrome in mustard (Schuster and Mohr, 1990), solely by nitrate in spinach (Seith *et al.*, 1991) and by the co-action of nitrate and light (phytochrome) in tobacco (Neininger *et al.*, 1992). NiR induction has been shown to require a positive control by a plastidic factor (Neininger *et al.*, 1992). NiR induction is also inhibited by the amino acids glutamine and asparagine (Vincentz *et al.*, 1993; Sivasankar *et al.*, 1997). The effect of carbohydrates on the induction of NiR differs between species; in maize sucrose enhances induction (Sivasankar *et al.*, 1997) whereas in tobacco induction is unresponsive to glucose (Vincentz *et al.*, 1993).

1.3.6 Post-transcriptional regulation of NiR

NiR enzyme level and NiR gene expression correlate well in barley (Seith *et al.*, 1994), whereas in spinach (Seith *et al.*, 1991), mustard (Schuster and Mohr, 1990) and tobacco (Neininger *et al.*, 1992) no quantitative relationship has been established. Thus suggesting that spinach, mustard and tobacco have regulation at the NiR protein level. NiR is also believed to be under post-transcriptional control. Plants grown on ammonium-containing medium and constitutively expressing NiR show strongly reduced protein levels and activities compared with those grown on nitrate containing medium (Crété *et al.*, 1997). The post-transcriptional control of NiR is different from that of NR. The reduction of NiR activity is due to a drop in the amount of NiR protein not protein inactivation. The NiR post-transcriptional regulatory mechanism(s) remain(s) to be determined. It has been suggested that NiR translation or incorporation into the chloroplast could be the steps subject to post-transcriptional control (Crété *et al.*, 1997).

1.3.7 The molecular nature of nitrate induction of NR and NiR

The molecular basis of nitrate-induced gene expression in higher plants has been studied to the greatest extent using the spinach NiR promoter and the *Arabidopsis* NR gene promoter (Rothstein and Sivasanker, 1999). Rastogi *et al.* (1997) revealed a significant similarity between higher plants and filamentous fungi in their machinery

for regulating nitrate induction. Rastogi *et al.* (1997) made NiR reporter plants with deletions between -330 bp and -200 bp (from the start of the promoter); these plants showed that the region between -200 and -230 bp is essential for nitrate induction of the NiR gene. Dimethyl sulfate footprinting identified several nitrate inducible footprints between -300 and -130 bp. One footprint coincided with the -230 to -200 bp region and contained 2 adjacent GATA elements separated by 24 bp. These elements are analogous to *cis*-regulatory sequences in nitrate inducible promoters of *Neurospora crassa* regulated by the *NIT2* Zn-finger protein. The -240 to -110 bp fragment of the NiR promoter was shown to bind *in vitro* to a fusion protein comprising the Zn-finger domain of *N. crassa NIT2* protein. GATA elements have also been discovered in the 5' upstream region of genes encoding NR in tobacco, tomato and *Arabidopsis* (Salanoubat and Ha, 1993; Lin *et al.*, 1994). Additionally, in the *Arabidopsis* NR promoter regions an AT-rich region followed by a sequence motif, A(C/G)TCA, has been identified as important in nitrate induction (Hwang *et al.*, 1997). These sequences have also been identified in the NR and NiR promoters of other plant species such as birch (Strater and Hachtel, 2000).

1.3.8 Diurnal changes in nitrogen assimilation in nitrate-replete plants

NR transcript decreases during the day and recovers again during the night, whereas NR activity increases during the first part of the light period and then decreases during the second part of the light period (Galangau *et al.*, 1988; Scheible *et al.*, 1997b; Geiger *et al.*, 1998; Scheible *et al.*, 2000). Whole tissue nitrate (presumably in the vacuole) decreases during the light and recovers at night (e.g. Steingröver *et al.*, 1986). Ammonium, glutamine, glycine and serine increase during the day and decrease at night, and 2-oxoglutarate increases after illumination and decreases during the last part of the light period (Scheible *et al.*, 1997b; Geiger *et al.*, 1998; Scheible *et al.*, 2000; Matt *et al.*, 2001). In the roots, nitrate uptake and transcripts of *NRT2* increase during the day (Matt *et al.*, 2001). Matt *et al.* (2001) combined these measurements to estimate diurnal changes in nitrate fluxes. During the first part of the light period nitrate reduction is twice as high as nitrate uptake and exceeds the rate at which reduced nitrogen is metabolised. Later in the diurnal cycle, NR expression and activity declines, *NRT2* expression and nitrate uptake remain high and leaf nitrate

is accumulated again. The regulatory network that underlies these changes is still not well understood.

1.4 Nitrate as a signal

The nutritional effect of nitrate fertilisation can be separated from those effects associated with nitrate signalling. Studies to determine the role of nitrate as a signal have frequently used NR deficient mutants. Supplying high nitrate to NR deficient mutants has generally shown the persistence of nitrate induced changes in metabolism despite the plants being severely deficient in organic nitrogen. The nutritional and signalling affects of nitrate can be further separated on the basis of concentration and rate of response. Nitrate rapidly (in minutes) induces the expression of genes encoding assimilatory enzymes at concentrations as low as 10 μM in plant cells which presumably has little nutritional affect (Crawford, 1995).

1.4.1 Nitrate signals regulating root development

It is well known that root growth and architecture are modified by nitrogen fertilisation; high nitrate inhibits root growth relative to shoot growth and lateral root formation. Additionally, local application of nitrate to nitrogen-limited plants produces localised root proliferation (Drew, 1973). The use of NR deficient mutants has shown that these regulatory signals persist in altering root growth and architecture even when nitrate no longer provides nutrition indicating a regulatory function for nitrate (Scheible *et al.*, 1997c; Zhang and Forde, 1998; Stitt and Feil, 1999).

1.4.1.1 Shoot:root ratios

Scheible *et al.* (1997c) investigated the significant correlation between shoot nitrate with shoot:root ratios. In wild type tobacco plants shoot:root ratio changes upon nitrate fertilisation, from 3.5:1 in well fertilised plants to 2:1 in nitrate-limited plants, whereas NR deficient mutants accumulated considerable amounts of nitrate in the shoot and had shoot:root ratios between 8:1 and 10:1. Ammonium or a product of ammonium assimilation was also implicated in the regulation of shoot:root growth, reducing root growth and stimulating shoot growth. A correlation between shoot:root

allocation and nitrogenous compounds in roots was not detected although there was a strong negative correlation with root sugar contents. The accumulation of nitrate in the leaves correlated with changes in photoassimilate partitioning, inhibition of starch synthesis and turnover in the leaves, and decreased transport of sucrose to the roots.

1.4.1.2 Lateral root formation

The molecular dissection of the lateral root signalling pathway was begun by Zhang and Forde (1998) who discovered a gene, *ANR1*, with homology to MADS box transcription factors. *ANR1* was rapidly induced by nitrate in the root of nitrogen starved seedlings and when expression of this gene was blocked, lateral root elongation in response to localised nitrate source stopped. MADS (MCM1, agamous deficiens, and serum response factor) box transcription factors are known to act as molecular switches during development (Theissen *et al.*, 1996). Zhang and Forde (1998) suggested therefore that *ANR1* was involved with transcriptional regulation of genes associated with the process of lateral root elongation. Further work by Zhang *et al.* (1999) has shown that the regulation of root branching by nitrate also involves the plant hormone auxin, since an auxin-resistant *Arabidopsis* mutant was insensitive to the localised stimulatory effect of nitrate.

1.4.2 Nitrogen metabolites affecting nitrogen metabolism

1.4.2.1 Nitrate regulating nitrogen metabolism

Nitrate induces the expression of NR and NiR (as described in Sections 1.3.1 and 1.3.6) and also induces other genes associated with nitrate uptake (Section 1.2.2) and assimilation (Stitt, 1999). Nitrate has also been shown to affect NR protein phosphorylation directly. It has been proposed that when nitrate binds to NR there is a conformational change that prevents its recognition by NR kinases (Rouby *et al.*, 1998).

1.4.2.2 Nitrate flux regulating nitrogen metabolism

Experiments altering nitrate flux to the leaves (reduced and then increased by cooling and then re-warming roots) showed that changes in NR activity corresponded to changes in nitrate flux and not to leaf nitrate content (Shaner and Boyer, 1976a). In a related study by the same authors (1976b), plants were desiccated slowly and then re-

watered to modify nitrate flux to the leaves. Re-watering produced an increase in NR activity that correlated with nitrate flux but not with leaf nitrate content. Shaner and Boyer (1976b) showed that this recovery depended on protein synthesis and by manipulating nitrate flux during desiccation showed that increased NR activity also depended on high nitrate flux.

1.4.2.3 Interaction with down-stream nitrogen metabolites

Down-stream metabolites appear to alter the induction of genes by nitrate. Nitrate induction is transient in wild type plants, whereas in NR deficient plants there is sustained over-expression of NR (Hoff *et al.*, 1994; Scheible *et al.*, 1997c; Krapp *et al.*, 1998). Wild type plants show sustained diurnal changes in these NR transcripts correlating with sugar, amino acid and organic acid pools (Scheible *et al.*, 1997a) whereas NR deficient mutants have high NR transcript levels during the day and night (Vaucheret *et al.*, 1990; Scheible *et al.*, 1997a). External application of glutamine and some other amino acids causes decreased nitrate uptake and assimilation (Hoff *et al.*, 1994). However, regulation by amino acids has been shown to be more complicated than this would imply. Spilt root experiments have shown feedback inhibition by a shoot derived signal that did not require increased amino acids in the phloem (Tillard *et al.*, 1998) and mutants deficient in GOGAT accumulated glutamine but did not show a decrease in NR expression (Dzuibany *et al.*, 1998).

1.5 Interactions between carbon and nitrogen metabolism

As described above, there are numerous points at which factors associated with carbon metabolism (e.g. light, carbon dioxide and sugars) have been shown to regulate nitrogen metabolism (e.g. transcriptional and post-transcriptional regulation of NR and NiR). The reverse is also true; factors associated with nitrogen metabolism regulate carbon metabolism.

1.5.1 Why regulate nitrogen and carbon metabolism?

There are two reasons why the co-ordinated regulation of nitrogen and carbon metabolism is essential to plants. The first is energetic expense; reductant and carbon

skeletons are required for the uptake and reduction of nitrate and in the subsequent incorporation of reduced nitrogen into organic compounds. The second is maintenance of cytosolic pH; nitrate assimilation leads to alkalisation and ammonium assimilation leads to acidification. Root cells are able to exchange protons with the soil but leaves must synthesise and export the organic acid malate to the roots for decarboxylation.

1.5.2 Nitrogen metabolites affecting the key enzymes of carbon metabolism

Figure 1.4 shows a schematic diagram representing the key enzymes of nitrogen and carbon metabolism in plant cells. Nitrogen metabolism alters the allocation of reduced carbon between organic acid and sucrose synthesis versus starch synthesis by regulating the key enzymes in these processes (Huppe and Turpin, 1994).

1.5.2.1 Organic acid metabolism

During nitrate assimilation, 2-oxoglutarate acts as an acceptor of ammonium in the GOGAT pathway and malate and citrate are required as counteranions to replace nitrate and prevent alkalinisation (Turpin *et al.*, 1997). Malate is synthesised from phospho*enol*pyruvate (PEP) via phospho*enol*pyruvate carboxylase (PEPcase) and citrate is synthesized by the concerted action of PEPcase, pyruvate kinase, pyruvate dehydrogenase and citrate synthase (Turpin *et al.*, 1997). The conversion of isocitrate into 2-oxoglutarate occurs in the cytosol and is catalysed by NADP- isocitrate dehydrogenase (NADP-ICDH) (Turpin *et al.*, 1997). Nitrate deficient wild type plants have low levels of *ppc* transcript (encoding for PEPcase), low PEPcase activity, low levels of malate and citrate and small pools of isocitrate and 2-oxoglutarate (Scheible *et al.*, 1997a). In comparison, in NR deficient mutants nitrate induces high *ppc* transcript levels and enhanced transcript levels of other genes encoding the synthesis of organic acids despite being unable to reduce and subsequently assimilate nitrate (Scheible *et al.*, 1997a).

1.5.2.2 Sucrose metabolism

Short-term exposure to nitrate causes a decrease in sucrose (van Quy *et al.*, 1991) and an increase in amino acid synthesis in nitrate deficient leaf cells while inorganic acid pools are maintained by a diversion of photosynthetic carbon into the anapleurotic

pathway (Champigny *et al.*, 1992). PEP was also shown to decrease under these conditions, leading to a small decrease in the precursors of sucrose synthesis and possibly contributing to the inhibition of sucrose synthesis. The inhibition of sucrose synthesis was also probably affected by a decrease in sucrose phosphate synthase (SPS) activity.

Champigny *et al.* (1991) also studied the affects of short-term nitrate application using ^{14}C tracer. This paper reported that short-term nitrate application had no affect on photochemical reactions but did depress the rate of carbon fixation and altered the allocation of photosynthetic carbon as reported by van Quy *et al.* (1991). Champigny *et al.* (1991) suggested that these changes were transient and preceded steady-state conditions of continuous high nitrate nutrition, increased carbon dioxide fixation and adequate supplies of carbon residues for protein and carbohydrate metabolism. A longer-term study, comparing nitrate deficient wild type and NR deficient mutant plants grown on high nitrate, showed that the NR deficient mutants have slightly higher levels of *sps* transcript (encoding SPS), higher SPS activity and no post-translational inactivation of SPS (Scheible *et al.*, 1997a). Scheible *et al.* (1997a) suggested that sucrose synthesis continues because sucrose constitutes a major osmoticum in the phloem. Synthesis and export of sucrose produces higher turgor in the phloem and promotes the export of amino acids from the leaves. In addition sucrose supply to growing tissue increases the demand for amino acids.

1.5.2.3 Diurnal regulation of sucrose and organic acid synthesis

The key enzymes of carbon metabolism associated with amino acid synthesis show diurnal regulation so that at the beginning of the light period when NR activity is high there is preferential synthesis of malate to act as a counter-anion for pH regulation (Turpin *et al.*, 1997). At the end of the light period there is preferential synthesis of 2-oxoglutarate to act as a nitrogen acceptor for accumulated ammonium when NR activity has decreased (Scheible *et al.*, 2000).

1.5.2.4 Starch metabolism

Accumulation of starch allows slow growing plants to store carbon in an osmotically inactive form (Rufty *et al.*, 1988). ADP glucose pyrophosphorylase (AGPase) plays a key role in the regulation of starch synthesis (Preiss *et al.*, 1991). Nitrate has been shown to interact with starch synthesis in two ways; nitrate inhibits the expression of

a regulatory subunit of AGPase, and NR deficient mutants grown on high nitrate have negligible amounts of starch even though they have low growth rates compared with nitrate deficient wild type plants (Scheible *et al.*, 1997a).

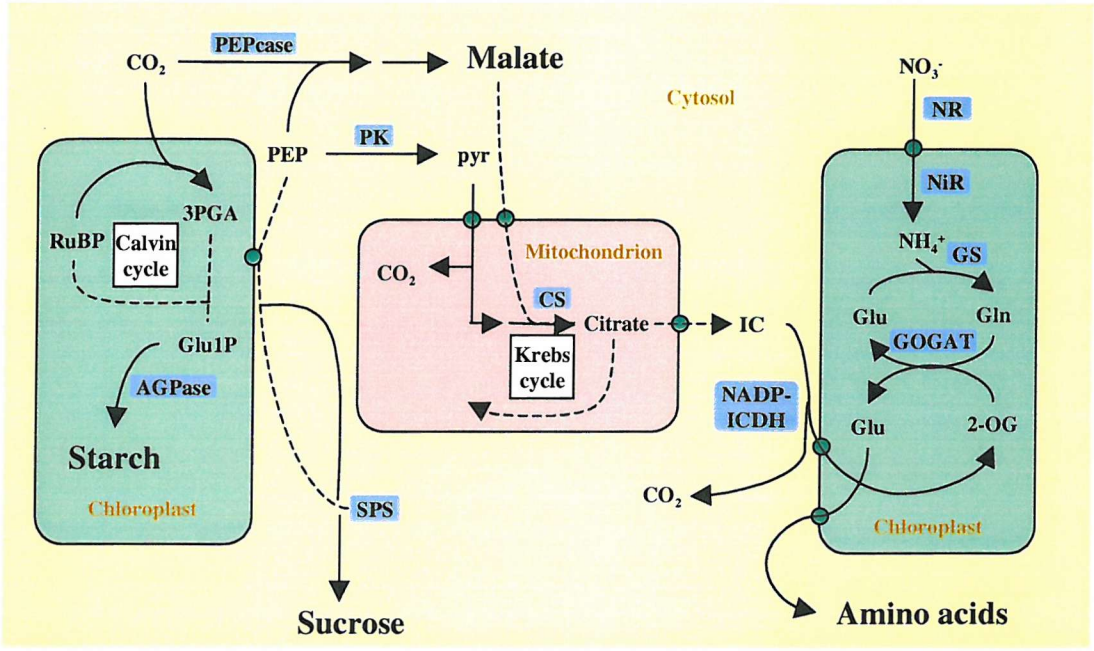

Figure 1.4 Pathways of primary nitrogen and carbon metabolism in an autotrophic plant cell.

Key: nitrate reductase, NR; nitrite reductase, NiR; glutamine synthetase, GS; glutamate-2-oxoglutarate aminotransferase, GOGAT; NADP-dependent isocitrate dehydrogenase, NADP-ICDH; citrate synthase, CS; pyruvate kinase, PK; phospho*enol*pyruvate carboxylase, PEPcase; sucrose phosphate synthase, SPS; ADP glucose pyrophosphorylase, AGPase; glutamine, Gln; glutamate, Glu; 2-oxoglutarate, 2-OG; isocitrate, IC; pyruvate, pyr; phospho*enol*pyruvate, PEP; glyerate-3-phosphate, 3PGA; glucose-1-phosphate, Glu1P; ribulose-1,5-bisphosphate, RuBP. Enzymatic reactions shown as thin black lines, transport processes indicated by green circles (drawn from Scheible *et al.*, 1997a).

1.5.3 Carbon metabolites affecting the key enzymes of nitrogen metabolism

The regulation of NR and NiR by factors associated with carbon metabolism (such as light and sucrose) is described in Sections 1.3.1, 1.3.2, 1.3.5 and 1.3.6. NR expression is linked to organic acid metabolism through inhibition by malate (Müller

et al., 2001). Sucrose feeding activates nitrate reduction, assimilation, amino acid and 2-oxoglutarate synthesis, and so complements the action of nitrate in increasing the nitrogen flow into amino acid synthesis (Morcuende *et al.*, 1998). At the whole plant level, alterations in carbon metabolism affect nitrogen metabolism. Transgenic plants with decreased expression of ribulose-1,5-biphosphate carboxylase-oxygenase and hence decreased rates of photosynthesis had higher shoot:root ratios to maximise leaf area but accumulated large amounts of nitrate in the leaf (Quick *et al.*, 1991). This suggests that nitrate assimilation is inhibited in response to low availability of photosynthate.

The response to enhanced atmospheric carbon dioxide depends on developmental age: the diurnal rhythm of nitrate reductase activity changes in older plants, whereas in young plants nitrate reductase activity is stimulated and more amino acids are synthesised (Geiger *et al.*, 1998). Starchless mutants of tobacco accumulated high concentrations of sugar phosphates in the afternoon and transient dark inactivation of NR also decreased in the afternoon relative to wild type plants (Bachmann *et al.*, 1995). This inhibition of dark inactivation was shown to be due to inhibition of a NR kinase. Regulation by carbon metabolism is by no means unimportant and can override signals from nitrogen metabolism, as demonstrated by Klein *et al.* (2000). NR deficient mutants grown in a light-dark regime continuously over-expressed NR transcript and transfer to continuous darkness resulted in a considerable decrease in NR transcripts. NR transcripts disappeared when sugars fell below a critical level but could be induced again by the application of sucrose (Klein *et al.,* 2000). The sugar-mediated control of NR transcript expression has also been shown to override regulation by nitrogenous compounds when sugar content of leaves was manipulated by altering day-length (Matt *et al.*, 1998)

1.5.4 Regulation by phosphorylation

Key enzymes of nitrogen (NR) and carbon metabolism (SPS and PEPcase) are located in the cytosol and are regulated post-transcriptionally by reversible phosphorylation. NR and SPS are inactivated whereas PEPcase is activated by phosphorylation. Regulation of NR by phosphorylation is described in Section 1.3.2. SPS catalyses the rate limiting step in the synthesis of sucrose (Worrel *et al.,* 1991). SPS activity is known to change in response to water stress (Quick *et al.*, 1989), accumulation of

sucrose (Stitt *et al.*, 1988) and in relation to photosynthesis or light/dark transitions (Pollock and Housley, 1985; Rodriguez-Sotres and Munos-Clares, 1987). PEPcase has a variety of functions in plants including a role in the production of malate. The activity of PEPcase also changes in response to light/dark transitions primarily regulated by a PEPcase-protein kinase (Champigny and Foyer, 1992). Some interactions between nitrogen and carbon metabolism are associated with regulation of phosphorylation status. For example, NR kinases are inhibited by sugar phosphates (Bachmann *et al.*, 1995). Also, the same type 2A phosphatase that activates NR activates SPS (Kaiser *et al.*, 1999). Nitrate has been suggested as an activator of the cytosolic protein kinases of PEPcase and SPS involved in the short-term diversion of carbon from sucrose to amino acids biosynthesis (Champigny and Foyer, 1992).

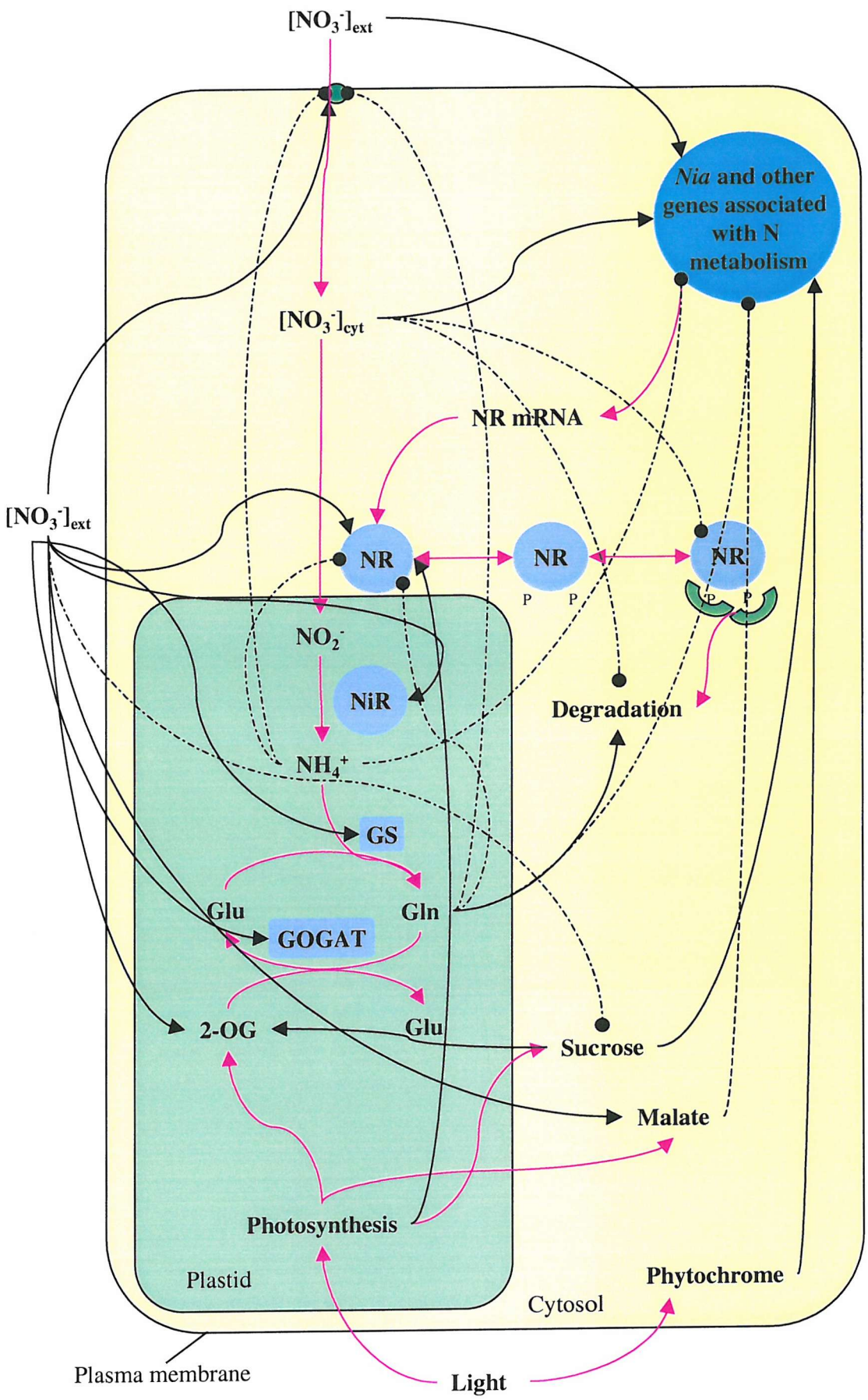
$[NO_3^-]_{ext}$
Nia and other genes associated with N metabolism
$[NO_3^-]_{cyt}$
NR mRNA
$[NO_3^-]_{ext}$
NR
NR
NR
P
P
P
P
NO_2^-
NiR
Degradation
NH_4^+
GS
Glu
Gln
GOGAT
2-OG
Glu
Sucrose
Malate
Photosynthesis
Plastid
Phytochrome
Cytosol
Plasma membrane
Light

Figure 1.5 Schematic diagram showing some of the main regulatory signals of nitrate uptake and assimilation in a simplified plant cell.

Key: nitrate reductase, NR; gene(s) encoding NR, *Nia;* nitrite reductase, NiR; glutamine synthetase, GS; glutamate-2-oxoglutarate aminotransferase, GOGAT; glutamine, Gln; glutamate, Glu; 2-oxoglutarate, 2-OG; enzymatic reactions indicated by pink arrows, stimulatory signals by solid black arrows, down-regulating signals by dashed black arrows.

1.6 Overview of nitrate signalling

The preceding sections of this chapter have provided a review of the published work associated with nitrate uptake, assimilation, regulation and signalling, the main features of which are summarised in Figure 1.5. This shows that nitrate assimilation is under complex regulation by environmental stimuli interacting with internal signals. This produces a wide range of responses that affect gene expression, enzyme activities and plant morphology. The nitrate signalling system has many components that are in complex and dynamic relationships with each other and external systems. To measure such systems poses considerable experimental difficulties since the measurement methods are in danger of perturbing the systems whose measurement is being attempted.

1.7 Methods used to study cytosolic ion signalling

The wide range of technologies available to image and/or measure cytosolic free calcium and pH changes has allowed the extensive study of these signalling ions. Some of these are briefly described below. The short time-scale over which signals occur within cells means that methods of measurement must be dynamic and capable of detecting changes with suitable resolution and sensitivity. They must also achieve this with minimal perturbation of the signalling system under examination.

1.7.1 Fluorescent indicator dyes

There are numerous examples of the imaging of cytosolic free calcium and pH changes using fluorescent indicator dyes (e.g. Shacklock *et al.*, 1992; Malhó *et al.*, 1994; Parton *et al.*, 1997). The technique is based on fluorescent probes that are loaded inside cells and change their fluorescent properties when bound to specific ions of interest (Roos, 2000). There are many indicator dyes that can be selected within different sensitivity ranges and tissue or compartmental specificity (Read *et al.*, 1992; Roos, 2000). Signals from single cells are visualised using conventional or confocal microscopy. Some of these fluorescent indicator dyes, called ratiometric dyes, can also be used to quantify ion concentration. Ratiometric dyes are those with either an excitation or emission wavelength that is insensitive to changes in ion concentration and thus can act as a reference value against fluorescence changes due to ion concentration.

1.7.2 Ion-selective microelectrodes

Changes in cytosolic free calcium and pH have also been studied using ion-selective microelectrodes (e.g. Miller and Sanders, 1987; Felle, 1993; Felle *et al.*, 1996; Miller and Smith, 1996; Miller *et al.*, 2001). Ion-selective microelectrodes have the advantage of being capable of measuring ion activity directly, but do not provide the spatial resolution of cytosolic free calcium changes reported by fluorescent indicator dyes.

1.7.3 Reporter proteins

Aequorin is the calcium sensitive luminescent protein found in the jellyfish, *Aequorea victoria.* Aequorin consists of two components, an apoprotein (apoaequorin) and coelenterazine, a hydrophobic luminophore. When reconstituted, aequorin binds calcium atoms with low affinity but high specificity. The calcium-aequorin complex undergoes a conformational change that results in the oxidation of bound coelenterazine and an accompanying emission of light. Genetically transforming plants with cDNA for apoaequorin and exogenous application of coelenterazine produces luminescent plants, the luminescence of which reports internal calcium ion concentrations. Many coelenterazines are available with different properties and

aequorin can be targeted to different cell compartments or attached to membranes by using specific promoters (Trewavas, 2000). This technique is now widely used in conjunction with low-light imaging technologies to study cytosolic free calcium changes (e.g. Johnson *et al.*, 1995). pH-sensitive mutants of green fluorescent protein (GFP) have recently been discovered and combined with compartment specific expression vectors. These new GFPs have various pH sensitivity ranges, from 5.5 to 8, and have been used to measure intracellular pH in animal cells (Llopis *et al.*, 1998).

1.8 Methods to study cytosolic nitrate activity changes

The techniques described above facilitated the study of cytosolic pH and free calcium signals in response to a wide range of stimuli (reviewed by Kurkdjian and Guern, 1989; Bush, 1995; Pandey *et al.*, 2000). The measurement of cytosolic nitrate activity changes is considerably more problematic. As yet, there are no fluorescent indicator dyes or reporter genes available to visualise cytosolic nitrate activity changes. Methods to measure cytosolic nitrate activity were reviewed by Miller and Smith (1996). Some of these are described below.

1.8.1 Anaerobic NR assay

The anaerobic NR assay is an indirect method based upon the measurement of nitrite formation in the absence of external nitrate under conditions designed to limit nitrite reduction (anoxia, darkness) (Ferrari *et al.*, 1973). This technique relies upon two assumptions. The first is that cytosolic nitrate is limiting nitrate reduction; however, it is feasible that the distribution and activity of NR, the supply of reductant or some other factors may limit nitrate reduction. The second is that the nitrate available for reduction is only made up of that in the cytosol and is not influenced by release of nitrate from the vacuole or efflux across the plasma membrane. Both assumptions need careful experimental verification before complete confidence can be placed in reported results. Cytosolic nitrate activity estimates from this approach range from 0.01 to 8 mM (Miller and Smith, 1996).

1.8.2 Compartmental tracer efflux

Compartmental tracer efflux analysis is a widely used and well-established technique (e.g. Lee and Clarkson, 1986; Siddiqi *et al.*, 1991). For this method, tissues are loaded with an isotopic tracer, transferred to an unloaded solution and the concentration of tracer in the solution determined periodically. Assuming that the plasma and tonoplast membrane have different resistances to tracer efflux, the kinetics of tracer loss are used to determine the tracer content in the estimated volumes of the apoplast, cytosol and vacuole. This technique also assumes that the nitrate tracer applied is not assimilated in the cytosol or transported elsewhere in the plant.

1.8.3 Cell fractionation

Cell fractionation estimates of cytosolic and vacuolar nitrate activity are based upon vacuole isolation from protoplasts (e.g. Martinoia *et al.*, 1981; 1986; 1987). This is a lengthy technique with the possibility of leakage or redistribution of solutes during preparation and estimates the whole nitrate content of cytosol including the organelles.

1.8.4 Nitrate-selective microelectrodes

All above techniques estimate average cytosolic nitrate of whole tissue samples, not single cells and require estimation of cytoplasmic volume, small changes of which could dramatically alter calculated cytosolic nitrate activity. None of the above lengthy methods could measure short-term transient changes like those reported for free calcium ion and pH signals. Therefore, a more direct, accurate approach is required, such as using nitrate-selective microelectrodes (Miller and Zhen, 1991). Nitrate-selective microelectrodes were also used in this study; a full desciption of this technique is given below. Calcium-selective microelectrodes are potentially unable to detect some signalling events because of the localised nature of some calcium signals. However, nitrate is a highly mobile ion and it is assumed that it would be homogeneously distributed within the cytoplasm.

1.9 Application of ion-selective electrodes

Ion-selective microelectrodes have been described as "the most widely used method in electrophysiology" (Ammann, 1986) and as "powerful and inexpensive tools for the elucidation of basic cellular processes" (Felle, 1993). Ion-selective microelectrodes allow the measurement of electrical and ionic gradients across cellular membranes and can be employed intra- or extracellularly. Intracellular measurements using this technique have been used to study the compartmentation of nutrients, intracellular signalling, and transport mechanisms (Miller, 1994).

The term 'microelectrode' describes a glass electrode pulled to a fine tip with dimensions in the order of 1 μm (Halliwell and Whitaker, 1987). An ion-selective microelectrode (ISE) additionally contains an ion-selective membrane in the electrode tip and forms an electrochemical half-cell. When used in conjunction with a 'ground' electrode to form a complete electrochemical cell, the measured potential differences (ISE versus ground electrode) are linearly dependent on the activity of a given ion in solution (Buck and Lindner, 1994). ISE theory is given in Appendix 1.

1.9.1 Intracellular use of ion-selective microelectrodes in plant cells

Plant cells pose several problems for the intracellular use of microelectrodes. The rigid cell wall of plant cells presents an obstacle to penetration, and cell turgor pressure acts to displace ion-selective membranes up the shaft of the micropipette (Brownlee, 1987). Prevention of displacement of ion-selective membranes has been achieved by the incorporation of physical strength using a matrix material (Sanders and Miller, 1986; Reid and Smith, 1988; Miller and Zhen, 1991). The highly localised measurement of ion activity by microelectrodes poses a further problem in vacuolate plant cells. It is important to be able to determine in which of the two major cellular compartments (cytoplasm or vacuole) the electrode tip is located. If enough measurements are taken, it may be possible to resolve intracellular measurements into vacuolar and cytoplasmic populations using statistical methods. Miller and Zhen (1991) reported that nitrate-selective microelectrode measurements in the giant alga *Chara corallina,* grown in nitrate replete conditions, could be resolved into two populations. The compartments of these two populations were assigned on the basis

of whole tissue analysis, assuming the majority of the sample was vacuolar. Zhen *et al.* (1991) showed similar resolution of nitrate-selective microelectrode measurements in the epidermal cells of barley roots. Certain ions such as Ca^{2+} and H^+ show measurable, constant differences in activity between cytosol and vacuole (Felle, 1993). Walker *et al.* (1995) used this fact to produce triple-barrelled microelectrodes, which, in addition to K^+- or NO_3^--selective and membrane potential-sensing barrels, contained a pH-selective barrel. Measurement of pH at the electrode tip allows immediate designation of activities sensed by the other barrel as cytosolic (pH 7.0-7.6) or vacuolar (pH 4.0-6.0) (Walker *et al.*, 1995).

1.9.2 Intracellular use of ion-selective microelectrodes in leaf cells

All microelectrode measurements require good electrical contact between the microelectrode tip (when in- and outside the cell of interest) and the ground electrode, so there is a low resistance pathway to complete the circuit. Good electrical connection is most easily achieved by submerging the cells of interest in an aqueous solution containing the ground electrode. Roots of hydroponically grown plants are therefore technically easy to prepare and make measurements on (Miller *et al.*, 2001). Aquatic plants have been selected for measurements in photosynthetically active cells for similar reasons (e.g. Lüttge and Higinbotham, 1979). Leaves of higher plants have also been studied using submerged (and sometimes vacuum infiltrated) leaves or leaf discs e.g. membrane potential measurements made in submerged barley leaves (Karley *et al.*, 2001). Microelectrode measurements in submerged leaves of *Arabidopsis* present difficulties because of possible stress to the leaf cells and consequent disruption of normal signalling events.

Methods have been recently developed for impaling microelectrodes into cells of intact, aerial leaves of whole plants. These methods require electrical contact to be made through the apoplastic water film of the leaf tissue (Hanstein and Felle, 1999). Hanstein and Felle (1999) made apoplastic measurements using blunt pH- and NH_4^+-selective microelectrodes inserted into stomata of the grass, *Bromus erectus*. The ground electrode was initially placed in a bath solution surrounding the stem but the resistance in the circuit was too high. A ground electrode was inserted through neighbouring stomata, and this made good electrical contact. Cuin *et al.* (1999) made K^+- and pH-selective microelectrode measurements on epidermal barley cells,

electrical contact was made from the microelectrode through the apoplast to a ground electrode in a bath solution at the leaf edge.

1.9.3 Nitrate activity measurements in plant cells using nitrate-selective microelectrodes

Nitrate-selective microelectrode measurements made in barley root cells have shown that nitrate activity in the cytoplasm is maintained at approximately 4 mM and nitrate activity in the vacuole varies according to the external supply of nitrate to the plant (Zhen *et al.,* 1991; van der Leij *et al.,* 1998). van der Leij *et al.* (1998) showed that the mean vacuolar nitrate activity in barley root epidermal cells ranged from greater than 80 mM in nitrate replete cells to 17 mM in plants starved of nitrate for 24 hours. van der Leij *et al.* (1998) also showed that cytosolic nitrate activity in nitrate replete epidermal cells was maintained after removal of external nitrate for at least 20 min. This apparent maintenance of steady-state cytosolic nitrate activity under changing environmental supply is a prerequisite of a signal ion. If ion activity fluctuated too widely it could not act as a signal. The well known signal ion calcium is maintained at a cytoplasmic concentration of approximately 100 nM by the action of transporters and buffers except during signalling events (Pandey *et al.*, 2000).

1.9.4 Plants for electrophysiological measurements

Electrophysiologists generally select large, robust plants (e.g. barley, *Chara corralina*) for experimental ease. *Arabidopsis thaliana* (commonly known as thale or mouse-ear cress, see Figure 1.6) is a small herbaceous annual of the family Brassicaceae. *Arabidopsis* is found in many different ecological and geographical regions, including the high mountains of equatorial Africa, the highlands of the Himalayas and most of temperate Europe (Bowman, 1994). Numerous wild populations (ecotypes) have been collected (Bowman, 1994). The advantages of using *Arabidopsis* as a model plant for genetic experiments were described nearly 60 years ago (Laibach, 1943). These advantages include small size, short generation time and small chromosome number. *Arabidopsis* has since become a uniquely important and well-studied laboratory species with numerous mutants characterised, the entire genome sequenced (The *Arabidopisis* Genome Initiative, 2000) and

transformation protocols perfected (described in Chapter 4). However, there are considerable disadvantages associated with using *Arabidopsis* for electrophysiology. It is a small, delicate plant that is difficult to grow in hydroponic culture and rapidly desiccates during manipulation into electrophysiological chambers. Despite the disadvantages the scientific importance of *Arabidopsis* makes it worthwhile extending electrophysiological studies to this species.

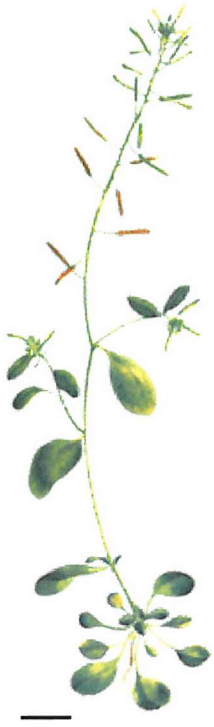

Figure 1.6 *Arabidopsis thaliana* plant, scale bar 2 cm.

1.10 Thesis overview

The thesis aims to investigate whether cytosolic nitrate activity changes could be a signal associated with modification of NR activity and the extent of NiR induction in *Arabidopsis thaliana.* The investigation was conducted in three parts. The first part was a study of cytosolic nitrate activity signals associated with changes in NR activity using nitrate-selective microelectrodes. The second part was a study of cytosolic pH changes associated with changing NR activity using ion-selective microelectrodes and pH indicator dyes. The third part was a study of cytosolic nitrate activity signals

associated with nitrate induction of NiR quantified using luminescent reporter *Arabidopsis* plants.

2 CYTOSOLIC NITRATE ACTIVITY CHANGES ASSOCIATED WITH MODIFICATIONS OF NITRATE REDUCTASE ACTIVITY

2.1 Aim

In order to study signalling in the laboratory, conditions must be created in which a signal would be expected to occur. This chapter describes experiments in which light/dark transitions were applied to leaf cells to produce changes in the activity and expression of nitrate transporters and assimilatory enzymes. Cytosolic nitrate activity was measured to determine whether its behaviour was consistent with a signalling role.

2.2 Introduction

The fulfilment of this aim first required the development of a technique to measure cytosolic nitrate activity in aerial leaves of intact *Arabidopsis* plants using nitrate-selective microelectrodes. After the technique was perfected cytosolic nitrate activity measurements were made under treatments in which NR activity was modified. NR activity is altered in response to changes in environmental conditions, such as anoxia, light, dark, pH and carbon dioxide concentration (Kaiser *et al.*, 1999). In this work, cytosolic nitrate activity was measured during light/dark transitions in *Arabidopsis* leaf cells. In order to link cytosolic nitrate activity changes observed to the presence of functional NR, measurements were made in the leaves of both wild type plants and those with non-functional NR.

2.2.1 Nitrate-selective microelectrode measurements in Arabidopsis *leaf cells*

The previous chapter described the use of nitrate-selective microelectrodes to study intracellular nitrate activity in plant cells (Section 1.8.4). In the current study, it was necessary to devise a technique to make ion-selective microelectrode measurements

of possible signalling events associated with specific environmental stimuli on the small delicate leaves of *Arabidopsis thaliana*. To ensure that measurements taken would be valid in natural conditions, this project required access to the cells of interest without damaging the surrounding cells and stimulating wound responses in the plant. This constraint meant that some easily applicable methods of ion-selective microelectrodes could not be used in this study such as submerging leaves in liquid (e.g. Karley *et al.*, 2001). Epidermal cells are easily identified and impaled with a microelectrode without causing significant damage (Cuin *et al.*, 1999). Making microelectrode measurements in mesophyll cells is technically more difficult. Previously reported methods have removed epidermal cells to gain access to the cells of interest (e.g. Elzenga *et al.*, 1995) or impaled mesophyll cells along cut edges of leaf sections (Prins *et al.*, 1980). Both of these methods cause significant trauma to the plant. To avoid this in this study mesophyll cells were impaled without causing damage to the surrounding cells by manoeuvring the microelectrode tip through stomata.

2.2.2 *Changes in membrane potential in response to light/dark transitions*

As part of nitrate-selective microelectrode measurements, cell membrane potentials are acquired (Appendix 1). Changes of the membrane potential of photosynthetic plant cells following changes in illumination have been reported since the first studies with microelectrodes (Pallaghy and Lüttge, 1970). The onset of illumination triggers a cascade of electrical events in thylakoid and plasma membranes of green plant tissues (Vredenberg and Tonk, 1975; Fujii *et al.*, 1978; Hansen *et al.*, 1987; 1989; 1993; Elzenga *et al.*, 1995; Johannes *et al.*, 1997). There are numerous vastly different reports of electrical responses to light in plant cells. There are differences in the shape of response, the magnitude and the number of phases for different species under different environmental conditions (Fujii *et al.*, 1978; Prins *et al.*, 1982; Elzenga *et al.*, 1995; Johannes *et al.*, 1997; Shabala and Newman, 1999). The typical response to a transition from dark to light is a quick initial depolarisation of the membrane potential, followed after 1 or 2 min by a slower repolarisation, which often results in a hyperpolarisation after 20 to 40 min (Fujii *et al.*, 1978; Prins *et al.*, 1980; Tazawa *et al.*, 1986; Marrè *et al.*, 1989; Spalding *et al.*, 1992; Hansten *et al.*, 1993; Blom-Zandstra *et al.*, 1995; 1997; Johannes *et al.*, 1997; Shabala and Newman, 1999).

Involvement of numerous ion transporters in electrical events at the plasma membrane, including H^+, K^+, Cl^- and Ca^{2+} has been documented (Spalding *et al.,* 1992; Blom-Zandstra *et al.,* 1997; Johannes *et al.,* 1997, Shabala and Newman, 1999). Shabala and Newman (1999) used ion-selective vibrating microelectrodes to measure the kinetics of H^+, K^+, Cl^- and Ca^{2+} fluxes and concentration changes due to illumination near the mesophyll and epidermal cells of a bean leaf. They showed that the influx of Ca^{2+} was the main depolarising agent in mesophyll responses to light and Cl^- was the main agent in the subsequent repolarisation. The situation is further complicated by different electrical responses of the plasma membrane of epidermal and mesophyll cells (Elzenga *et al.,* 1995).

2.2.3 Producing plants without NR activity

A suitable control for the study of nitrate signalling possibly associated with changes in NR activity is to use plants without NR activity. Loss of NR activity can be achieved by various means, such as tungstate application and selecting mutant plants without functional NR. Tungstate application causes a loss of NR activity in plant cells because tungstate is an analogue of molybdate (Heimer *et al.,* 1969; Deng *et al.,* 1989). This disruption is caused because molybdate is an essential part of MoCo component of NR. Resistance to chlorate can select for mutant plants without functional NR. Chlorate is converted to toxic chlorite by NR (Åberg, 1947). NR deficiency may be conferred in different ways, including mutations to the genes associated with MoCo biosynthesis ('MoCo mutants') as well as structural mutations of NR (Wray and Kinghorn, 1989; Caboche and Rouze, 1990; Crawford and Campbell, 1990; Kleinhofs and Warner, 1990). Nine chlorate resistance loci have been identified in *Arabidopsis*; a mutation in any one of these loci produces a chlorate resistant plant (Braaksma and Feenstra, 1982; Crawford, 1992). MoCo mutants and tungstate fed plants were not selected for this study because the effects of disruption to MoCo biosynthesis are not restricted to NR (Mendel 1997; Mendel and Schwarz, 1999)). Plants with disrupted molybdenum cofactor biosynthesis are also deficient in other enzymes, for example, xanthine dehydrogenase and aldehyde oxidase (Mendel, 1997). Since the measurements made here were to be in as natural condition as possible, these methods were excluded.

One of the genes conferring chlorate resistance in *Arabidopsis* was identified as the NR structural gene *NIA2* (Wilkinson and Crawford, 1991). These *nia2* deletion mutants were characterised by having 10 % of the wild type level of shoot NR activity and being capable of maintaining normal vegetative growth when provided with nitrate as the sole nitrogen source (Wilkinson and Crawford, 1991). A second NR gene was identified during DNA cloning experiments and was designated *NIA1* (Cheng *et al.*, 1988). Together, these results indicate that *Arabidopsis* has two structural genes, *NIA2* encoding for most of the NR activity in the shoot. The *nia1nia2* double deficient structural mutant (NR^- mutant) was produced and characterised by Wilkinson and Crawford (1993); the mutant was isolated by a further chlorate selection of the *nia2* deficient mutants. The *NIA1* gene was shown to encode for the residual NR activity in the *nia2* deficient mutant. The NR^- mutant had 0.5 % of the wild type NR activity. Wilkinson and Crawford (1993) compared the fresh weight (FW) of the NR^- mutants with that of the *nia2* deficient mutants. NR^- mutants grew almost as well on NH_4^+ as the sole nitrogen source (83 % of FW). When grown on NH_4NO_3 medium the NR^- mutants had 40 % of the FW of the *nia2* mutants and had the morphology of the NH_4^+ grown plants (smaller, rounder leaves with short petioles). When grown on nitrate as the only nitrogen source the NR^- mutants grew very poorly; the FW was 10 % of the *nia2* mutants and the plants were yellowish. The structural NR^- mutant *Arabidopsis* plant produced by Wilkinson and Crawford (1993) was selected as a suitable control for this project because the only detected difference between these plants and wild type plants is the absence of NR activity.

2.3 Materials and methods

This section describes the material and methods associated with culturing *Arabidopsis thaliana* material, assaying whole tissue nitrate concentration and making nitrate-selective double-barrelled microelectrode measurements in *Arabidopsis* leaf tissue. All chemicals were from Sigma-Aldrich Company Ltd., Poole, UK unless otherwise stated; catalogue numbers are given where appropriate.

2.3.1 Culturing plant material

Nitrate-selective microelectrode measurements were made on three to four weeks old *Arabidopsis* plants grown in either hydroponic or sterile culture, as described below. Plants were cultured in a controlled environment cabinet at 20 °C, with 75 % relative humidity, a 16 h day and photon fluence of 280-300 μmol m^{-2} s^{-1}.

2.3.1.1 Hydroponic culture of wild type plants

Arabidopsis thaliana (Col 0) plants obtained from the Nottingham *Arabidopsis* Stock Centre (Plant Science Division, University of Nottingham, Nottingham, UK) for microelectrode measurements were grown hydroponically in order to control the nutrient supply accurately. A successful hydroponic culture method was devised, as described and also illustrated in Figure 2.1. 0.5 ml black tubes (Polypropylene Microtubes, 96.7456.0.01, Anachem Ltd., Luton, UK) with the lids removed were filled with 0.4 ml of 1% purified agar in deionised water solution. The agar was left to solidify. Approximately 3 mm of the bottom of each tube was cut off using a microtube cutter (Z21708-5, Aldrich Company Ltd., Poole, UK). The 0.8 l containers selected for hydroponic culture were blackened with black electrical tape or black paint. 10 mm thick black polyethylene cross-linked closed cell foam rubber (303-2296, RS Components Ltd., Corby, UK) was cut into the shape of the top of the hydroponic culture container to produce a float. This foam rubber was selected because of its resistance to weathering and its light excluding and floating properties. A number of 4 mm diameter holes were punched out of the foam float approximately 2 cm apart. The tubes were placed in the holes of the foam float and *Arabidopsis* seeds were placed on the surface of the agar using a damp cocktail stick. Nutrient solution (described below) was added to the container, the float was placed on the solution and an airline, attached to an aquarium pump, was fed though an additional hole in the foam to gently aerate the nutrient solution.

Wild type plants were grown on a modified Hoagland's nutrient solution (Gilbeaut *et al.* (1997) adapted from Hoagland and Arnon (1950)). This solution contains: 1.25 mM KNO_3, 0.5 mM KH_2PO_4, 0.75 mM $MgSO_4$, 1.5 mM $Ca(NO_3)_2$, 50 µM KCl, 50 µM H_3BO_3, 10 µM $MnSO_4$, 2 µM $ZnSO_4$, 1.5 µM $CuSO_4$, 0.075 µM $(NH_4)_6Mo_7O_4$, 72 µM ethylenediaminetetra-acetic acid ferric monosodium salt and 0.1 mM Na_2O_3Si at pH 6.0.

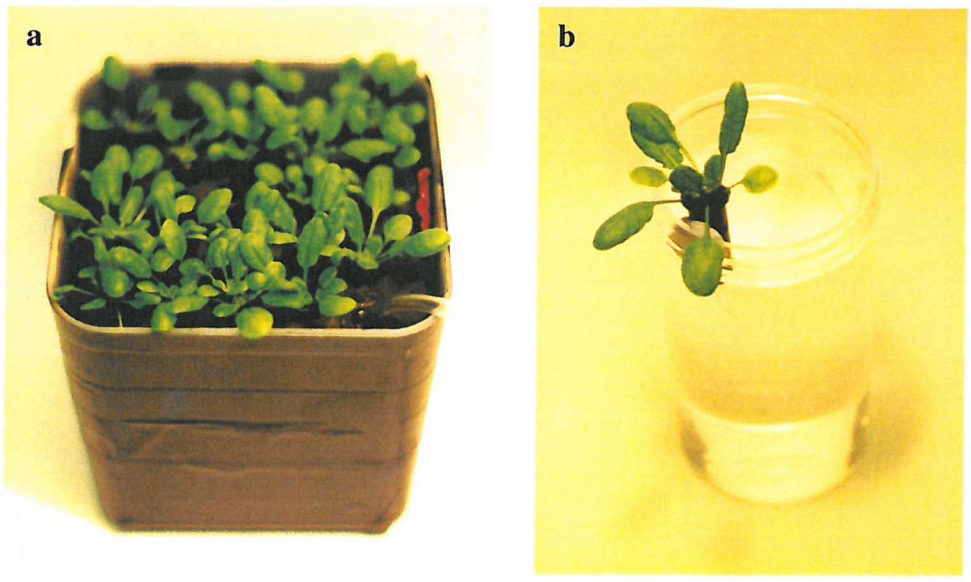

Figure 2.1 a) *Arabidopsis* plants grown in hydroponic culture with airline to aerate the solution, b) *Arabidopsis* plant removed from hydroponic culture.

2.3.1.2 Hydroponic culture of NR^- mutant plants

The NR^- mutant *Arabidopsis* seedlings were grown in hydroponic culture on a mixed nitrogen source modified Hoagland's nutrient solution; KNO_3 and $Ca(NO_3)_2$ were removed from the nutrient solution and replaced by 1.25 mM KCl and 0.1 mM NH_4NO_3.

2.3.1.3 Sterile culture of NR^- mutant plants

The NR^- mutant plants were also grown on sterile vertical agar plates (100mm square petri dishes, 109, Bibby Sterilin Ltd., Nottingham, UK). The agar solution contained di-ammonium succinate as the nitrogen source. Approximately 50 ml of the agar solution was added to each plate and left to solidify in a sterile laminar flow workstation (Microflow, Intermed, Rodhikde, Denmark). The agar solution contained a modified Hoagland's nutrient solution; KNO_3 and $Ca(NO_3)_2$ were removed from the nutrient solution and replaced by 1.25 mM KCl, 2.125 mM di-ammonium succinate, 0.8 % (w/v) purified agar and 2 % (w/v) sucrose. The NR^- mutant plants cannot assimilate nitrate so were supplied with nitrate for 3 days prior to measurement in order to fill the vacuoles with sufficient nitrate to allow determination of the location of the microelectrode tip within the cell.

Seeds were then sterilised according to the following protocol. Approximately 100 *Arabidopsis* seeds were placed in a 1.5 ml microcentrifuge tube. 1 ml of 70 % (v/v) ethanol solution was added to the tube, the tube was shaken for 1 min and transferred to a sterile laminar flow workstation. The tube was placed in a vertical position, the seeds were allowed time to settle to the bottom of the tube and the 1 ml of 70 % ethanol solution was removed by pipetting using a sterile 1 ml auto-pipette tip. 1 ml of 20 % (v/v) sodium hypochlorite solution (Fisher Scientific UK Ltd., Loughborough, UK) was added to the tube, the tube was placed on its side and shaken at intervals for 15 min. The sodium hypochlorite solution was removed and the seeds were then rinsed 6 times with sterile distilled water using the above technique.

Once the seeds were sterilised, a 0.1 ml suspension containing approximately 10 seeds in sterile water was pipetted onto each agar plate and then evenly distributed with sterile forceps. The agar plates were positioned vertically in the controlled environment cabinet.

2.3.2 Assaying whole tissue nitrate concentration

The method used to assay whole tissue nitrate concentration in *Arabidopsis* leaf tissue was based upon the protocol described in Gilliam *et al.* (1993). This method is based upon converting the nitrate present in the sample to nitrite using *Aspergillus* NR (EC 1.6.6.2.) and then assaying the nitrite produced colorimetrically.

Nitrate was extracted from the leaf tissue by boiling the tissue in a small volume of distilled water for 10 min. In some cases it was necessary to dilute the sample with deionized water to gain accurate measurements of tissue nitrate concentration.

The *Aspergillus* NR was dissolved in deionized water at a concentration of 5 U/ml (1 unit will reduce 1.0 μM of nitrate min^{-1}) and allowed to reactivate for 30 min at 23 °C. This stock was then diluted to 3.5 U/ml in 0.14 M $KHPO_3$ buffer (KH_2PO_4, P/4800/53 and K_2HPO_4, P/5245/53 both from Fisher Scientific UK Ltd., Loughborough, UK), pH 7.5. The enzyme was stored on ice. One mM FAD and 12.5 mM NADPH (β-nicotinamide adenine dinucleotide phosphate, reduced form, tetrasodium salt) were prepared and stored on ice. Just before analysis the FAD mixture was diluted 1:10 with deionized, distilled water. One hundred mM sodium nitrate was diluted (from 0.001 to 100 mM) to produce standard curves. The final

reaction volume of 100 µl contained 40 µl of 0.14 M $KHPO_3$ buffer, 30 µl deionised water, 2.5 µl of 100 µM FAD, 0.8 µl of 12.5 mM NADPH, 1.7 µl of NR (3.5 U/ml) and 25 µl of sample or standard. Each reaction was repeated three times in wells of nunc-immuno plates (Intermed, Rodhikde, Denmark) left at room temperature for 1 h.

The reaction was stopped by the addition of sulfanilamide (1 % (w/v) in 3.0 M HCl) and N-(1-naphthyl) ethylenediamine dihydrochloride (N/1252, Fisons plc., Loughborough, UK, 0.02 % (w/v)) which also produced a pink colour (after 30 min at room temperature) proportional to the concentration of nitrite in the sample. The nitrite concentration in the sample was then determined spectrophotometrically (MR5000, Dynatech, Guernsey, Channel Islands) at 540 nm based on the intensity of pink colour produced.

2.3.3 Manufacture of nitrate-selective double-barrelled microelectrodes.

Nitrate-selective membranes for the microelectrodes used in this project were constructed according to the protocol devised by Miller and Zhen (1991) as detailed in Table 2.1. Polyvinylchloride (PVC, high molecular weight polymer) and nitrocellulose were the matrix materials in the nitrate-selective membranes and methyltridodecylammonium nitrate ($MTDDA.NO_3$) was the nitrate-selective component of the membranes. The plasticiser or membrane solvent in the nitrate-selective membranes was 2-nitrophenyloctyl ether. The additive methyltriphenyl phosphonium bromide, a lipophilic cation, was included in the membranes to reduce interference by any lipophilic cations in a sample. These components were mixed together in a suitable solvent to form a sensor 'cocktail'. The nitrate-selective membrane was solvent cast from the cocktail in a micropipette. The manufacture of nitrate-selective double-barrelled microelectrodes, which involves pulling glass micropipettes, silanising glass and backfilling the micropipette with a nitrate-selective sensor cocktail, is described below.

2.3.3.1 Pulling

Double-barrelled filamented borosilicate glass (Hilgenberg Glass, Malsfeld, Germany) with barrels of differing diameters (external diameters 1.0 and 0.75 mm, internal diameters 0.58 and 0.35 mm respectively) was used to make micropipettes. 10 cm lengths of glass were clamped into the chucks of a vertical micropipette puller

(Narishige model PE-2, Tokyo, Japan, Figure 2.2) covered with a protective sleeve of plastic tubing. The puller had been modified to include an electric motor to twist the glass 360° in 1 min. The glass was heated and the lower chuck was allowed to fall 4 mm as the glass softened. Heating was continued for a further 30 s and then the glass was twisted. After the twisting was completed the micropipette was pulled by means of a magnet to a fine point. Two 5 cm double-barrelled micropipettes were produced with both barrels twisted together within an overall tip diameter of less that 1 μm (see Figure 2.3). Adjustment of the puller magnet and heater allowed the manufacture of micropipettes with different tip geometry; the tip geometry was optimised to produce electrodes capable of impaling *Arabidopsis* leaf cells. The smaller diameter barrel was broken back using a razor blade so that it was approximately 2.5 cm shorter than the larger diameter barrel. The micropipettes were then placed on a steel plate in a fume hood under a heating lamp (140 °C) to dry for 45 min.

Figure 2.2 Modified electrode puller.

Key: upper chuck, U, lower chuck, L, heating element, H, magnet, M, control unit (for adjustment of magnet and heater settings), C. *Inset:* motor attached to upper chuck.

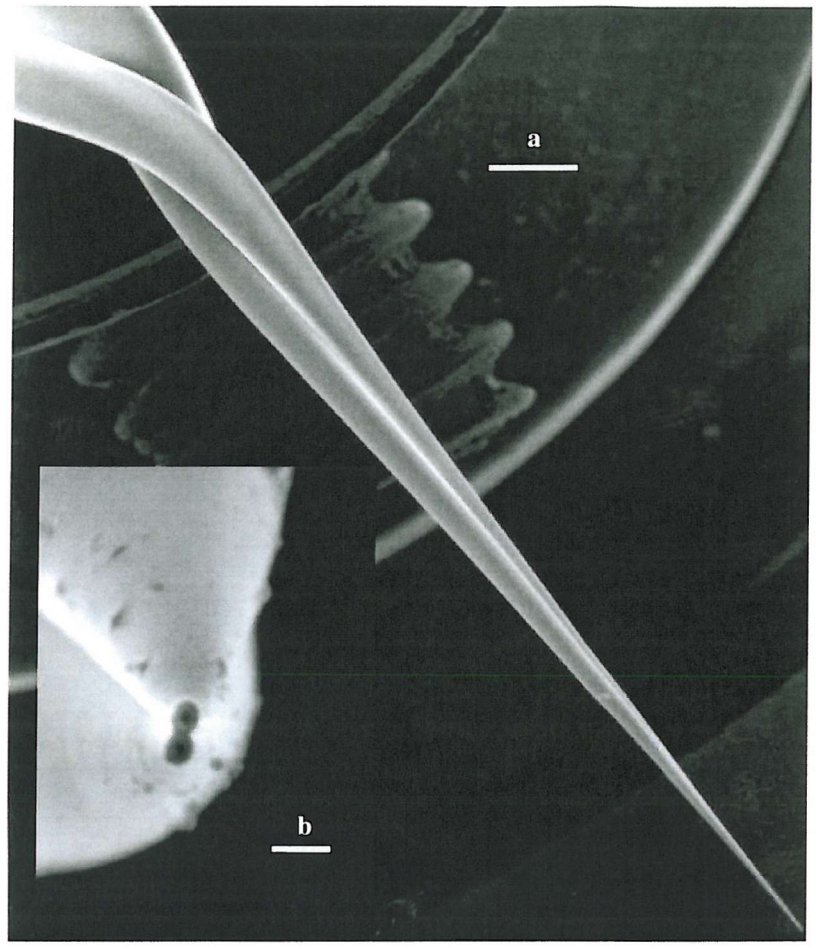

Micrographs courtesy of D.J. Walker

Figure 2.3 Electron micrographs of double-barrelled micropipettes to show the twisted tip and final pore size. Scale bars: a = 0.5 mm, b = 0.6 μm.

2.3.3.2 Silanising

Silanising was necessary to produce a high resistance seal between the glass of the internal wall of the micropipette and the hydrophobic nitrate-selective membrane. Silanising is the process of replacing hydrophilic hydroxyl groups at the glass surface with hydrophobic chlorosilanes (Ammann, 1986). The pipettes were silanised using 2 % (v/v) dimethyldichlorosilane (DCDMS, 40140, Fluka Chemicals, Gillingham, UK) in chloroform (AnalR grade, BDH Laboratory Supplies, Poole, UK). Two drops of silanising mixture were placed at the blunt end of the longer barrel of each micropipette using a 1 ml plastic syringe (Becton Dickinson S.A, Madrid, Spain) and a 19 gauge metal needle (Terumo Europe N.V., Leuven, Belgium). Care was taken not to silanise the shorter barrel, which was to be used as the membrane potential recording or 'reference' barrel. The mixture vaporised on contact with the pipette

(DCDMS has a boiling point of 60 °C) and the vapour entered the pipette to silanise the internal surfaces. The micropipettes remained under the heating lamp for a further 45 min to complete the silanisation process.

2.3.3.3 Backfilling

The components of the nitrate-selective sensor cocktail were mixed according to the proportions in Table 2-1 and dissolved in approximately 0.5 ml of the solvent tetrahydrofuran (THF). Cocktails were stored at 4 °C in screw-capped glass specimen vials with tetrafluoroethylene/silicon liners (98893, Alltech Associates Applied Science Ltd., Carnforth, UK). Vials were stored inside light-tight pots containing self-indicating silica gel (Fisher Scientific UK Ltd., Loughborough, UK).

Table 2-1 The components of a nitrate-selective microelectrode sensor membrane (Miller and Zhen, 1991).

Component	*% (w/w)*
MTDDA-NO_3. 91664, Fluka Chemicals, Gillingham, UK.	6
Methyltriphenylphosphonium bromide. M-7883, Sigma-Aldrich Company Ltd., Poole, UK	1
2-Nitrophenyl octyl ether. 73732, Fluka Chemicals, Gillingham, UK	65
Nitrocellulose. 7184002, Whatman International Ltd., Maidstone, UK.	5
PVC. 81392, Fluka Chemicals, Gillingham, UK	23

Approximately 8 μl of sensor cocktail was introduced to the silanised barrel of the double-barrelled micropipette using a 1 ml glass syringe and 38 mm long 29 gauge stainless steel hypodermic needle (Scientific Laboratory Supplies Ltd., Nottingham, UK). The micropipettes were attached tip downwards with blu-tack (Bostik Findley Ltd., Stafford, UK) to the inner walls of an airtight plastic container containing self-indicating silica gel. After 48 h the solvent phase of the cocktail evaporated to form a solvent cast nitrate-selective membrane in the tip of the micropipette. The internal filament aided the sensor filling the tip of the micropipette. The resulting microelectrodes were stored in silica-dried air and used within a month.

2.3.4 *Using nitrate-selective microelectrodes*

The microelectrodes were calibrated and subsequently used in a Faraday cage to minimise electrostatic interference as shown in Figure 2.4. Equipment was electrically grounded to a common earth as required.

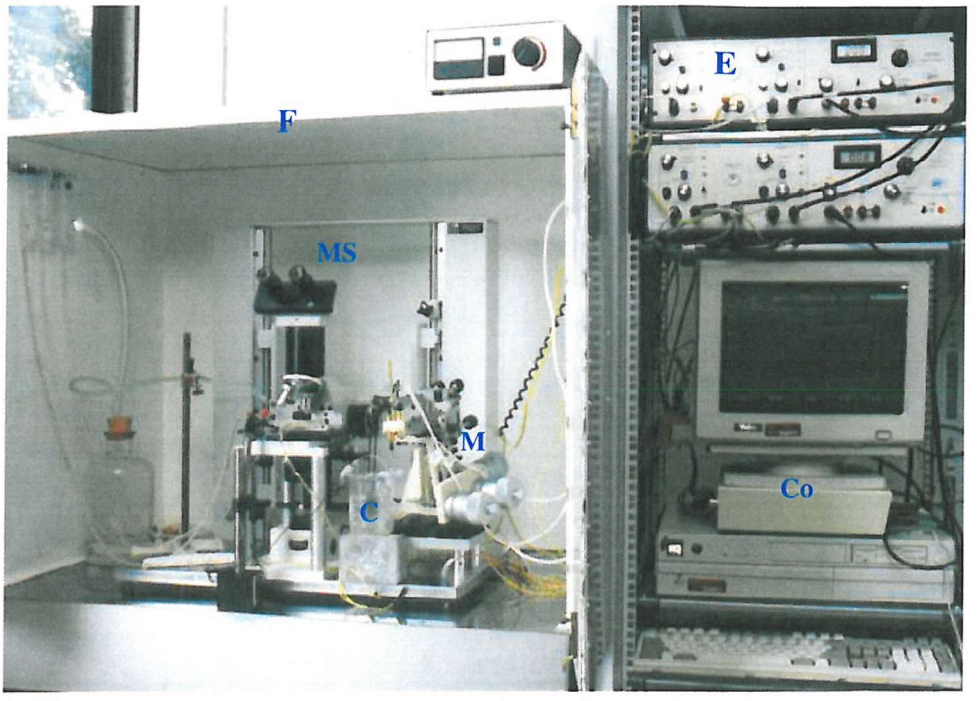

Figure 2.4 Arrangement of equipment for intracellular electrophysiological recordings.

Key: electrometer, E; micromanipulator, M; microscope, MS; Faraday cage, F; calibration funnel, C; computer, Co.

2.3.4.1 Setting up the equipment

Microelectrodes were backfilled with electrolyte solution (nitrate-selective barrel with 100 mM KCl, 100 mM KNO_3 and reference barrel with 100 mM KCl) using a plastic syringe and a MicroFil™ flexible needle (World Precision Instruments Inc., Stevenage, UK). The nitrate-selective barrel was connected directly into a microelectrode holder (model ESP-F10N, Harvard Apparatus Ltd., Edenbridge, UK) filled with the 100 mM KCl, 100 mM KNO_3 electrolyte using a plastic syringe with 38 mm long 29 gauge stainless steel hypodermic needle. The shorter reference barrel was connected with silver wire (0.38 mm diameter silver wire, AGW1510, World Precision Instruments Inc., Stevenage, UK) from the microelectrode to a 100 mM KCl

filled microelectrode holder. The microelectrode holders contained a Ag/AgCl pellet with a 2 mm socket which was connected to the jack of the headstage amplifier of a high impedance differential electrometer (model FD223, World Precision Instruments Inc., Stevenage, UK). The output from the electrometer was passed via an analogue to digital converter and data acquisition card (PC-LabCard model PCL-818H, Advantech Co. Ltd., Taipei, Taiwan) to an IBM-compatible personal computer. Data were displayed, analysed and stored using VISER software (**V**ersatile **I**on-**S**elective **E**lectrode **R**ecording software, Version 4.0, I. R. Jennings, University of York, York, UK). The headstage/holder/electrode assembly was clamped to a x-y-z micromanipulator (Goodfellow Cambridge Ltd., Cambridge, UK) to allow accurate positioning of the microelectrode tip. A half-cell connected to plastic tubing with an agar plug (100 mM KCl, 3.2 % (w/v) purified agar) was filled with 100 mM KCl; this 'ground electrode' provided connection between the ground of the electrometer and the sample solution.

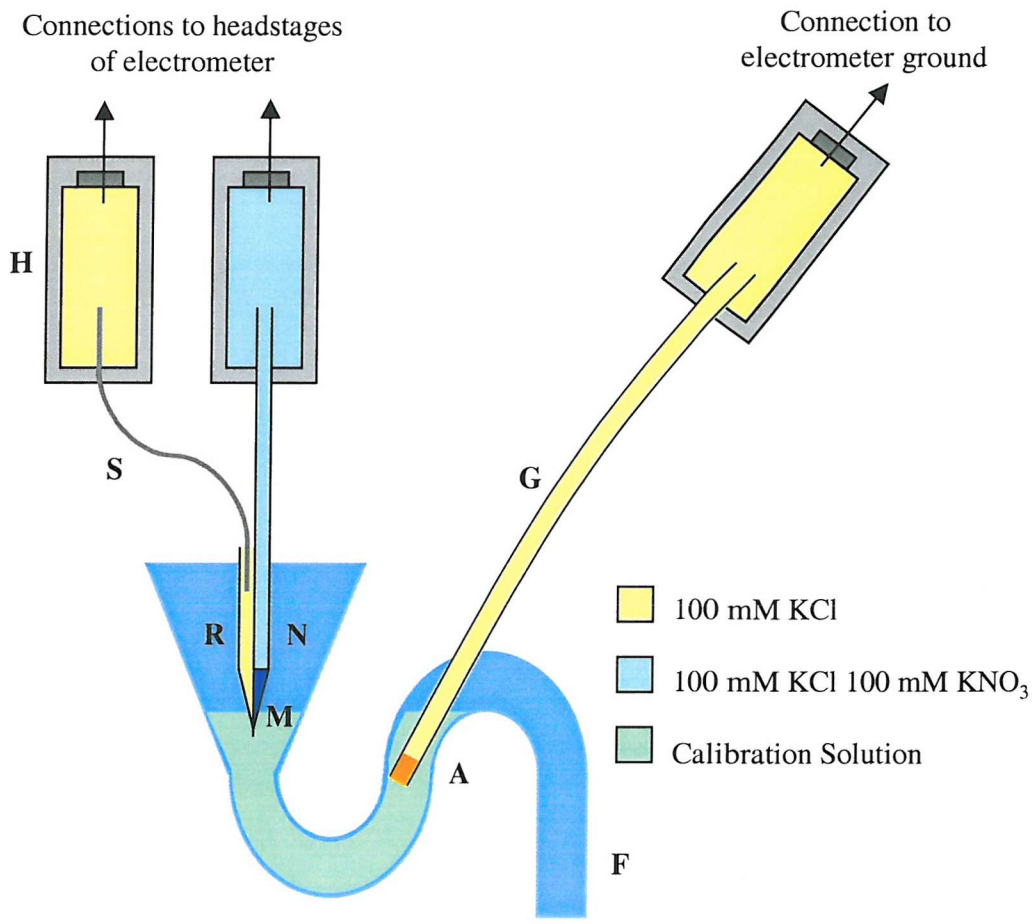

Figure 2.5 Arrangement of equipment for calibration.

Key: microelectrode holder H; silver wire, S; reference barrel, R; nitrate-selective barrel, N; nitrate-selective membrane, M; agar plug, A; ground electrode, G; calibration funnel, F.

2.3.4.2 Calibration

The nitrate-selective barrel gives an output voltage or EMF (electromotive force) dependent on the activity of nitrate at the microelectrode tip, and requires calibration before use. The tips of nitrate-selective microelectrodes were immersed in a series of calibration solutions of known ionic concentration (shown in Table 2-2, Miller and Zhen, 1991) held in a glass funnel (Soham Scientific, Cambridge, UK) as shown in Figure 2.5. The shank of the funnel was modified to form a U-bend so that the level in the funnel remained constant whilst changing solutions. An opening in the U-bend allowed the reference half-cell electrode to be located in the solution at all times,

allowing constant operation of the electrometer during calibration (the headstage amplifier of the electrometer could otherwise be damaged by a break in the recording circuit). The arrangement of the calibration equipment is shown in Figure 2.6.

Table 2-2 Composition of solutions to calibrate nitrate-selective microelectrodes for intracellular measurements (Miller and Zhen, 1991).

Nitrate activity (mM)	*pNO_3*	*HEPES (mM)*	*KNO_3 (mM)*	*KH_2PO_4 (mM)*	*Ionic strength (mM)*
0.01	5	5	0.0121	50.0	140
0.1	4	5	0.122	50.0	140
1.0	3	5	1.22	50.0	141
10.0	2	5	12.20	46.5	140
100.0	1	5	130.00	15.0	142

All solutions were at pH 7.9 to ensure the major anion determining ionic strength, other than nitrate, was HPO_4^{2-}. pNO_3 is the negative $\log_{10}$ [NO_3^- activity]. HEPES, N-(2-hydroxyethyl)piperazine-N'-(2-ethanesulfonic) acid.

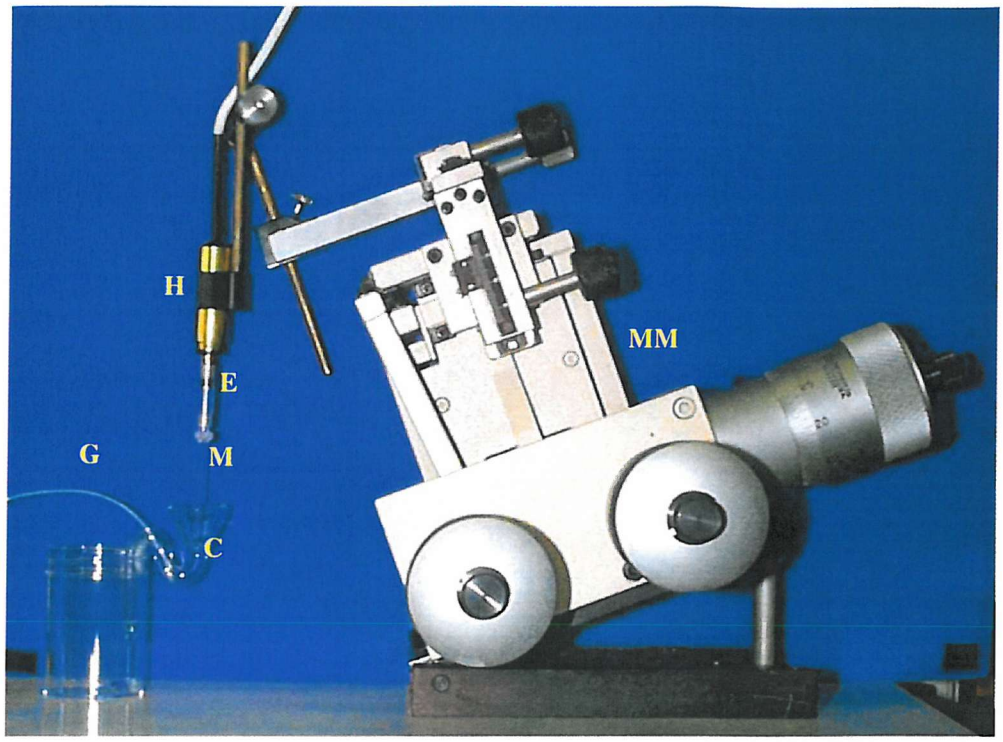

Figure 2.6 Calibration equipment.

Key: micromanipulator, MM; headstage amplifier of electrometer, H; electrode holder, E; microelectrode, M; calibration funnel, C; ground electrode G.

The VISER software calculated a calibration curve using the Nicolsky-Eisenman equation for each electrode as described in Appendix 1, an example of a typical nitrate-selective microelectrode calibration response and curve is shown in Figure A.2. Nitrate-selective microelectrodes are considered suitable for intracellular measurements if the slope of the calibration curve is between –50 and –60 mV (Fluka, 1996).

2.3.4.3 Making nitrate-selective microelectrode measurements

Leaves of intact plants were impaled with most of the leaf in the air; one edge of the leaf was dipped into a bath solution (¼ Hoaglands solution) in order to make electrical contact through the leaf to a ground electrode in the bath solution (Figures 2.7 and 2.8). A leaf was held in a transparent perspex chamber firmly secured under a polythene strap. The polythene strap had 1.5 mm diameter holes punched through it so that the microelectrode tip could access the cells of interest. The leaf was

positioned at an angle of 45° to the base of the chamber. The impaled cells were free from the bath solution touching the lower edge of the leaf. The plants were placed in the chamber on the microscope stage; the light conditions required for the measurement were maintained for at least 1 h before each measurement was taken, to allow the leaf to adjust to the new environment of the chamber and recover from possible handling stress.

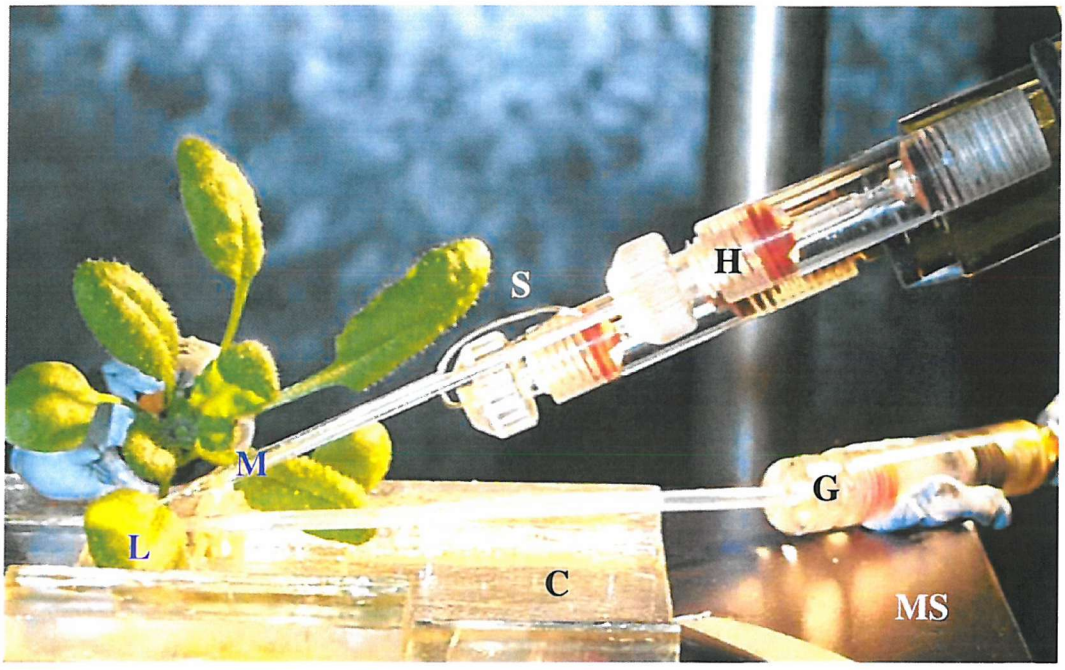

Figure 2.7 Impaling an *Arabidopsis* leaf cell with a nitrate-selective microelectrode.

Key: chamber, C; ground electrode, G; microelectrode holder, H; leaf, L; microelectrode, M; microscope stage, MS; silver wire, S.

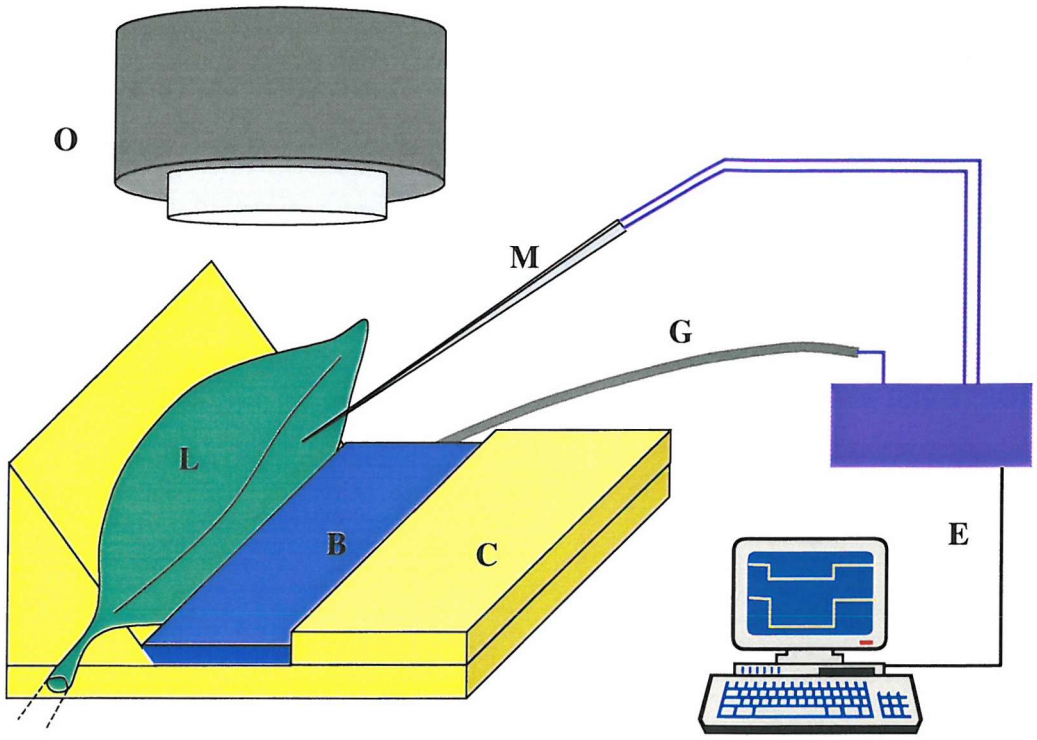

Figure 2.8 Diagrammatic representation of the experimental arrangement used for microelectrode measurements in leaf cells.

Key: microscope objective (long working distance), O; leaf (whole plant not shown), L; double-barrelled nitrate-selective microelectrode, M; perspex chamber, C; ground electrode, G; bath solution, B; high impedance electrometer, E.

After a successful calibration, the microelectrode was carefully manoeuvered close to the leaf using the micromanipulator. The microelectrode tip was viewed under a light microscope (ME2, Oxford Micro Instruments, Oxford, UK) with a magnification of x400. The tip was positioned in the apoplast surrounding the cell type of interest. At x400 magnification epidermal cells can be easily identified and impaled. Guard cells were also identifiable and manoeuvring the microelectrode tip through the stomata allowed measurements in mesophyll cells. Mesophyll cell measurements were technically more difficult as the exact location of the microelectrode tip was not visible.

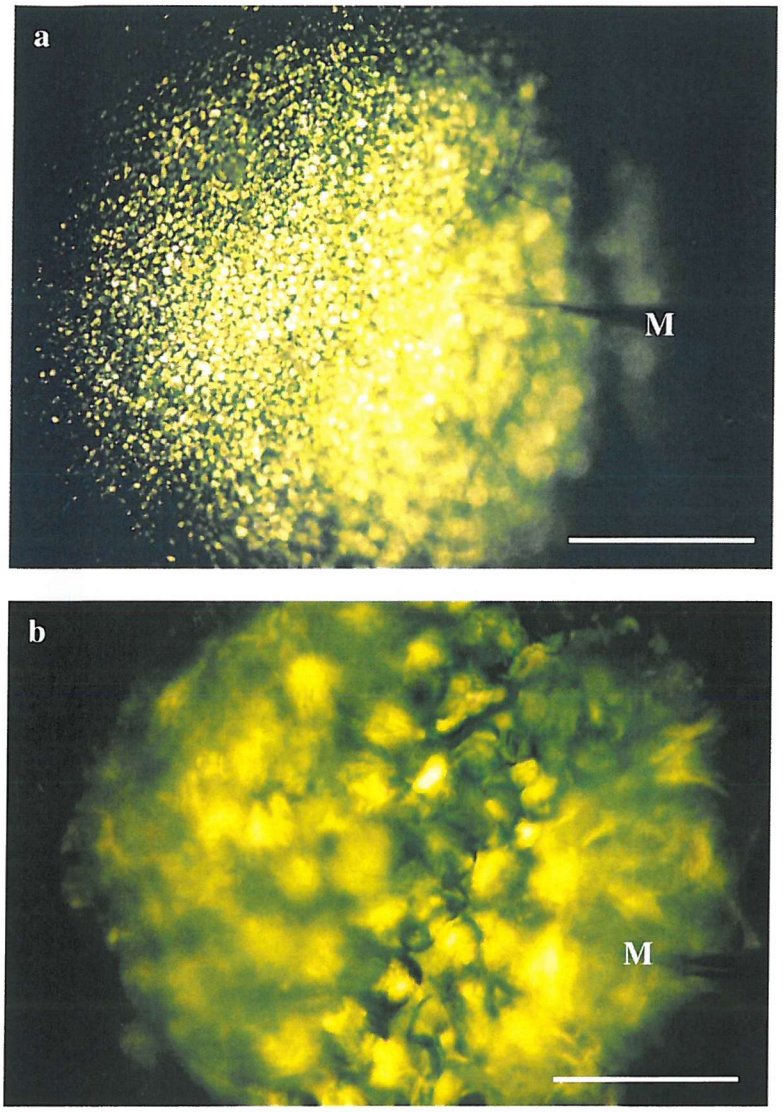

Figure 2.9 Light micrographs of an impaled *Arabidopsis* leaf cell using a nitrate-selective microelectrode, magnification: a) x50, b) x400, scale bars: a) 1200 μm, b) 150 μm.

Key: microelectrode tip, M.

The voltage of the membrane potential or 'reference' barrel was manually offset to zero on the electrometer. A successful impalement was indicated by a response of the reference barrel of approximately –100 mV. The VISER software calculated the mM nitrate activity by subtracting the voltage output of the reference barrel from the nitrate-selective barrel, and then applying the calibration curve (see Appendix I). The microelectrode was re-calibrated after a successful impalement.

Readings were discarded if the difference between calibration curves before and after measurement was greater than the normal limits of experimental variation. Where necessary corrections associated with drift in the reference barrel of the microelectrode were applied.

2.3.4.4 Illumination treatments

Dynamic nitrate-selective microelectrode measurements (in which the responses to treatments were studied) were made after a minimum 5 min of steady recording of both the barrels of the microelectrode. The illumination treatment was then applied; initially measurements were made with the light on (350 μmol m^{-2} s^{-1}), so the first treatment was to turn the light off. A new steady state was achieved, and then the treatment was reversed; the light was turned on, and recording continued until the previous steady state was restored. The electrode was then removed from the cell carefully and recalibrated.

2.3.5 Statistical analysis of data

Data were analysed using the statistical computer package SPSS (**S**tatistical **P**ackage for **S**ocial **S**ciences), version 6.0, SPSS Inc., Chicago, USA.

2.4 Results

Electrophysiological techniques are notoriously difficult; Miller *et al.* (2001) reported a successful measurement and recalibration rate of 24 % for steady-state double-barrelled nitrate-selective microelectrode in root cells. Ion-selective microelectrode measurements in leaf cells are technically more difficult due to the positioning of the microelectrode tip in the apoplast before impalement and the length of measurement time required for dynamic measurements. The data given here represents the manufacture, calibration and testing of over 350 nitrate-selective microelectrodes for measurement attempts.

2.4.1 Steady-state nitrate-selective microelectrode measurements made in wild type and NR⁻ mutant Arabidopsis *leaves*

Nitrate-selective microelectrode measurements were made in wild type and NR^- mutant *Arabidopsis* leaves. Figure 2.10 is an example of a nitrate-selective microelectrode measurement in a NR^- mutant mesophyll cell. The microelectrode tip is initially in the apoplast and then positioned in the cytosolic compartment. The membrane potential barrel rapidly responds to the impalement whereas the nitrate-selective barrel settles down more slowly.

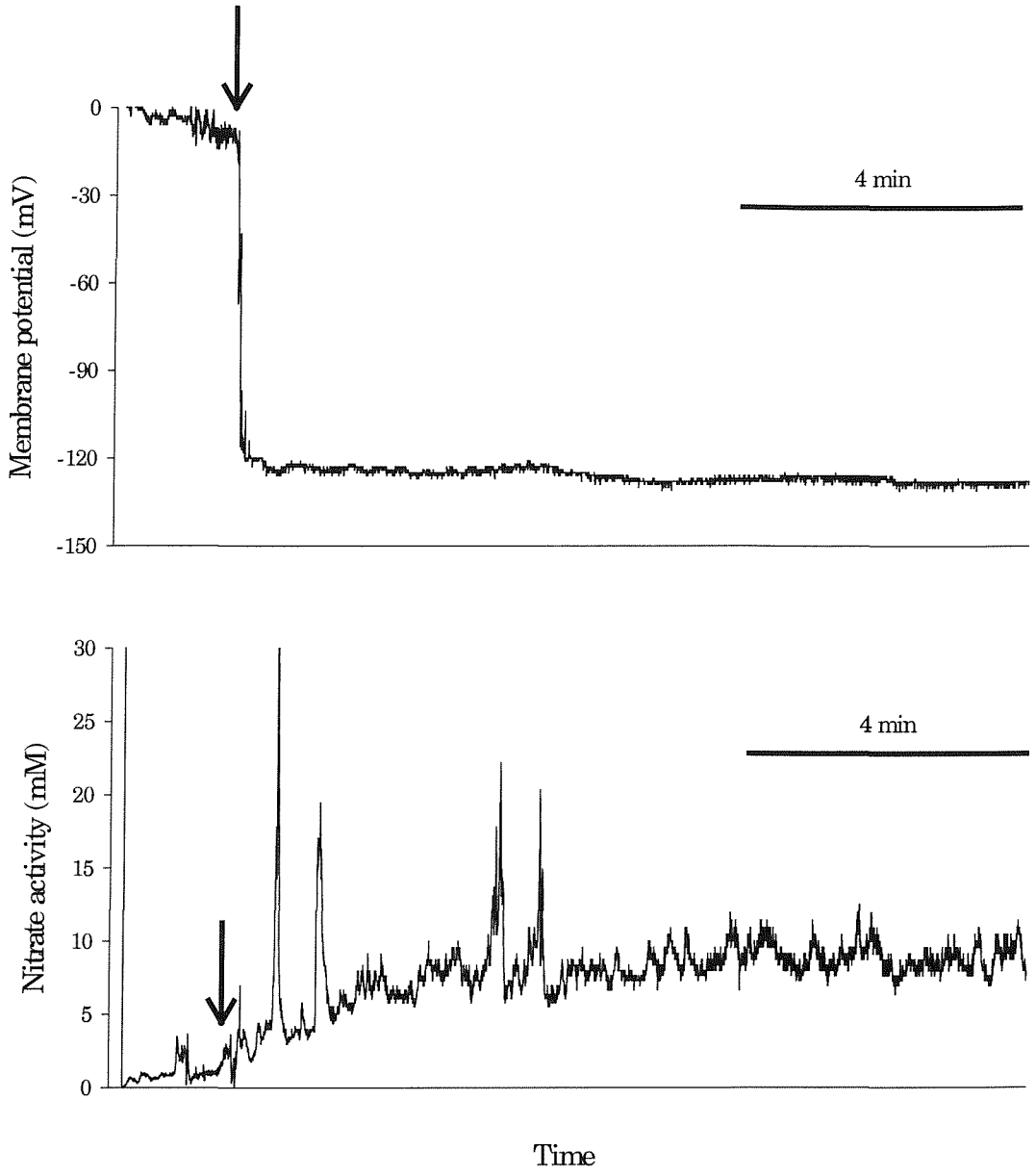

Figure 2.10 An example of a nitrate-selective microelectrode measurement in a NR^- mutant mesophyll cell; arrow indicates the time at which the microelectrode tip was manoeuvered from the apoplast into the cytosol.

Figure 2.11 shows scatter plots of the nitrate activity versus membrane potential of measurements made in wild type and NR^- mutant plants. These results must represent measurements in either the vacuole or cytoplasm of a leaf cell. For both wild type and NR^- mutant measurements the data were analysed using a hierarchical cluster analysis. In both cases the data resolved clearly into two clusters. The higher nitrate activity and less negative membrane potential cluster was ascribed to the vacuole on the basis of whole tissue nitrate analysis (30 and 50 mM for the wild

type and NR^- mutant plants respectively) assuming that the majority of the shoot consists of vacuole. Therefore, the lower nitrate activity and more negative membrane potential cluster was ascribed to the cytoplasmic population.

The mean nitrate activities of the apoplastic, cytosolic and vacuolar populations from wild type and NR^- mutant plants are shown in Figure 2.12. These data are shown in more detail in Table 2-3; the mean measurements are further sub-divided into those of epidermal and mesophyll cells. The mean cytoplasmic nitrate activity in the wild type epidermal and mesophyll cells was lower than the NR^- mutant plants and this difference was proven to be statistically significant at the 5 % level using a Mann-Whitney U-test. The mean cytoplasmic nitrate activity of epidermal cells was lower than that of mesophyll cells in both wild type and NR^- mutant leaves. The mean vacuolar nitrate activity in both the wild type and NR^- mutant epidermal and mesophyll cells was considerably higher than that of the cytosol, between 25 and 50 mM. The mean tonoplast potential was approximately 35 mV for all cells studied. The measurements of nitrate activity in wild type and NR^- mutant leaf apoplast were very low with means of 0.3 and 0.7 mM respectively; the means were not statistically significantly different at the 5 % level when tested using a Mann-Whitney U-test.

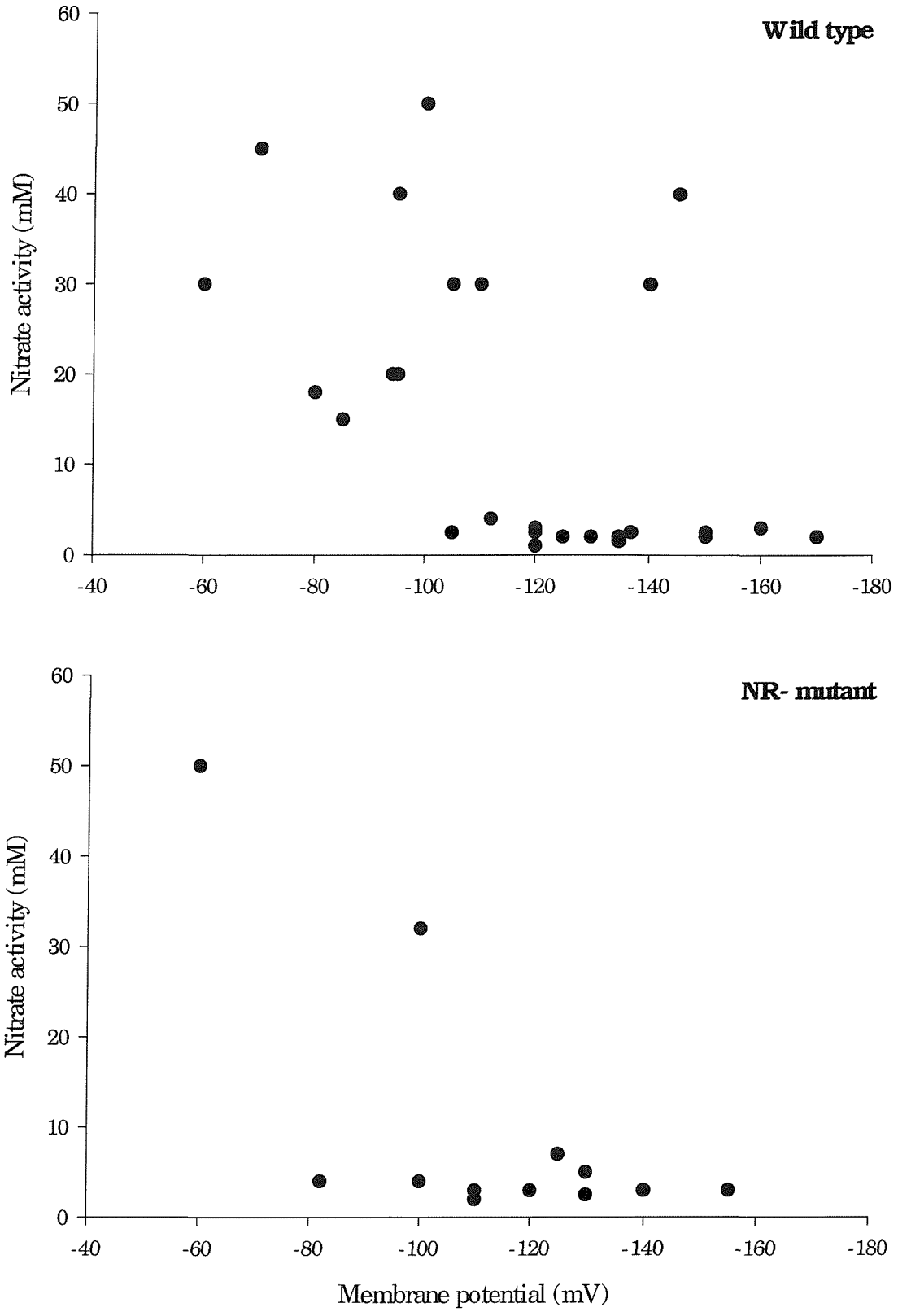

Figure 2.11 Scatter plots of nitrate-selective microelectrode measurements made in wild type and NR^- mutant leaf cells.

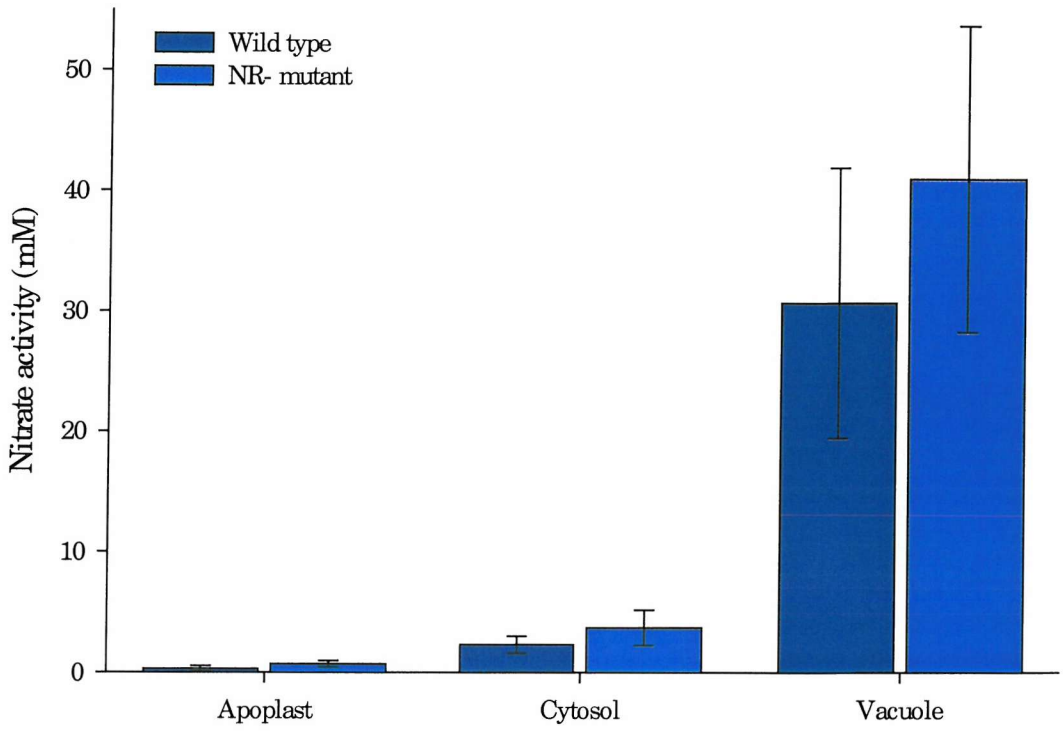

Figure 2.12 Means of nitrate-selective microelectrode measurements made in the apoplast, cytosol and vacuole of wild type and NR^- mutant leaf cells, standard deviations shown.

Table 2-3 Mean values of steady-state nitrate-selective microelectrode measurements in wild type and NR^- mutant epidermal and mesophyll cells.

Compartment	*Plant*	*Cell type*	*Mean nitrate activity (mM)*		*Mean membrane potential (mV)*	
Cytoplasm	Wild type	Epidermal	2.2	(0.50)	-147.0	(15.75)
		Mesophyll	2.4	(0.80)	-128.6	(20.25)
	NR^- mutant	Epidermal	3.2	(1.61)	-123.3	(11.55)
		Mesophyll	3.9	(1.46)	-118.6	(24.44)
Vacuole	Wild type	Epidermal	25.0	(7.07)	-99.5	(7.78)
		Mesophyll	31.8	(11.84)	-98.0	(27.61)
	NR^- mutant	Epidermal	50.0	(*)	-60.0	(*)
		Mesophyll	32.0	(*)	-100.0	(*)
Apoplast	Wild type		0.3	(0.24)	0	(0.00)
	NR^- mutant		0.7	(0.28)	0	(0.00)

Standard deviations shown in brackets n > 5, * insufficient data

2.4.2 *Dynamic nitrate-selective microelectrode measurements in* Arabidopsis *leaves during light-dark and dark-light transitions*

Figures 2.13 to 2.16, 2.18, 2.19, 2.23 and 2.24 are typical examples of sections of nitrate-selective microelectrode measurements in *Arabidopsis* leaves during light/dark transitions. The upper trace of each figure shows the membrane potential and the lower trace shows the nitrate activity of the cell compartment. Transients on electrophysiological traces are due to electrical noise.

2.4.2.1 Measurements in wild type epidermal and mesophyll cells.

Figures 2.13 and 2.14 are examples of a measurement in the vacuole of an epidermal cell, Figures 2.15 and 2.16 are examples of a measurement in the cytoplasm of an epidermal cell and Figures 2.18 and 2.19 are examples of a measurement in the cytoplasm of a mesophyll cell.

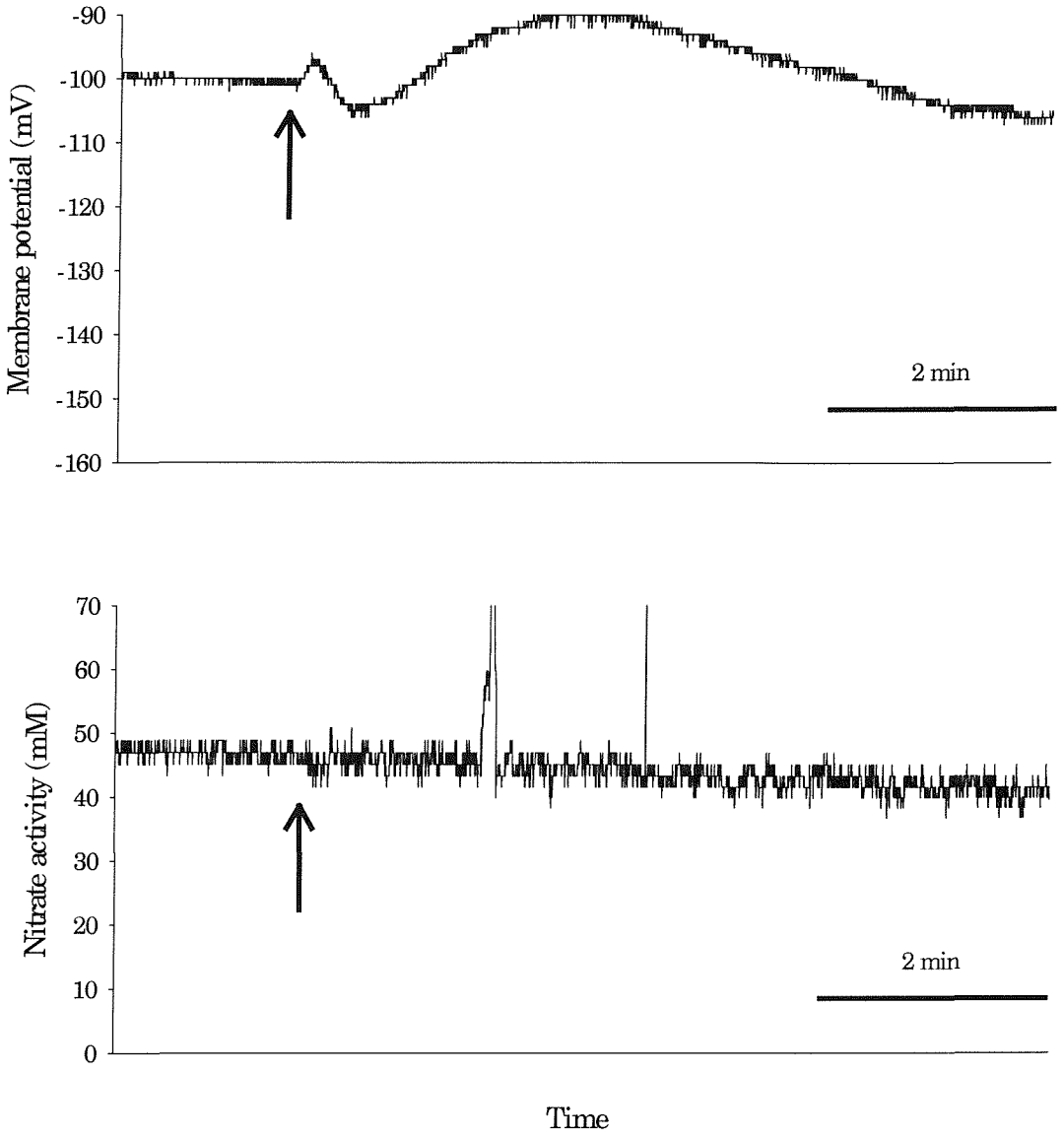

Figure 2.13 A typical example of a recording from a nitrate-selective microelectrode in a vacuole of an epidermal cell of a wild type plant, arrow indicates the time at which the light to dark transition occurred.

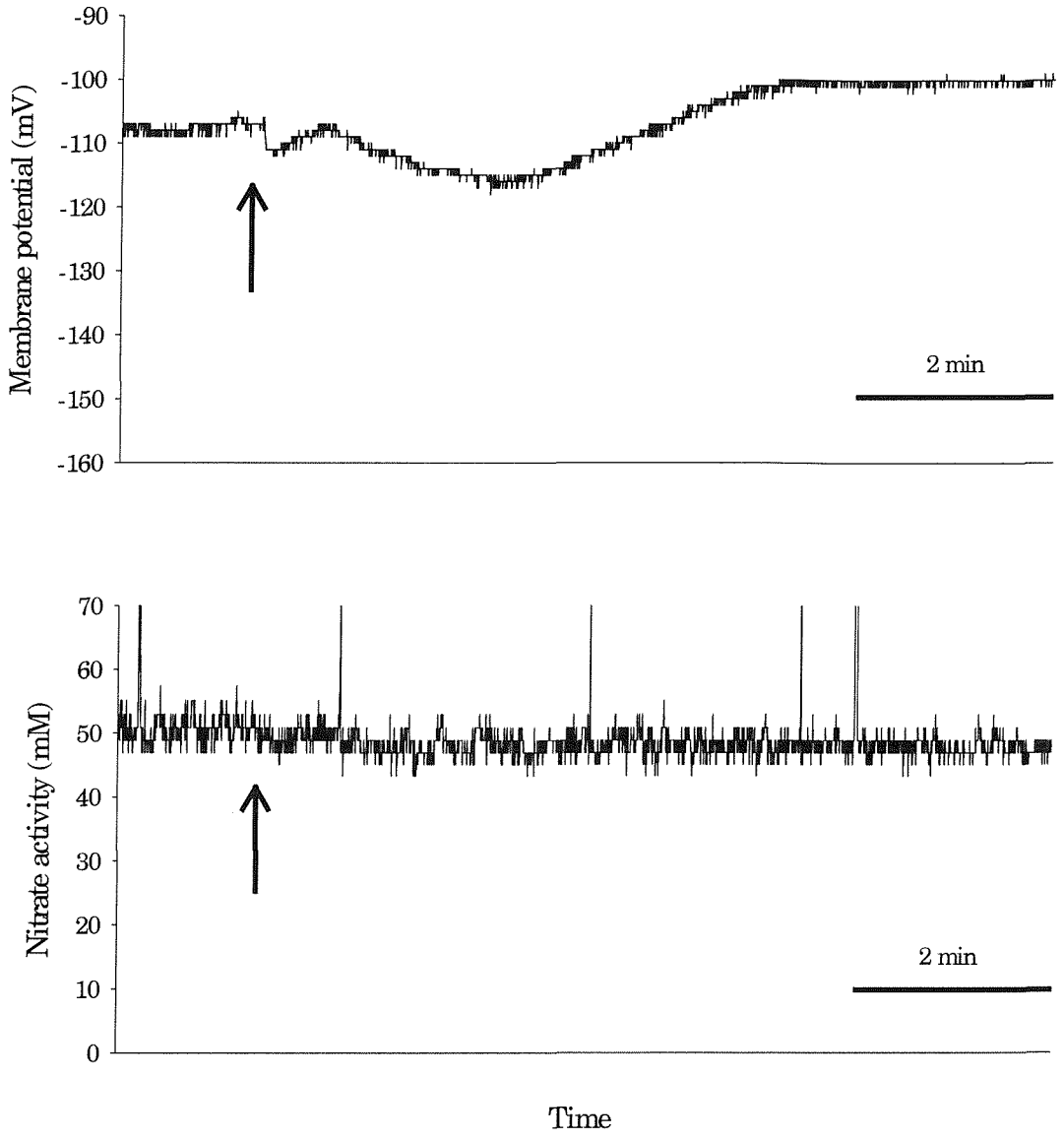

Figure 2.14 A typical example of a recording from a nitrate-selective microelectrode in a vacuole of an epidermal cell of a wild type plant, arrow indicates the time at which the dark to light transition occurred.

Figures 2.13 and 2.14 show that there was no change in vacuolar nitrate activity (in these examples approximately 50 mM) in response to light-dark and dark-light transitions in epidermal cells. The membrane potential of the cell did change in response to light-dark and dark-light transitions in a multiphase, transient response. The examples shown are typical responses in terms of magnitude, duration and shape of response. Generally, epidermal cells respond to light-dark transitions (see Figure

2.13) by a fast small initial depolarisation followed by a subsequent small hyperpolarisation and then a more prolonged depolarisation and then another slow hyperpolarisation before returning to a steady resting membrane potential. Generally, epidermal cell membrane potentials respond to dark-light transitions (see Figure 2.14) in the opposite sense to light-dark transitions. A rapid small hyperpolarisation is followed by a small depolarisation, then by a further prolonged hyperpolarisation and depolarisation before returning to a steady resting membrane potential. Generally, the resting membrane potential of a cell is slightly more negative in the dark compared with the light.

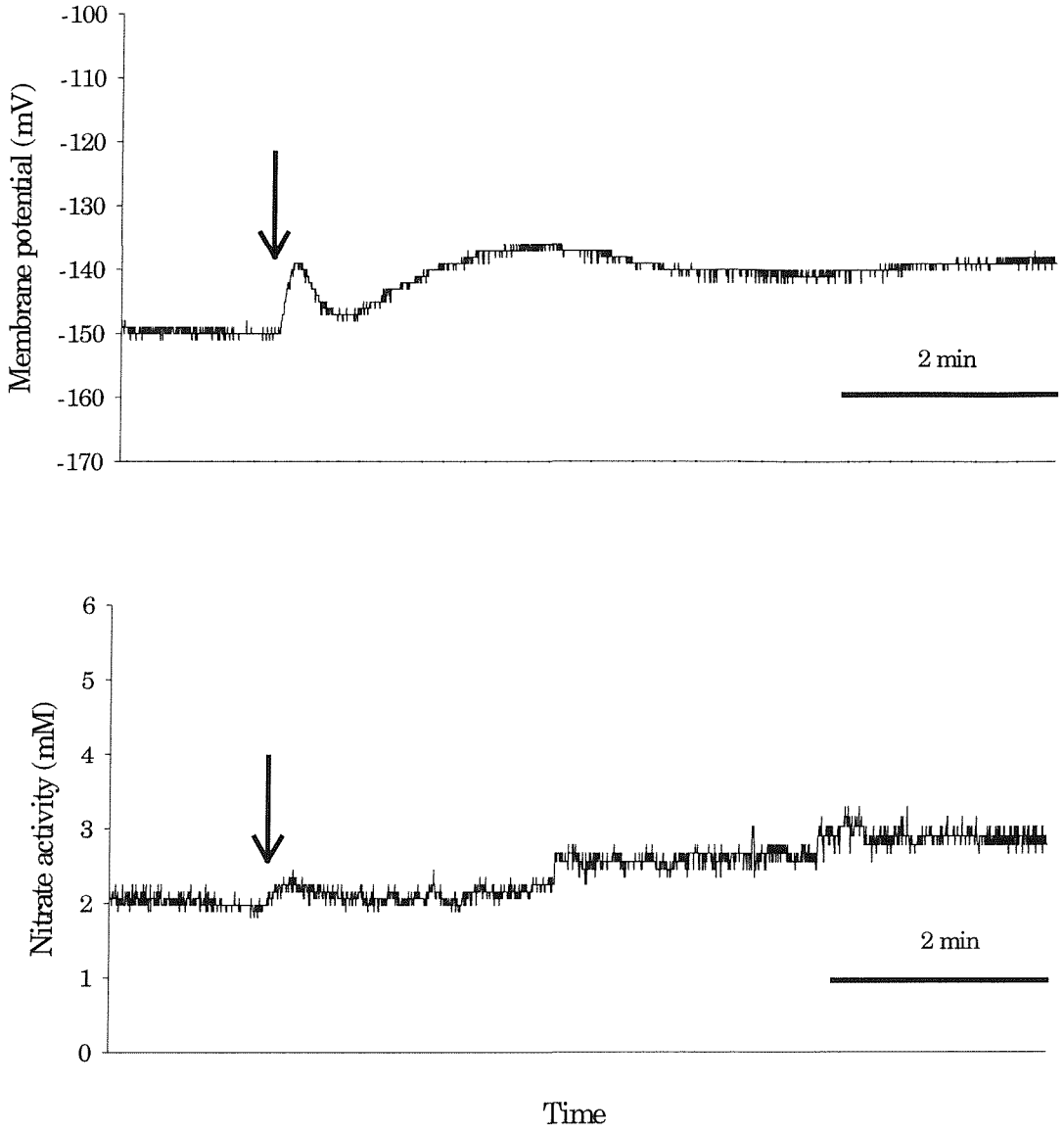

Figure 2.15 A typical example of a recording from a nitrate-selective microelectrode in the cytosol of an epidermal cell of a wild type plant, arrow indicates the time at which the light to dark transition occurred.

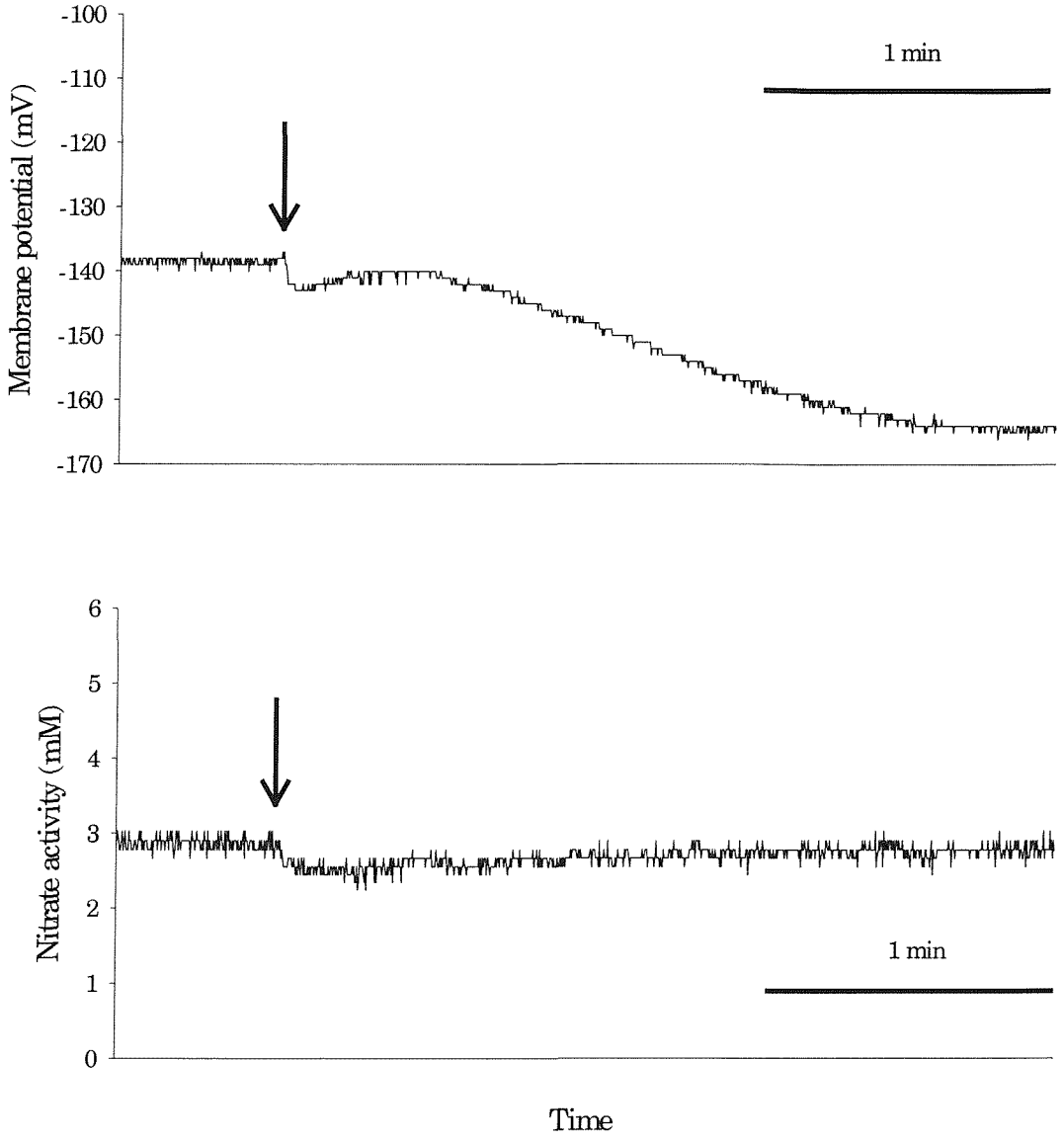

Figure 2.16 A typical example of a recording from a nitrate-selective microelectrode in the cytosol of an epidermal cell of a wild type plant, arrow indicates the time at which the dark to light transition occurred.

Figures 2.15 and 2.16 show that there was little or no change in cytoplasmic nitrate activity (maintained at approximately 3 mM in these examples) in response to light-dark and dark-light changes in epidermal cells. The membrane potential of the cell changed in response to the light-dark and dark-light transitions with the same response as described and shown previously for responses recorded from vacuoles of epidermal cells (Figures 2.13 and 2.14).

2.4.2.2 Tonoplast potential changes in wild type epidermal cells

Light-dark transition induced changes in the tonoplast potential of the wild type epidermal cells (Figure 2.17) were calculated by subtracting the membrane potential of a cytosolic measurement (Figure 2.15) from a vacuolar measurement (Figure 2.13). The cytosolic and vacuolar measurements were made in different epidermal cells of the same leaf.

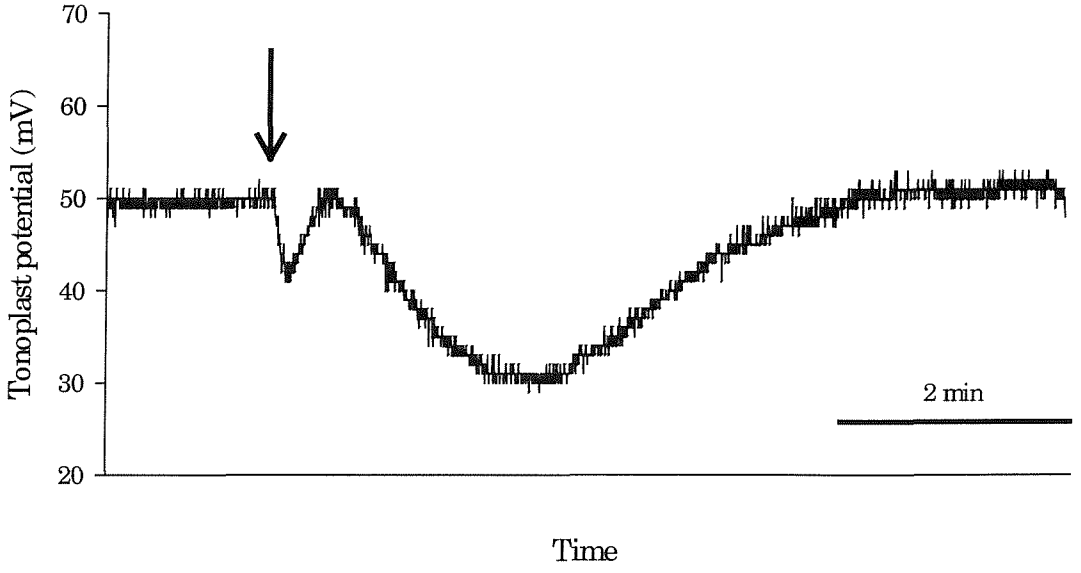

Figure 2.17 Calculated tonoplast potential response to the transition from light to dark (indicated by arrow) of an epidermal cell of a wild type plant.

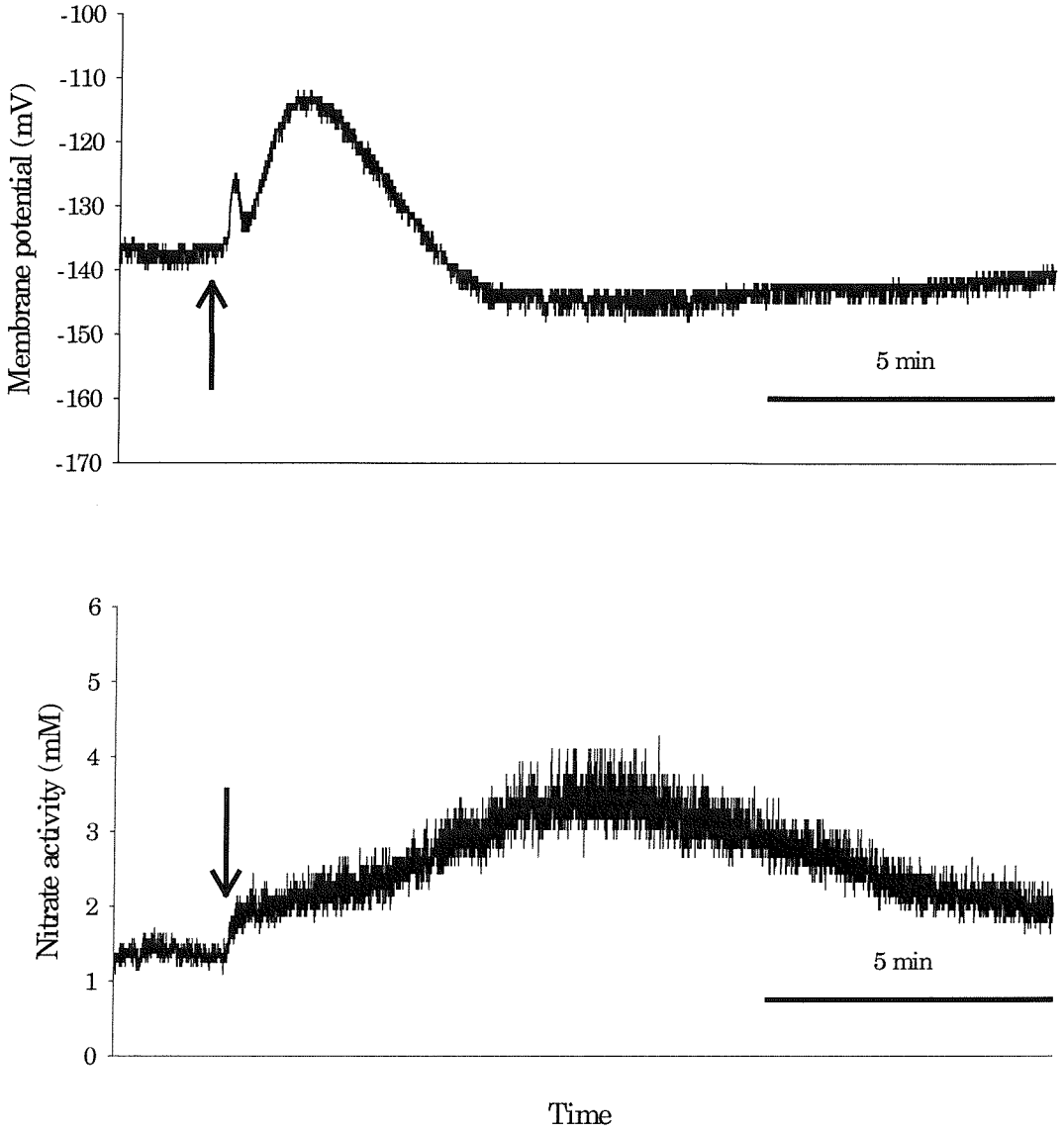

Figure 2.18 A typical example of a recording from a nitrate-selective microelectrode in the cytosol of a wild type mesophyll cell, arrow indicates the time at which the light to dark transition occurred.

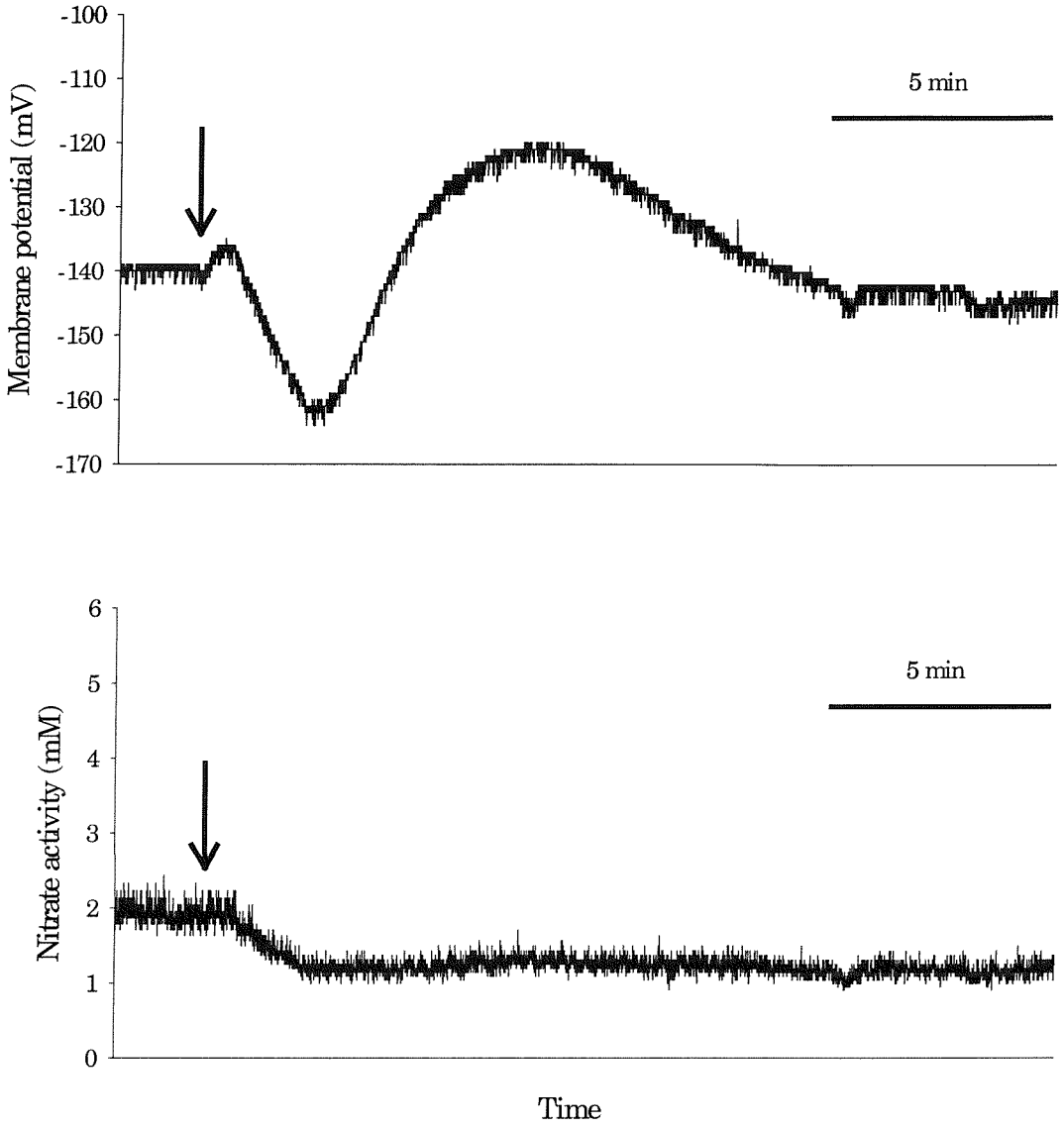

Figure 2.19 A typical example of a recording from a nitrate-selective microelectrode in the cytosol of a wild type mesophyll cell, arrow indicates the time at which the dark to light transition occurred.

Figures 2.18 and 2.19 show that there was a change in cytoplasmic nitrate activity in response to light-dark and dark-light changes in mesophyll cells. Whilst the cell was under the dark treatment cytosolic nitrate activity was maintained at around 2 mM, after the application of the light treatment the cytosolic nitrate activity rapidly decreased to 1.3 mM (see Figure 2.19). Figure 2.18 shows the reverse process; during the light treatment the cytosolic nitrate activity was 1.3 mM. After application of the dark treatment cytosolic nitrate activity quickly increases to 2 mM,

then more gradually increases to 3.5 mM over the following 7 min and then a steady state nitrate activity of 2 mM was restored after a further 7 min. The membrane potential of the cell changes in response to the illumination transitions in a pattern similar to that of the epidermal cells (as shown in Figures 2.13 to 2.16). The mean magnitude of membrane potential response to light off and light on in mesophyll cells was greater than the response in epidermal cell and this was proven to be statistically significant at the 5 % level using a Mann-Whitney U-test (as shown in Figure 2.20). The mean duration of the perturbation in the membrane potential in response to illumination changes was significantly longer (tested with a Mann-Whitney U-test at the 5 % level) in mesophyll cells compared with that of the epidermal cells (as shown in Figure 2.21).

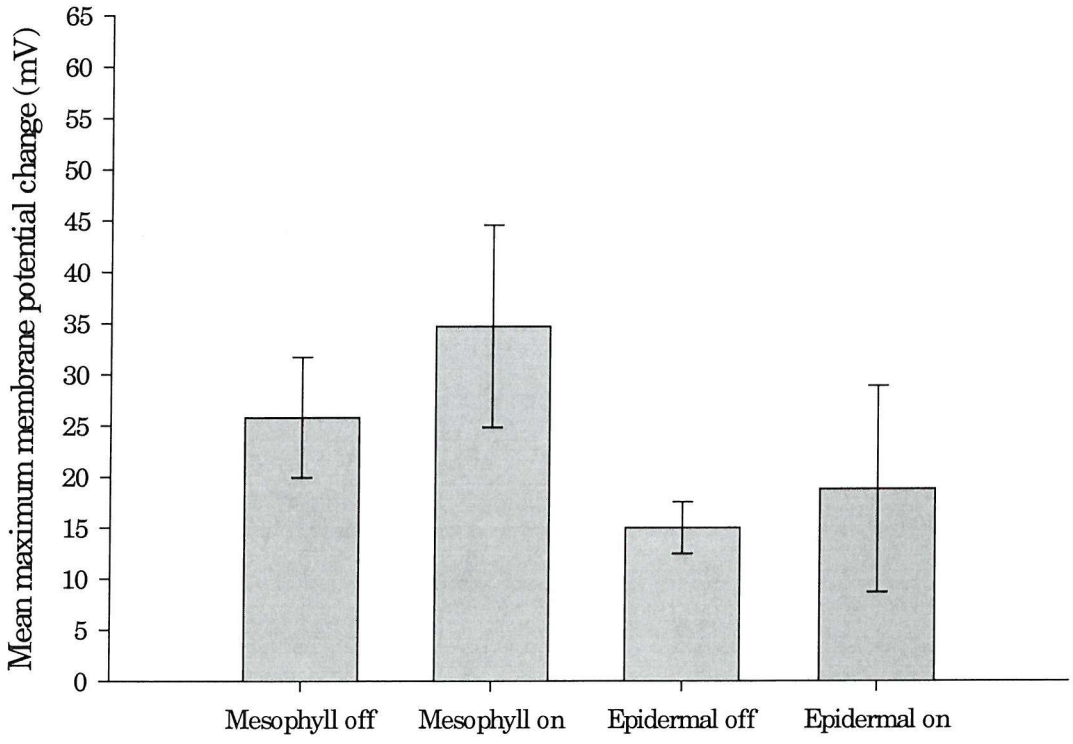

Figure 2.20 Mean maximum magnitude of perturbation of the membrane potential in response to either light off or light on in wild type mesophyll and epidermal cells, n > 5 in each category, standard deviations shown.

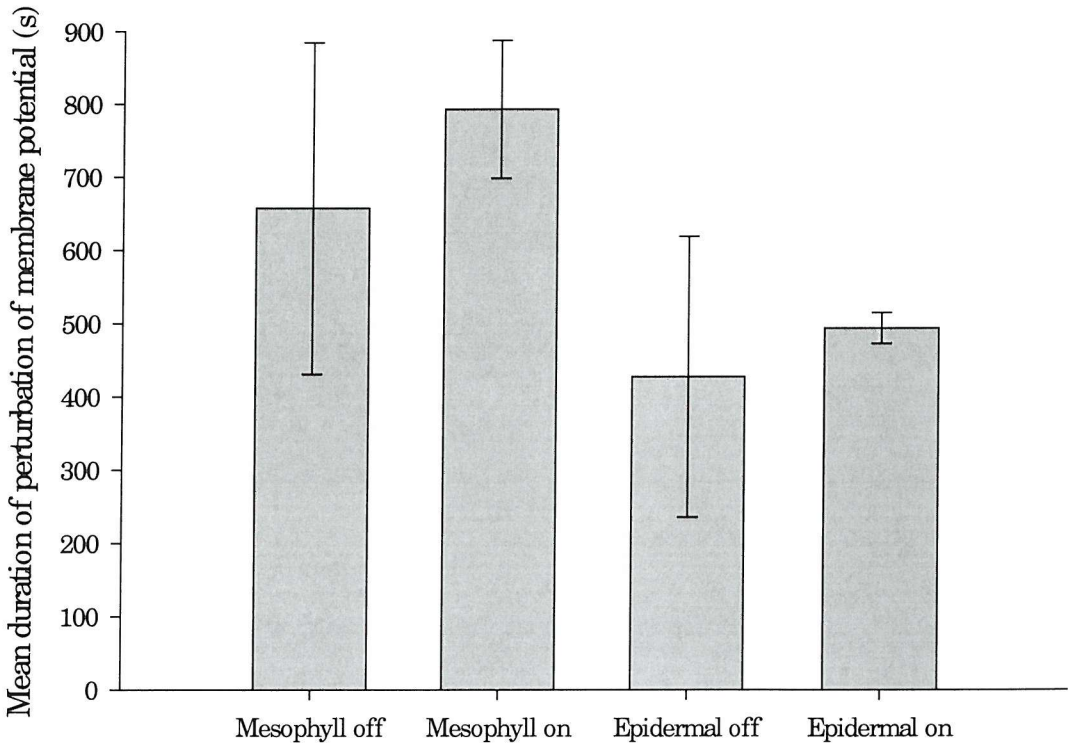

Figure 2.21 Mean duration of perturbation of the membrane potential in response to light off or light on in wild type mesophyll or epidermal cells, n > 5 in each category, standard deviations shown.

Figure 2.22 shows the mean cytosolic nitrate activity of wild type epidermal and mesophyll cells during light and dark treatments. Mean cytosolic nitrate activity in mesophyll cells was significantly different (Mann-Whitney U-test at the 5 % level) during the light and dark treatments. However, in the epidermal cells there was no significant difference in cytosolic nitrate under the two treatments.

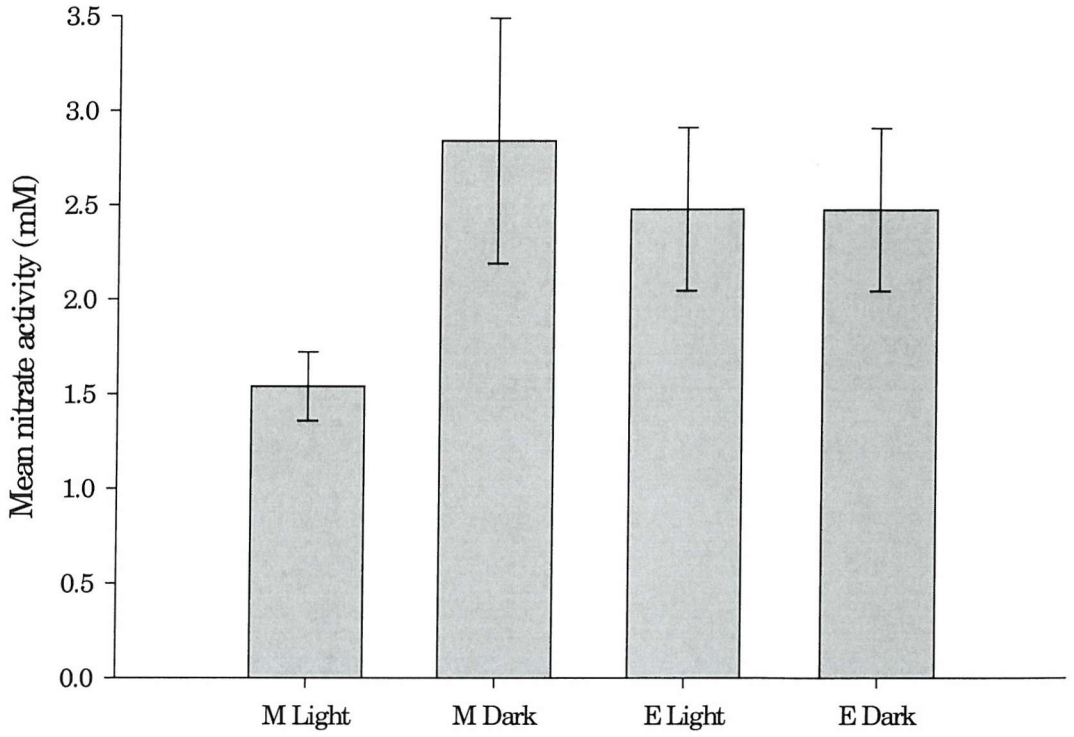

Figure 2.22 Mean cytosolic nitrate activity measurements of mesophyll (M) and epidermal (E) cells under light or dark treatments, n = 5 in each category, standard deviations shown.

2.4.2.3 Measurements in NR^- mutant mesophyll cells.

Figures 2.23 and 2.24 are examples of sections of nitrate-selective microelectrode measurements in the cytoplasm of an NR^- mutant mesophyll cell during dark-light and light-dark transitions.

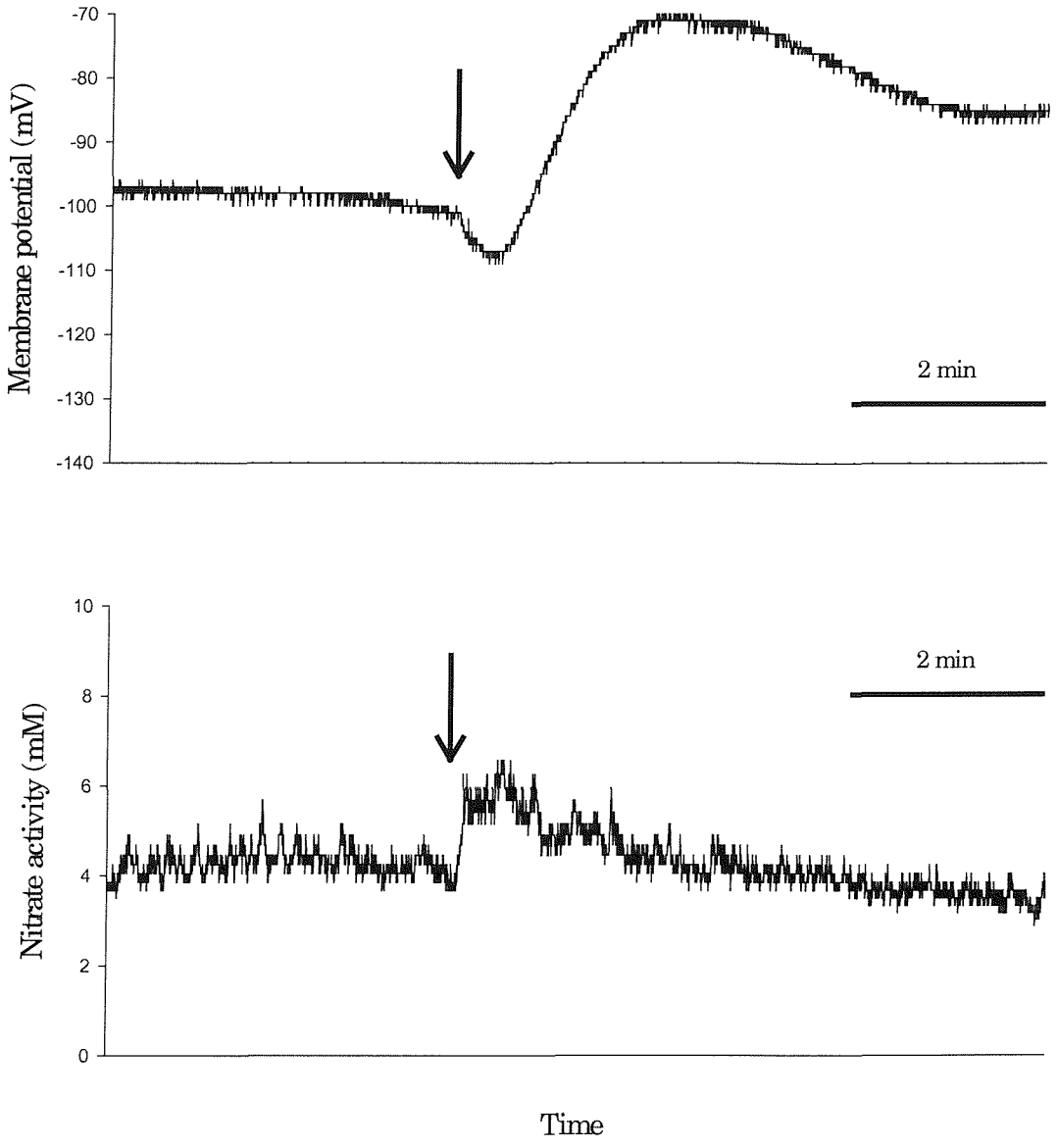

Figure 2.23 A typical example of a recording from a nitrate-selective microelectrode in the cytosol of an NR^- mutant mesophyll cell, arrow indicates the time at which the light to dark transition occurred.

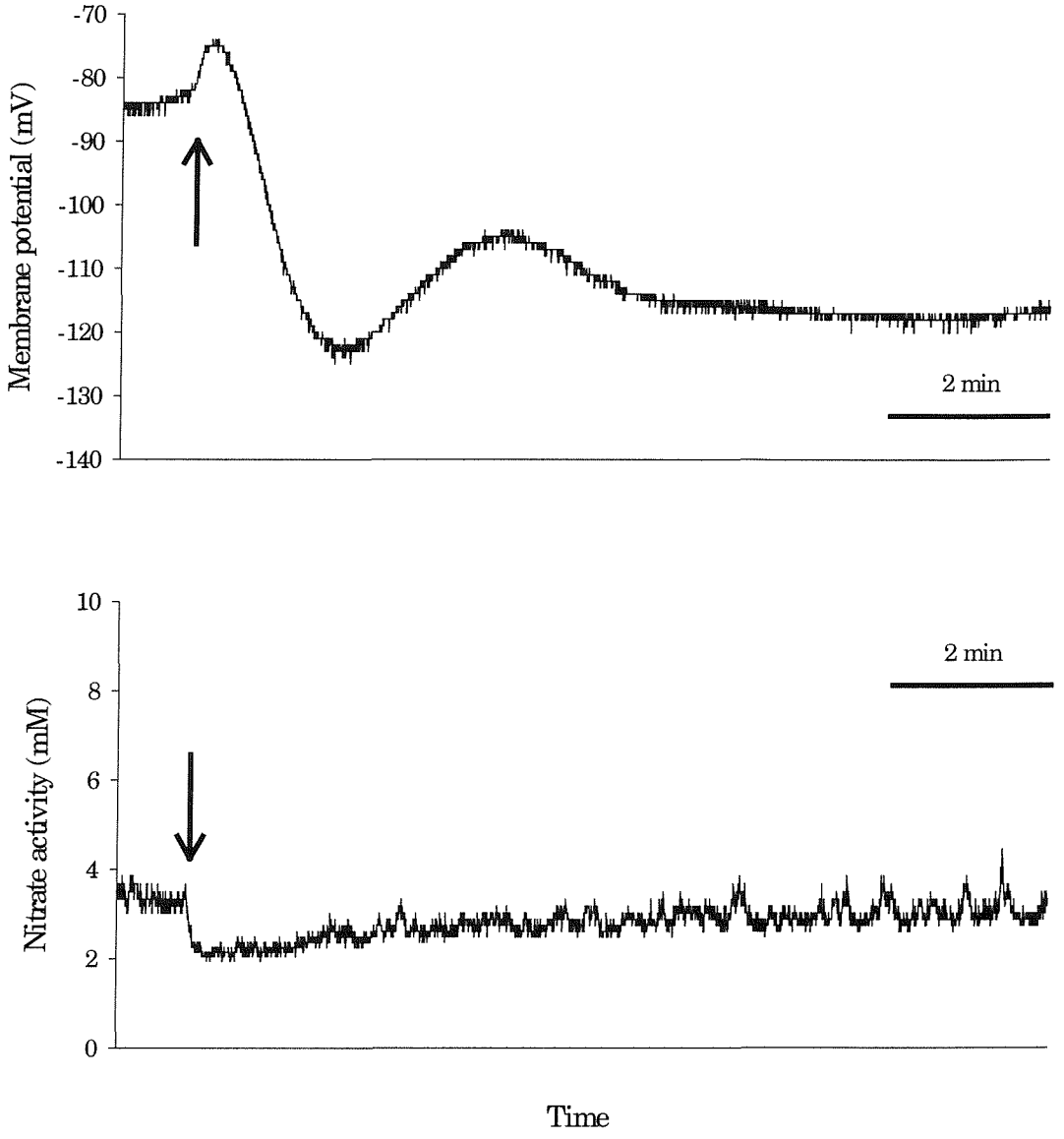

Figure 2.24 A typical example of a recording from a nitrate-selective microelectrode in the cytosol of an NR^- mutant mesophyll cell, arrow indicates the time at which the dark to light transition occurred.

Figures 2.23 and 2.24 show that cytosolic nitrate activity in the NR^- mutant mesophyll cells showed small, rapidly recovering changes in response to light-dark and dark-light transitions. The magnitude, pattern and duration of membrane potential perturbation in NR^- mutant mesophyll cells was similar to those of the wild type mesophyll cells (as shown in Figures 2.18 and 2.19).

The mean maximum magnitude of membrane potential responses to light off and light on in the mesophyll cells of wild type and NR^- mutants was not significantly different when tested at the 5 % level using a Mann-Whitney U-test (as shown in Figure 2.25). The mean duration of the perturbation in the membrane potential in response to illumination changes not significantly different (tested with a Mann-Whitney U-test at the 5 % level) between wild type and NR^- mutant mesophyll cells (as shown in Figure 2.26).

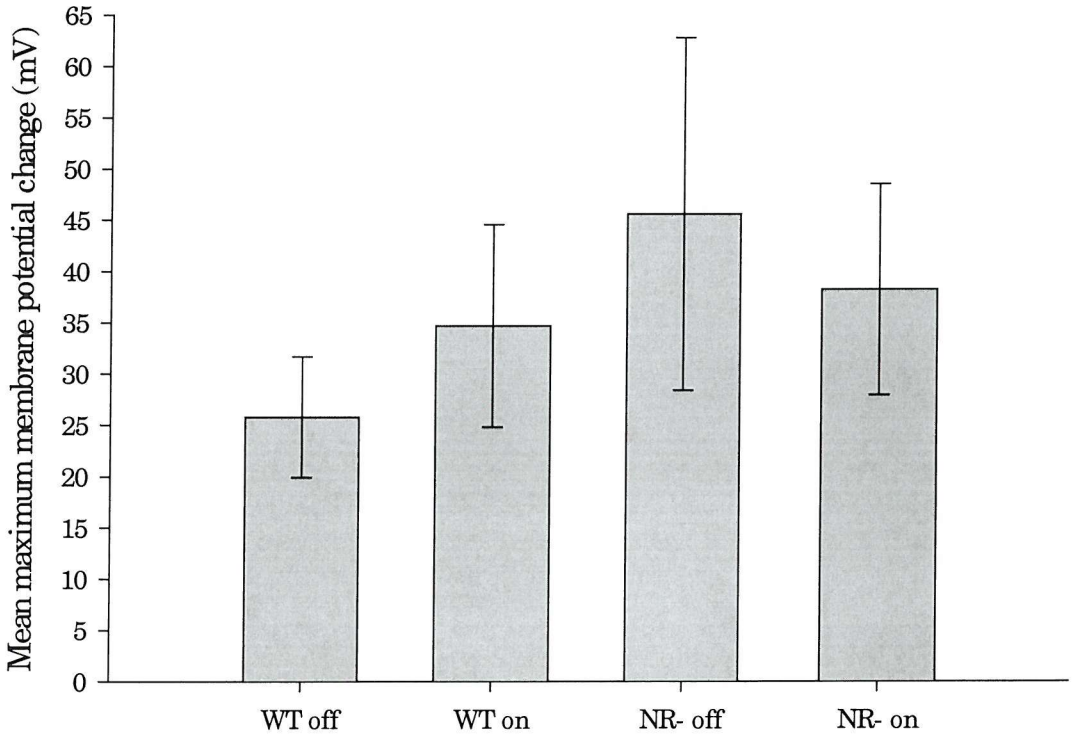

Figure 2.25 Mean maximum magnitude of perturbation of membrane potential in response to either light off or light on in wild type (WT) or NR^- mutant (NR^-) mesophyll cells, $n > 5$ in each category, standard deviations shown.

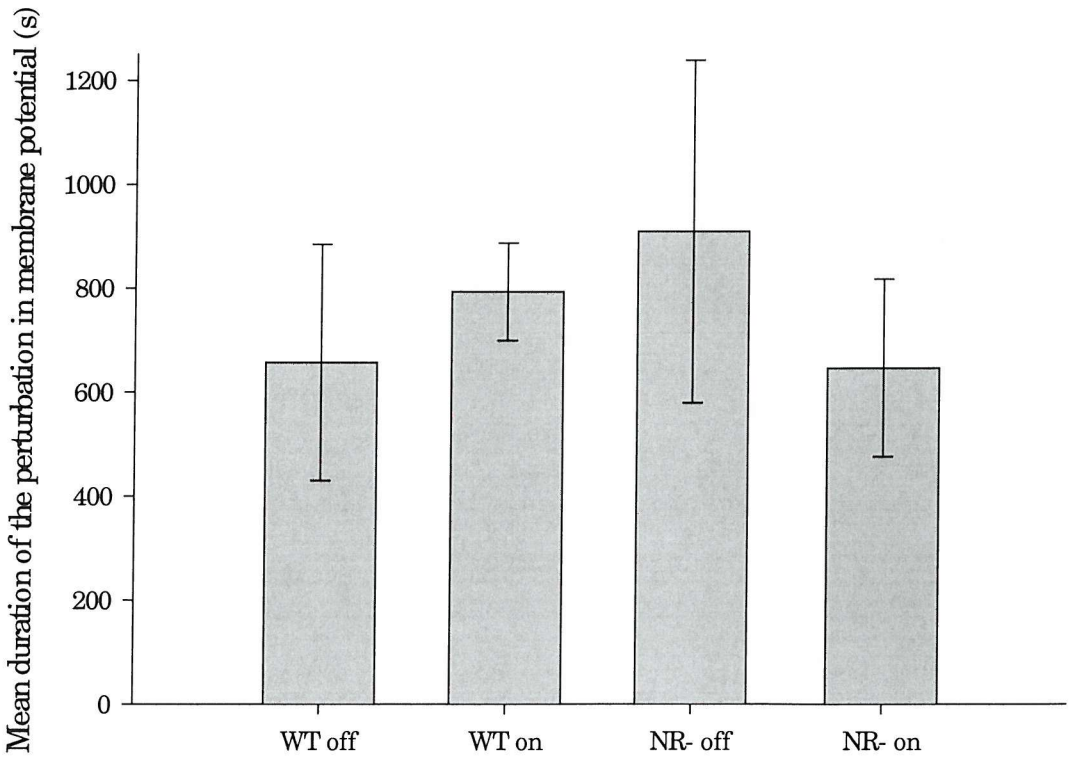

Figure 2.26 Mean duration of perturbation of the membrane potential in response to light off or light on in wild type (WT) and NR^- mutant (NR^-) mesophyll cells, $n > 5$ in each category, standard deviations shown.

Figure 2.27 shows the mean cytosolic nitrate activity in mesophyll cells of wild type and NR^- mutant plants under light and dark treatments. The mean cytosolic nitrate activity in the NR^- mutant mesophyll cells was not significantly different (tested using a Mann-Whitney U-test at the 5 % level) under the light and dark treatments. The mean cytosolic nitrate activity of the wild type mesophyll cells was significantly (tested using a Mann-Whitney U-test at the 5 % level) higher under the dark treatment compared with that of the light treatment. The cytosolic nitrate activity in the mesophyll cells of the NR^- mutant was higher than the wild type for both light and dark treatments, although there was no significant difference between the NR- mutant and dark wild type mesophyll cell mean cytosolic nitrate activities.

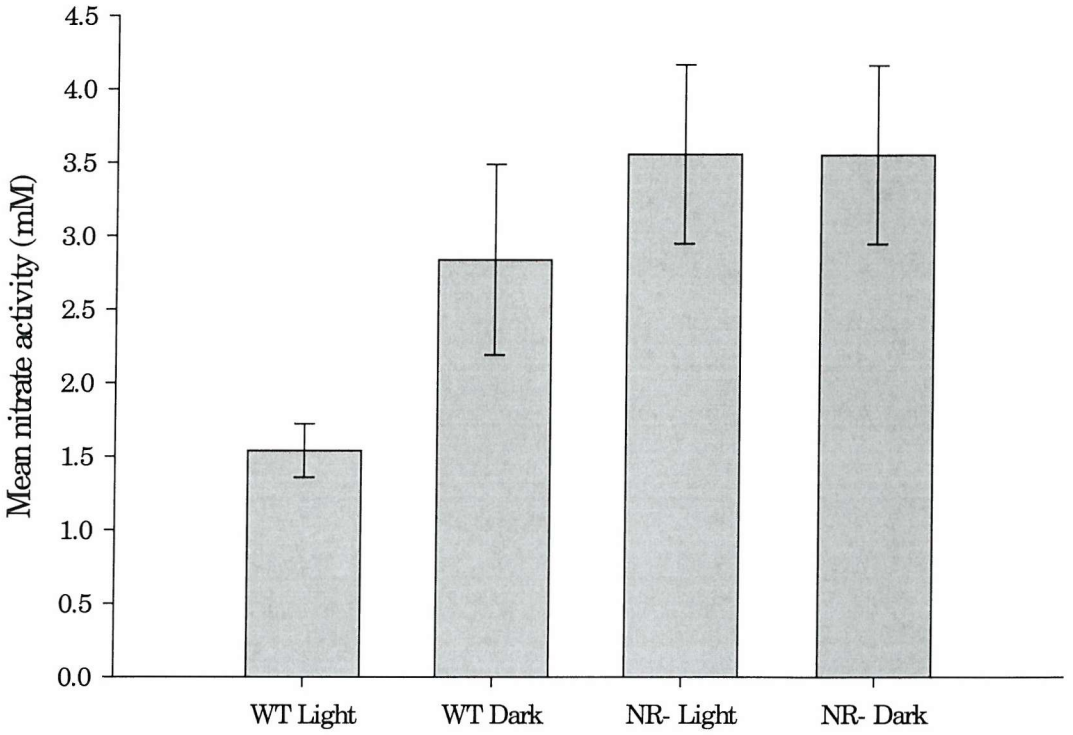

Figure 2.27 Mean cytosolic nitrate activity measurements of mesophyll cells under light or dark treatments in wild type (WT) and NR^- mutant (NR^-) plants, $n > 5$ in each category, standard deviations shown.

Table 2-4 summarises the means of the extent and duration of membrane potential change in response to light/dark transitions, and the steady-state nitrate activity in the light and dark of the dynamic nitrate-selective measurements in wild type and NR^- mutant leaf cells shown in Figures 2.13 to 2.27.

Table 2-4 Mean values of dynamic nitrate-selective microelectrode measurements in wild type and NR^- mutant epidermal and mesophyll cells during light/dark transitions.

a. Mean maximum magnitude of perturbation in membrane potential.

Plant type	*Cell type*	*Light treatment*	*Mean membrane potential change (mV)*	
Wild type	Epidermal	Light On	18.8	(10.12)
		Light Off	15.0	(2.52)
	Mesophyll	Light On	34.7	(9.36)
		Light Off	25.8	(5.88)
NR^- mutant	Mesophyll	Light On	38.3	(10.30)
		Light Off	45.6	(17.23)

b. Mean duration of perturbation in membrane potential.

Plant type	*Cell type*	*Light treatment*	*Mean duration of membrane potential change (s)*	
Wild type	Epidermal	Light On	495	(21.2)
		Light Off	428	(192.0)
	Mesophyll	Light On	793	(94.5)
		Light Off	658	(227.6)
NR^- mutant	Mesophyll	Light On	648	(171.4)
		Light Off	910	(330.2)

c. Mean cytosolic nitrate activity.

Plant type	*Cell type*	*Light treatment*	*Mean nitrate activity (mM)*	
Wild type	Epidermal	Light	2.48	(0.432)
		Dark	2.48	(0.432)
	Mesophyll	Light	1.54	(0.182)
		Dark	2.84	(0.650)
NR^- mutant	Mesophyll	Light	3.56	(0.612)
		Dark	3.56	(0.612)

Standard deviations shown in brackets, $n > 5$.

2.4.3 Summary of key results

1. Apoplastic nitrate activity is very low.
2. During the light treatment, cytosolic nitrate activity is higher in NR^- mutant mesophyll cells than in those of wild type plants.
3. In epidermal cells, vacuolar and cytosolic nitrate does not change in response to light/dark transitions.
4. In mesophyll cells, mean cytosolic nitrate activity increases upon dark treatment and decreases upon light treatment in wild type, but does not change in NR^- mutant plants.

2.5 Discussion

2.5.1 Steady-state nitrate-selective microelectrode measurements made in wild type and NR^- mutant Arabidopsis *leaf cells*

The ability to identify two clusters within nitrate-selective microelectrode measurements in root cells of barley and *Chara corallina* plants grown with sufficient nitrate has been reported previously (e.g. Miller and Zhen, 1991; Zhen *et al.,* 1991; Miller and Smith, 1992; van der Leij *et al.,* 1998). Generally the cytosolic cluster had lower nitrate activity and more negative membrane potentials, whereas the vacuolar cluster had higher nitrate activity and a less negative membrane potential. The previous reports have cited tonoplast potentials of approximately 10 to 35 mV (e.g. Miller *et al.*, 2001).

The results of nitrate-selective microelectrode measurements in wild type leaf cells presented here are similar to previous reports; the two clusters separated well and had similar properties to previously reported values. The cytosolic nitrate activity of epidermal cells was lower than that of mesophyll cells. This is consistent with the reported cytosolic nitrate activities of barley roots, lower in epidermal than cortical cells (Miller and Smith, 1992). The steady resting cytosolic nitrate activity during the light treatment in the NR^- mutants was statistically significantly higher than that of the wild type leaf cells. The reason for the higher cytosolic nitrate activity in the NR^- mutants may be due to culturing these plants on ammonium succinate, sucrose and/or the absence of NR. If so, either NR or application of ammonium succinate and/or

sucrose may have a role in maintaining cytosolic nitrate activity during the light treatment.

The apoplast of plants is a very difficult environment to study and knowledge of ion concentration in the apoplast is very limited (as discussed by Mühling and Sattelmacher (1995)). There are no previous reports of leaf apoplastic nitrate activity in *Arabidopsis* leaf tissue; nor are there previous reports of measurements using nitrate-selective microelectrodes in any species. The results presented here are novel.

In most of the previous reports of apoplastic nitrate concentration, estimates are made from apoplastic washing fluids (e.g. Mühling and Sattelmacher, 1995; Sattelmacher *et al.,* 1998; Solomon and Oliver, 2001). Solomon and Oliver (2001) reported apoplastic nitrate concentrations of approximately 4 mM in tomato leaves. Mühling and Sattelmacher (1995) reported apoplastic nitrate concentrations of 0.01 to 0.03 mM in the field bean, *Vicia faba,* grown for 6 weeks on 5 mM nitrate or ammonium as the sole nitrogen source. Sattelmacher *et al.* (1998) reported considerably higher apoplastic nitrate concentrations in *Vicia faba* (2.1 mM), *Zea mays* (1.8 mM) and *Helianthus annuus* (6.2 mM) grown on 5 mM nitrate for 5 weeks. The reason for these species-specific differences was attributed to the contribution of root NR activity to overall plant NR activity in the order *Helianthus annuus* < *Zea mays* < *Vicia faba*. The apoplastic nitrate activity in *Vicia faba* reported by these two papers is vastly different, although the plants were cultured in identical condition. It may be that these differences are attributable to the different age of the plants used in these studies (6 and 5 weeks). However, it is questionable whether apoplastic nitrate activity would change by two orders of magnitude in one week. It may be significant that a recent review by Sattelmacher (2001) does not refer to the results of Sattelmacher *et al.* (1998) but does make reference to the earlier paper, Mühling and Sattelmacher (1995), which reported low apoplastic nitrate.

Apoplastic nitrate activity has also been estimated at approximately 0.2 mM in nitrate-replete spruce roots by compartmental efflux analysis (Kronzucker *et al.*, 1995). Both apoplastic washing fluids and compartmental efflux analysis have the disadvantages of requiring an estimate of apoplastic volume, calculating whole-tissue average apoplastic nitrate activity and the activities measured may depend upon the apoplast extraction conditions (Lohaus *et al.*, 2001).

Nitrate activity in the apoplast of the *Arabidopsis* leaf tissue presented in this chapter was approximately 0.3 mM, which is similar to Mühling and Sattelmacher

(1995) and Kronzucker *et al.* (1995). Possible reasons for relatively low apoplastic nitrate activity are the high NR activity of *Arabidopsis* shoots and the fact that the apoplast is a compartment of high cation exchange capacity in which anions are excluded. Also, since nitrate is frequently the nutrient limiting plant growth, plant cell membranes contain many transporters to take up nitrate (Forde, 2000) and probably remove nitrate from the apoplast very effectively. Apoplastic nitrate activity was not significantly different for the NR^- mutant and wild type leaves, possibly suggesting that NR does not have a role in maintaining apoplastic nitrate activity under these conditions.

The possible effects on the leaf cells of the electrical contact bath solution in which the leaf edge was placed were a cause of concern. However, the solution contained a concentration of 4.25 mM nitrate and as apoplastic nitrate activity was measured at 0.3 mM it is unlikely that the solution affected the results.

2.5.2 *Dynamic nitrate-selective microelectrode measurements made in* Arabidopsis *leaves during light-dark and dark-light transitions*

The membrane potential responses presented here were similar to previous reports of membrane potential changes in response to light-dark and dark-light transitions in *Arabidopsis* and other species in terms of shape, magnitude and duration of response (e.g. Fujii *et al.,* 1978; Prins *et al.,* 1980; Tazawa *et al.,* 1986; Marrè *et al.,* 1989; Spalding *et al.,* 1992; Hansten *et al.,* 1993; Blom-Zandstra *et al.,* 1995; 1997; Johannes *et al.*, 1997, Shabala and Newman, 1999). The membrane potential response to light-dark transitions in mesophyll cells was different from the response of epidermal cells. This is also similar to previous work with other plant species, for example Elzenga *et al.* (1995), although the results presented here are the first for *Arabidopsis*.

Differences in the ion fluxes across the plasma membrane in response to illumination transitions between mesophyll and epidermal cells have been previously reported. Shabala and Newman (1999) found considerable fluxes of H^+ and Ca^{2+} from mesophyll cells but negligible fluxes from attached epidermal cells of field bean. Elzenga *et al.* (1995) discovered that isolated mesophyll and epidermal cells of *Pisum sativum* give different light-induced membrane potential responses. In mesophyll cells these changes were dependent on photosynthesis and external Cl^-, whereas in

epidermal cells the changes were not dependent on photosynthesis but involved H^+ and Ca^{2+} ion fluxes.

Epidermal cells of *Arabidopsis* leaves do not contain chlorophyll-containing plastids (see Figure 3.13). This could suggest that the light-induced membrane potential responses in the epidermal cells reported here are mediated by a photoreceptor rather than by some aspects of the process of photosynthesis. It is widely accepted that chlorophyll deficient tissues, like those of *Arabidopsis* leaf epidermal cells, exhibit electrical changes in response to light transitions. For example, Stahlberg *et al.* (2000) studied the effects of light transitions on isolated white and green mesophyll cells of variegated leaves. The white and green mesophyll cells responded differently to light transitions. The white cells showed a response dependent upon the H^+-ATPase pump, whereas the green cells produced a biphasic response initially dependent upon photosynthesis and not the H^+-ATPase pump, and subsequently not dependent upon photosynthesis but on the H^+-ATPase pump.

Elzenga *et al.* (1995) studied the light-induced membrane potential responses of epidermal cells attached to mesophyll cells and found that under these conditions the epidermal cell membrane potential response reflected the membrane potential responses of the underlying cells. Given the similarity in the shape of the membrane potential responses of the epidermal and mesophyll cells in the current study, some component of the membrane potential change in epidermal cells could reflect that of the underlying mesophyll cells.

Vacuolar nitrate activity in wild type epidermal cells did not change in response to light transitions; this is not surprising as the vacuole represents a large store of nitrate so would be unlikely to change quickly under different environmental conditions.

Cytosolic nitrate activity in wild type epidermal cells showed small transient changes during light transitions. The response may be genuine or an artifact due to the different response times of the nitrate-selective and the membrane potential recording barrels of the microelectrode. The small or non-existent nitrate activity response to changing illumination conditions in epidermal cells may be due to the absence of chlorophyll-containing plastids in this cell type. The illumination change signals within such cells are likely to be small and any changes in cytosolic nitrate below the detection capabilities of nitrate-selective microelectrodes.

The calculated tonoplast potential showed a multiphasic depolarisation in response to light to dark transition indicating that there was a transient (6 min) flux of ion(s) across this membrane as well as the plasma membrane. The depolarisation of the tonoplast is presumably not due to a flux of protons because it is not accompanied by a cytosolic pH change in this cell type (see Chapter 3, Figure 3.2). (Tonoplast potential responses were not calculated for mesophyll cells because vacuolar measurements during light-dark transitions were not made.)

Cytosolic nitrate activity in wild type mesophyll cells showed large changes maintained for at least 20 min in response to light transitions. The duration of the changes in cytosolic nitrate activity negate the possibility that the different response times of the nitrate-selective and reference barrels produce artifacts in these recordings. In the examples shown the cytosolic nitrate activity in mesophyll cells was maintained at approximately 1.5 and 2.0 mM during the light and dark treatment respectively. The onset of darkness also triggered a transient increase in nitrate activity from 2 to 3.5 mM, which peaked after 7 min of darkness and then returned to the steady-state level. The different steady-state nitrate activities during the light and dark treatments and the transient increase in nitrate activity caused by the onset of darkness may be examples of cytosolic signalling events in association with illumination transitions. Mesophyll cells are more likely to have detectable nitrate signalling events associated with changing NR activity under different light transitions because these cells are very photosynthetically active with a large number of chlorophyll-containing plastids (see Figure 3.13). Furthermore, mesophyll cells of *Arabidopsis* leaves probably contain considerable amounts of NR. Vaughn and Campbell (1988) showed that the cytoplasm of mesophyll cells was the exclusive location of NR within maize leaves.

The membrane potential changes in response to illumination transitions for the wild type and NR^- mutant mesophyll cells were similar in terms of magnitude, direction and duration of response. This is important as it suggests that although the NR enzyme has been inactivated the plant cell responds normally to light transitions in terms of membrane potential changes and confirms that the same process is being repeated in the mesophyll cells in both types of plant.

The absence of detectable nitrate activity change in the wild type epidermal cells strongly suggested that further investigation into the responses of the NR^-

mutants would not be of value. For this reason, measurements on these cells were not made.

Cytosolic nitrate activity in NR^- mutant mesophyll cells showed small transient (2 min) responses to light transitions. This response may be genuine or an artifact due to the different response times of the nitrate-selective and the membrane potential recording barrels of the microelectrode. The membrane potential of a mesophyll cell changes rapidly and considerably in response to illumination changes, and so the differing response times of the microelectrode barrels could have a considerable effect during the first few minutes of the light transition. After the apparent transient change the nitrate activity returned to the pre-treatment level, a response different from that of the wild type mesophyll cell.

2.5.3 Conclusion

As described in Section 1.9.3, the only previous dynamic microelectrode measurements investigating changes in cytosolic nitrate activity did not demonstrate cytosolic nitrate activity changes in barley epidermal cells (van der Leij *et al.*, 1998). In the current study cytosolic nitrate activity changes were also not detected in epidermal cells of *Arabidopsis* leaves.

The major finding of this work is that the mean cytosolic nitrate activity changed in response to illumination transitions in wild type and not significantly in NR^- mutant mesophyll cells. The absence of cytosolic nitrate activity change following illumination transitions in the NR^- mutants suggests a role for NR activity in this response. The direction and rate of the change also support this suggestion. Cytosolic nitrate activity is higher in the dark when NR is inactive than the light when NR is actively reducing nitrate. The rate of NR activity change in response to illumination transitions is rapid, with a half-life of 2 to 15 min in spinach (Huber *et al.*, 1992; Kaiser *et al.*, 1992; Riens and Heldt, 1992). The duration of cytosolic nitrate activity responses to illumination transitions shown here also ranges from 2 to 15 min, which is consistent with the timescale for NR activity changes. Huber *et al.* (1992) showed that the rate of NR activation change in response to dark-light transitions was faster than that of light-dark transitions. In this study the establishment of steady-state cytosolic nitrate activity in mesophyll cells of wild type was faster in response to dark-light than light-dark transitions, which is in agreement

with the results of Huber *et al.* (1992) in spinach. Furthermore, supporting evidence for the role of NR in regulating cytosolic nitrate activity is provided by the higher mean cytosolic nitrate activity under the light treatment in NR^- mutant leaf cells compared with those of the wild type containing active NR. Mean cytosolic nitrate activity in NR^- mutant leaf cells under the light treatment was not significantly different to that of the wild type under the dark treatment when NR was inactive. This suggests that active NR is essential to lowering cytosolic nitrate activity in wild type leaf cells in the light treatment.

Well-known cytosolic signalling ions, such as free calcium and protons, have certain characteristics in common; they are maintained within the cytosol and then change consistently in response to particular environmental stimuli. The apparent maintenance of cytosolic nitrate activity during periods of nitrate starvation and re-supply (Zhen *et al.*, 1991; van der Leij *et al.*, 1998) suggests that nitrate fulfils this criterion for a cytosolic signal ion. The current study has shown that light/dark transitions trigger repeatable changes in cytosolic nitrate activity in wild type mesophyll cells further suggesting that cytosolic nitrate is a signal.

The next question is how may this fit into a signalling cascade. Light transitions in photosynthetically active tissue have long been known to affect free calcium and pH (Pallaghy and Lüttge, 1970; Miller and Sanders, 1987). Calcium ion activity and pH may be involved with an illumination transition signal cascade to regulate NR activity in leaf cells; NR activity is affected by changes in pH and at least one calcium-dependent NR kinase has been identified. The NR-dependent cytosolic nitrate activity changes reported here might be the next step in the signalling cascade. The next question to address is what might these nitrate activity signals originating from NR regulate? Champigny and Foyer (1992) have provided a possible answer. Champigny and Foyer (1992) suggested the role of nitrate as a signal metabolite associated with carbon partitioning between carbohydrates (principally sucrose) and amino acid biosynthesis. They proposed the light activation by nitrate of protein kinase(s) that either activated or inactivated the enzymes that regulate carbon partitioning. Their hypothesis was based upon the diversion of photosynthetic carbon away from carbohydrate synthesis toward organic acid and amino acid synthesis in leaves fed with nitrate. Van Quy *et al.* (1991) demonstrated the requirement of NR in signalling the application of nitrate to regulate carbon partitioning in leaves. In this work, nitrate starved leaves were removed from plants and nitrate fed through the

transpiration stream to illuminated leaves. Sucrose synthesis showed an inverse relationship to nitrate application, uptake and assimilation. This alternation in sucrose synthesis was not seen in leaves that absorbed nitrate but were pre-treated with tungstate, which inactivates NR. The conclusions of this chapter are in agreement with the hypothesis presented in Champigny and Foyer (1992) and are supported by the results reported by van Quy *et al.* (1991).

3 CYTOSOLIC PH CHANGES ASSOCIATED WITH MODIFICATIONS OF NITRATE REDUCTASE ACTIVITY

3.1 Aim

As described in Chapter 1, cytosolic pH change has been implicated in the regulation of NR activity. The aim of the work described here was to investigate possible interactions between NR activity and cytosolic pH. This was studied by measuring cytosolic pH under environmental conditions in which NR and cytosolic nitrate activity are known to change in *Arabidopsis* wild type and NR^- mutants leaf cells.

3.2 Introduction

It is well established that pH affects the activity of NR since NR is activated by acidic pH (Kaiser and Brendle-Behrisch, 1995). Nitrate reduction consumes protons and produces hydroxide ions and it is thought that this process may have a role in altering cytosolic pH. This work aims to identify the role of NR activity modifications in the maintenance of cytosolic pH homeostasis after the application of cytosolic pH perturbing treatments. NR activity and cytosolic pH are known to change in response to light/dark transitions in wild type photosynthetic cells. Experiments are described which were designed to determine whether light/dark transition-induced cytosolic pH changes in wild type also persist in NR^- mutant *Arabidopsis* leaf cells. The following sections of this introduction describe the distribution, maintenance and signalling role of protons within plant cells.

3.2.1 The pH of plant cell compartments

It is well established that there are large trans-membrane pH differences across the plasma membrane and tonoplast (Kurkdjian and Guern, 1989). The approximate pH of the apoplast is 5.5, the cytosol is 7.2 and the vacuole is 5.0 (Kurkdjian and Guern,

1989; Zimmermann *et al.*, 1999; Yu *et al.*, 2000). Cytosolic pH is maintained at relatively constant values despite the existence of pH-perturbing processes whereas the vacuole generally has a variable pH from 4.0 to 6.5 (Kurkdjian and Guern, 1989; Zimmermann *et al.*, 1999).

3.2.2 Cytosolic pH maintenance

Cytosolic pH is maintained (Felle, 1988). The maintenance of pH may be established by three mechanisms. Firstly, the cytosol does have some degree of buffering capacity (Roos and Boron, 1981) but this is relatively low compared with the extent of pH change (Kurkdjian and Guern, 1989). The second mechanism is the transport of protons from the cytosol to the external medium or vacuole. It is not clear how this is done, but it is assumed that the plasma membrane H^+-ATPase has a considerable role in maintaining cytosolic pH (Morsomme and Boutry, 2000). Cytosolic pH is maintained at about 7.5. The optimum pH of this H^+-ATPase is slightly below 7.0 so there is scope for cytosolic acidification activating this H^+-ATPase, excluding protons and restoring cytosolic pH (Morsomme and Boutry, 2000). It has also been proposed that H^+/Na^+ and H^+/K^+ antiporters are involved in counteracting cytoplasmic acidification and that anion exchangers transporting bicarbonate are involved in cytoplasmic pH modification (Kurkdjian and Guern, 1989). Thirdly, in leaves the production and consumption of organic acids is believed to have a role in maintaining cytosolic pH (Kurkdjian and Guern, 1989).

3.2.3 Cytosolic pH change

There are a number of processes capable of perturbing cytosolic pH associated with metabolism, the transport of solutes, or the effect of various environmental conditions. Some of these pH-perturbing processes may be associated with nitrate utilisation; nitrate assimilation causes cytosolic alkalisation and nitrate is transported into cells with two protons. Cytosolic pH is affected by the uptake of NO_3^- causing a transient alkalinisation contrary to the predicted acidification associated with the uptake of protons (Ullrich and Novacky, 1990). Presumably this effect is caused by rapid nitrate reduction rates.

Cytosolic pH is well known to change in response to changing environmental conditions (Kurkdjian and Guern, 1989). Cytosolic pH is known to decrease in response to anaerobiosis (by 0.4 to 0.8 pH units) and increased carbon dioxide or other acidic gases (e.g. NO_2 and SO_2). Cytosolic pH has long been known to decrease (by 0.2 to 0.6 pH units) in response to transition from light to dark in photosynthetic cells (Pallaghy and Lüttge, 1970). This is believed to be most likely due to the transport of protons from the stroma to the cytoplasm. When 'light' treatment is applied to photosynthetic cells, the photosynthetic electron transfer reactions begin immediately and protons are taken up into the interior of the thylakoids. The chloroplast stroma becomes more alkaline and the cytoplasm could lose protons to the stroma. There are also light-induced changes in carbon dioxide consumption and other metabolic effects may have a role in modifying cytosolic pH. Cytosolic pH decreases in response to increasing temperature. Generally, vacuolar pH is not modified by these changing environmental conditions but is more sensitive than the cytosol to external pH change from pH 4.0 to 9.0.

3.2.4 Vacuolar pH

Ion exchanges across the tonoplast have the ability to influence not only the pH of the vacuole but also that of the cytosol. The tonoplast contains several transporters capable of modifying the pH of the surrounding compartment: vacuolar H^+-ATPase (V-ATPase)(Ratajczak, 2000), H^+-pyrophosphatase (Maeshima, 2000), Na^+/H^+ antiporter (Blumwald *et al.*, 2000) and other systems that exchange H^+ or H^+ equivalents. Contrary to the requirement of pH homeostasis in the cytosol, plants can sustain large variations in their vacuolar pH (Kurkdjian and Guern, 1989).

3.2.5 Cytosolic pH signalling

Changes in pH are well known to have a role in plant cells regulating key enzymes (including NR, described in Section 3.2.6 below) and metabolic steps (Kurkdjian and Guern, 1989; Roos *et al.*, 2000). Change in cytosolic pH has been implicated in the regulation of diverse processes in plants, including gravitropic responses (Scott and Allen, 1999), plant defence responses (Guern *et al.*, 1992), nodulation (Felle *et al.*, 1996) and responses to hormones (Swanson and Jones, 1996; Beffagna *et al.*, 1997).

3.2.6 Cytosolic pH changes associated with NR activity

Kaiser and Brendle-Behrisch (1995) studied the acid-base modulation of NR activity in spinach leaf tissues. They found that in the dark, when NR was usually inactivated, addition of acid activated NR and inhibitors of protein phosphatases prevented this response. They suggested that this acid induced activation was mediated by protein de-phosphorylation. In the light, when NR was usually active, an alkaline pH (9.0) had no effect on the activation of NR. Also, addition of ammonium ions caused an increase in pH and a subsequent decrease in NR activity. Kaiser and Brendle-Behrisch (1995) suggested that this was a possible example of cytoplasmic pH change acting as a signal to modulate the activity of NR. They also suggested a role for NR in the regulation of cytoplasmic pH because the reduction of nitrate to ammonium ions (involving NR) consumes protons and produces hydroxide ions, potentially facilitating acid induced activation of NR to restore cytosolic pH homeostasis.

3.2.7 Methods to measure cellular pH

There are numerous methods to measure cytosolic pH, such as pH-selective microelectrodes, microscopy using fluorescent pH indicator dyes, NMR spectroscopy and single cell sampling to study the vacuole (described in Section 1.7; reviewed by Kurkdjian and Guern, 1989). In the current study two methods were used. The first used pH-selective microelectrodes and the second used confocal microscopy and pH indicator dyes. In the following sections these two approaches are described separately.

3.3 pH-selective microelectrodes

3.3.1 Introduction

Various types of pH-selective microelectrodes have been developed and are widely used. These were originally made from H^+-selective glass and subsequently made from H^+-selective liquid resins (Ammann, 1986). To overcome the problem of plant

cell turgor Felle and Bertl (1986) added a PVC plug beneath the liquid resins. Double-barrelled microelectrodes were then developed to ensure that the tip of each barrel was in the same compartment (Felle, 1987). pH-selective microelectrodes have proven to be very useful in the study of cytosolic and vacuolar pH, particularly because of their fast response time. This means that they can resolve fast and transient pH changes *in vivo* (Felle, 1993; Miller and Smith, 1996; Miller *et al.*, 2001), although as described in the previous chapter (Section 2.5.2.6) ion-selective microelectrodes can produce artifacts due to the different response times of the reference and ion-selective barrels. The pH cocktail used in this study was based on a commercial formulation ("Hydrogen Ionophore II – Cocktail A", 95927, Fluka Chemicals, Gillingham, UK). This cocktail contains the ionophore ETH1907 (4-nonadecylpyridine) as the sensor, 2-nitrophenyl octyl ether as a plasticiser, and potassium tetrakis(4-chlorophenyl) borate as an additive (Chao *et al.*, 1988). To this cocktail was added PVC and nitrocellulose as matrix materials (Miller and Smith, 1992).

3.3.2 Methods

3.3.2.1 Culturing plant material

Plants were cultured under the same conditions as those described in Section 2.3.1.

3.3.2.2 Manufacture of pH-selective double-barrelled microelectrodes

The initial steps of ion-selective microelectrodes manufacture, pulling and silanizing, were the same as those used in the manufacture of nitrate-selective microelectrodes (described in the previous chapter, Sections 2.3.3.1 and 2.3.3.2). The back-filling step (Section 2.3.3.3) was also the same except that the sensor membrane was as outlined in Table 3-1. The components of the membrane were dissolved in THF (0.15 μg of cocktail μl^{-1} THF) to produce a cocktail to allow solvent-casting (described in Section 2.3.3.3).

Table 3-1 The components of a pH-selective microelectrode sensor membrane (Miller and Smith, 1992).

Component	*% (w/w)*
PVC	28
Hydrogen ionophore II cocktail A.	61.5
Nitrocellulose	10.5

3.3.2.3 Using pH-selective microelectrodes

The pH-selective microelectrodes were used as described in Section 2.3.4 except that these microelectrodes were backfilled with a different electrolyte solution, calibration solution pH 4.0 (Table 3-2).

The calibration of pH-selective microelectrodes was as described in Section 2.3.4.2 except different calibration solutions were used (shown in Table 3-2). The pH-selective barrel was calibrated using a series of solutions that span the physiological range. The pH of each solution was adjusted to the correct value measured by a digital pH-meter (Model 3310 pH meter, Jenway Ltd., Dunmow, England).

Table 3-2 Composition of solutions to calibrate a pH-selective microelectrode for intracellular measurements.

pH calibration solution	*KCl (mM)*	*$NaH_2PO_4.2H_2O$ (mM)*	*20 mM buffer*
4	120	10	KHP
6	120	10	MES
7	120	10	MOPS
8.5	120	10	TAPS

(pH was adjusted with 1 M NaOH or HCl. All buffers were purchased from Sigma-Aldrich Company Ltd., Poole, UK: KHP, potassium hydrogen phthalate; MES, 2-[N-morpholino]ethanesulfonic acid; MOPS, 3-[N-morpholino]propanesulfonic acid; TAPS, N-tris[hydroxymethyl]methyl-3-amino propanesulfonic acid. Calibration solutions from Walker *et al.* (1995) adapted from Reid and Smith (1988))

Measurements were made as described in Section 2.3.4.3 and the illumination treatments were as described in Section 2.3.4.4.

3.3.3 Results

pH-selective microelectrode measurements made in the cells of intact, aerial *Arabidopsis* leaves proved to be extremely technically demanding. The results presented here represent the outcome of the manufacture and testing of over 60 pH-selective microelectrodes. Measurements of mesophyll cells were particularly difficult; the microelectrode results below refer exclusively to epidermal cells of wild type plants.

3.3.3.1 Steady-state pH-selective microelectrode measurements made in wild type epidermal cells

Figure 3.1 shows mean pH values of the apoplast, cytosol and vacuole of wild type epidermal leaf cells under the 'light' treatment. The mean pH values of the apoplast and vacuole were acidic, 5.4 and 5.8 respectively, whereas the mean pH value of the cytosol was more alkaline (pH 7.6).

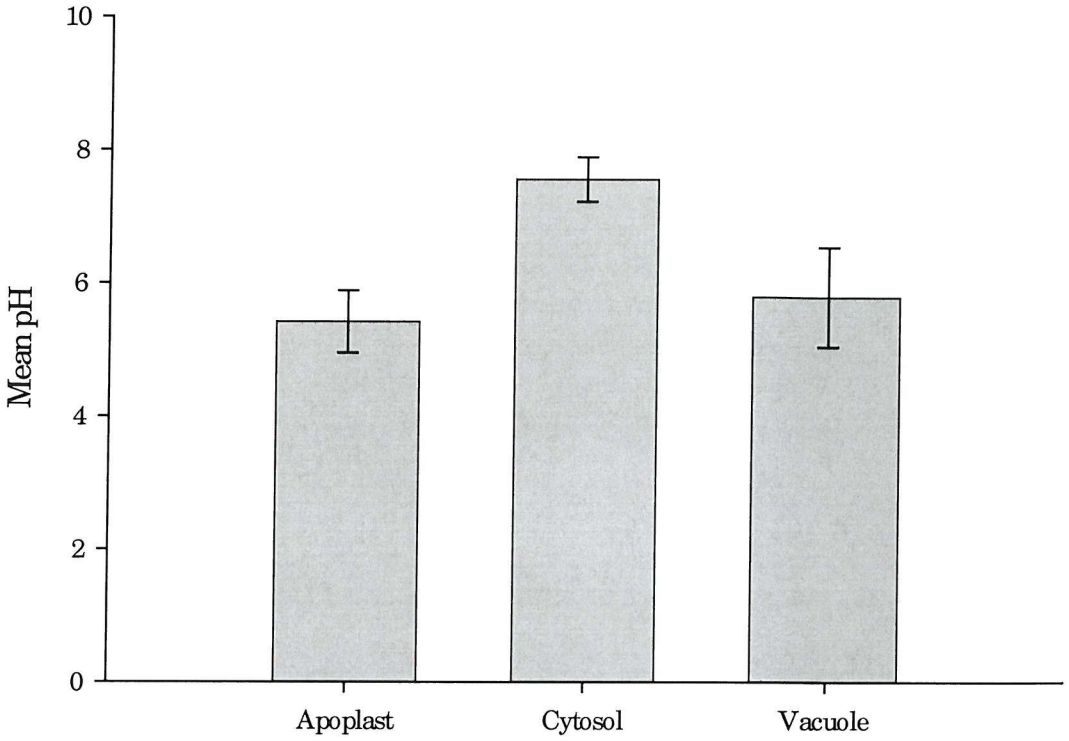

Figure 3.1 Means of pH-selective microelectrode measurements made in the apoplast, cytosol and vacuole of wild type epidermal cells, standard deviations shown (n > 5).

3.3.3.2 Dynamic pH-selective microelectrode measurements in wild type epidermal cells during light-dark and dark-light transitions.

Dynamic pH-selective microelectrode measurements were made under the same conditions as the nitrate-selective microelectrode measurements described in the previous chapter. Figures 3.2 to 3.5 are typical examples of sections of pH-selective microelectrode measurements during light/dark transitions. The upper trace of each figure shows the cell membrane potential and the lower trace shows the pH of the cell compartment.

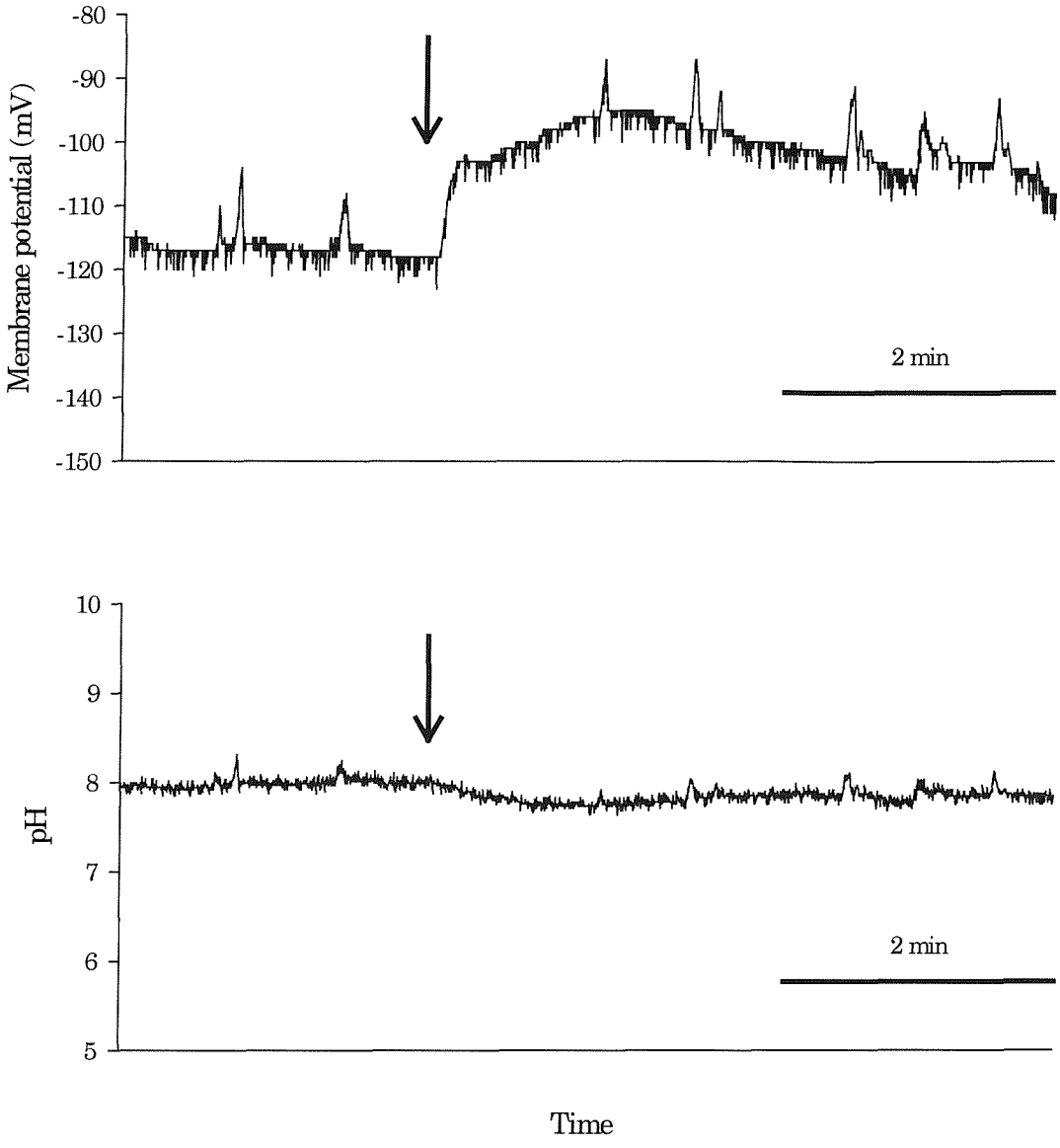

Figure 3.2 A typical example of a recording from a pH-selective microelectrode in the cytosol of an epidermal cell of a wild type plant, arrow indicates the time at which the light to dark transition occurred.

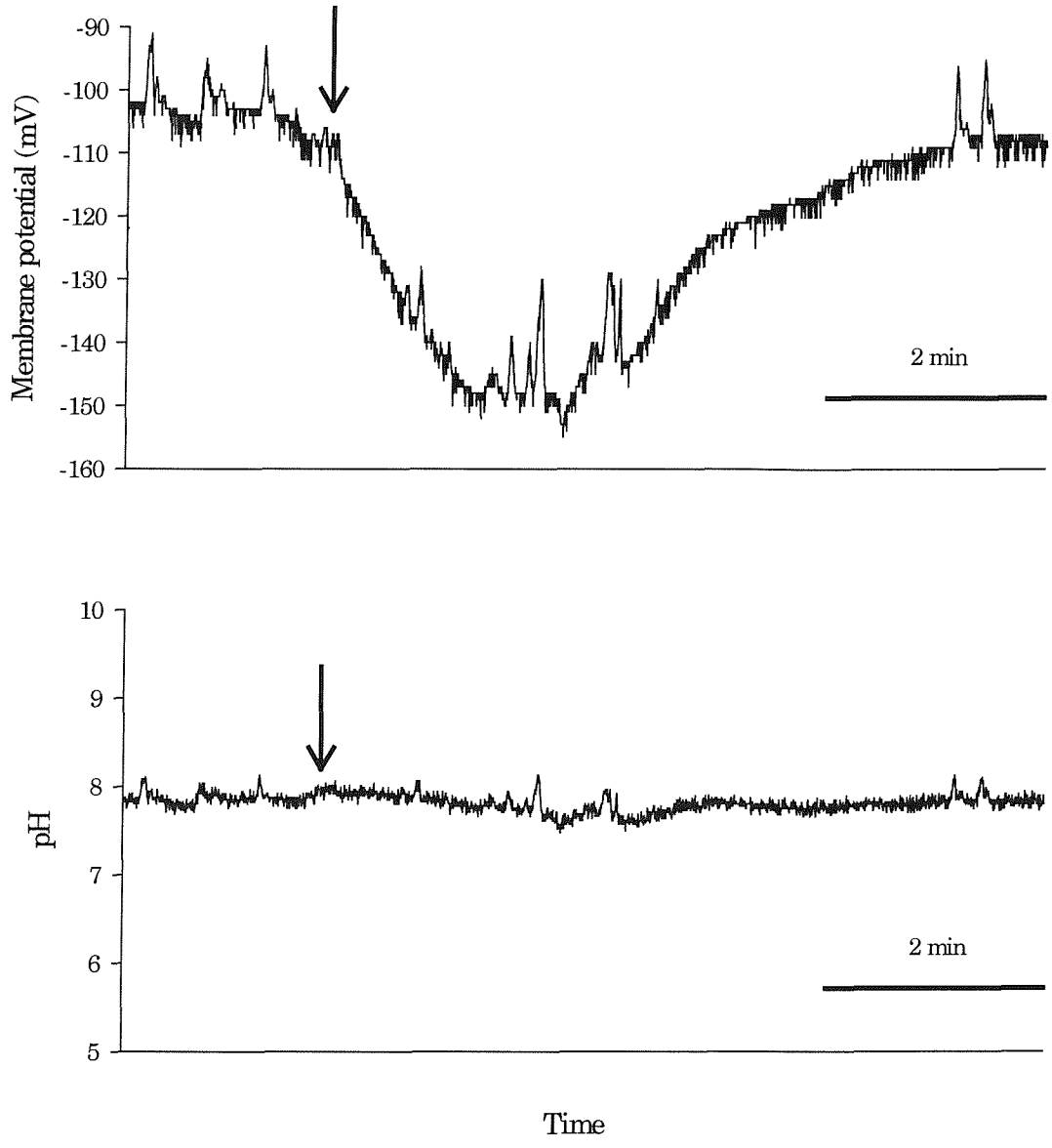

Figure 3.3 A typical example of a recording from a pH-selective microelectrode in the cytosol of an epidermal cell of a wild type plant, arrow indicates the time at which the dark to light transition occurred.

Figures 3.2 and 3.3 are examples of pH-selective microelectrode measurements in the cytosol of an epidermal cell during light/dark transitions. These figures show that there was little or no cytosolic pH change in response to light/dark transitions.

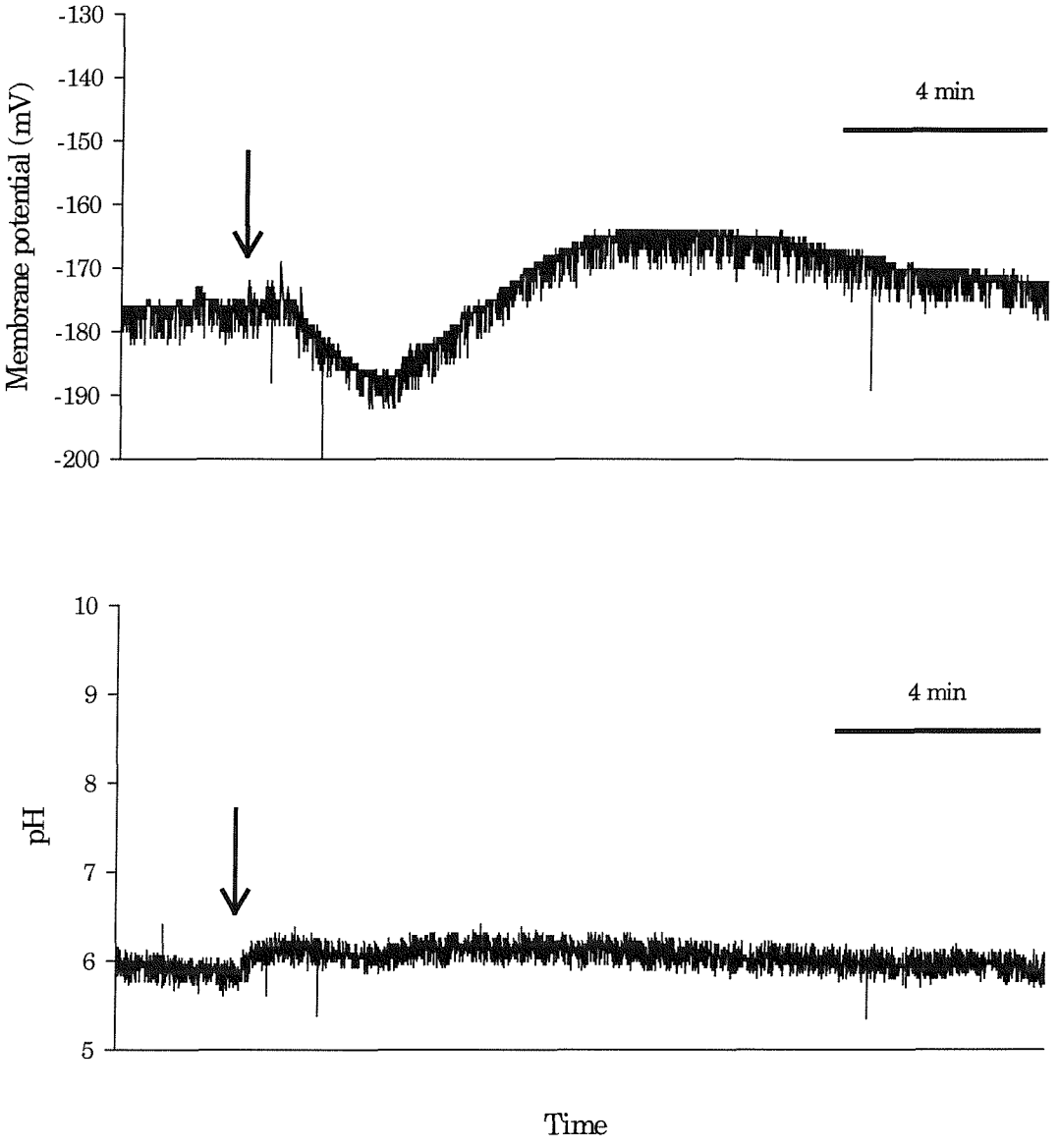

Figure 3.4 A typical example of a recording from a pH-selective microelectrode in the vacuole of an epidermal cell of a wild type plant, arrow indicates the time at which the light to dark transition occurred.

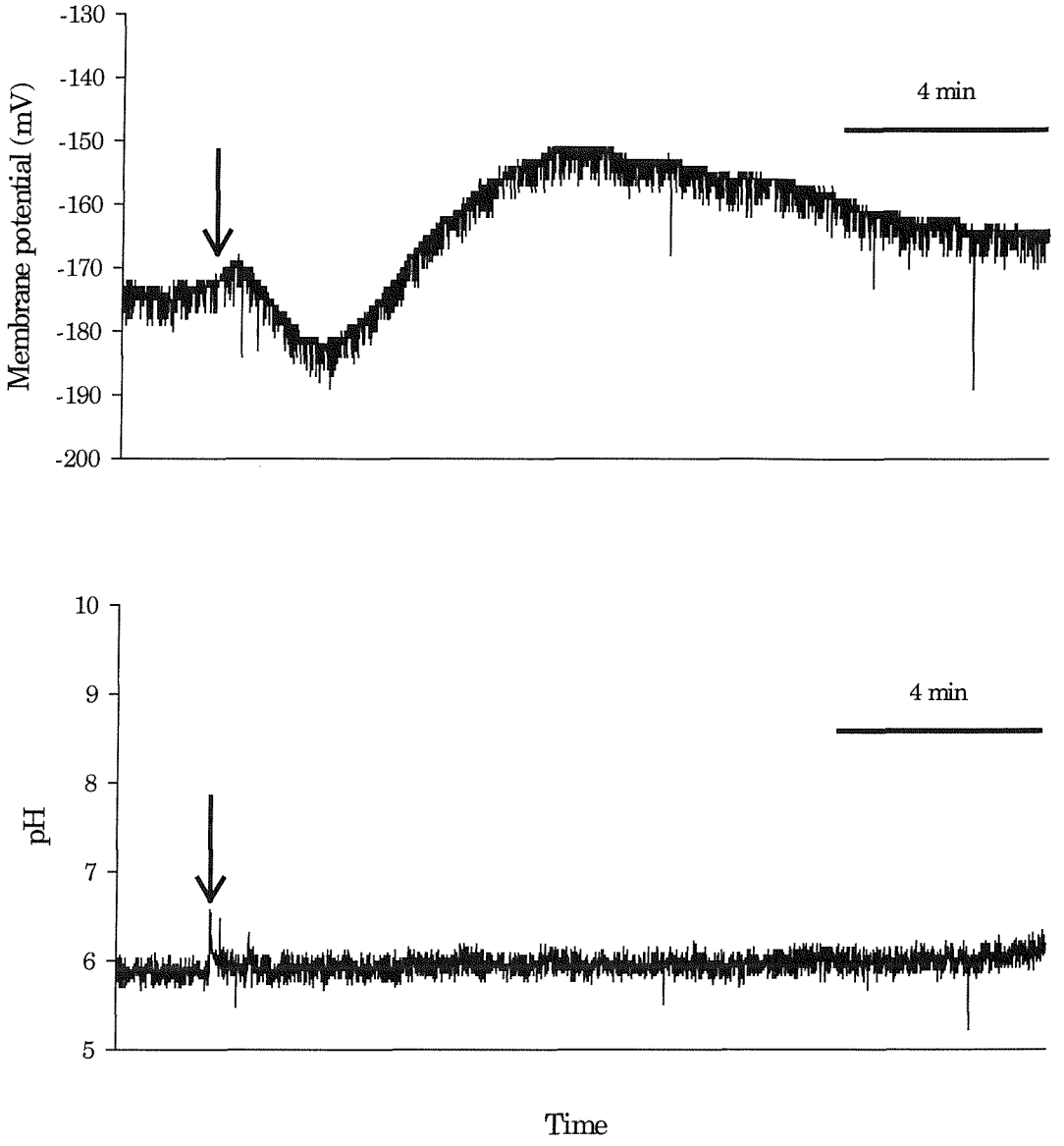

Figure 3.5 A typical example of a recording from a pH-selective microelectrode in the vacuole of an epidermal cell of a wild type plant, arrow indicates the time at which the dark to light transition occurred.

Figures 3.4 and 3.5 are examples of pH-selective microelectrode measurements in the vacuole of an epidermal cell during light/dark transitions. These figures show that there was no vacuolar pH change in response to light/dark transitions.

3.3.4 Discussion

The steady-state pH measurements presented here are in agreement with the previous measurements made in plant cells (Kurkdjian and Guern, 1989; Zimmermann *et al.*, 1999; Yu *et al.*, 2000).

The membrane potential changes triggered by light/dark transitions in the examples of pH-selective microelectrode measurements presented in this chapter are similar in terms of shape, magnitude and duration to those of nitrate-selective microelectrodes shown in the previous chapter (Figures 2.13 to 2.16). Dynamic measurements were made in epidermal cells. Both vacuolar and cytoplasmic pH showed no response to illumination transitions. The fact that the pH-sensor membrane was not responsive to illumination transitions suggests it could be useful in the study of cytosolic pH changes in response to illumination in other cell types.

The absence of cytosolic pH change combined with the presence of membrane potential response to illumination transitions in epidermal cells seems intriguing because it could be expected that the movement of protons across the plasma membrane would be the depolarising event. The absence of light induced cytosolic pH responses in *Arabidopsis* leaf epidermal cells may suggest that H^+ fluxes are small or absent during light transitions. A possible candidate ion flux for these membrane potential responses may be K^+ combined with Ca^{2+} and/or Cl^-, suggested by a study into light-induced K^+-channels in *Arabidopsis* mesophyll cells (Spalding *et al.*, 1992)

3.3.5 Conclusion

The pH-selective microelectrode technique was successful in delivering measurements of epidermal cells in both steady-state and under light/dark transitions. The results showed that cytosolic and vacuolar pH did not change in response to light/dark transitions although membrane potential did, suggesting that the movement of other ions across the plasma membrane was the depolarising event. Owing to the low sucess rate in obtaining epidermal cell measurements there was insufficient time to extend the study to mesophyll cells using this technique. An alternative technique, confocal microscopy of pH indicator dyes, was employed in the hope that the mesophyll measurements could be made in the time available.

3.4 Confocal microscopy of pH indicator dyes

3.4.1 Introduction

This section describes experiments to determine whether fluorescent pH indicator dyes viewed with a confocal microscope can be used to investigate the effects of light-dark transitions on leaf cells of NR^- mutant and wild type *Arabidopsis* plants. The aim of this section was to study these changes in the mesophyll cells. Many authors (e.g. Hepler and Gunning, 1998; Roos, 2000) have reviewed the use of fluorescent indicator dyes to measure intracellular pH. The technique is based on fluorescent probes that are loaded inside cells and change their fluorescent properties when bound to specific ions of interest (Roos, 2000). The fluorescence from pH indicator dyes is generally monitored using microscopy. The spatial resolution of the fluorescence distribution detected by conventional microscopy is degraded because the specimen is illuminated by a cone of excitation light and the detector detects both in-focus regions and out-of-focus blur. Images with better spatial resolution are produced by confocal microscopy.

3.4.1.1 Confocal microscopes

Confocal laser scanning microscopy (CLSM) produces images of relatively thin sections within a thicker sample without physical sectioning and consequent specimen compression (Entwistle, 2000). The CLSM achieves optical sectioning by the combination of two related effects (see Figure 3.6). Firstly, illumination (typically from a laser light source) is sharply focused on a single point within the object, the regions above and below the point of focus (defocused) being much less brightly illuminated. Secondly, the light emanating from the point of focus is collected and sharply focused on an aperture, the confocal pinhole, positioned in front of the detector. Light emanating from the defocused regions above, below or to the side of the point of focus is focused behind, in front of or to the side of the pinhole respectively. These emissions are therefore largely prevented from entering the pinhole and reaching the detector and so the point of focus is imaged preferentially. Scanning the point of focus by moving the microscope stage or the light beam horizontally produces two-dimensional images, and moving the microscope stage

vertically collects transverse sections at different depths forming data sets of three-dimensional images. Images from the CLSM are collected and processed by computer.

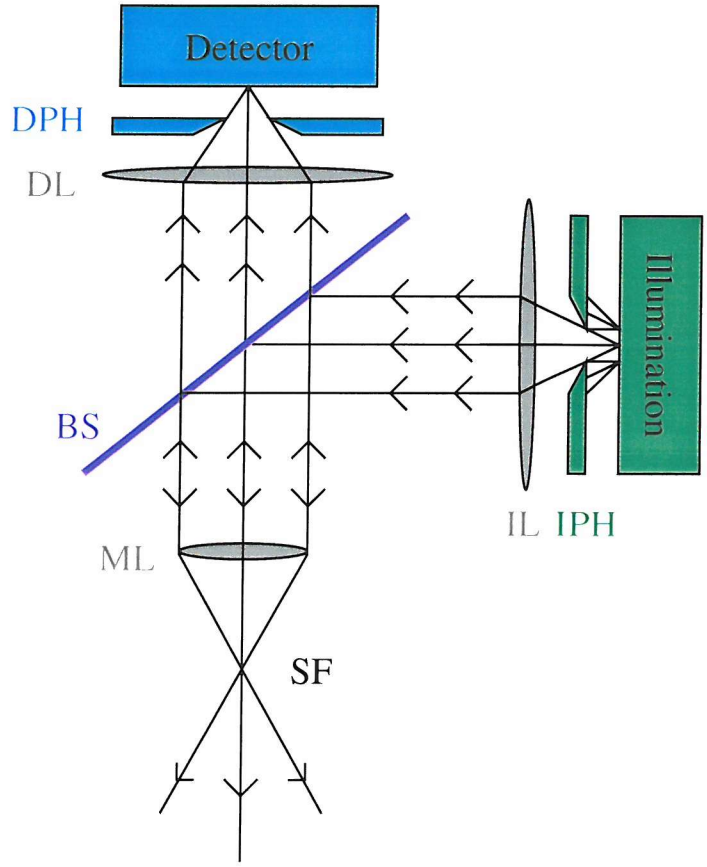

Figure 3.6 Schematic representation of CLSM.

Key: illumination passes through the illumination pinhole (IPH) and is focused by the illumination lens (IL). Illumination is then reflected by a beam splitter (BS) and focused to a point within the specimen (SF) by a microscope (ML) and any optical beam scanning components. Fluorescence from the SF is collected and focused sharply through the ML and detector lens (DL) onto an aperture, the confocal pinhole (DPH) placed before the detector.

3.4.1.2 pH indicator dyes

There are numerous pH indicator dyes available (Haugland, 1999). Indicator dyes may be concentrated differently in organelles and cellular compartments. To quantify cellular pH accurately both concentration and fluorescence intensity of dye need to be measured (Hepler and Gunning, 1998; Roos, 2000). Ratiometric techniques use dyes

that possess an excitation or emission wavelength insensitive to changes in ion concentration that can act as a reference point against fluorescence changes due to ion concentration. Other dyes change their fluorescence intensity in response to pH at the same wavelength and therefore there is no reference value to give dye concentration.

3.4.1.3 Selecting a suitable pH indicator dye

Before experiments studying pH changes in the cytosol of mesophyll cells could begin a suitable pH indicator dye had be selected, based upon the following. The dye of choice should have a strong shift in the fluorescence spectrum or intensity upon binding of the target ion (to provide sufficient detection and responsiveness within the pH range likely to be detected). The dye should have a high quantum yield of light emission and high photo-stability (to record low concentrations of dye with minimum intracellular buffering). The dye of choice should have sufficient intracellular accumulation, slow leakage from the target area and low cyto-toxicity.

3.4.1.4 Dye loading strategies

Various dye-loading strategies have been developed to apply dyes to target areas. A commonly used approach is to apply permeant esters. Permeant esters have been produced from many fluorescent ion probes and have hydroxyl- and carboxyl groups available as acetyl- or acetoxymethyl (AM) esters, respectively. These lipophilic molecules are designed to penetrate cellular membranes and then be cleaved by cellular esterases, the anions formed being trapped inside the cell. These permeant esters have been used successfully; however in mature plant cells insufficient loading has been frequently reported (Roos, 2000). These problems have been ascribed to cell wall-bound esterases that cleave the esters before they can cross the plasma membrane (Cork, 1986). Other strategies include acid loading of lipophilic acid pH indicators in low external pH and microinjection of dye (Roos, 2000). Lipophilic acid loading and microinjection have disadvantages; lipophilic acid loading may alter cytosolic pH and other cellular processes, and microinjection is invasive, possibly triggering wound reactions and diluting the cytoplasm. Yin *et al.* (1990) described the use of the pH indicator dye pyranine to measure cytosolic pH in leaf mesophyll cells. Pyranine is a highly charged trisulfonate anion, which would presumably not cross the hydrophobic plasma membrane, yet is reported to accumulate within

mesophyll cells. Yin *et al.* (1990) suggested that pyranine uptake was carrier-mediated.

3.4.2 Methods

Wild type *Arabidopsis* plants were hydroponically cultured as described in Section 2.3.1. Initial investigations were done to establish the suitability of *Arabidopsis* leaves for confocal microscopy studies. Experiments were designed to establish the distribution of a number of pH indicator dyes within the leaf tissue and to select a suitable dye to study the cytosol of mesophyll cells.

3.4.2.1 Chamber design

A chamber (Figure 3.7) was designed and constructed to hold the leaves flat and securely under the microscope. To collect a good resolution image a detached leaf was submerged in ¼ Hoagland's solution (see Section 2.3.1.1) and where appropriate the dyes were added to the ¼ Hoagland's solution.

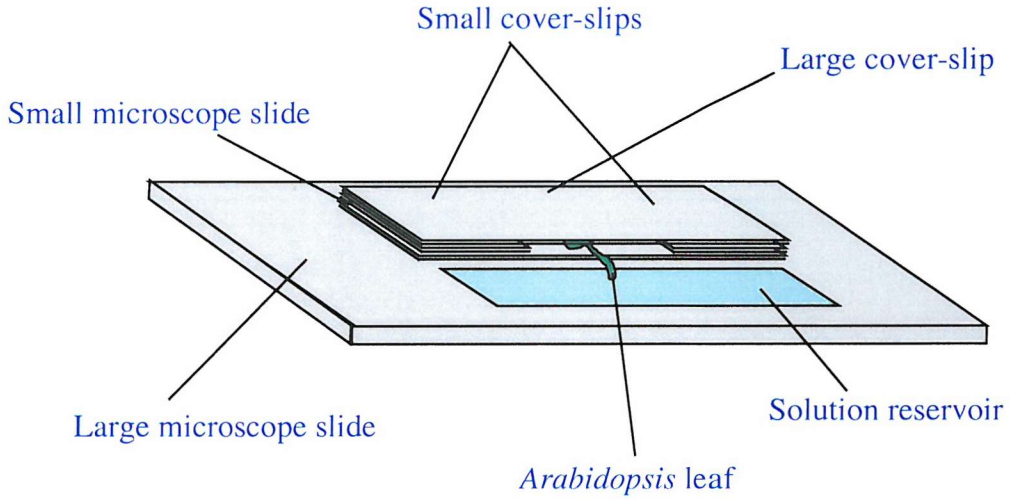

Figure 3.7 CLSM chamber design

3.4.2.2 The dyes

All the dyes were obtained from Molecular Probes, Eugene, USA. The dyes were excited by blue light of 488 nm and green fluorescence was measured at 505 to 550 nm. The fluorescence of the dyes used in this study increases upon alkalisation. The dyes tested during this study are described below.

5-Carboxyfluorescein diacetate acetoxymethyl ester (CFDA-AM, C-1354) is electrically neutral and readily crosses membranes. Upon hydrolysis by cellular esterases, CFDA-AM ester yields carboxyfluorescein (CF). Compared with fluorescein (described below), CF contains extra negative charges and is therefore better retained within cells. CF has a pH dependent spectral response similar to that of fluorescein. CFDA-AM was dissolved in acetone, then diluted to 10 μM in ¼ Hoagland's solution to produce the dye solution.

Dextran conjugates of dyes are relatively inert polysaccarides with different chemical properties from those of the dyes themselves, being highly water-soluble and therefore not readily membrane permeable. A red coloured dextran (10 mM rhodaminated-dextran) was used to determine the exact location of CFDA-AM.

The neutral species of fluorescein (at approximately pH 5) contains both phenol and carboxylic acid functional groups. Upon alkalisation (at approximately pH 6.4) the monoanion is produced by the ionisation of the carboxylic acid functional group. Further alkalisation yields the dianion by the ionisation of the phenol functional group. Only the monoanion and dianion are fluorescent; the fluorescence emission spectrum is dominated by the dianion even at acidic pH. Fluorescein is excited by (absorbs at) 488 nm and emits at approximately 515 nm. The emission spectrum of fluorescein is relatively independent of pH. The intensity of fluorescence increases with increasing pH as a result of fluorescein ionisation. Neutral fluorescein rapidly penetrates membranes whereas the ionic forms do not; therefore theoretically fluorescein would easily enter the cell, be retained to some degree in the cytosol (pH ~7.5) and any fluorescein in the vacuole (pH ~5.5) would readily diffuse into the cytosol. Fluorescein (F-1300) was diluted to 10 μM in ¼ Hoagland's solution to produce an appropriate dye solution.

8-Hydroxypyrene-1,3,6-trisulfonic acid (HPTS, also known as pyranine; H-348) is a highly water soluble, membrane impermeable pH indicator. Pyranine was excited by 488 nm and fluorescence detected at 520 nm. Although this dye does not normally cross membranes Yin *et al.* (1990) reported good uptake by barley, spinach, tobacco and *Pelargonium zonale* leaves. They fed the dye through the petiole at a concentration of 200 μM in a 2 mM MES buffer solution at pH 7.0 for 90 min. They reported that pyranine was one of the best pH indicator dyes for the pH range of interest in leaf cytoplasmic pH measurements. Savchenko *et al.* (2000) used 500 μM in a 2 mM HEPES (N-[2-Hydroxyethyl]piperazine-N'-[2-ethanesulfonic acid]) buffer

for 20 min to 3 h in spinach, potato, *P, zonale* and *Rumex acetosa* leaves. For the current study, pyranine was used at a concentration of 500 μM in a 2 mM HEPES buffer, with various loading times covering the ranges reported by Yin *et al.* (1990) and Savchenko *et al.* (2000).

3.4.2.3 Application methods for the dyes

Different techniques were used to determine the best method to apply each dye. Dyes were applied to leaves excised by cutting the petiole near the stem. Three methods were used: submerging the leaves in dye solution, cutting across the leaves and submerging in dye solution, and feeding the dye through the petiole dipped in dye solution.

3.4.2.4 The microscope

Image data sets were collected on an LSM510 confocal laser scanning microscope (Figure 3.8, Zeiss, Welwyn Garden City, UK) set up and aligned as described in Entwistle and Noble (1994). The specimens were scanned with 488 and 633 nm illumination simultaneously sometimes followed with 545 nm illumination, in which case these were alternated on a line-by-line basis. The illumination was directed onto the specimen by a broadband biased (10% reflective) beam-splitter. The signal emanating from the specimens was collected with either a x40 NA 1.3 objective (high magnification) or a x10 NA 0.3 objective (low magnification). The signal was then split into two channels that were filtered with a 505-550 nm bandpass filter, a 650 nm long pass filter and also, when appropriate, an additional single channel of data was collected with a 560 nm long pass filter. The collection of the various channels was synchronised with the changes in the illumination. Images were collected as three channel data sets with a bit depth of 12 using a matrix of either 512 x 512 or 1024 x 1024 pixels. The confocal microscope was also used as a conventional light microscope with ultra-violet illumination.

Figure 3.8 The Zeiss confocal laser scanning microscope (CM) and data collection system (PC).

3.4.2.5 Image analysis

Images were analysed and selected areas quantified using the Zeiss 3D software associated with driving the microscope.

3.4.3 Results

3.4.3.1 Confocal microscopy of *Arabidopsis* leaves

In examining the suitability of *Arabidopsis* leaves for confocal microscopy study the first parameter to be assessed was the extent and possible interfering properties of auto-fluorescence from chlorophyll and other fluorescent pigments (Figure 3.9). There were strong auto-fluorescent signals in the blue channel (B, excited by 633 nm emitting greater than 650 nm), very small signals in the red channel (R, excited by 545 nm emitting greater than 560 nm) and only tiny signals in the green (G, excited by 488 nm emitting 505-550 nm) channel; this was encouraging as pH indicator dyes emit a green colour. The auto-fluorescence from blue oval structures, presumably chlorophyll-containing chloroplasts, was strong in the mesophyll cells and guard cells; however no chlorophyll-containing chloroplasts were detected in the epidermal cells (also shown clearly in Figure 3.13).

The next parameter to be examined was the ability of the laser to penetrate the leaf tissue. The *Arabidopsis* leaves used in these experiments were approximately 75 μm thick. Adjustments to the size of the pinhole can alter the penetration of the laser into the tissue; opening the pinhole generally increases penetration at the expense of the resolution of the image. In this case, opening the pinhole produced no enhancement of laser penetration (data not shown).

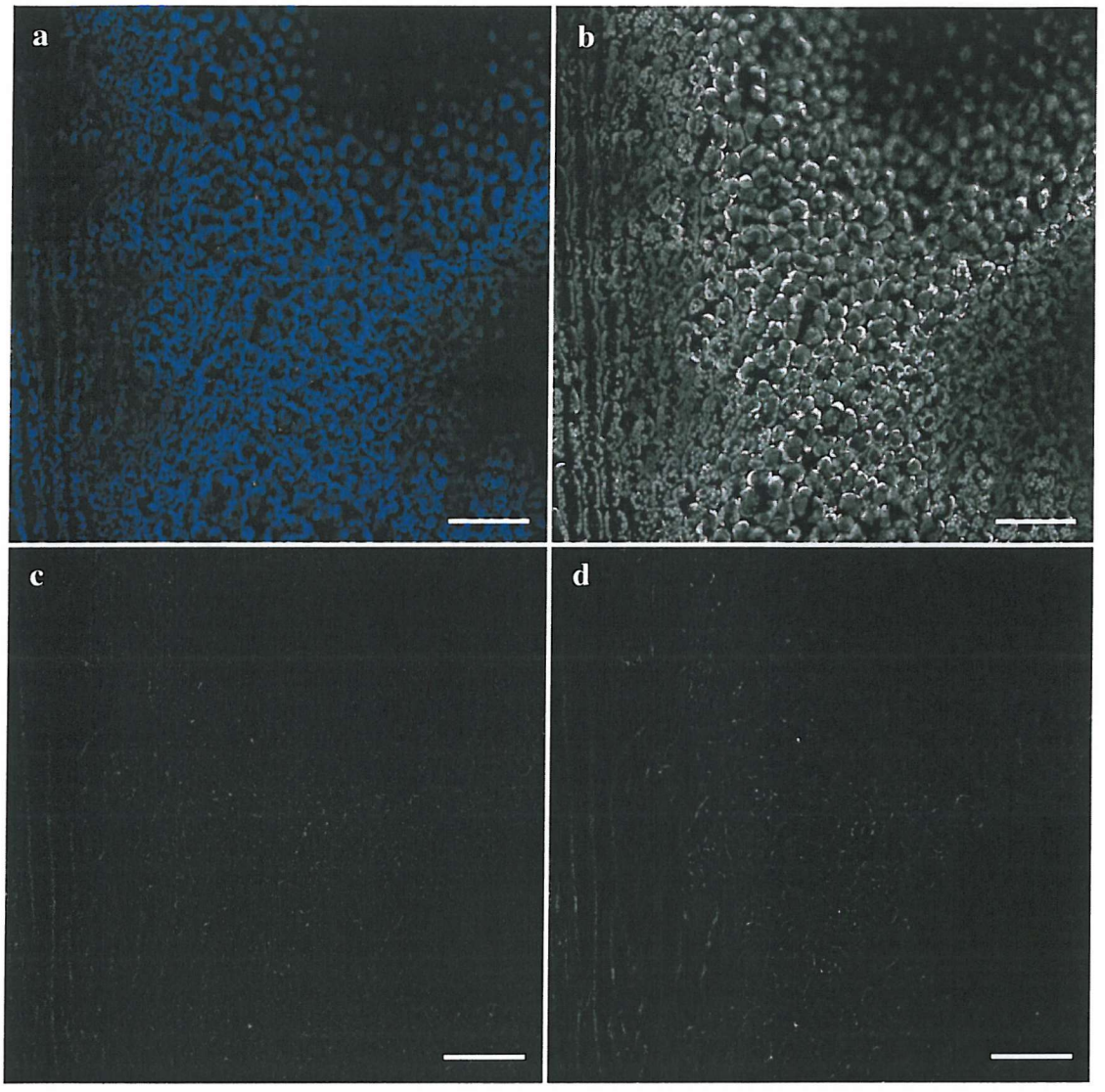

Figure 3.9 Auto-fluorescence from an *Arabidopsis* leaf: a) RGB channels shown in colour, separated b) blue (strong signals from oval shaped chloroplasts), c) green and d) red channels shown in black and white, all channels with the same contrast application, scale bar 125 μm.

3.4.3.2 The pH indicator dyes

Initial experiments were done to ascertain the best means to apply CFDA-AM to the cytosol of mesophyll cells. Cut leaf loading of CFDA-AM was poor, only the first 4 or 5 mesophyll cells next to the cut surface were loaded after 40 min (data not shown). Petiole loading of CFDA-AM was slow, diffusing only 0.4 mm along the petiole in 1 h (data not shown). Submerged loading of CFDA-AM was not particularly effective; the dye rapidly reached the epidermal but not the mesophyll cells (data not shown).

After these initial studies, the petiole loading method of dye application was repeated for a longer time-scale (approximately 20 h, data not shown). This experiment showed that the dye loaded at the highest concentrations near the main vein of the leaf, at the edges of the epidermal cells, in the vascular tissue and in the vacuoles of the mesophyll cells. Further away from the main vein, the dye was at highest concentration in the mesophyll vacuoles. After the completion of these initial studies a time course experiment was done using submerged loading of CFDA-AM (Figure 3.10) to see if there was an optimum time after dye application for detecting the dye in the cytosol of mesophyll cells. The first image in Figure 3.10a shows the auto-fluorescence of the leaf prior to dye application. The dye was then loaded and an image collected every 5 min. Figure 3.10b showed that CFDA-AM was rapidly cleaved by esterases at the edges of the epidermal cells (either in the cytosol or apoplast) with some CF visible after only 5 min. Over time the intensity of CF fluorescence at the edges of the epidermal cells became stronger. After 60 min (see Figure 3.10o) CF was visible in the vacuoles but not in the cytosol of mesophyll cells. The distribution of dye was then examined in a series of transverse (x-y) sections at increasing depths (Figures 3.11 and 3.12) and the dye was shown to be at highest concentration in the mesophyll vacuoles, at the edges of the epidermal cells and in the trichomes.

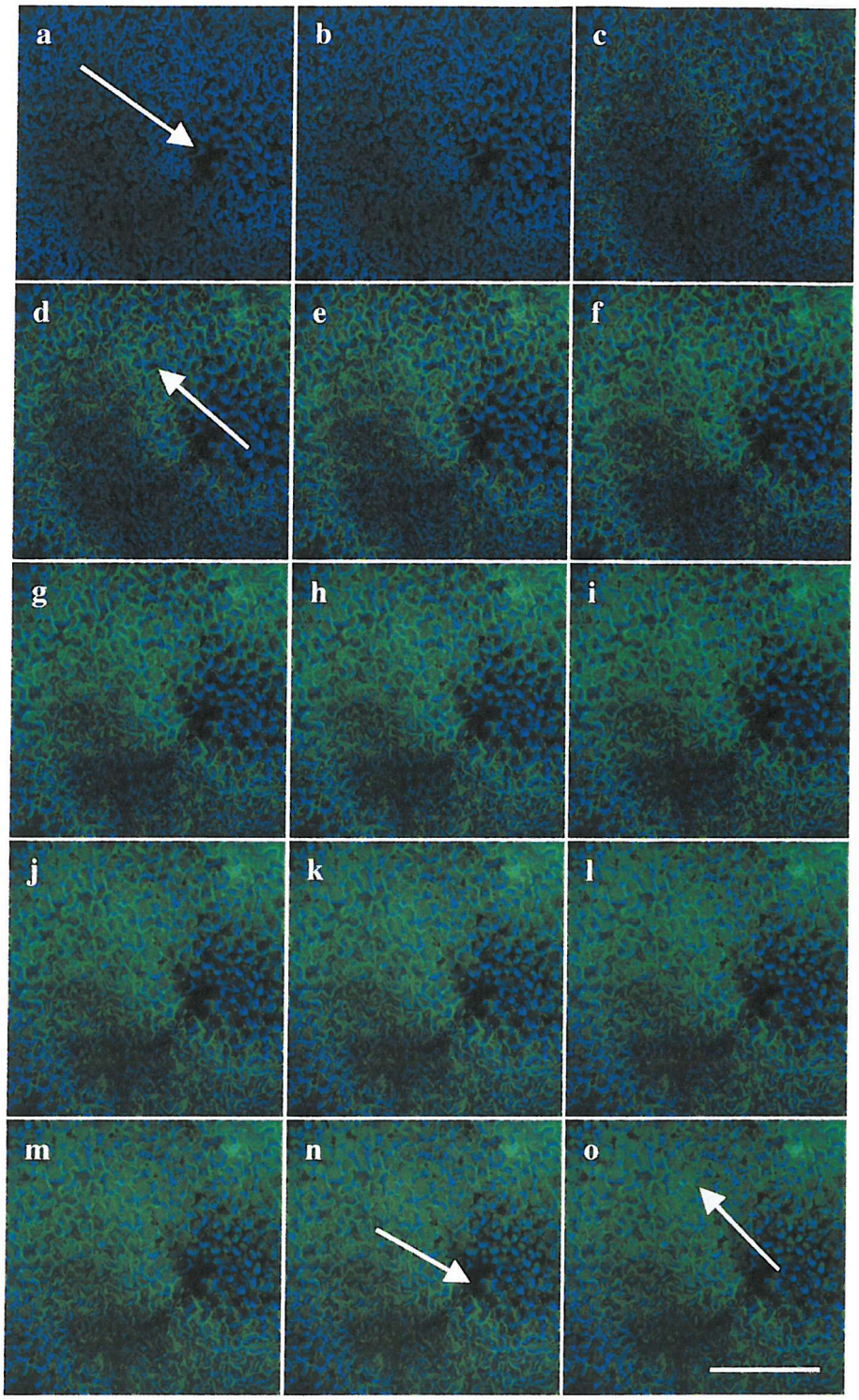

Figure 3.10 Submerged loading of CFDA-AM into an *Arabidopsis* leaf, images of the same x-y transverse section: a) before addition of dye, blue auto-fluorescence from chloroplasts, arrow marks the shadow of a trichome, b) immediately after application of the dye, c) to o) images taken every 5 min, d) arrow indicates esterase cleaving of CF around the edges of epidermal cells, n) arrow marks the shadow of the trichome and o) arrow marks the accumulation of CF in the vacuoles of mesophyll cells, scale bar 200 μm.

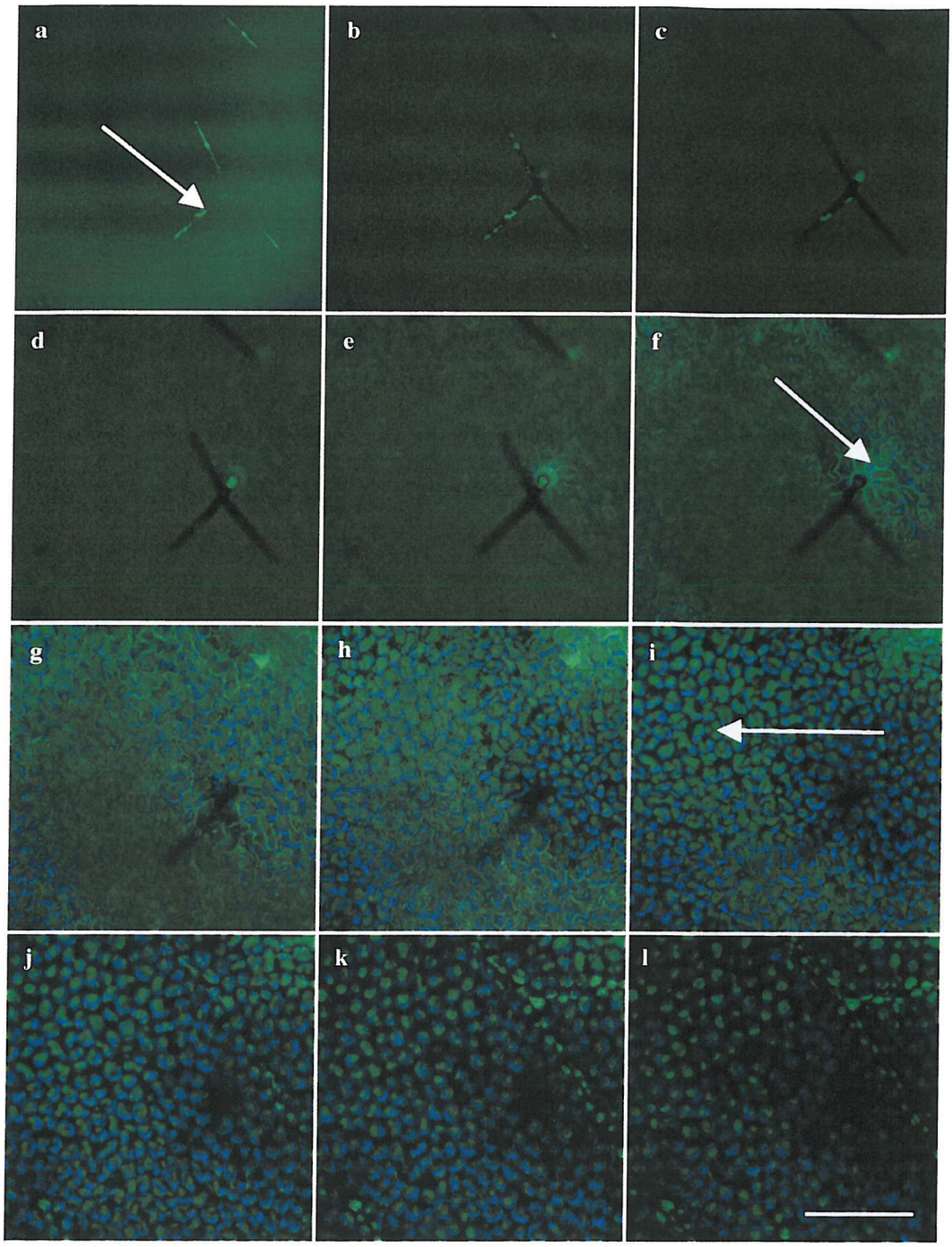

Figure 3.11 Submerged loaded (1 h 20 min) CFDA-AM into an *Arabidopsis* leaf, images of x-y transverse sections at increasing depths within the leaf: a) arrow marks accumulated CF in trichome on leaf upper surface, f) arrow marks the accumulation of CF surrounding the basal cells of the trichome and epidermal cells, i) arrow marks the accumulation of CF within the vacuoles of mesophyll cells surrounded with blue auto-fluorescent chloroplasts, scale bar 250 μm.

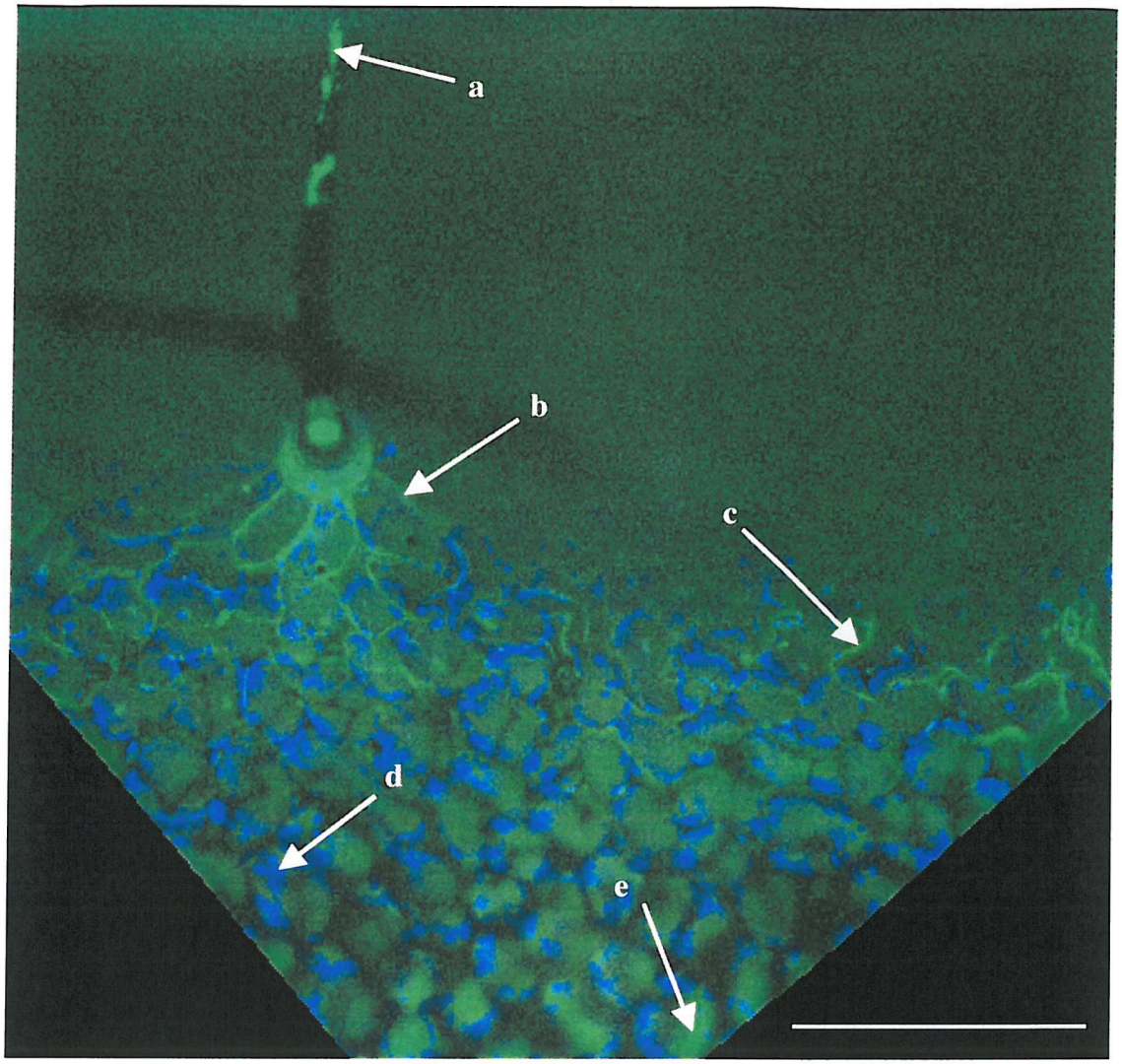

Figure 3.12 3-dimensional reconstruction of the x-y transverse sections shown in Figure 3.11, x = 585, y = 454, z = 8, pitch = 15° and view angle = 139°, scale bar 150 μm. Arrows mark: a) the accumulation of CF (shown in green) in the trichome, b) the accumulation of CF in the basal cells of the trichome, c) the accumulation of CF surrounding the epidermal cells, d) auto-fluorescence from chloroplasts (shown in blue) and e) the accumulation of CF in the vacuoles of mesophyll cells.

In order to establish the exact location of CF associated with epidermal cells images were collected at high magnification (Figure 3.13). Figure 3.13 shows red faint auto-fluorescence in the apoplast and blue auto-fluorescence from chlorophyll-containing chloroplasts in the mesophyll and guard cells. The high magnification image revealed that the CF at the edge of the epidermal cells was in an uneven distribution of localised patches of high intensity. This patchy distribution may be due

to cytosolic or apoplastic accumulation of CF with the localised high intensity patches reflecting organelle sequestered or patches of high esterase activity respectively. CF was not detected in the mesophyll cells unless the contrast was increased massively.

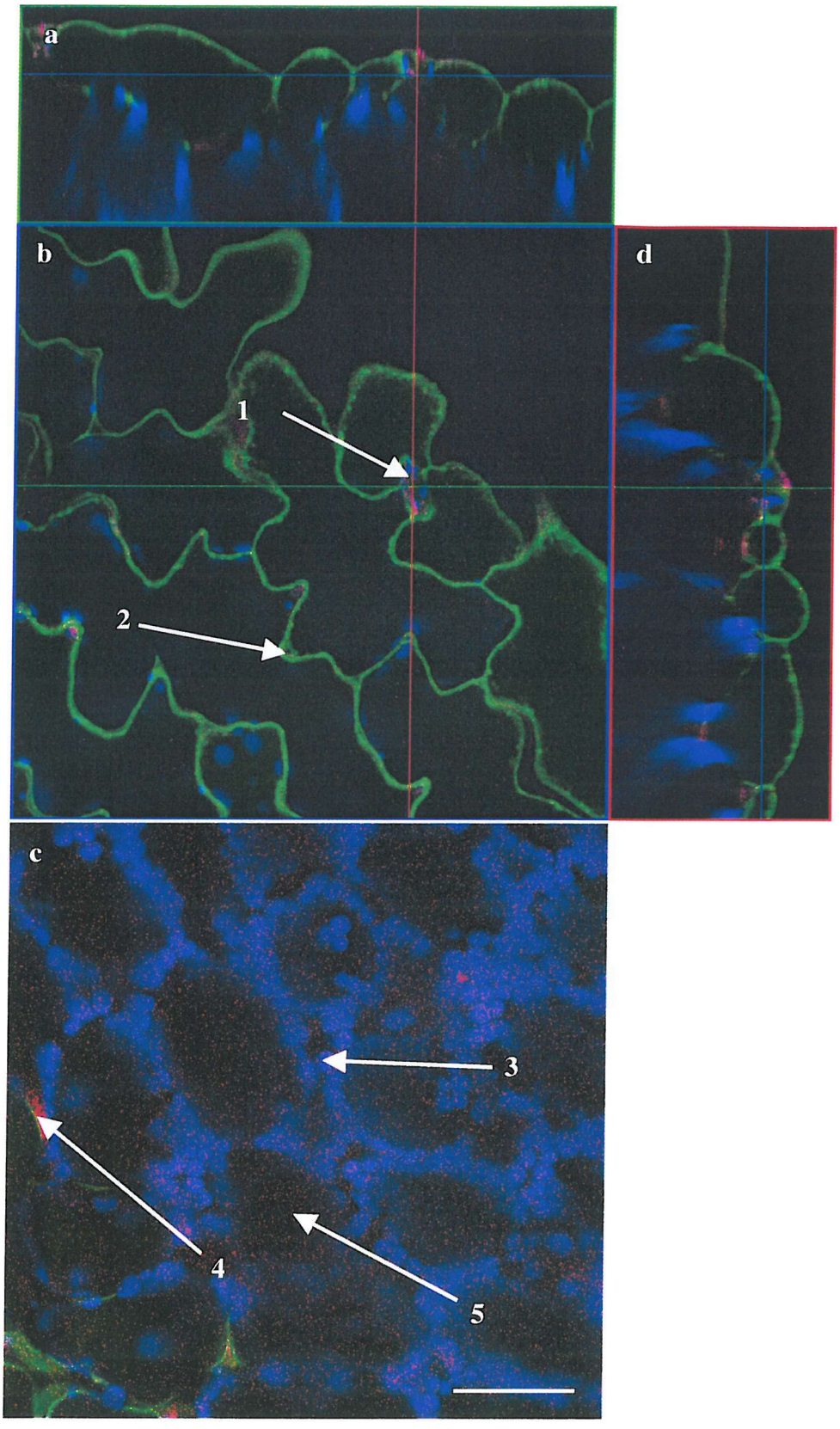
a
b
d
1
2
c
3
4
5

Figure 3.13 Submerged loaded (for 20 min) CFDA-AM into an *Arabidopsis* leaf: a) x-z cross section, b) x-y transverse section through epidermal and guard cells (CF surrounding epidermal cells (arrow 1) and guard cells (arrow 2) shown in green), c) x-y transverse section at greater depth through mesophyll cells, auto-fluorescence from chloroplasts shown in blue (marked by arrow 3), apoplastic auto-fluorescence shown in red (marked by arrow 4) and non-fluorescent vacuoles (marked by arrow 5) and d) y-z cross section, scale bar 50 μm.

Determination of the exact location of the CF around/in the epidermal cells was done using a mixture of rhodaminated dextran and CFDA-AM (Figure 3.14). Figure 3.14 showed that the dextran overlaid the CF suggesting a cytosolic localisation of CF within the epidermal cells.

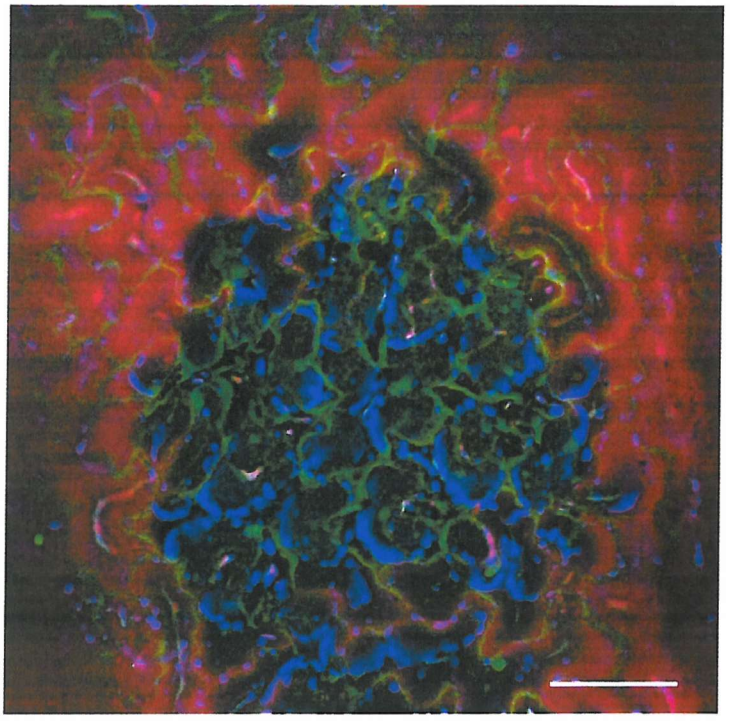

Figure 3.14 Transverse (x-y) section of an *Arabidopsis* leaf, submerged loaded CFDA-AM and rhodaminated dextran for 30 min, CF at the edges of epidermal cells shown in green, auto-flourescence from chloroplasts of mesophyll cells shown in blue and rhodaminated dextran shown in red, scale bar 100 μm.

Generally, CFDA-AM loaded well around the base cells surrounding and inside the trichomes themselves, in the cytosol of epidermal cells and in the vacuoles

of mesophyll cells. Most importantly for this project CF fluorescence was not seen to accumulate in the cytosol of mesophyll cells. CF was used to determine the behaviour of permeant esters in *Arabidopsis* leaves although it is not sensitive within the range of expected cytosolic pH change. The use of permeant esters was therefore not considered suitable for studies of cytosolic pH under these conditions. If these experiments had been successful the alternative pH indicator dye, carboxy-SNARF-1-AM ester acetate (C-1271) would have been tested.

Initial tests were done to study the loading of membrane-permeant fluorescein. Submerged and cut leaf edge loading produced images with a very bright background; however penetration of dye was not very good, with only some label visible in the vacuoles (data not shown). The auto-fluorescence in images taken with leaves submerged in fluorescein was reduced because (exciting and emitted) light was absorbed by the overlying fluorescent dye. Petiole feeding for 2.5 h was fairly successful, highest concentration being in the edges of epidermal cells, in the vascular tissue, in mesophyll cell vacuoles and in the tips of the trichomes (see Figures 3.15 and 3.16). Petiole loading overnight was less successful with the dyes being mainly localised in the vascular tissue. Most importantly, fluorescein was not at sufficiently high concentrations in the cytosol of mesophyll cells to be used to study cytosolic pH changes.

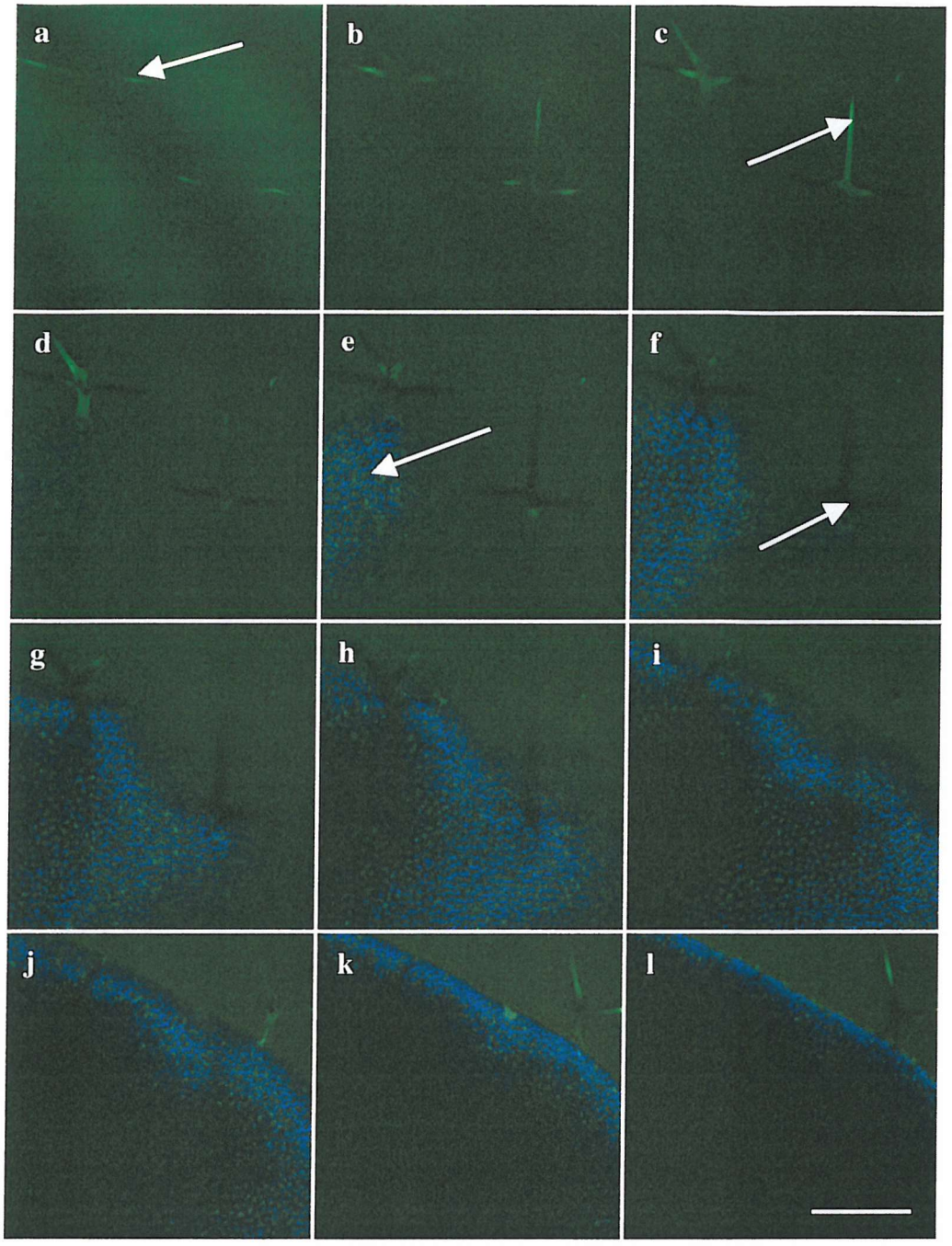

Figure 3.15 Transverse (x-y) sections at increasing depth through an *Arabidopsis* leaf after 2.5 h petiole loading of fluorescein (shown in green): a-d) fluorescein accumulation in trichomes on the upper surface of the leaf marked by arrows, e) blue auto-fluorescence from chloroplasts of mesophyll cells, the accumulation of fluorescein in mesophyll cells marked by arrow and f) shadow of trichome marked by arrow, scale bar 250 μm.

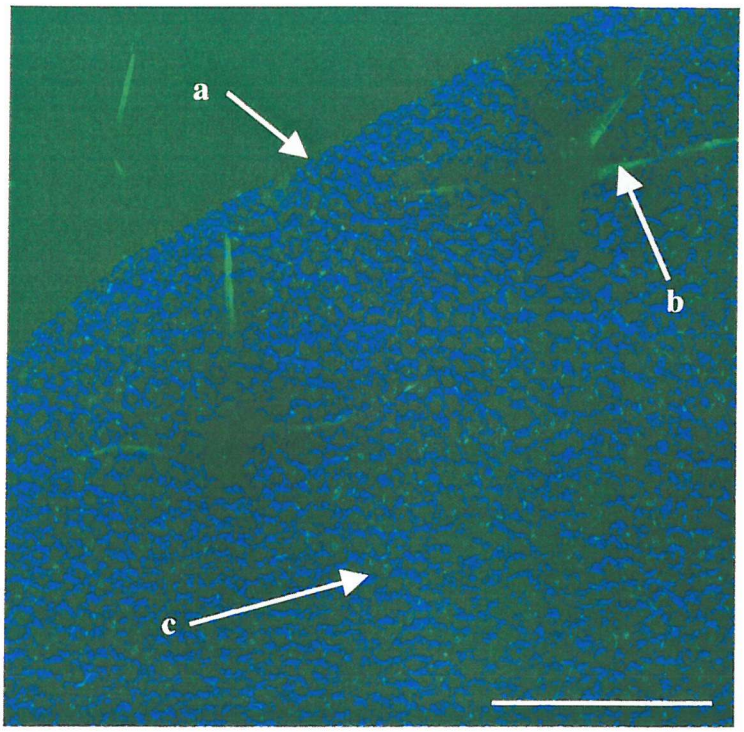

Figure 3.16 Maximum intensity projection of the transverse (x-y) sections shown in Figure 3.15, fluorescein (shown in green) accumulated in the trichomes (marked by arrow b) and mesophyll cell vacuoles (marked by arrow c), auto-fluorescence from chloroplasts of mesophyll cells are shown in blue, arrow a marks the edge of the leaf, scale bar 250 μm.

After 40 min of pyranine loading the leaf was viewed under ultra-violet light. The dye was present at high concentration along the vascular tissue and in the trichomes of the leaf. A time course study of pyranine uptake by mesophyll cells was done, from 57 min to 1 h 57 min (Figure 3.17). There was little change in the distribution of the dye, which remained high only in the vascular tissue. A subsequent CLSM series of x-y sections at increasing depth through the leaf (Figure 3.18) showed that the dye was at high concentration in the vascular tissue and trichomes but at low concentration elsewhere. A maximum intensity projection of the 3D data set collected (shown in Figure 3.19) confirms the distribution of dye concentration.

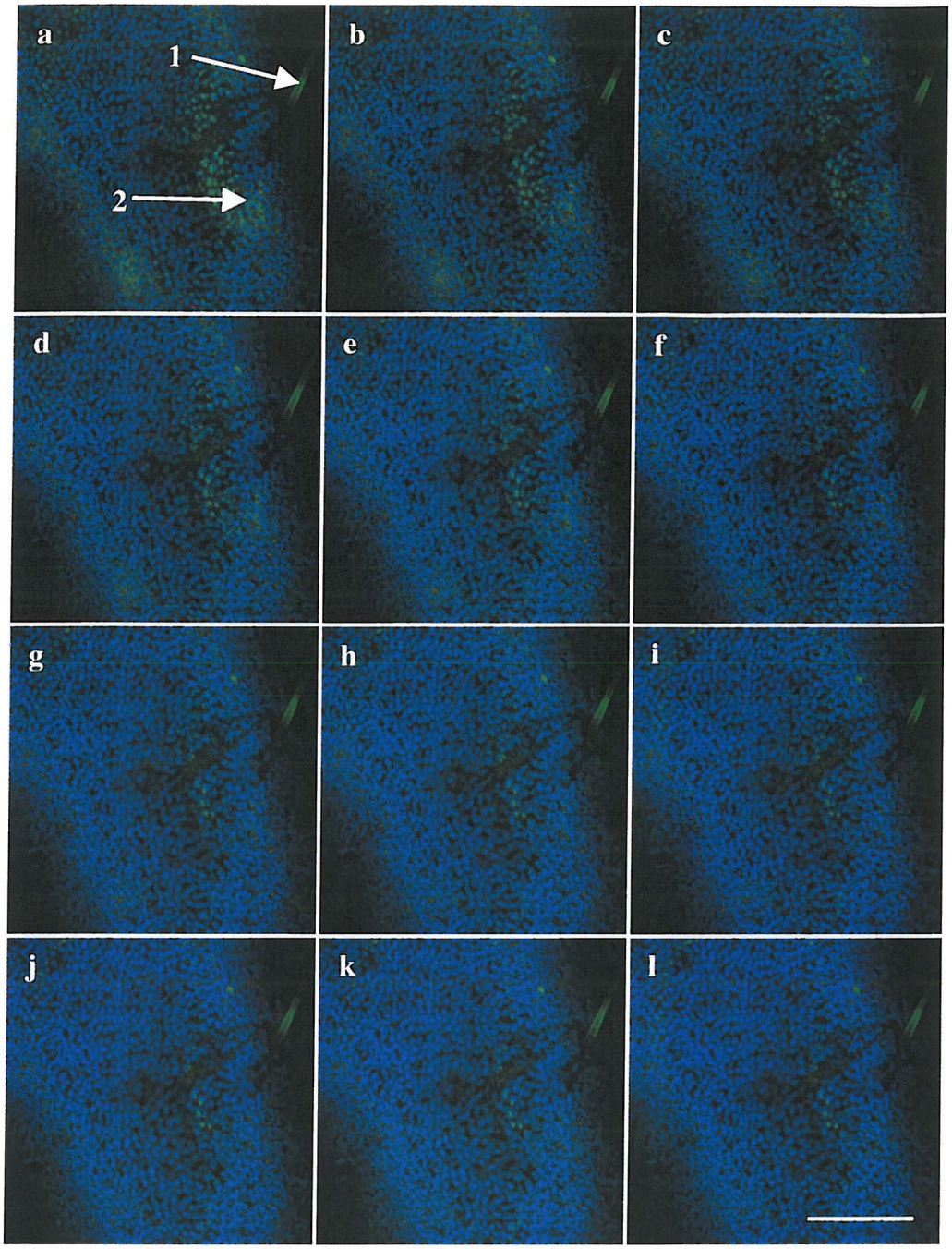

Figure 3.17 Uptake and distribution of pyranine (shown in green) within an *Arabidopsis* leaf after 57 min of exposure to the dye, a) to l) images of the same transverse (x-y) section taken at 5 min intervals: arrow 1 marks the accumulation of pyranine in a trichome, arrow 2 marks the accumulation of pyranine in the vacuoles of mesophyll cells, auto-fluorescence from chloroplasts in the mesophyll cells is shown in blue, scale bar 250 μm.

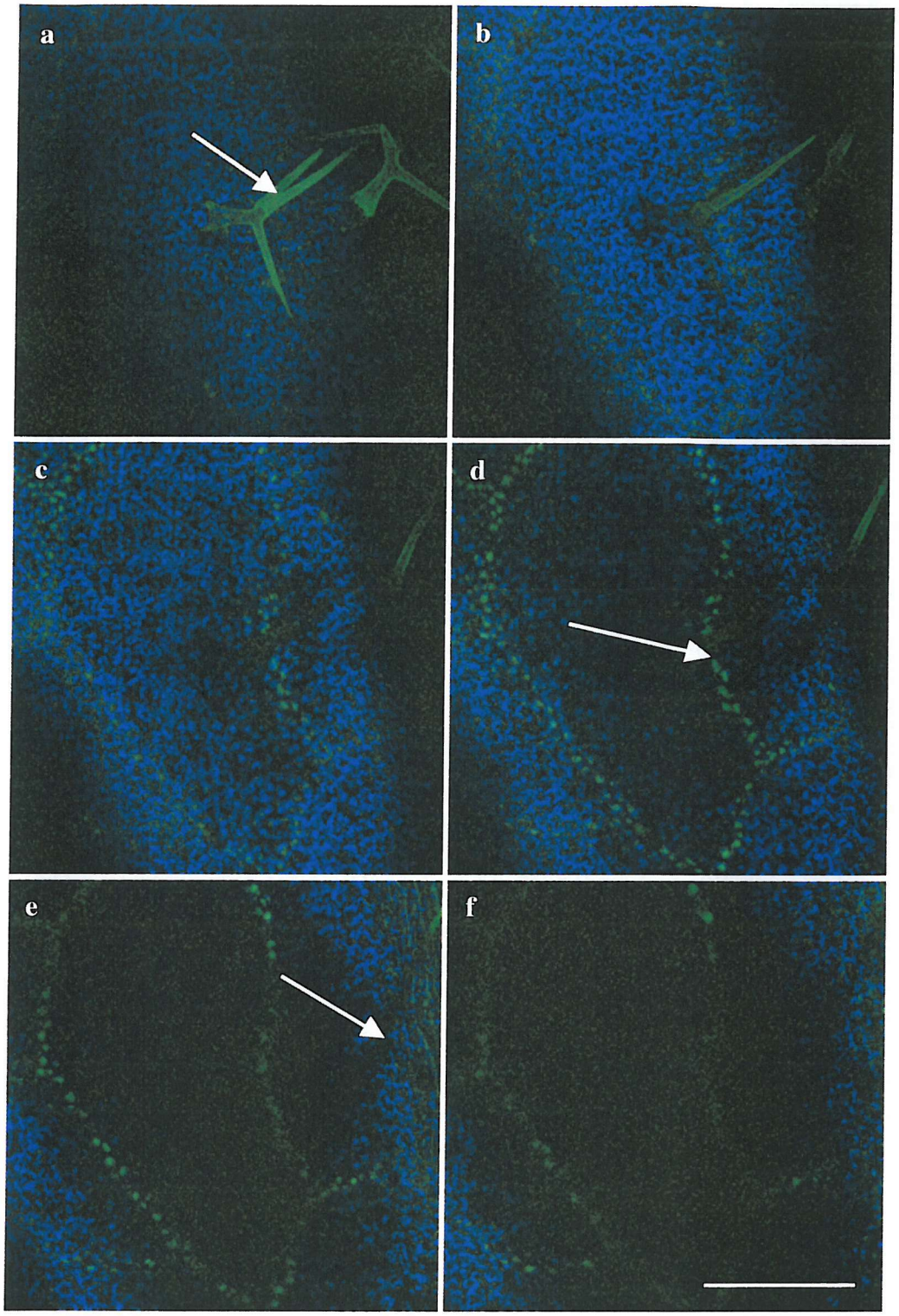

Figure 3.18 Transverse (x-y) sections of an *Arabidopsis* leaf at increasing depths after 2 h petiole loading of pyranine (shown in green), auto-fluorescence from mesophyll cell chloroplasts (shown in blue), a) leaf upper surface with trichomes (marked by arrow), d) section through mesophyll cells, accumulation of pyranine in the vascular tissue (marked by arrow), e) arrow marks the shadow of a trichome, scale bar 250 μm.

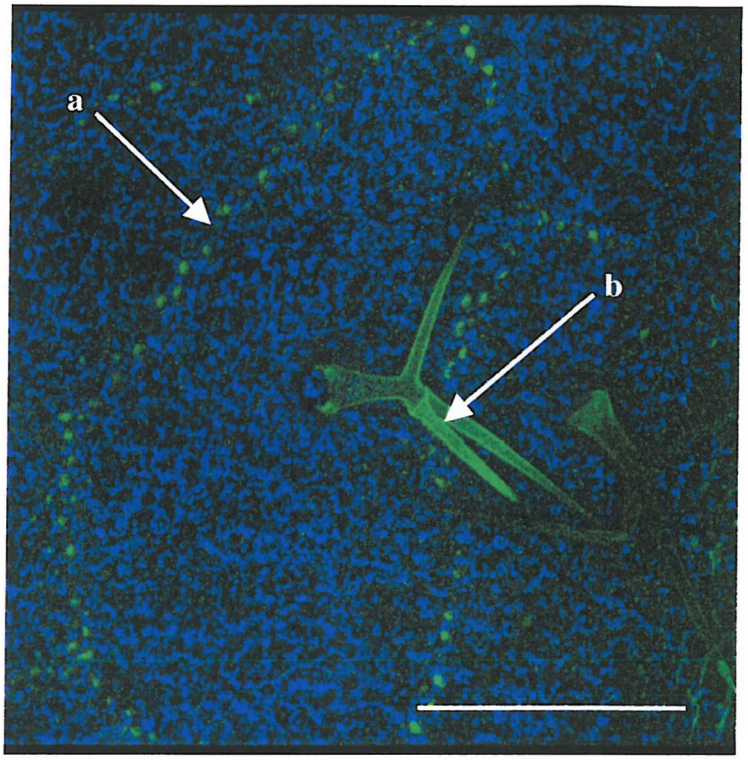

Figure 3.19 Maximum intensity projection of the transverse sections shown in Figure 3.18, auto-fluorescence from chloroplasts in the mesophyll cells shown in blue, the accumulation of pyranine (shown in green) in the vascular tissue (marked by arrow a) and trichomes (marked by arrow b), scale bar 250 μm.

The distribution of petiole fed pyranine was also examined at high magnification (see Figure 3.20). Pyranine was shown to accumulate in association with the epidermal cells. It was only detected within the mesophyll cells when the contrast was massively increased and was therefore in very low concentration.

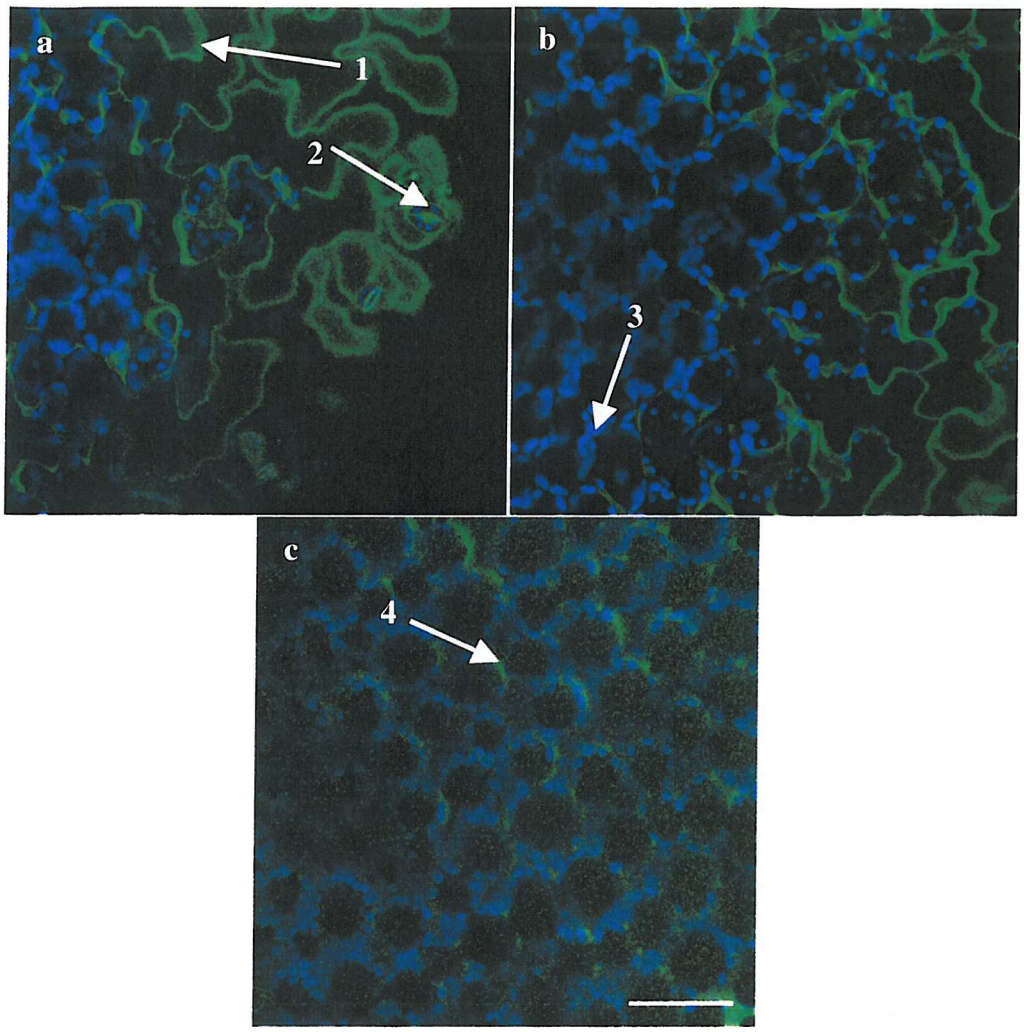

Figure 3.20 Transverse (x-y) sections through an *Arabidopsis* leaf at increasing depths loaded with pyranine (shown in green) via the petiole: arrow 1 marks the accumulation of pyranine at the edges of the epidermal cells, arrow 2 marks a chloroplast (shown in blue) inside a guard cell, arrow 3 marks the auto-fluorescence from the chloroplasts in the mesophyll cells and arrow 4 marks the accumulation of pyranine in the cytosol of the mesophyll cells, high magnification, scale bar 100 μm.

3.4.3.3 Light-dark transitions

Cytosolic pH change in mesophyll cells during light/dark transitions was not measured due to the unsuitability of all the dyes tested.

3.4.4 Discussion

There were problems associated with the loading of each dye. The use of permeant esters is frequently unsuccessful in mature leaf cells because of the activity of apoplastic esterases that cleave the dye before it enters the cell (Roos, 2000). However, in *Arabidopsis* leaves this did not occur; in the *Arabidopsis* leaves the CF appeared to be cleaved inside the epidermal cells. However, CF was not shown to accumulate in the cytosol of mesophyll cells, therefore the use of permeant esters to load dyes was considered unsuitable for the study of cytosolic pH change in the mesophyll. The loading of membrane permeant fluorescein into the cytosol of *Arabidopsis* mesophyll cells was unsuccessful as fluorescein rapidly accumulated in other cell types in preference to the mesophyll cells.

The loading of membrane impermeant pyranine into the cytosol of *Arabidopsis* mesophyll cells was also too low to study pH changes although pyranine has been used successfully to study mesophyll cytosolic pH in other species. This may be due to the species-specific differences in dye intracellular localisation and even extrusion, which have been reported elsewhere (Fricker *et al.*, 1993; Williams *et al.*, 1993).

All the dyes tested accumulated rapidly at the edges of the epidermal cells, presumably in the cytosol, in the vacuoles of mesophyll cells and within the trichomes, regardless of their mode of loading. This accumulation pattern may represent a detoxification mechanism for the dyes within *Arabidopsis* leaves. Plants encounter a wide range of phytotoxic natural and synthetic chemicals, called xenobiotics, in the environment and contain versatile detoxification mechanisms to counter the effects of these compounds (Coleman *et al.*, 1997). One important mechanism is the chemical modification of the xenobiotic by covalent linkage to the endogenous tripeptide glutathione and subsequent export from the cytosol into the vacuole (Dixon *et al.*, 1998). Xenobiotics may also be sequestered into the ER and other membrane bound organelles (Coleman *et al.*, 1997).

Trichomes are hair-like structures that extend from the epidermis of aerial tissues. The botanical literature contains more than 300 descriptions to characterise various morphological types of trichomes. Many plant species contain a range of trichomes within a single leaf (Rodriguez *et al.*, 1984). The function of trichomes has been difficult to demonstrate clearly; however it is generally accepted that trichomes

have a role in the reduction of heat and water loss, the protection against pathogen and insect attack by secreting chemicals or by physically limiting access and as guide to potential pollinators. Some trichomes are more specialised and produce secretions associated with plant-insect interactions and survival under desert conditions (Wagner, 1991). Trichomes have also been implicated in the detoxification of heavy metals and they are involved in salt tolerance mechanisms (e.g. Fahn *et al.*, 1988; Choi *et al.*, 2001). *Arabidopsis* leaves have only one type of stellate trichome that does not have a secretory anatomy but a role in the prevention of herbivore access has been proposed (Szymanski *et al.*, 2000). Gutierrez-Alcala *et al.* (2000) reported extremely high glutathione concentrations within the trichomes of *Arabidopsis* and suggested an additional function as a sink for detoxification processes, which is consistent with the findings of this study.

The distribution of pH indicator dyes reported here may represent dye detoxification mechanisms in which the dyes are sequestered into the vacuoles of mesophyll cells, into organelles of the cytosol of epidermal cells and into trichomes. This cellular compartmentation of pH indicator dyes away from the cytosol is consistent with previous reports reviewed elsewhere (Hepler and Gunning, 1998; Roos, 2000). There has only been one report of the accumulation of a fluorescent indicator dye (fluorescein) into trichomes (of tomato leaves) (Barclay *et al.,* 1982)

There are many potential problems in using pH indicator dyes to monitor pH changes (Hepler and Gunning, 1998; Roos, 2000) particularly in loading the dye into the compartment of interest. Additionally, measurements in the cytosol are complicated by the need to ascertain whether the dye is actually inside the cytosol or within endomembranal vesicles or organelles. The application of pH indicator dyes can affect cellular ions and metabolism, potentially altering cellular function. Any ion-indicator dye inevitably adds to the cellular buffering capacity for the ion of interest, which may influence its local concentration, although in this case this effect is probably negligible when compared with the relatively high H^+ buffering capacity of the cytosol (Roos, 2000). Also, as described in the previous chapter, the submergence of leaves whilst studying signalling events associated with environmental stimuli is not an ideal method as it is likely to cause some trauma to the plant. Although not tested during this study, the confocal laser may cause problems by illuminating the leaves even in the 'dark' treatment. This could potentially be overcome by turning the intensity of the laser down. Some of the problems outlined

in this chapter could possibly be circumvented by using the recently discovered pH sensitive mutants of GFP combined with compartment specific expression vectors.

Vacuolar pH heterogeneity in barley root epidermal cells has been discovered by Miller and Smith (personal communication); two populations were identified with more acidic or alkaline vacuoles. The pH indicator dyes used in this study were not sufficiently sensitive within the pH range required to study vacuolar pH and therefore two populations of vacuolar pH could not be identified.

Plant leaves contain various auto-fluorescent chemicals other than those associated with the reactions of photosynthesis such as phenolic compounds, flavinoproteins, NAD(P)H, anthocyanins and lignins (Buschmann *et al.*, 2000). Studies into the localisation of phenolic compounds and other auto-fluorescent chemicals have typically involved using the CLSM under excitation by UV or blue light (e.g. Hulzler *et al.*, 1998). This technique has revealed the presence of phenolic compounds in a wide variety of locations including some in the apoplast and stomata (Hulzler *et al.*, 1998; Liakopoulos *et al.*, 2001). The auto-fluorescence shown here may originate from such phenolic compounds.

3.4.5 Conclusion

The dyes tested in this study were all shown to be unsuitable to monitor cytosolic pH changes in mesophyll cells under the conditions described. Confocal microscopy revealed the distribution of chlorophyll-containing chloroplasts within *Arabidopsis* leaves in mesophyll and guard cells but not in epidermal cells.

3.5 Conclusion

The use of pH indicator dyes with a confocal microscope was unsuitable to achieve the required results for this study. It was concluded that the use of pH-selective microelectrodes is a better method to investigate cytosolic pH change than use of pH indicator dyes with CLSM. The major disadvantage of using pH-selective microelectrodes in mesophyll cells of intact, aerial *Arabidopsis* leaves is the extremely technically demanding nature of the measurements. As an example, some

60 microelectrodes were manufactured and tested which yielded only 5 dynamic measurements in epidermal cells of wild type plants.

Measurements of cytosolic pH in mesophyll cells of wild type and NR^- mutant leaves during light/dark transitions are still needed as they may reveal the role of NR in the maintenance of cytosolic pH. Cytosolic pH in wild type plants would be expected to decrease in response to a light to dark transition and vice versa as previously reported for other photosynthetic tissues (Pallaghy and Lüttge, 1970). However, there are no previous reports of pH measurements made during light/dark transitions in NR^- mutant leaf cells. If the pH response in NR^- mutant mesophyll cells were the same as the wild type response then this would suggest no role for NR in maintaining cytosolic nitrate. Alternatively, if the pH response had been different then the role of NR in this process would have been confirmed. For these reasons further work on measurement in mesophyll cells using pH-selective microelectrodes should to be undertaken despite the technical difficulties.

4 LUMINESCENCE QUANTIFICATION OF NITRATE-INDUCIBLE LUCIFERASE-REPORTER PLANTS

4.1 Aim

The primary aim of the work described in this chapter was to develop a photomultiplier tube/fibre optic cable system to quantify luminescence ultimately from single cells of nitrate-inducible luciferase-reporter *Arabidopsis* plants. A second aim was to combine this technique with electrophysiology to study possible cytosolic ion activity changes associated with nitrate-induction of gene expression in single cells.

4.2 Introduction

The application of nitrate to plant cells induces many genes associated with nitrate uptake and utilisation (Wang *et al.*, 2000). In Chapter 2 the role of cytosolic nitrate activity in possible signalling events associated with changes in NR activity during light/dark transitions was investigated. This chapter describes experiments designed to investigate whether similar changes in cytosolic nitrate activity are associated with the induction of genes by nitrate. The extent of nitrate-induction was to be determined using nitrate-inducible luciferase-reporter plants and parallel changes in cytosolic nitrate activity measured using nitrate-selective microelectrodes.

Genes coding for enzymes that can be detected visually can be used to report (detect or quantify) gene expression in transgenic organisms, for example, genes coding for dyes or luminescence. Bioluminescence genes have been introduced as reporter genes to bacterial, mammal, yeast, viral and plant cells, (DeWet *et al.*, 1987; Mudge *et al.*, 1996; Aflalo, 1997). The light emitted from the bioluminescent enzymes, coded by the reporter genes, can be detected non-invasively using luminometers, photon counters, film and cameras (Ow *et al.*, 1986; Millar *et al.*, 1992; Michelet and Chua, 1996).

The North American firefly (*Photinus pyralus*) produces the enzyme luciferase that reacts with luciferin to produce light. The light emitted can be in various colours from yellow (582 nm) to green (522 nm) (DeLuca, 1976). In *Photinus*, luciferase is synthesised from a single copy of the *Luc* gene (DeWet *et al.*, 1987). This reaction was first characterised by DeLuca (1976). Initially luciferase catalyses the formation of D-luciferin adenylate (from D-luciferin and Mg-ATP). This is followed by the oxidation of acyladenylate by molecular oxygen, leading to the formation of an enzyme bound molecule in excited state. This decays to ground state oxyluciferin with emission of light. A simplified equation for the luciferin-luciferase reaction is given.

$$\text{Luciferin} + \text{Mg-ATP} + O_2 \rightarrow$$
$$\text{Oxyluciferin} + \text{AMP} + \text{Pi} + CO_2 + \text{Light}$$

At neutral pH luciferin carries a single negative charge and it is generally assumed that it will not cross the hydrophobic layer in the plasma membrane. Barnes (1990) extracted luciferin and measured its penetration in plant tissue and concluded that luciferin concentration was the same throughout the tissue after 20 min of exposure, except in senescent leaves. Schneider *et al.* (1990) studied the light distribution of plants expressing luciferase in different tissue to test whether the light distribution reflected the distribution of ATP, peroxisomes, luciferin or luciferase. It was concluded that the distribution represented luciferase activity. This evidence suggests that luciferase reporter genes give a good indication of the expression of a gene of interest. An additional advantage is that luciferin has no detectable toxicity (Ow *et al.*, 1986).

Luciferase is an excellent reporter gene; it is short lived in plant cells (Michelet and Chua, 1996), assaying luciferase activity is non-destructive and this reporter gene is capable of providing sensitive assays in real-time (Mudge *et al.*, 1996; Schneider *et al.*, 1990).

The experiments described in this chapter are sub-divided into three sections. The first describes the development of the photomultiplier tube/fibre optic cable system. The second describes the production of new and improved nitrate-inducible reporter plants and the third describes experiments to characterise them.

4.3 Quantifying luminescence from luciferase-reporter plants

4.3.1 Introduction

The *Arabidopsis* reporter plants used in this study were provided by Prof. M Caboche, INRA-Versailles, France. These plants contained the luciferase gene linked to the foliar *Nii* promoter encoding NiR from tobacco (Dorbe *et al.*, 1998). These reporter plants were called NiR*Luc*. The tobacco NiR promoter is 1.1 kb in length. Dorbe *et al.* (1998) showed that deletions from the start of the *Nii* gene of –962, -678 and –202 bp retained nitrate-inducibility whereas a deletion of –76 bp did not. Plants grown on reduced nitrogen sources, such as glutamine, contained little or no luciferase activity. Ten μM nitrate was sufficient to induce the β-glucuronidase (GUS) reporter gene attached to the full length tobacco *Nii* promoter in similarly produced GUS reporter plants (Dorbe *et al.*, 1998), although higher GUS activity was measured after induction with higher concentrations of nitrate. In order to develop the photomultiplier tube/fibre optic cable system, some positive control plants with the luciferase reporter gene linked to the strong CaMV (**Ca**uliflower **M**osaic **V**irus) 35S promoter were also provided by Prof. M Caboche. These strong constitutive luciferase expression plants were called 35S*Luc*.

4.3.2 Materials and Methods

Sigma-Aldrich Company Ltd., Poole, UK supplied all chemicals unless otherwise stated where appropriate catalogue numbers are given.

4.3.2.1 Culturing plant material

Plant material was cultured on sterile, vertical agar plates as described in Section 2.3.1.3. The agar solutions used were modified Hoagland's nutrient solutions (Section 2.3.1.1), either containing 10 mM nitrate (Hoagland's nutrient solution with the addition of 2.85 mM $Ca(NO_3)_2$) or 5 mM glutamine (added to a modified Hoagland's solution without KNO_3 and $Ca(NO_3)_2$, with the addition of 1.25 mM KCl and 4.35 mM $CaSO_4$).

4.3.2.2 Quantification of luminescence

Two methods were used to quantify luminescence from luciferase-reporter plants. The first technique used the photomultiplier tube / fibre optic cable (PTFOC) system developed as part of the work described here. The second method used a CCD camera system at the University of Warwick.

4.3.2.3 Photomultiplier tube / fibre optic cable system (PTFOC system)

This system was designed around a photomultiplier tube (9125A, Electron Tubes Ltd., Ruislip, UK in housing QL30F/RF1 with electrical screening and a voltage divider). Photomultiplier tubes are extremely sensitive light detectors providing current output proportional to light intensity. They have a large surface area for light detection and are able to detect single photons. The photomultiplier detects light at the photocathode, which emits electrons. These electrons are accelerated and focused onto the first dynode of an electron multiplier. On impact each electron liberates a number of secondary electrons, which are in turn accelerated and focused onto the next dynode. The process is repeated many times until the secondary electrons are collected at the anode.

The output from the photomultiplier tube was fed into the computer via a transimpedance amplifier (AD6, Electron Tubes Ltd., Ruislip, UK). This system required collection of photons from a very small area; therefore an adaptation was made to the front of the photomultiplier tube to connect a fibre optic cable (400 and 600μm diameter, 77512 and 77511, Oriel Lazers and Technology, Stratford, USA with a 77572 5MA connector on one end and the other open).

Data were output to an IBM-PC compatible computer. A computer counter timer board (CT1, Electron Tubes Ltd., Ruislip, UK) was put into the computer and data were collected and recorded using the associated computer software (Thorn EMI Photon Counter 1.1a, Electron Tubes Ltd., Ruislip, UK). This software could only collect data for 1.5 h at a time, so new files were opened during long experiments leading to interruptions in data gathering. The arrangement of the components of the PTFOC system is shown in Figure 4.1.

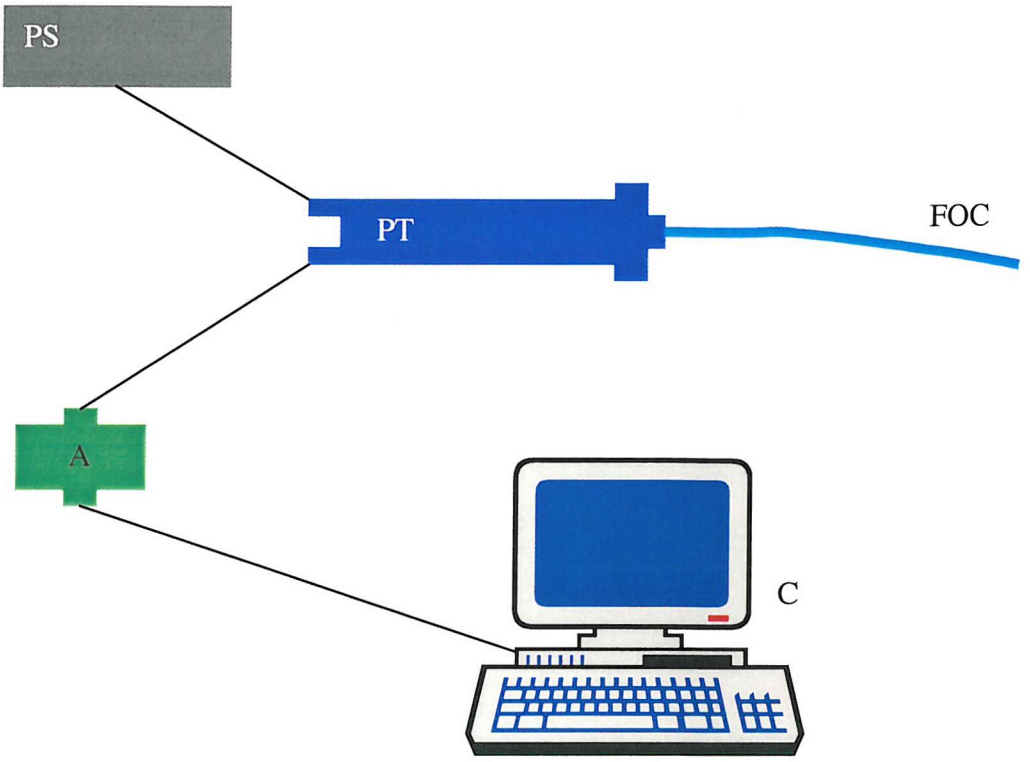

Figure 4.1 PTFOC system for measuring luciferase production plant cells.

Key: power supply, PS; photomultiplier tube, PT; fibre optic cable, FOC; amplifier, A; computer, C.

The 35S*Luc* plants were grown on nitrate containing agar plates. The NiR*Luc* plants were grown on glutamine containing agar plates; the leaves were immersed in a 4.25 mM nitrate solution for between 3 and 24 h prior to making a photon counting recording. Luminescence measurements from the PTFOC system were made in a dark room. Before developing the PTFOC system to study single cells, tests were done to measure luminescence (photon counts) from groups of cells by placing the fibre optic cable onto the leaves of plants. The photon counts from 600 μm diameter areas of leaf were measured for both the NiR*Luc* reporter and 35S*Luc* control plants. Photon counting recordings involved adding 1 mM D-luciferin (D-luciferin sodium salt, D-(-)-2-(6'hydroxy-2'-benzothiazolyl)-thiazoline-4-carboxylic acid, 1400, Analytical luminescence Laboratory, Sparks, USA) and 10 % (v/v) DMSO (dimethyl sulfoxide) after 3.5 min of steady background recording and recording continued for at least 1.5 h. If initial studies of leaf areas proved successful, the aim was to develop the PTFOC system to quantify luminescence from single cells. The fibre optic cable was to be placed down the barrel of a microelectrode attached to a micromanipulator

and luminescence combined with electrophysiological measurements made whilst the microelectrode was inserted into a cell.

4.3.2.4 CCD camera

Luminescence from luciferase-reporter plants cannot be adequately detected using conventional photography or video cameras. Specialised cameras or video systems are required, such as image intensified photon counting cameras or cooled slow scan CCD (charged coupled device) cameras (reviewed by Hooper *et al.,* 1994). The current study used a highly light sensitive, photon counting, imaging CCD camera (C2400-25 Hamamatsu Photonics Systems, Bridgewater, USA) in the laboratory of Dr. I. Carre, Department of Biological Sciences, University of Warwick. An ARGUS-200 controller (Hamamatsu Photonics Systems, Bridgewater, USA) accumulated signals from the camera. The associated image processing software corrected for background counts of thermal electrons, produced false colour images and performed area analysis to quantify luminescence from individual seedlings.

Luciferase expression in reporter plants is often 'leaky' (Dr. I. Carre, personal communication) therefore the 'baseline' luciferase activity has to be 'reset' to remove this luciferase by applying luciferin. 24 h prior to quantification of luciferase activity leaky luciferase activity was removed from the seedlings by 3 repeats (every 6 h) of spraying the seedlings with 5 mM D-luciferin and 0.01 % (v/v) triton X-100.

Nitrate-induction of the NiR*Luc* reporter plants was studied by comparing the luciferase activity of plants grown on either 10 mM nitrate or 5 mM glutamine as the sole nitrogen source (a direct comparison with the nitrate-induction experiments reported by Dorbe *et al.* (1998)). Immediately before image collection the seedlings were sprayed with 1 mM D-luciferin and 0.01 % (v/v) triton X-100.

4.3.3 Results

4.3.3.1 PTFOC system

Figure 4.2 shows an example of photon counts from a number of leaf cells from 35S*Luc* under the 600 μm diameter fibre optic cable. Photon counts from individual seedlings were very variable but always measurable under these conditions (n = 12).

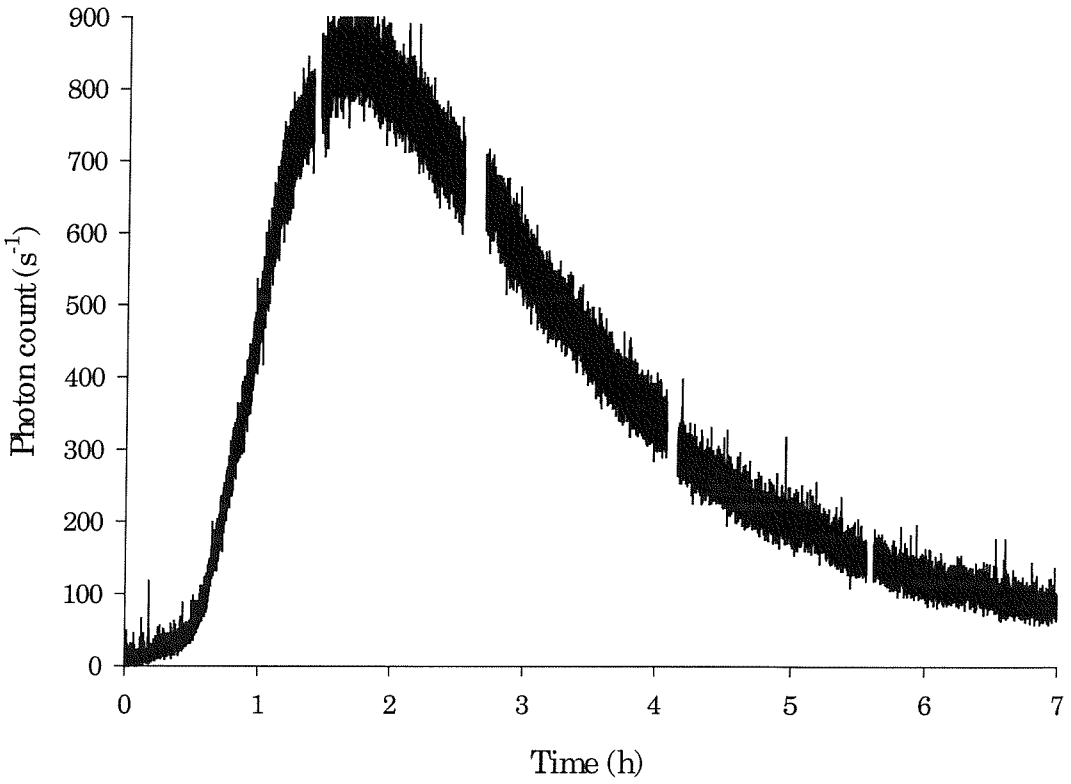

Figure 4.2 PTFOC measurement of a 35S*Luc* leaf, 1 mM D-luciferin applied after 5 min of recording.

The photomultiplier system was unable to detect signals above background photon counts from the 600 μm areas of leaves of NiR*Luc* reporter plants (n = 10) (data not shown). Consequently it was not appropriate to proceed to develop measurements from single cells.

4.3.3.2 CCD camera

Photon counting images of over 200 35S*Luc* and NiR*Luc* seedlings were obtained. Typical examples are shown in Figure 4.3. Figure 4.3a clearly shows a false colour image of luminescence from 35S*Luc* seedlings. Figure 4.3b shows a false colour image of NiR*Luc* seedlings; in this case luminescence was not detected.

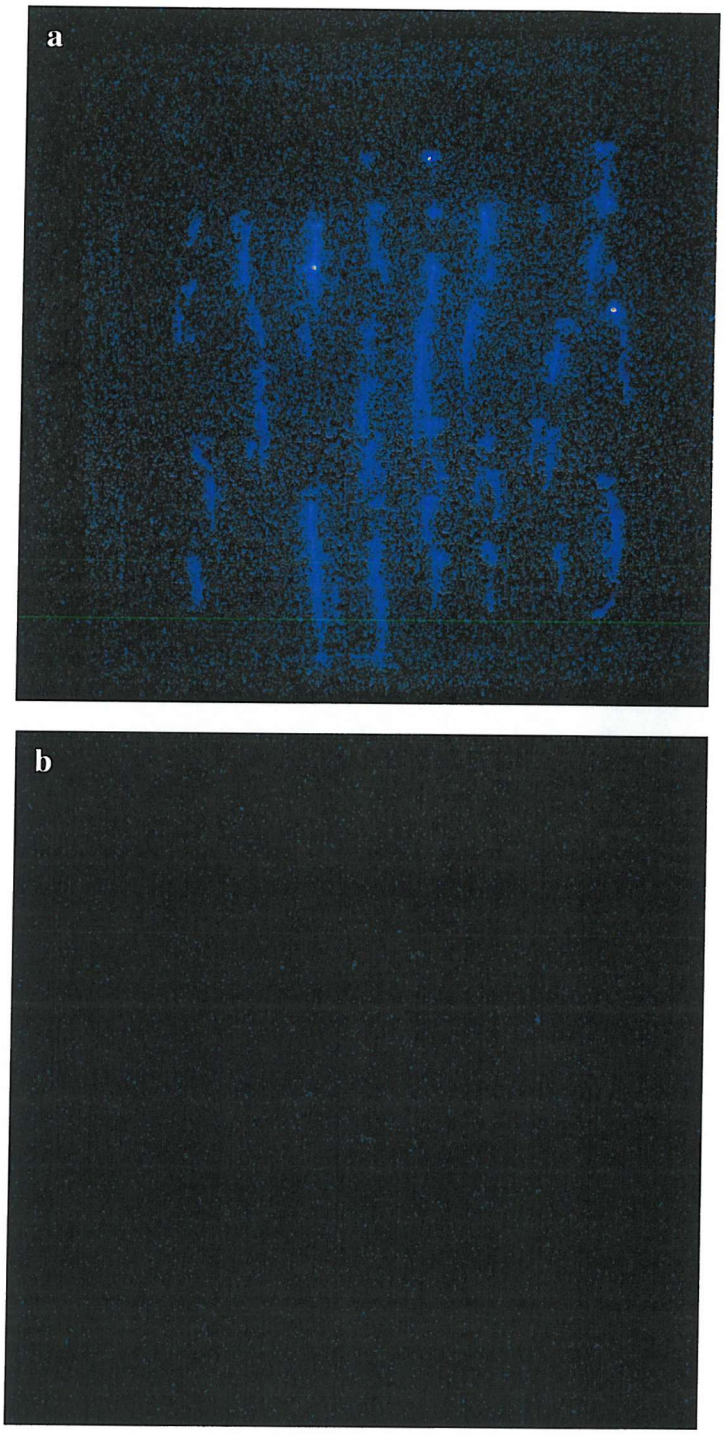

Figure 4.3 False colour CCD camera images of a) 35S*Luc* and b) NiR*Luc* seedlings grown for 2 weeks on sterile vertical agar plates containing 4.25 mM nitrate after being sprayed with 1 mM luciferin, images collected for 25 min.

4.3.4 Discussion

The ability of the PTFOC system to detect luminescence from the 35S*Luc* plants demonstrated the suitability of this system to quantify luminescence from small leaf areas of luciferase expressing plants. However, no luminescence was detected from the NiR*Luc* plants. This failure of the PTFOC system to detect luminescence from the NiR*Luc* reporter plants prompted an investigation of these reporter plants with an already established technique, using a photon-counting imaging CCD camera. The results of studying the NiR*Luc* plants with the camera showed that the luciferase activity was undetectable. Additionally, the luciferase activity in both the NiR*Luc* and 35S*Luc* seedlings was extremely poor in comparison with other luciferase-reporter plants (Dr. I. Carre, personal communication).

These luciferase-reporter plants had been produced using an old, low efficiency luciferase reporter gene (Riggs and Chrispeels, 1987) based upon the native firefly enzyme (De Wet *et al.*, 1985). Better reporter genes are now commercially available. In fireflies, luciferase is localised in the lantern (photocyte); the enzyme is targeted to the peroxisomes by a peptide signal of the last three c-terminal amino acids, Lys-Ser-Leu (Gould *et al.,* 1987; 1989). Removal of these terminal amino acids does not influence enzyme activity but converts the peroxisomal luciferase to a cytoplasmic enzyme (Gould *et al.,* 1989). The adapted luciferase reporter gene is called *Luc*+ (Promega Corporation, Madison, USA) and gives 10 to100 times greater expression.

4.3.5 Conclusion

Although the PTFOC system was developed successfully, the low luciferase activity produced by the NiR*Luc* reporter plants precluded the achievement of the secondary aim of this study. The extent of nitrate-induction of the reporter plants provided could not be determined using either of the methods described above. Consequently the measurement of cytosolic ion activity during nitrate-induction was not attempted. To achieve this aim it would be necessary to produce new reporter plants incorporating the new improved luciferase reporter gene, *Luc*+. The production of the new nitrate-inducible reporter plants is the subject of the following section.

4.4 Making new improved nitrate-inducible luciferase-reporter plants

4.4.1 Introduction

This introduction is a review of the background to the production of improved nitrate-inducible luciferase-reporter plants, comprising the selection of the component genes used for transformation and the method of effecting the *Arabidopsis* transformation.

4.4.1.1 Selecting the components of improved nitrate-inducible reporter plants

The application of nitrate is known to induce many genes such as nitrate transporters and assimilation enzymes. Wang *et al.* (2000) have shown that the genes strongly and rapidly induced by nitrate are those associated with nitrite reduction and those generating reductant; this is unsurprising as nitrite is toxic. The strong induction of NiR by nitrate makes NiR an ideal gene to use in producing nitrate-inducible reporter plants.

The study described in the previous section used plants provided by Dorbe *et al.* (1998). These plants contained an old, low-efficiency, luciferase reporter gene; an alternative could contain the newly developed luciferase reporter gene, *Luc*+. The NiR*Luc.* reporter plants also contained the *Nii* tobacco promoter encoded for foliar NiR. The value of reporter plants for future electrophysiology experiments could be increased by using a promoter that was also expressed in root cells. A possible alternative could be the nitrate-inducible 330 bp region of the spinach *Nii* promoter, which is expressed in foliar and root cells (Rastogi *et al.,* 1993). The spinach *Nii* promoter was cloned and sequenced by Back *et al.* (1991). It is called NiR792. The upstream regulatory region is 3.1 kb. Back *et al.* (1991) used this region to express the GUS reporter gene in transgenic tobacco. They found that the synthesis of GUS was regulated by nitrate availability; changes in GUS reflected changes in NiR mRNA.

Rastogi *et al.* (1993) showed that NiR was not induced in plants grown on ammonium as the sole nitrogen source. Leaves of plants supplied with nitrate had the highest GUS expression in the mesophyll cells. GUS activity was also high in the vascular tissue and stems. Roots of plants supplied with nitrate had high GUS activity in the vascular tissue and the surrounding cortical cells, but none in the root tip or epidermal cells. Rastogi *et al.* (1993) also studied the kinetics of nitrate-induction;

plants were grown on ammonium as the sole nitrogen source and then 20 mM nitrate was applied. GUS activity was not detected after 1 h. In root tissue weak GUS activity was detected after 2 h and maximum activity after 6 h. In leaf tissue GUS activity was detected weakly after 6 h and well after 24 h. This is similar to NR induction reported by Galangau *et al.* (1988) and NiR induction in maize (Kramer *et al.*, 1989).

Sivansanker *et al.* (1998) showed that NiR gene was repressed by products of nitrogen assimilation (e.g. glutamine and asparagine) in promoter fragments of -3.1 kb to -230 bp from the start of the *Nii* gene. The untranslated leader region of 0 to +67 is important in minimal induction in the presence of nitrate, and Sivansanker *et al.* (1998) showed the concentration-dependent competitive binding of a factor in tobacco nuclear extracts to this region.

Odell *et al.* (1985) studied the strong, non-tissue specific expressing CaMV 35S promoter and discovered the presence of a region of the sequence that increased the level of transcription. They suggested the use of these 'enhancer' sequences in increasing the transcription of a foreign promoter. Kay *et al.* (1987) was the first report of the use of these enhancer sequences to enhance gene expression in plants. Enhancer sequences (generally tetramers) incorporated into plasmids have been used in a wide variety of experiments (e.g. Walden *et al.*, 1994).

4.4.1.2 Transforming *Arabidopsis*

The ability to express or inactivate plant genes via the stable introduction of specific transgenes has become a powerful tool in the study of physiological, biochemical and molecular systems. The introduction of transgenes may be achieved by various means such as physical methods (electroporation, ballistics, ultrasonication, microinjection) or *Agrobacterium tumefaciens* or *rhizogene* mediated transformation. In the past these techniques have transformed *in vitro* cultured cells or tissues but more recent techniques have eliminated the time-consuming tissue culture procedures and developed transformation *in planta* (Katavic *et al.*, 1994).

The transformation method used here is based on that of Bechtold *et al.* (1993). This is now the most efficient, reproducible and widely used technique for transforming *Arabidopsis thaliana*. The method consists of the vacuum infiltration of *A. tumefaciens* into premature flower buds and the transfer of transgenes into the gametophytic tissues of the developing flower, to produce transformants, which can

be selected from the T_1 seed. The female reproductive tissues are the primary target of *A. tumefaciens* mediated transformation by this method. Transformants from the same seed pod represent independent T-DNA insertion events (Desfeux *et al.*, 2000).

The first step towards the development of the technique used in this study was the discovery of a large extrachromosomal plasmid of the virulent strains of the 'Crown Gall' bacterium *A. tumefaciens,* which possesses all of the genes necessary for gall-tumour induction (Zaenen *et al.*, 1974). This plasmid was named the Ti plasmid (**T**umour **i**nducing). One study of gall cell cultures detected 20 copies of a section of Ti plasmid from *A. tumefaciens* (Chilton *et al.*, 1977). The DNA section that transferred into the plant genome is referred to as T-DNA (**T**ransfer-**DNA**).

Proteins encoded by a 40 kb operon (known as *vir*- or virulence region) of the Ti plasmid located outside the T-DNA are essential to the T-DNA transfer process. This process begins with the formation of 'nicks' in 24 bp imperfect-repeat sequences at the left and right borders of the T-DNA. A single stranded T-DNA template is then synthesised from the sequence between the nicks (Stachel *et al.*, 1986). The T-DNA is accompanied into the host cell by a *vir* operon-encoded protein which contains sequences for nuclear targeting in plant cells and which also protects the T-DNA from nuclease denaturation prior to incorporation into the plant genome (Herrera-Estrella *et al.*, 1990). This discovery implied that the transfer of DNA by *A. tumefaciens* could be exploited for specific genetic engineering purposes.

The most commonly used *A. tumefaciens* transformation strategy and the one used here employs a binary vector (BIN vector) system (Bevan, 1984). This system involves two separate plasmids that are introduced into *A. tumefaciens* to facilitate the gene transfer. The first plasmid is a modified version of the naturally occurring Ti plasmid, 'disarmed' by the removal of the T-DNA and the 24 bp imperfect-repeat sequences to prevent the transfer of tumour inducing genes, the *vir* genes remain intact (Hoekema *et al.*, 1983). The second plasmid, or binary vector, is smaller and easier to manipulate in the laboratory possessing a multicloning site between artificial T-DNA borders (Hoekema *et al.*, 1983). A gene conferring antibiotic resistance is also included between the T-DNA borders, usually the neomycin phosphotransferase (*npt*II) gene that confers resistance to kanamycin (Bevan *et al.*, 1983). Any gene can be cloned into the multicloning site of the T-DNA region and if successfully incorporated into the genome will be expressed in a host plant. The number of copies

of the T-DNA and the positions at which they are incorporated into the host genome result in a wide variation of expression levels between transformant lines.

4.4.2 Materials and Methods

All general molecular biology methods were as described in Maniatis *et al.* (1982). Sigma-Aldrich Company Ltd., Poole, UK supplied all chemicals unless otherwise stated (where appropriate catalogue numbers are given).

4.4.2.1 Restriction digestion of plasmid DNA

Restriction enzymes and buffers were from MBI Fermentas (supplied by Helena Biosciences Ltd., Sunderland, UK), GIBCO BRL Life Technologies Ltd., Paisley, UK or Stratagene Ltd., La Jolla, USA. Usually 2.0 μg of plasmid DNA was digested in a reaction volume of 10 μl. A reaction consisted of 5 units of each restriction endonuclease (0.5 μl), 1 μl of the appropriate 10 x buffer, 2.0 μl of the plasmid preparation with the reaction volume made up with sterile deionised water. The reaction was incubated for 1 h at 37 °C.

4.4.2.2 Electrophoresis of agarose gels

DNA was separated on an agarose gel. A 1 % (w/v) agarose gel was prepared in TAE buffer (40 mM Tris base, Tris(hydroxymethyl)aminomethane, approximately 1 M glacial acetic acid, 50 mM EDTA, ethylenediaminetetraacetic acid, pH 8.0) with 0.5 μg ml^{-1} ethidium bromide. The DNA sample was mixed in a 5:1 ratio with loading buffer (0.25 % (w/v) bromophenol blue, 0.25 % (w/v) xylene cyanole FF and 15 % (w/v) Ficoll 400). The sample was then loaded into a well at the cathode end of the gel in a gel tank containing TAE buffer solution. Electrophoresis was typically done at 80 volts for 45-90 min, according to the size of the gel tank and the expected size of the fragments of interest. The DNA fragment size was compared with a 1 kb DNA Ladder (201115, Stratagene Ltd., Cambridge, UK). DNA was visualised using a short wavelength ultra-violet transilluminator (Eagle Eye II, Strategene Ltd., Cambridge, UK).

4.4.2.3 Recovery of DNA from agarose gels

DNA was recovered from agarose gels using a 'QIAquick Gel Extraction Kit' (28704, QIAGEN Ltd., Crawley, UK) using a microcentrifuge.

4.4.2.4 Phenol:chlorform extraction of DNA

DNA was extracted from aqueous solution by adding one volume phenol:chloroform isoamylalcohol (25:24:1) pH 8.0 to the sample, mixing thoroughly and then centrifuging at 13000 g for 5 min. The two phases separated and the upper aqueous phase was carefully removed and put in a new Eppendorf tube. Traces of phenol were removed using a column made of a 1:1 mix of Sepharose CL-68 in a tris-EDTA buffer (10 mM Tris base and 1 mM EDTA, pH 8.0).

4.4.2.5 Ethanol precipitation of DNA

Two volumes ethanol and a 0.1 volume 3 M sodium acetate (pH 5.2 adjusted with acetic acid) were added to the DNA sample and incubated for at least 1 h at -20 ^{o}C. The sample was centrifuged at 13000 g at 0 ^{o}C for 20 min. The supernatant was discarded and the pellet was dried. The pellet was then resuspended in an appropriate solution.

4.4.2.6 Phosphatase procedure

Some of the sub-cloning required ligating new fragments into plasmids that were capable of self-ligation. In order to prevent the plasmid from self-ligating the phosphate groups at the end of the digested plasmid were removed using a phosphatase kit (Alkaline Phosphatase, 600015, Stratagene Ltd., Cambridge, UK) according to the manufacturer's instructions. After the procedure the phosphatase enzyme had to be removed; it is a long-lived enzyme that would continue to remove the phosphate groups in subsequent reactions and prevent them from successful completion. The enzyme was initially denatured by heat shock to 70 ^{o}C for 15 min and was then removed by phenol:chloroform extraction (see Section 4.4.2.4).

4.4.2.7 Ligating new fragments of DNA into a new plasmid vector

When necessary, phosphate groups were removed from the digested vector (see Section 4.4.2.6). The fragment to be inserted retained the phosphate groups to allow the ligation reaction to proceed. Concentrations of the vector and the fragment DNA

were ligated at the approximate compatible end molar ratios of 1:3, 1:1 and 1:$^1/_3$. A typical 10 µl ligation reaction mixture contained 1 µl of T4 DNA ligase enzyme (equivalent to 5 units), 1 µl of T4 DNA ligase buffer, vector and fragment DNA. The reaction was incubated in a water bath at 23 °C for 2 h. Each ligation reaction was accompanied by control reactions. One control used only digested plasmid to test the efficiency of the T4 DNA ligase. A second control used where appropriate comprised only phosphatased digested plasmid to test the efficiency of the phosphatase procedure. The third control contained only the insert fragment to test for contamination.

4.4.2.8 Transforming *Escherichia coli* competent cells

The *E. coli* ultra-competent cells used were the XL2-Blue strain (200150, Stratagene Ltd., Cambridge, UK). These cells were transformed according to the recommendations of the manufacturer. Each *E. coli* competent cell transformation was accompanied by suitable positive and negative controls. A positive control of circularised plasmid DNA was used. 50 µl of transformed cells was plated onto Luria – Bertani (LB) agar plates containing the appropriate antibiotic (l^{-1}, 10 g NaCl, 10 g bacto – tryptone (0123-17-0, DIFCO Laboratories, Detroit, USA), 5 g yeast extract (Merck KGaA, Darmstadt, Germany), 1 l deionised water adjusted to pH 7.0 with NaOH, 20 g bacto-agar (0140-01, DIFCO Laboratories, Detroit, USA), autoclaved, poured and allowed to solidify in a sterile laminar flow work station). The plates were inverted and incubated overnight at 37 °C.

4.4.2.9 Plasmid DNA isolation from *E. coli*

Plasmid DNA was isolated using the 'QIAprep Miniprep Kit' (27106, QIAGEN Ltd., Crawley, UK), following manufacturer's recommendations.

4.4.2.10 Production of nitrate-inducible constructs

The backbone of the cloning plasmid used was from the cloning vector pAL25, a 6603 bp plasmid containing: carbenicillin resistance, the *Luc+* gene (accession number: U47122, pGL3, Promega Corporation, Madison, USA) under the *Ubi1* ubiquitin promoter and leader intron. In order to use the pAL25 plasmid the *Ubi1* promoter and leader intron were removed using a *Pst*I restriction enzyme cutting at sites 2251 and 4237. The appropriate fragment was extracted from the gel and ligated

together to form the *Luc*+ cloning plasmid vector, p*Luc*+, for subsequent cloning experiments. Figure 4.4 below shows a diagrammatic representation of pAL25.

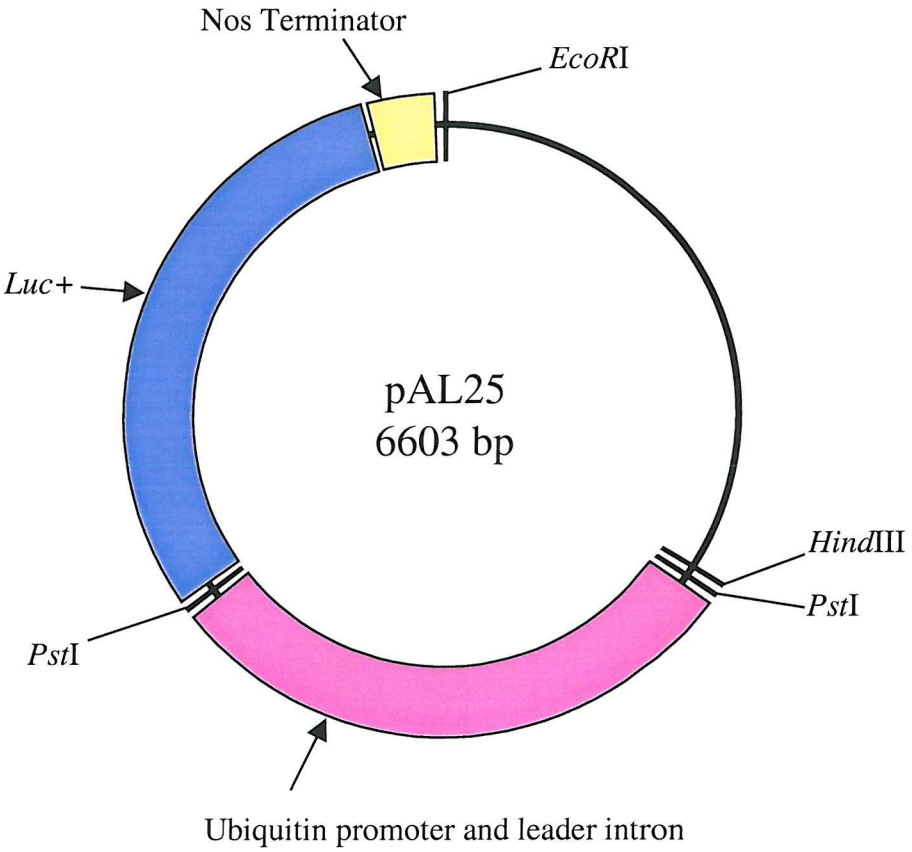

Figure 4.4 Diagrammatic representation of pAL25 with the genes and restriction sites of interest marked.

Key: transcription termination region of the **No**paline **s**ynthase (Nos) gene, Nos terminator.

Rastogi *et al.* (1993) discovered that the spinach NiR gene (accession number 17031) required only a 330 bp region of the promoter to be nitrate-inducible (as described in Section 4.4.1.1). A plasmid produced by Back *et al.* (1991), NiR792, was used for cloning as it included a *BamH*I site before the 330 bp region and introduced 2 extra bases to create a *Bgl*II site at the other end of the 330 bp region. The NiR792 plasmid was digested with *BamH*I and *Bgl*II and the appropriate fragment was excised from the gel and purified. The fragment produced was

approximately 460 bp in length containing the 330 bp nitrate-inducible region of the promoter and 130 bp of untranslated leader sequence.

Plasmid p*Luc*+ contained a unique *BamH*I site before the start of the *Luc*+ gene (site 4251) and was digested using the *BamH*I restriction enzyme. The resulting fragment was run on an agarose gel to check that the p*Luc*+ vector had been fully digested. The phosphatase procedure was used to prevent the p*Luc*+ cloning vector from self-ligating at the *BamH*I site. The resulting plasmid vector was ligated to the NiR fragment that retained the phosphate groups. *E. coli* competent cells were transformed using the ligation mixtures and selected using carbenicillin (60 μg ml^{-1}, C3416) resistance on LB agar plates. Twelve of the resulting colonies were used to inoculate liquid LB media and grown in overnight shaking cultures. Plasmids were extracted from the liquid media cultures. The plasmids containing the NiR promoter fragment in the correct orientation were selected by digesting the resulting colonies with *BamH*I and another restriction enzyme (*EcoR*I or *Nco*I) that cuts elsewhere in the plasmid. This test for orientation was based upon the knowledge that the combination of a *BamH*I and a *Bgl*II site would destroy the restriction site whereas the combination of two *BamH*I sites would preserve the site. Plasmids containing the NiR promoter fragment in the correct orientation in the cloning vector plasmid were subsequently called pNiR*Luc*+ plasmids (as shown in Figure 4.5).

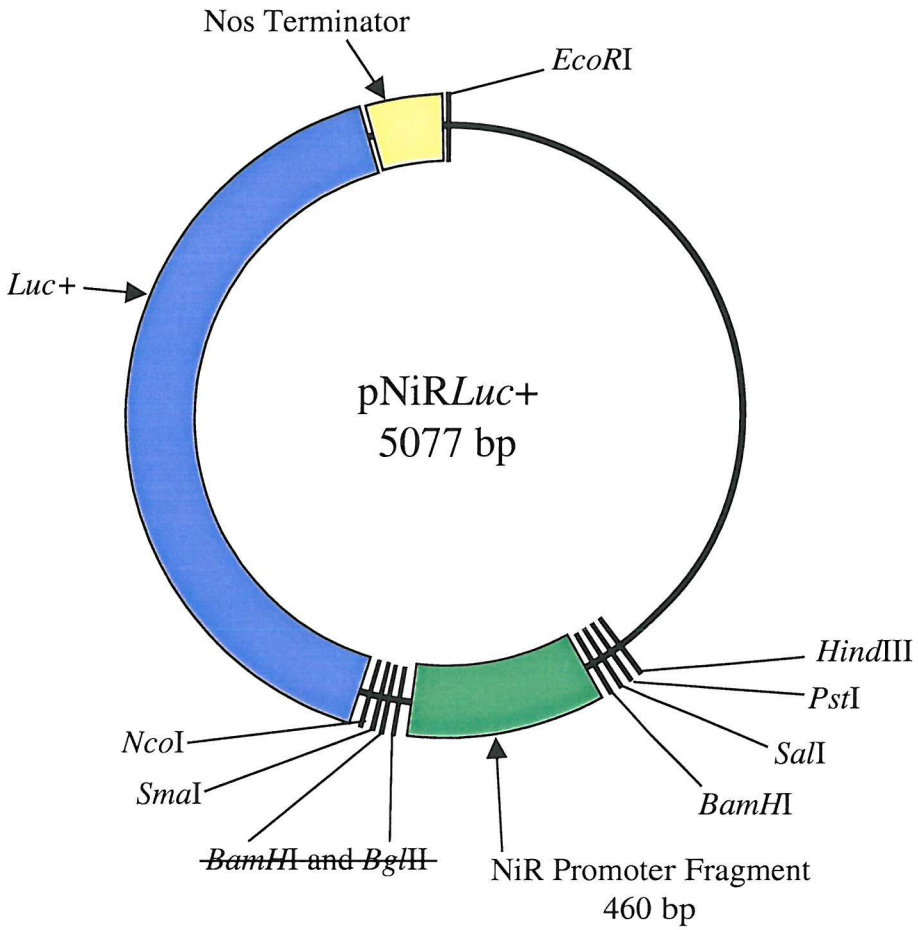

Figure 4.5 Diagrammatic representation of the pNiR*Luc*+ plasmid with genes and restriction sites of interest marked, *BamH*I and *Bgl*II restriction site destruction shown.

Regions of the 35S CaMV promoter are able to enhance transcription of the downstream promoter; these regions are called enhancer sequences (Odell *et al.*, 1985). Some of these 35S enhancer sequences were added in front of the NiR promoter region to increase transcription of the *Luc*+ but retain the nitrate inducibility of the promoter. The pCS101 plasmid (Guilley *et al.*, 1982) containing the 35S CaMV promoter (accession number: af044029) was used as a template for a polymerase chain reaction (PCR) to clone the promoter sequence. The region of interest was from -423 to –90; primers were designed to add a *BamH*I site to the start of the fragment and a *Bgl*II site to the end of the fragment (as shown below).

Primers 5' – 3' produced by Sigma-Genosys Ltd., Poole, UK:

1. CGGGATCCAAAAATATCAAAGATACAGTCTC
2. GAAGATCTTTATTTGTTCCTATTGTGCGTCAT

Primer 1 binds at the -420 region of the 35S enhancer sequence and a *BamHI* was added at the 5' end. Primer 2 binds at the -90 region of the 35S enhancer sequence and a *Bgl*II was added at the 5' end.

The reaction was mixed according to the manufacturer's instructions, using the enzyme *PfuTurbo*^{TM} DNA polymerase (Stratagene Ltd., Cambridge, UK) and a Hybaid Omnigene PCR machine (A3114, Omnigene HBTR3CM, Hybaid Ltd., Teddington, UK). The cycle used is shown below.

PCR cycle:
94 °C for 1 min, 57 °C for 45 s, 72 °C for 1 min cycled 10 times and then 94 °C for 45 s, 68 °C for 55 s, 72 °C for 1 min cycled 20 times followed by a polishing step of 10 min at 72 °C.

The first method devised to produce pNiR*Luc*+ with multiple 35S enhancer sequences was to digest the 35S enhancer PCR products with *BamHI* and *Bgl* II to reveal the restriction sites. These PCR products were then ethanol precipitated to remove any fragments of DNA and then ligated together. The ligated 35S enhancer sequences were then run on a gel. Some 2 x, 3 x and 4 x 35S enhancer sequence fragments were produced and these were extracted from the gel. These 35S enhancer sequence fragments were then digested with *BamHI* and *Bgl*II to break down any multiple 35S enhancer sequences in the incorrect orientation. The resulting digests were then run on a gel, and the 2 x, 3 x and 4 x 35S enhancer sequences (with all enhancers in the correct orientation) were gel extracted. The multiple 35S enhancer fragments were then ligated to phosphatased pNiR*Luc*+ plasmids. (This ligation was repeated six times unsuccessfully, possibly because there were insufficient quantities of the multiple 35S enhancer sequences in the ligation reactions.)

The second method attempted to produce pNiR*Luc*+ with multiple 35S enhancer sequences was to ligate into the construct a single 35S enhancer fragment, then to open the construct again and add another 35S enhancer fragment. The pNiR-

Luc+ plasmid was digested before the NiR promoter region using *BamH*I and the phosphate groups removed. The 35S enhancer sequence PCR products were digested with *BamH*I and *Bgl*II to reveal these restriction sites. The 35S enhancer sequence fragments produced were then ethanol precipitated in order to remove the small fragments of DNA produced during the digestion of the restriction sites. An excess of individual 35S enhancer sequence fragments were then ligated for 48 h into the pNiR*Luc*+ plasmid (with repeated additions of 0.5 μl T4 DNA Ligase during the reaction). *E. coli* were transformed with the ligation reactions. 36 of the colonies produced were used to inoculate liquid media, grown in shaking culture overnight and then plasmid DNA isolated. Plasmids containing the 35S enhancer inserts were screened on the basis of the *BamH*I to *Bgl*II restriction site destruction by digesting with *BamH*I and either *Nco*I or *EcoR*I.

The intention of this part of the cloning was to make successive *BamH*I digestions of the plasmid vectors containing 35S enhancer sequences and to insert more single 35S enhancer sequences. The objective was to create 35S enhancer tetramers in the construct, all in the correct orientation (tested with restriction digestion on the basis of the destruction on combination of *BamH*I and *Bgl*II at either end of the 35S enhancer fragment). However, only monomers and dimers of the 35S enhancer sequences were successfully incorporated into pNiR*Luc*+.

Three plasmid constructs suitable for the *Arabidopsis* transformation were produced, as illustrated in Figure 4.6. One construct did not contain any of the 35S enhancer sequences pNiR*Luc*+ whereas the other two contained either one or two 35S enhancer sequences, pNiR*Luc*+35S and pNiR*Luc*+35S35S respectively.

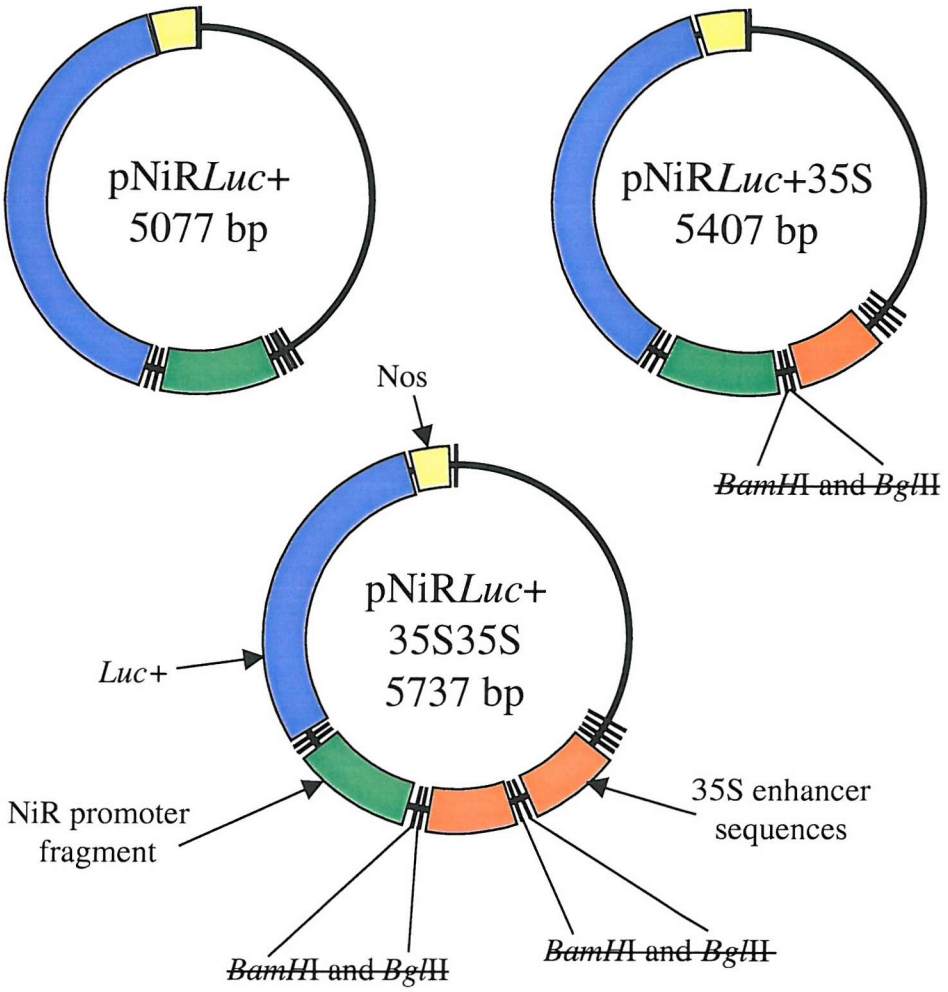

Figure 4.6 Diagrammatic representation of the plasmid constructs selected for *Arabidopsis* transformation, genes of interest and the destruction of *BamH*I and *Bgl*II restriction sites marked.

4.4.2.11 Sequencing of double stranded plasmid DNA

Plasmid DNA was sequenced using a 'DNA Sequencing Kit' (Dye Terminator Cycle Sequencing, Ready Reaction, 402079, ABI Prism, PE Applied Biosystems, Warrington, UK). Each sequencing reaction was assembled according to the manufacturer's instructions and the mixture was overlaid with two drops of mineral oil. The reaction cycle was done according to the manufacturer's instructions on a Hybaid Omnigene PCR machine. Data were collected using ABI Prism™ 310 Genetic Analyser linked to a Power Macintosh 7300/200 using sequence analysis software v.3 as supplied with the system. Sequence data were exported to the

STADEN suite of sequence handling programs where fluorescence traces were reconciled with the automated sequence data, and ambiguities resolved manually. Data was converted into GCG format (Wisconsin package version 10.1, **G**enetics **C**omputer **G**roup Inc., Madison, USA)) and compared with sequence data available in the NCBI database (National Center for Biotechnology Information, Bethesda, USA) via the world wide web (http://www.ncbi.nlm.nih.gov/).

4.4.2.12 Transferring the NiR*Luc*+ plasmids to the *A. tumefaciens* vector

The *A. tumefaciens* vector pBIN19 (Bevan, 1984) was used for transformation; this vector contained genes encoding for kanamycin resistance. The pNiR*Luc*+ plasmids (with or without the 35S enhancer sequences) were digested at the unique restriction sites *EcoR*I and *Hind*III to remove the genes of interest from the cloning vectors. The pBIN19 contained an extensive multiple cloning site that included *EcoR*I and *Hind*III in the correct orientation; therefore pBIN19 was also digested with these enzymes. The resulting digests were run on a gel and the appropriate sized fragments excised from the gel and gel purified. The fragments were then ligated together, *E. coli* transformed and the *A. tumefaciens* vector clones selected on kanamycin (50 μ ml^{-1}) containing LB plates. Colonies of *E. coli* were used to inoculate liquid LB media and grown overnight in shaking culture. Plasmids were isolated and those containing the appropriate fragment were identified by restriction enzyme digestion. These plasmids were then given the names pBIN-NiR*Luc*+ (without 35S enhancer sequences), pBIN-NiR*Luc*+35S (with a single 35S enhancer sequence) and pBIN-NiR*Luc*+35S35S (with two 35S enhancer sequences). The empty pBIN19 vector was also used as a control.

4.4.2.13 Electroporation to introduce the *A. tumefaciens* vector to the *A. tumefaciens* strain

Cultures of *A. tumefaciens* (strain GV3101 pmp90, Koncz and Schell, 1986) were grown overnight in YEB (yeast extract-beef) liquid medium (l^{-1}, 5 g beef extract powder, 1 g yeast extract, 5 g bacto-peptone (0118-17-0, DIFCO Laboratories, Detroit, USA), 5 g sucrose, 0.5 g $MgSO_4$ and the antibiotics gentamycin (50 $\mu g\ l^{-1}$) and rifampicin (25 $\mu g\ l^{-1}$)).

The preparation of the *A. tumefaciens* for electroporation was as follows. Step 1 was to cool on ice 20 ml of the culture. In step 2 cells were centrifuged at 12000 rpm, 4 ^{o}C for 10 min and the supernatant was discarded. In step 3 the resulting pellet

was re-suspended in 20 ml of 10 % glycerol (also cooled on ice). Step 4 repeated step 3 but re-suspended the pellet in 10, 4, 0.4 and 0.2 ml of 10 % glycerol (cooled on ice). 40 µl of the *A. tumefaciens*/glycerol mixture was added to the electroporation cuvette along with 10 µl of the appropriate *A. tumefaciens* plasmid vector (at a concentration of 5 ng DNA/µl). The 0.2 cm electroporation cuvettes were then placed in the electroporator (Gene Pulser™, BIORAD Ltd., Hemel Hempstead, UK). The field strength required was 12.5 kV cm^{-1} so field strength was set to 2.5kV/0.2 cm. The capacitance was set to 25 µF, the resistance set to 400 Ω and the time constant was 7.5 ms. Electroporation was then done. 1 ml of the appropriate medium was added to the contents of the cuvette and shaken at 28 °C and 125 rpm for 3 h. This was then centrifuged and the pellet resuspended in 110 µl of medium and spread out on agar plates containing antibiotics selecting for the *A. tumefaciens* strain and the *A. tumefaciens* vector. The plates were placed upside down in an incubator and allowed to grow for 3 d at 28 °C. Successfully electroporated *A. tumefaciens* colonies were confirmed using PCR with primers specific to the gene of interest.

4.4.2.14 'Floral dip' vacuum infiltration of *A. tumefaciens*

A large pot of compost and sand was covered in polythene and 9 individual plants were transplanted in the holes in the polythene and left to grow. 3 pots per construct were set up. The plants were grown in a controlled environment cabinet (20 °C , 75 % relative humidity with a 16 h day and a photon fluence of 280 - 300 µmol m^{-2} s^{-1}) for 4 to 6 weeks until the main bolts were 10 cm in height. The main bolts of all plants were clipped to 2.5 cm of bare stem to encourage the formation of multiple secondary bolts. After 5 d these plants were ready for transformation.

Two days before infiltration, each of the 4 types of transformed *A. tumefaciens* colonies were used to inoculate 50 ml of YEB medium and then grown overnight in shaking culture at 28 °C. The next day 10 ml of each culture was used to inoculate 500 ml of liquid culture then grown in the same conditions.

The *A. tumefaciens* cells were pelletted by centrifuging for 20 min at 7000 rpm and then resuspended in 200 ml of infiltration medium (l^{-1}, 2.2 g MS salts (Murashige and Skoog basal medium with Gamborg's vitamins), 50 g sucrose, 0.5 g MES, 0.044 µM benzylaminopurine, 200 µl Silwet L-77 (vac-in-stuff, VIS-01, OSI Specialities, Lehle Seeds, Texas, USA) and pH to 5.7 with KOH). The *A. tumefaciens* solution was further diluted with infiltration medium to give an $O.D._{600}$ of 2.4 to 2.6.

Approximately 500 ml of infiltration medium containing *A. tumefaciens* was placed in the bottom of a vacuum dessicator; one pot was inverted into the solution making sure all the flowers and buds were covered. A strong vacuum was applied for 5 min and then the plants were removed and drained. This was repeated using the same solution for a further 2 pots of plants. The plants were placed back into the greenhouse and covered with plastic film for 24 h and grown for a further 4 weeks until the seeds could be harvested.

4.4.2.15 Screening the seeds produced on kanamycin resistance plates

The pBIN19 vector transferred the genes of interest as well as the *nptII* gene (conferring resistance to the antibiotic kanamycin) to some of the plants. The putative transformed plants were selected on agar plates (l^{-1} 4.3 g MS salts, 0.5 g MES, pH 5.8, 8 g agar and 50 μg ml^{-1} kanamycin) as described in Section 2.3.1.3. Transformed plants were green and healthy whereas the un-transformed were yellow and died after 2 weeks. Putative transformants were confirmed by PCR and then transferred into soil culture. T_1 seeds were collected. The T_1 seeds were also screened on agar plates and those with kanamycin resistance planted to harvest the seeds. Then the seeds of T_2 homozygous lines were screened.

4.5 Characterising the nitrate-inducible luciferase-reporter plants

4.5.1 Introduction

This section describes some investigations into the nitrate-induction characteristics of the luciferase-reporter plants whose production was described in the previous section. Initial tests were done to ascertain whether the transformants were nitrate-inducible. Nitrate-inducible transformants were then identified and the best lines were selected. Further experiments were done to investigate the characteristics of nitrate-induction of the NiR promoter.

4.5.2 Methods

Plant material was cultured on sterile, vertical agar plates as described in Section 2.3.1.3. Seedlings were grown for 10 to 15 d on various nitrogen sources, either nitrate or reduced nitrogen sources such as ammonium succinate or glutamine.

One of the experiments investigating the properties of nitrate-induction of the NiR promoter was to examine the influence of functional NR. As described in Section 2.2.3, plants without functional NR may be produced by various means. Plants deficient in functional NR were produced by adding 0.5 mM tungstate to the growth medium. Tungstate inhibition of NR activity has been used previously in *Arabidopsis* plants (Zhuo *et al.,* 1999).

The light sensitive, photon counting, imaging CCD camera (as described in Section 4.3.2.4) was used in studies of the nitrate inducibility of the reporter plants. Leaky luciferase activity was removed by pre-spraying with luciferin as described in Section 4.3.2.4. All images were collected after 10 min exposure. Seedlings were nitrate-induced by a spray of nitrate solution.

4.5.3 Results

4.5.3.1 Luciferase-reporter *Arabidopsis* plants transformed with pBIN-NiR*Luc*+35S and pBIN-NiR*Luc*+35S35S

Images from the CCD camera revealed that the kanamycin resistant plants were also expressing the luciferase-reporter gene, as shown in Figure 4.7 below.

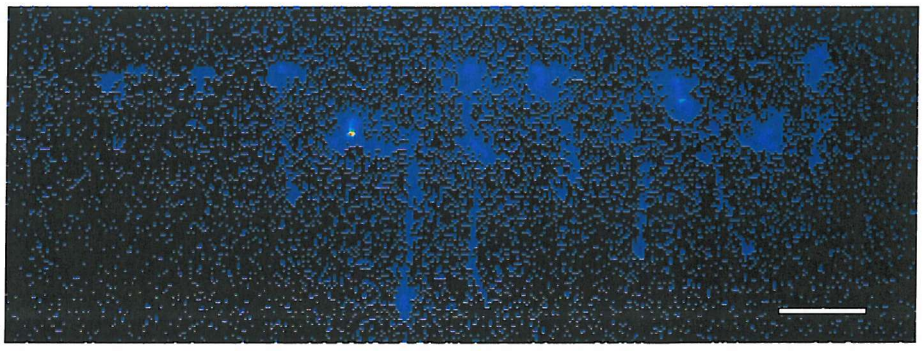

Figure 4.7 False colour CCD camera image of seedlings transformed with pBIN-NiR*Luc*+35S grown on sterile vertical agar plates containing 4.25 mM nitrate, scale bar 1 cm.

Figure 4.8 shows the results of a nitrate-induction experiment of plants transformed with the pBIN-NiR*Luc*+35S construct. The seedlings were grown on 5 mM glutamine and then sprayed with 10 mM of either calcium sulphate or nitrate. Whole seedling luminescence measurements were taken from 9 seedlings under each treatment. Prior to analysis dark frames were collected and subtracted from the recorded luminescence measurements. Seedling luminescence is expressed as a percentage of the pre-nitrate-induction photon count to remove the effect of seedling size differences, bars contain 95 % of the observations. There was no indication of significant nitrate-induction in these reporter plants; the average seedling luminescence changed to 112 % of pre-treatment level in those sprayed with sulphate solution and 148 % in those sprayed with nitrate solution. The average photon count per seedling was very high relative to other *Arabidopsis* luciferase-reporter plants (Dr. I. Carré, personal communication). Under both treatments seedling luminescence decreased transiently after 1 h under the CCD camera.

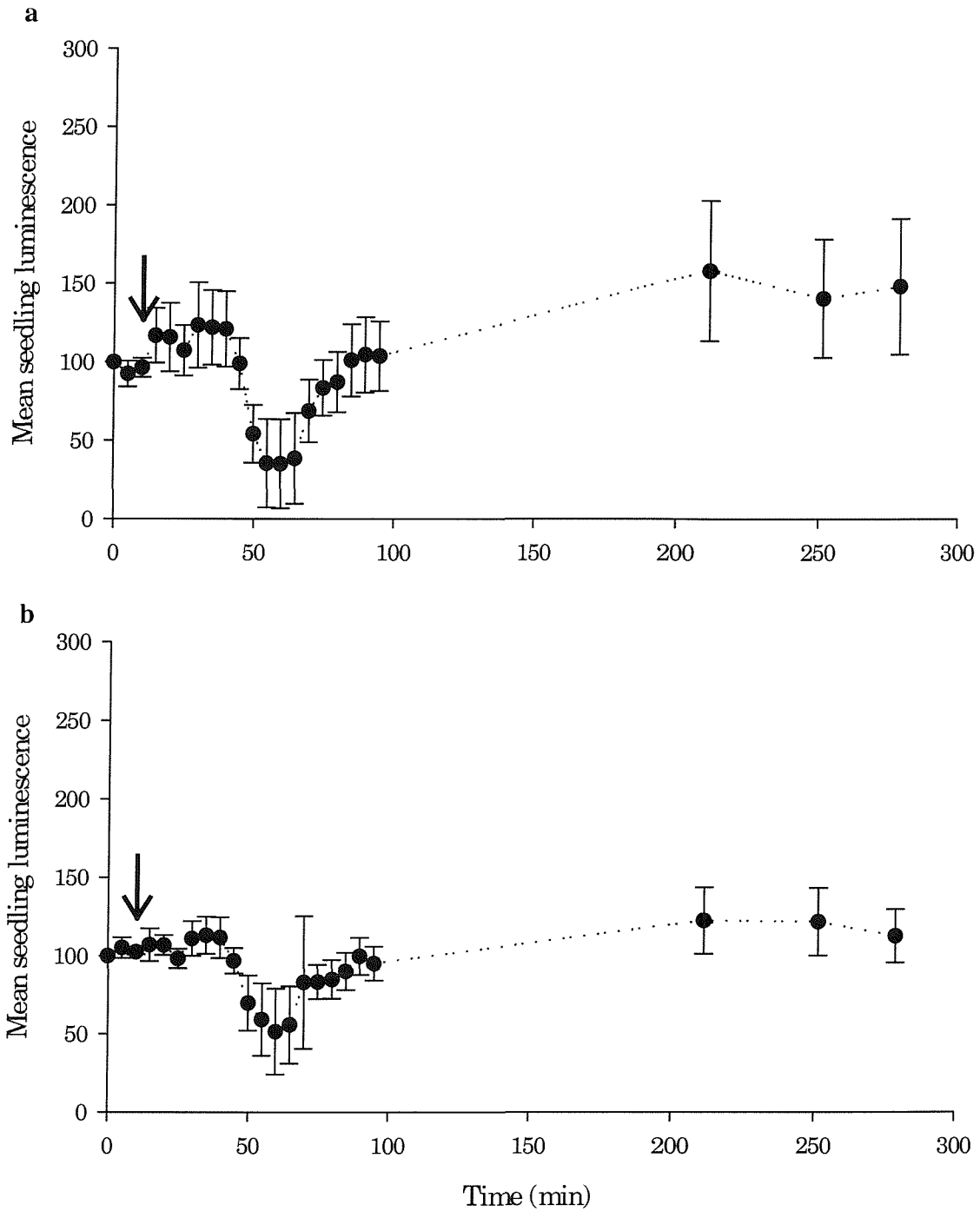

Figure 4.8 Mean percentage change in seedling luminescence (photon counts for 10 min) pBIN-NiR*Luc*+35S transformants grown on 5 mM glutamine, arrow indicates the time at which a spray of either 10 mM a) calcium nitrate or b) calcium sulphate solution occurred.

4.5.3.2 Luciferase-reporter *Arabidopsis* plants transformed with pBIN-NiR*Luc*+

Transformation of *Arabidopsis* with the pBIN-NiR*Luc*+ plasmid did not produce any kanamycin resistant plants on the first two attempts, but generated some transformants on the third attempt. Three pBIN-NiR*Luc*+ transformant lines were produced and were all shown to be nitrate-inducible as illustrated in Figure 4.9 below.

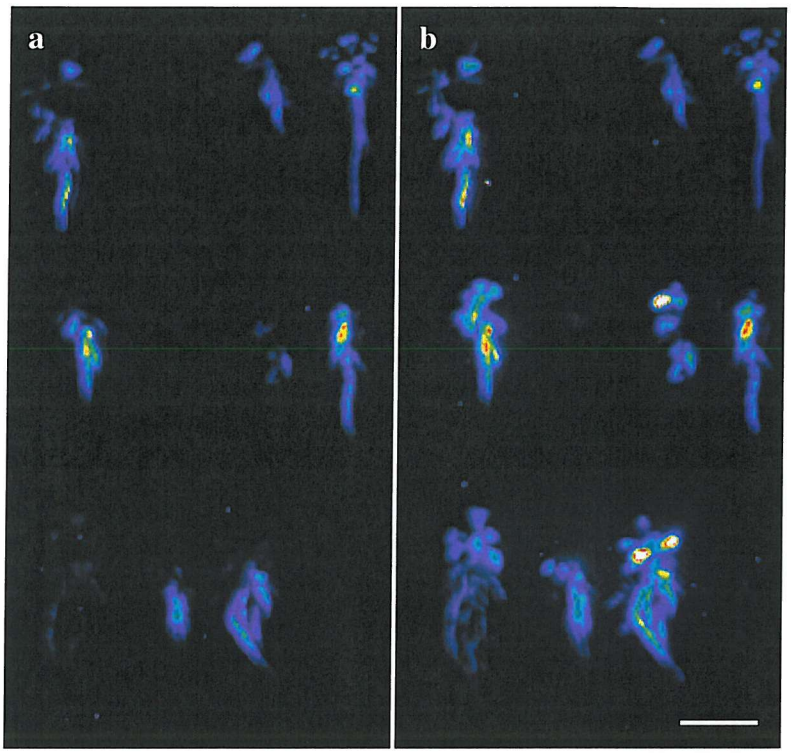

Figure 4.9 False colour CCD camera images of seedlings transformed with pBIN-NiR*Luc*+. The top row of seedlings is of Line 1, the second row is of Line 2 and the bottom row is of Line 3. This Figure shows a) seedlings grown for 15 d on a vertical agar plate containing ammonium succinate, b) the same seedlings 2.5 h after spraying with 10 mM nitrate, scale bar 1 cm.

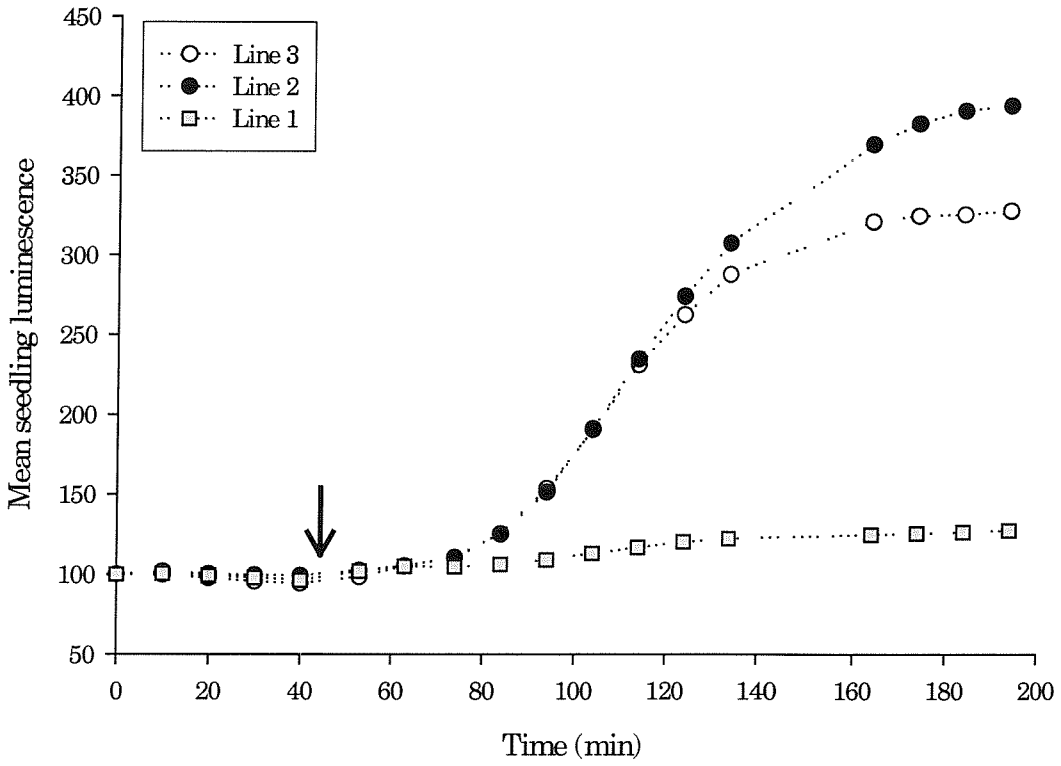

Figure 4.10 Mean percentage change in seedling luminescence (photon counts for 10 min) for each line of pBIN-NiR*Luc*+ transformants grown on ammonium succinate, arrow indicates the time at which the spray of 10 mM nitrate solution occurred.

Figure 4.10 shows the mean seedling luminescence for each line of pBIN-NiR*Luc*+. Line 1 produced the least nitrate-induction whereas Lines 2 and 3 produced very good induction. Further experiments were done using only Lines 2 and 3.

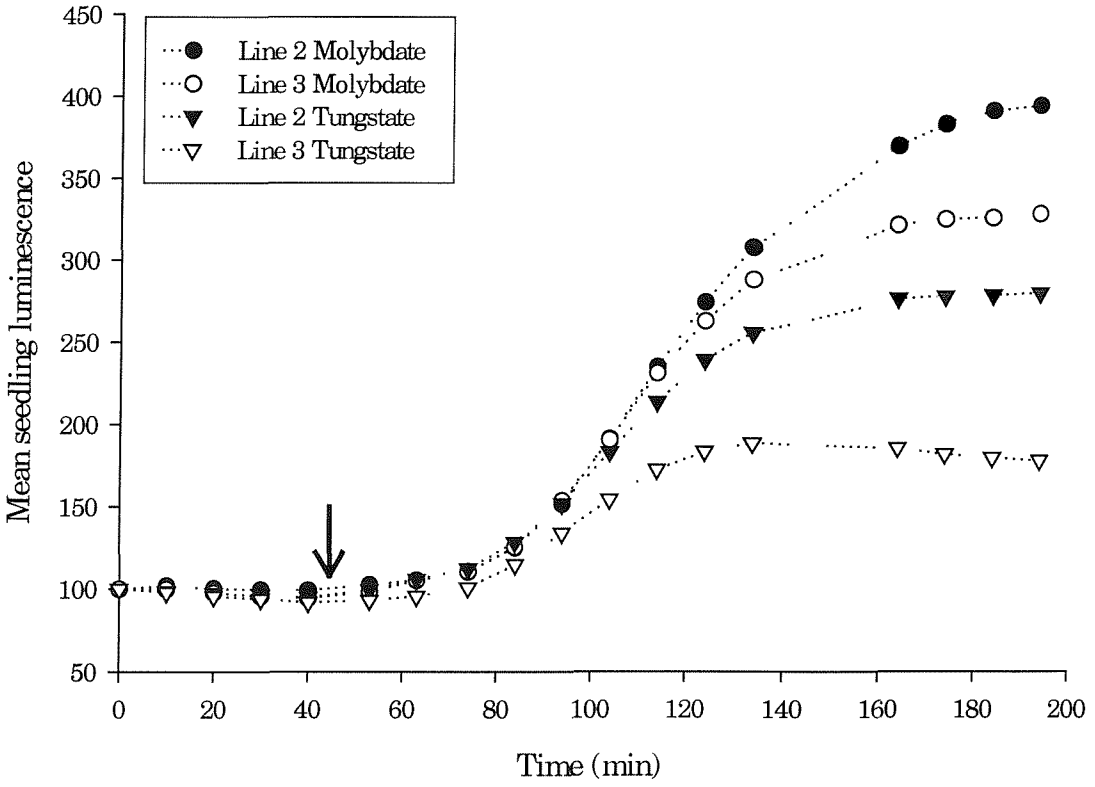

Figure 4.11 Mean percentage change in seedling luminescence (photon count for 10 min) of Line 2 (closed symbols) and Line 3 (open symbols) pBIN-NiR*Luc*+ transformants grown on ammonium succinate and either tungstate (▼) or molybdate (●), arrow indicates the time at which the spray of 10 mM nitrate solution occurred.

Figure 4.11 shows the mean percentage change in seedling luminescence for the two best pBIN-NiR*Luc*+ lines, Lines 2 and 3, grown on ammonium succinate with either 0.5 mM tungstate or 0.075 μM molybdate. In both lines, tungstate application reduced the intensity of nitrate-induced seedling luminescence.

4.5.4 Discussion

4.5.4.1 Luciferase-reporter *Arabidopsis* plants transformed with pBIN-NiR*Luc*+35S and pBIN-NiR*Luc*+35S35S

Rastogi *et al.* (1993) used the same NiR promoter fragment as the one used here connected to the GUS reporter gene. Rastogi *et al.* (1993) showed that there was only minimal expression in the root tip, whereas in the pBIN-NiR*Luc*+35S and pBIN-

NiR*Luc*+35S35S transformed plants the root tip was an area of strong luciferase activity (Figure 4.7). The pattern of luciferase expression from the plants transformed with pBIN-NiR*Luc*+35S and pBIN-NiR*Luc*+35S35S differed from a previous report of the expression pattern of the spinach NiR promoter (Rastogi *et al.*, 1993), indicating the loss of nitrate inducibility in these plants.

The pBIN-NiR*Luc*+35S and pBIN-NiR*Luc*+35S35S transformed plants were unsuitable for further use because they were not sufficiently nitrate-inducible for at least 4 h. The addition of 35S enhancer sequences has proved successful in numerous studies (e.g. Kay *et al.*, 1987; Walden *et al.*, 1994) but in this study such additions were not beneficial. The loss of promoter mediated inducibility and the subsequent gain of constitutive expression has been reported previously (e.g. Dorbe *et al.*, 1998). The inducibility of promoters with 35S enhancer sequences is highly unpredictable; however these enhancer sequences can greatly improve the expression of promoters of interest.

4.5.4.2 Luciferase-reporter *Arabidopsis* plants transformed with pBIN-NiR*Luc*+

The distribution of high luciferase activity in the pBIN-NiR*Luc*+ transformants was consistent with the expression patterns reported by Rastogi *et al.* (1993) using the same NiR promoter fragment with the GUS reporter gene. Maximum luciferase activity was usually located in the leaves and a few mm behind the root tip.

All three pBIN-NiR*Luc*+ lines produced were shown to be nitrate-inducible but to differing extents. Wide variation between transformants of different lines under induced and non-induced conditions has been reported previously and ascribed to the chromosomal location of the transgene (Rastogi *et al.*, 1993). There is also substantial variation between individual plants of the same line, which was reflected here and in the results reported in Rastogi *et al.* (1993).

Detection of nitrate-induction in the pBIN-NiR*Luc*+ transformants was considerably faster than that reported for GUS activity by Rastogi *et al.* (1993). Luciferase-reporter plants are generally more sensitive than GUS reporter plants (Schneider *et al.*, 1990). Luminescence changes were detected less than 1 h after nitrate application in the pBIN-NiR*Luc*+ plants. However, the conditions for the experiments reported and the species transformed here were not the same as those of Rastogi *et al.* (1993).

Tungstate application inhibited nitrate-induction of the pBIN-NiR*Luc*+ transformants replete in reduced nitrogen. Tungstate is assumed to affect the function of NR although effects on other MoCo containing enzymes are possible. Aslam and Huffaker (1989) also showed partial inhibition of NiR induction by tungstate in barley. Tungstate inhibition of nitrate transporters has been reported in *Arabidopsis* (Zhuo *et al.*, 1999). The inhibition of high affinity nitrate transporters has been shown to persist in *Arabidopsis* NR^- mutants (Lejay *et al.*, 1999). This inhibition of expression of high-affinity nitrate transporters is dependent upon the presence of a reduced nitrogen source during induction; in N starved plants there is no inhibition or even a stimulation of expression (Vidmar *et al.*, 2000). NR has been shown to regulate the expression of nitrite uptake and NiR activities in *Chlamydomonas-reinhardtii* (Navarro *et al.*, 1996) but they suggest that this could be due to a signalling role of nitrite produced. The tungstate inhibition of NiR and high affinity nitrate transporter induction indicate that the down regulation of these components is not entirely due to the products of nitrate assimilation. Therefore suggesting that NR itself may have a role in the regulation of NiR and high affinity nitrate transporter induction.

4.5.4.3 Decrease in luminescence

The decrease in luminescence from the seedlings under both conditions after approximately 1 h of camera recording may have been a result of transferring the seedlings to the dark, due to a decrease in cytosolic ATP limiting the luciferase-luciferin reaction.

4.6 Conclusion

The primary aim of the work described in this chapter, the development of the PTFOC system to quantify luminescence from luciferase-reporter plants, was successfully achieved. Studies using the PTFOC system developed to measure luminescence from the luciferase-reporter plants originally provided by Prof. M. Caboche revealed that they were unsuitable. As a consequence construction of new improved luciferase-reporter plants was begun and successfully completed. The luciferase-reporter plants without 35S enhancer sequences described in this chapter

were proven to be nitrate-inducible and provide a basis for further development of the work.

There is considerable scope for additional induction experiments using these newly developed plants. The *Nii* gene is regulated by numerous factors and investigations into these factors, such as nitrate, reduced N metabolites, light, hormones, sucrose, circadian rhythms, etc., may yield valuable results. Crossing these reporter plants with the NR^- mutants could assist the investigation into the requirement of NR for nitrate-induction of NiR.

A logical and valuable extension of the work described in this chapter would be to study nitrate-induction of single cells, the second aim of this chapter, if such a project were technically feasible. The variability between individuals of the same line of pBIN-NiR*Luc*+ transformants may pose a potential problem in such studies.

5 GENERAL DISCUSSION

5.1 Introduction

As described in Chapter 1, transporters associated with nitrate uptake and the enzymes of nitrate assimilation are under complex regulation. They are induced by nitrate, down regulated by down-stream metabolites and synchronised with carbon metabolism. Much research effort has gone into searching for the metabolite(s) that regulate nitrate uptake and assimilation, so far without unambiguous success. The subject of this study was cytosolic ion activity changes associated with modifications of NR activity and the nitrate-induction of NiR at the single-cell level. This chapter discusses the realisation of the objectives of this study and the conclusions that can be drawn from it, and how these relate to previously published work.

5.2 Novel technical developments

The completion of the practical work required the successful achievement of technical developments in a number of areas. The first of these was the hydroponic culture of *Arabidopsis*, which is known to be problematic (Prof. W.M. Kaiser, personnal communication). However the time and effort devoted to this development was essential for the accurate control of the nutrient supply to the plants.

The next development was the design of a chamber to hold *Arabidopsis* leaves during electrophysiological measurements. The measurements required were of aerial leaves of intact plants in as near natural conditions as possible so that normal signalling processes were not disrupted. The delicate nature and small size of the *Arabidopsis* leaves pose problems for electrophysiological measurements, which is one of the reasons why other species have usually been selected. Plant material needs to be held securely to allow the impalement of cells by the microelectrode tip and to ensure its retention in the cell. The new chamber was designed to allow electrical connection through the apoplast to the bath solution whilst keeping the leaves dry.

This development led to the first electrophysiological measurements of mesophyll cells of intact plants in near natural conditions. Previous measurements in mesophyll cells have involved significant trauma to the plant (Prins *et al.*, 1980; Elzenga *et al.*, 1995). The collection of confocal microscopy images also necessitated the design and construction of a new glass chamber to hold *Arabidopsis* leaves.

The PTFOC system constructed in this study and demonstrated to be capable of quantifying luminescence from small areas (600 μm) of luciferase-reporter plants was a further new development. The quantification of luminescence from small areas of cells could be of use for other projects in which imaging technologies (such as CCD cameras) cannot sufficiently resolve and quantify the spatial heterogeneity of luciferase expression. A significant part of the work described here involved the design and manufacture of reporter gene constructs and the production of new nitrate-inducible luciferase-reporter plants.

5.3 Theoretical and experimental limitations

The ability of the PTFOC system to quantify single-cell luminescence has not been demonstrated. The results presented in this thesis suggest there are serious technical difficulties that may prevent the successful completion of this objective. Placing the fibre optic cable next to a leaf collected luminescence from approximately 400 cells (estimated by counting the number of cells in a 600 μm diameter circle of the confocal microscopy data sets collected in Chapter 3). The pBIN-NiR*Luc*+ luciferase-reporter plants produced in the project were at least three times more luminescent than those of the 35S*Luc* plants provided by Prof. M. Caboche (based upon the images collected with the CCD camera, Chapter 4). Typical PTFOC system measurements from the 35S*Luc* plants were approximately 850 photons s^{-1} (see Figure 4.2). Therefore, a single-cell of a pBIN-NiR*Luc*+ leaf could be predicted to produce approximately 6 photons s^{-1}, which would be indistinguishable from the background photon count. These calculations suggest that the PTFOC system is unsuitable to quantify luminescence from single-cells of luciferase-reporter plants. These predictions are based upon the luminescence from a fibre optic cable placed next to the leaf. An experimental system that provided a liquid connection between

the cytosol emitting luminescence and the photomultiplier tube may be more effective at harvesting photons.

There are other potential difficulties with quantifying luminescence from single-cells of luciferase-reporter plants. As mentioned in Chapter 4, variation between individual seedlings transformed with pBIN-NiR*Luc*+ could produce problems with using the PTFOC system to quantify luminescence changes as well as unknown variations between individual cells of the same leaf. Additionally, the extent of light contamination from neighbouring cells would need to be established, possibly by comparing luminescence from cells loaded with luciferin as described in Chapter 4 with single-cells loaded with caged luciferin.

5.4 Interpretation of experimental results

The interpretation of results both here and elsewhere in the literature often relies upon a comparison between the responses of NR-deficient mutants and wild type plants. However, the use of NR-deficient mutants in the identification of nitrate signalling processes may be problematic. NR-deficient mutants require culture on a reduced nitrogen source, whereas wild type plants are typically cultured on nitrate containing media to maximise the expression of NR. The culture of plants on a reduced nitrogen source may, in itself, be a signal to the regulation mechanism(s) of nitrate uptake and assimilation (Hoff *et al.*, 1994). It is widely accepted that the application of reduced nitrogen sources affects the activity and expression of assimilatory enzymes and transporters. As discussed in Chapter 3, the absence of NR may also affect cytosolic pH (Kaiser and Brendle-Behnisch, 1995), potentially affecting nitrate uptake as well as numerous other cellular processes.

5.4.1 The regulation of nitrate uptake and assimilation

Despite much previous research, no individual carbon or nitrogen metabolite has been identified as the regulating agent for nitrate uptake and assimilation. It is therefore appropriate to consider alternative regulatory signals.

5.4.1.1 Regulation by the rate of nitrate entry

It has been shown that in maize plants and detached maize leaves (Shaner and Boyer, 1976a; 1976b) and in tobacco plants (Geiger *et al.*, 1998) the rate of nitrate entry changes NR transcription and activity even though the total tissue nitrate remains unaltered. However this conflicts with the observation that in leaves of intact plants, NR expression declines after illumination whilst root nitrate uptake, translocation to the shoot and presumably shoot uptake increase (Matt *et al.*, 2001). Therefore it seems unlikely that NR expression is regulated by the rate of nitrate entry *per se*. The apparent conflict in evidence for the hypothesis that NR expression is regulated by nitrate uptake could be explained by the presence of different nitrate pools in specific cell types. These cells could differ in their response to nitrate application under illumination, either sequestering it in the vacuole or assimilating it in the cytosol. Experiments in which the average response of whole tissue samples is measured would be unable to distinguish the characteristics of individual cells. Although the presence of two types of cell is possible it would seem unnecessary to partition these processes into different cell types, since these processes occur in separate compartments and therefore could both be regulated and function in the same cell. If there is only one type of cell with respect to the regulation of nitrate uptake and assimilation, the regulation of NR expression by rate of nitrate entry seems unlikely.

5.4.1.2 Regulation by the pool of cytosolic nitrate

An alternative and more likely explanation is that a pool of nitrate within each cell, which reflects the balance between nitrate entry and use, regulates nitrate uptake and assimilation. An obvious candidate is the pool of cytosolic nitrate, as has been proposed by many authors, e.g. Matt *et al.*, 2001. There are two questions that must be answered to test the hypothesis that cytosolic nitrate activity signals regulate nitrate uptake and assimilation. Firstly, does cytosolic nitrate activity change in conditions when expression and activity of nitrate transporters and assimilatory enzymes are changing? Secondly, do experimental systems that can alter the pool of cytosolic nitrate trigger changes in nitrate uptake and assimilation?

The results described in Chapter 2 have answered the first question. Cytosolic nitrate activity in mesophyll cells of *Arabidopsis* changes in response to light/dark transitions, conditions in which the activity and expression of nitrate transporters and assimilatory enzymes change. These results could be interpreted as providing

evidence for cytosolic nitrate activity signals maintained for at least 20 min (Figures 2.18 and 2.19).

The answer to the second question could be inferred indirectly from the results described in Chapters 2 and 4. Chapter 2 showed that in the light treatment the pool of cytosolic nitrate was higher in the mesophyll cells of mutant plants with non-functional NR than in the wild type. Under light/dark transitions the pool of cytosolic nitrate did not change in mesophyll cells of mutant plants whereas in wild type plants a response was detected. Chapter 4 demonstrated that the nitrate-induction of NiR decreased in plants with non-functional NR. Cytosolic nitrate activity in mesophyll cells was shown to increase in the dark (Chapter 2), a condition in which the expression of nitrate transporters and assimilatory enzymes decreases (Bowsher *et al.*, 1991; Matt *et al.*, 2001). Increased cytosolic nitrate activity in mesophyll cells decreased the expression of nitrate transporters and assimilatory enzymes. These results imply that in conditions in which cytosolic nitrate activity was altered the expression of nitrate transporters and assimilatory enzymes changed. The results described in Chapters 2 and 4 provide the answers to the two questions above, and in doing so strongly support the hypothesised role of cytosolic nitrate activity signals in the regulation of nitrate uptake and assimilation.

Cytosolic nitrate activity fulfils the criteria of an ion capable of producing signals (described in Section 1.1.1.). Cytosolic nitrate activity is homeostatically controlled and under nitrate-replete conditions there are considerable stores within the vacuole (Zhen *et al.*, 1991; Miller and Smith, 1996; van der Leij *et al.*, 1998). Thus, providing means for the release of vacuolar nitrate to alter cytosolic nitrate activity. The work described in Chapter 2 has provided evidence of cytosolic nitrate activity changing in response to an environmental condition.

The sophisticated regulation of NR and its ability to alter cytosolic nitrate activity suggest it may be important in the regulation of nitrogen metabolism. The ability of NR activity to change rapidly and reversibly in response to changing environmental conditions implies a potential capacity to co-ordinate associated metabolism. Additionally, nitrogen status (at least nitrate availability and internal concentrations of glutamine) has been shown to regulate NR degradation (Scheible *et al.*, 1997b). This provides a mechanism for active NR to respond to environmental changes via phosphorylation and to respond to internal nitrogen pools via NR degradation. The role of NR in directly modifying cytosolic nitrate activity seems

unlikely because the K_m of NR is in the micromolar range (e.g. Kanayama *et al.*, 1999) whereas the cytosolic nitrate activity is in the millimolar range. However, K_m values of enzymes *in vitro* may be very different to those operating *in vivo* because of the regulation by allosteric modulators. The K_m of other enzymes such as GS and pyruvate kinase also appears to be unrelated to the substrate concentrations (reviewed by Britto *et al.*, 2001). They also suggested that the catalytic rates of enzymes subject to allosteric modulation were determined by the concentration of regulatory molecules rather than by substrate concentration. Alternatively, NR may regulate cytosolic nitrate activity indirectly possibly by altering the properties of transporters surrounding the cytosol.

The dramatic diurnal changes in whole leaf nitrate levels, presumably requiring a switch between rapid release of nitrate from the vacuole during the day and transport into the vacuole during the night, requires some sort of regulation. The cytosolic nitrate activity changes associated with light-dark transitions reported here may offer a possible regulatory signal. The decrease in cytosolic nitrate activity during the light may trigger the release of nitrate from the vacuole.

The light/dark changes in cytosolic nitrate activity in wild type mesophyll cells reported here are apparently contradicted by Steingröver *et al.* (1986). They reported maintenance of cytosolic nitrate activity during diurnal cycles. However, they used the considerably less accurate anaerobic NR assay to determine cytosolic nitrate activity and the results were very variable. In support of the hypothesis and results presented here, compartmental efflux analysis has shown that cytosolic nitrate activity is maintained at different levels in barley root cells of plants grown on different nitrogen treatments (Britto and Kronzucker, 2001). This suggests cytosolic nitrate activity signals are associated with external nitrogen supply, which would be consistent with a role for cytosolic nitrate activity in the regulation of nitrate uptake and assimilation. As reviewed in Section 1.8, work using compartmental efflux analysis and the anaerobic NR assay should be interpreted with caution because of the number and nature of the assumptions made when using these methods.

Studies using the more accurate and sensitive method of nitrate-selective microelectrodes have revealed that cytosolic nitrate activity is maintained under conditions in which nitrate is supplied and removed when sufficient vacuolar stores are available (Zhen *et al.*, 1991; Miller and Smith, 1996; van der Leij *et al.*, 1998). Van der Leij *et al.* (1998) also showed that cytosolic nitrate activity of nitrate-replete

barley root epidermal cells is maintained for at least 20 min when nitrate is withdrawn. This observation satisfies one criterion for a signal, that steady-state activity should be maintained during conditions in which the supply changes (Chapter 2).

Miller and Smith (personal communication) have shown that cytosolic nitrate activity in root tip cells changes more rapidly than mature cells during removal and re-supply of nitrate. This could be due to the fact that root tip cells do not contain fully developed vacuoles and therefore do not have the nitrate buffering capacity of mature root cells. Siebrecht *et al.* (1995) proposed that the root tip is a nitrate-sensing zone and reported high concentrations of NR there. This provides further support for the hypothesis that cytosolic nitrate activity changes in association with NR activity changes are signals.

Nitrate-selective microelectrodes have shown that cytosolic nitrate activity decreases in response to the application of ammonium chloride in barley root cells (Miller and Smith, personal communication; Kronzucker *et al.*, 1999b). The decrease in cytosolic nitrate activity may be due to the inhibition of nitrate uptake (Ingemarsson *et al.*, 1987; King *et al.*, 1993; Kronzucker *et al.*, 1999a). Ammonium application has been shown to cause a partial inactivation of NR *in vivo*, but this effect does not persist under *in vitro* conditions, possibly indicating that this change is caused by changes in cytosolic pH (Kaiser and Brendle-Behnisch, 1995). The application of reduced nitrogen metabolites decreases the activity and expression of nitrate assimilatory enzymes (Stitt, 1999). The ammonium application induced cytosolic nitrate activity change reported by Miller and Smith and Kronzucker *et al.* (1999b) supports the current hypothesis. However, the direction of cytosolic nitrate activity change apparently contradicts the hypothesis presented here. This apparent contradiction may be resolved if different mechanisms of cytosolic nitrate activity regulation operate in roots and shoots.

5.4.2 Summary of the experimental results

- Apoplastic nitrate activity in wild type and NR^- mutant *Arabidopsis* leaves is very low, approximately 0.3 mM (under the growth conditions used here).

- The first measurements of steady-state cytosolic and vacuolar nitrate activity and pH, and apoplastic pH made in wild type *Arabidopsis* leaves were reported in Chapters 2 and 3, and are consistent with those values reported for other species.
- The steady-state cytosolic nitrate activity in NR^- mutant is higher than that of wild type *Arabidopsis* leaf mesophyll cells during the light treatment.
- Cytosolic nitrate activity in *Arabidopsis* mesophyll cells rapidly changes in response to light/dark transitions. The onset of darkness triggers a transient increase in cytosolic nitrate activity followed by maintenance of higher steady-state nitrate activity when compared with that of light treatment.
- Light/dark transition induced cytosolic nitrate activity changes are dependent upon the presence of functional NR.
- Mesophyll and guard cells have chlorophyll-containing chloroplasts whereas epidermal cells do not.
- The PTFOC system is capable of quantifying luminescence from small areas of luciferase-reporter plants.
- Some component of NiR induction requires functional NR.

These results are shown diagramatically in Figure 5.1.

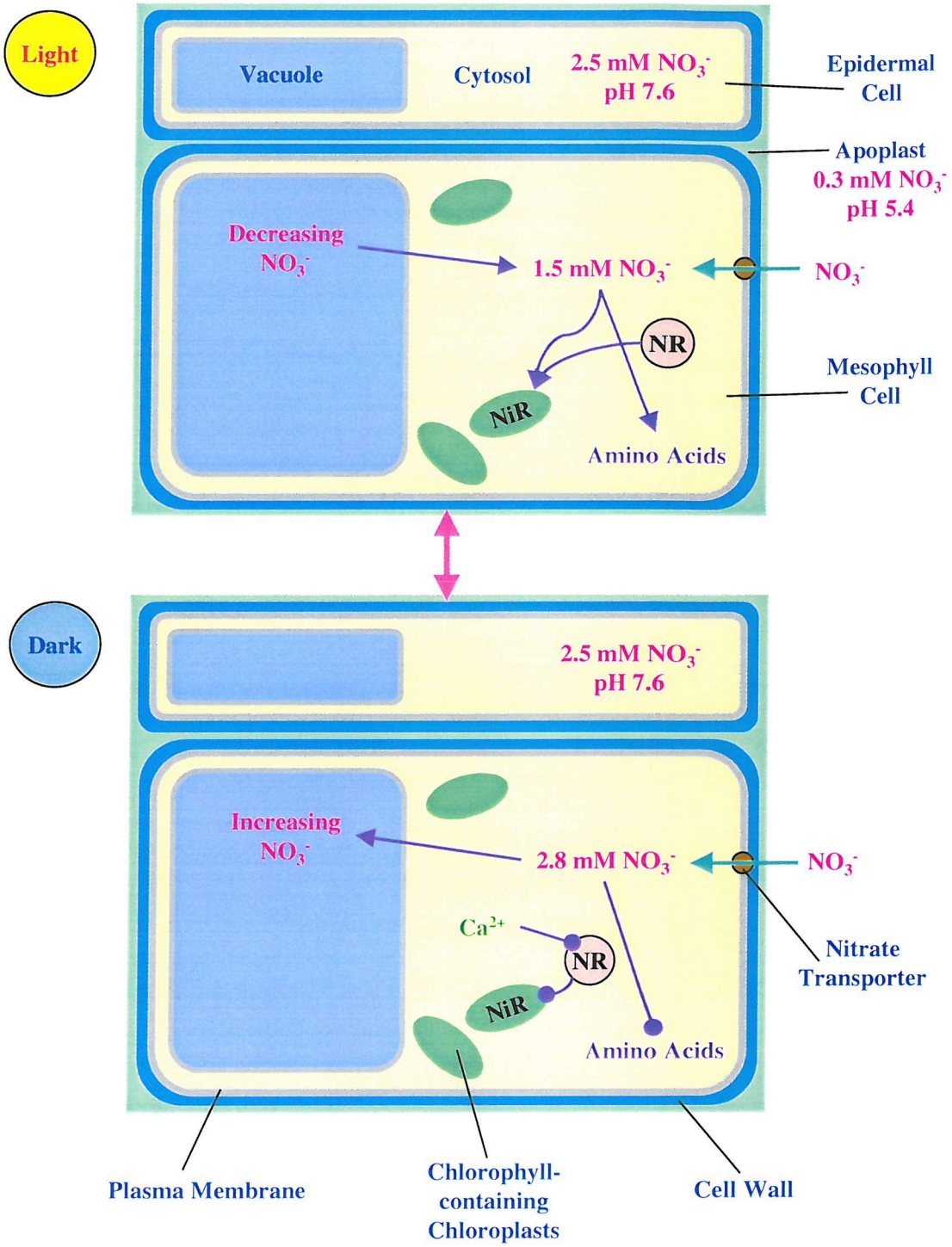

Figure 5.1 Schematic diagram summarising light/dark cytosolic and apoplastic nitrate activity and pH, the distribution of chlorophyll-containing chloroplasts and the effects of light/dark on nitrate reduction and assimilation in an *Arabidopsis* leaf.

Key: nitrate reductase, NR; nitrite reductase, NiR

5.5 Future work

The work described in this thesis used ion-selective microelectrodes to study possible cytosolic ion activity signalling events in wild type and NR^- mutant leaf cells. Further experiments primarily using nitrate-selective microelectrodes could provide additional data relating to the results and conclusions of the current study.

5.5.1 Cytosolic nitrate activity changes associated with NR activity modifications

Nitrate-selective microelectrode measurements could further test the hypothesis that cytosolic nitrate activity changes dependent on functional-NR are central to the regulation by nitrogen status. Illumination transitions were the changing environmental condition that modified NR studied here. Changing carbon dioxide concentration has also been shown to modify NR activity, which is reduced by decreasing carbon dioxide concentration (Kaiser and Förster, 1989; Kaiser and Brendle-Behnisch, 1991). The effects of altered carbon dioxide concentration on nitrate uptake and assimilation are difficult to interpret because of complex interactions with plant nitrogen status (Stitt and Krapp, 1999). Generally, under nitrate-replete conditions elevating carbon dioxide concentration has been shown to increase nitrate uptake, NR activity and nitrogen assimilation (Stitt and Krapp, 1999). In agreement with the hypothesis that cytosolic nitrate activity regulates nitrate uptake and assimilation, the application of increased carbon dioxide concentration to plant cells would increase NR activity, presumably triggering a decrease in cytosolic nitrate activity and inducing the activity and expression of nitrate transporters and assimilatory enzymes.

Anoxia causes hyper-activation of NR (Glaab and Kaiser, 1993) and according to the hypothesis presented here would be predicted to cause a decrease in cytosolic nitrate activity and a corresponding increase in the expression and activity of nitrate transporters and assimilatory enzymes. However, the reverse has been demonstrated; anoxia inhibits nitrite and ammonium assimilation (Botrel *et al.*, 1996). The cause of the inhibition has been ascribed to a lack of NAD(P)H and ATP. It is possible that extremely low cytosolic nitrate activity, due to the hyper-activation of NR, could produce a regulatory signal to decrease the expression and activity of nitrate

transporters and assimilatory enzymes or that a lack of NAD(P)H and ATP could increase cytosolic nitrate activity.

Further work to determine the effects of changing carbon dioxide concentration and anoxia on cytosolic nitrate activity could provide further support for the hypothesis that functional-NR dependent cytosolic nitrate activity changes regulate nitrate uptake and assimilation.

5.5.2 Cytosolic nitrate activity changes associated with the amount of NR protein

The cytosolic nitrate activity changes in response to illumination transitions reported in Chapter 2 were dependent upon the presence of functional NR. A plant's nitrogen source affects the induction and degradation of NR (Scheible *et al.*, 1997b) and this may be important in modifying cytosolic nitrate activity and regulating nitrogen assimilation. Culturing plants on different nitrogen sources may provide evidence of the maintenance of different levels of cytosolic nitrate related to the amount of NR protein (e.g. Britto and Kronzucker, 2001). Miller and Smith (personal communication) and Kronzucker *et al.* (1999b) have shown that nitrate activity changes in response to the application of ammonium. The application of other nitrate assimilation products, for example glutamine, may also provide further evidence of nitrate signals associated with regulating NR activity when reduced nitrogen forms are available.

5.5.3 Nitrate-inducible reporter plants

Further work needs to be done on the detailed characterisation of the nitrate-inducible luciferase-reporter plants produced in this project. There is huge scope for further investigation. The *Nii* gene is regulated by numerous factors, for example, nitrate, reduced N metabolites, light, hormones, sucrose and circadian rhythms. Experiments determining the role of these factors may yield valuable results.

The development of a technique to study nitrate-induction of single-cells may not be achievable. As discussed above, the PTFOC system is unlikely to be capable of quantifying luminescence from single-cells of the pBIN-NiR*Luc*+ plants. The variability between individuals of the same line of plants transformed with pBIN-

NiR*Luc*+ may pose a potential problem for any technique based on single-cell measurements.

Experiments using the pBIN-NiR*Luc*+ reporter plants could however be designed to investigate the relationships between cytosolic nitrate activity signals and the extent of nitrate-induction. The PTFOC system could be used to quantify luminescence from small areas of cells adjacent to those studied with ion-selective microelectrodes. Experiments could be done to establish whether the root tip has a sensing role as proposed by Siebrecht *et al.* (1995). Nitrate-selective microelectrode and luminescence measurements made during periods of nitrate starvation and subsequent nitrate replenishment in root tip cells may provide evidence of cytosolic nitrate activity changes related to nitrate availability and nitrate-induction. Other experiments investigating the effects of modifications of NR activity (by altering carbon dioxide and oxygen concentrations) on cytosolic nitrate activity could be expected to establish the nature of any relationships between cytosolic nitrate activity and the induction of genes by nitrate.

5.5.4 Manipulating cytosolic nitrate activity

Manipulating cytosolic nitrate activity experimentally could provide further evidence for the hypothesis that cytosolic nitrate activity changes regulate nitrate uptake and assimilation. In this study, cytosolic nitrate activity was affected by the disruption of functional NR. Other methods to alter cytosolic nitrate activity may provide further evidence to confirm or refute the hypothesis suggested here. Iontophoresis of nitrate down a barrel of a microelectrode could directly alter cytosolic nitrate activity and the affects on the induction of genes by nitrate could be quantified using the nitrate-inducible luciferase plants and PTFOC system produced in this project. These experiments could also determine whether the rate of nitrate entry or cytosolic nitrate activity regulates nitrate uptake and assimilation.

5.5.5 Other aspects of NR regulation

There are many other aspects of NR regulation that remain to be understood, such as the physiological significance of having multiple isoforms of NR. *Arabidopsis* has two isoforms that are regulated differently. There are also three NR kinases and two

NR phosphatases that are regulated differently. The contribution of these phosphorylation enzymes to the regulation of NR is unknown. The complexity of NR regulation may also be due to the role of NR in nitrate signalling.

5.6 Conclusion

The aim of this study was to investigate two aspects of nitrate signalling. The first of these was possible changes in cytosolic ion activity associated with changing NR activity. This objective was successfully achieved (Chapter 2). Cytosolic nitrate activity was shown to change in response to an environmental condition in which NR activity was known to be modified and this change was shown to be dependent upon the presence of functional NR. This is the first report of functional NR dependent cytosolic nitrate activity change in any plant tissue or species under any conditions in which NR activity is known to change. Further work is necessary to complete the pH-selective microelectrode measurements described in Chapter 3. The use of pH indicator dyes with confocal microscopy was tested and shown to be unsuitable as an alternative experimental approach because of the tissue localisation of the pH indicator dyes. The role of NR in maintaining cytosolic pH homeostasis remains to be determined.

The second aspect of the work was the study of cytosolic ion activity changes associated with nitrate-induction of NiR using luciferase-reporter plants. Originally it was intended to use luciferase-reporter plants provided by Prof. M. Caboche. These luciferase-reporter plants showed poor luciferase activity and were unsuitable for the planned single-cell photon counting (see Chapter 4). Improved reporter plants were produced and shown to be nitrate-inducible.

The regulatory mechanism of nitrogen metabolism has been a subject of considerable research and debate for many years and it is still not fully understood. The work described here provides evidence to support the hypothesis that cytosolic nitrate activity changes are a regulatory mechanism by which processes of nitrogen metabolism are controlled. As Crawford (1995) pointed out 'it is a mystery why a highly regulated enzyme that catalyses a critical step is present in such excess'. The work described in this thesis may shed light on this mystery. The apparent excess NR may have a role in the cytosolic nitrate activity signals associated with the regulation

of nitrate uptake and assimilation. The fact that functional NR has a role in at least some aspects of cytosolic nitrate activity change suggests a role for this enzyme that is broader than that of a simple step in nitrate reduction.

APPENDIX 1 ION-SELECTIVE MICROELECTRODE THEORY

Ion-selective microelectrodes respond to changes in ionic activity. The activity of an ion in solution is the product of its activity coefficient and concentration:

$$a_i = f_i\,[i] \qquad (1)$$

where a_i is the activity of ion i (M), f_i is the activity coefficient, and [i] its concentration (M). The activity coefficient f_i is calculated using the Debye-Hückel equation:

$$-\log_{10} f_i = A\, z_i^2\, \sqrt{I}/(1 + å\, B\, \sqrt{I}) \qquad (2)$$

where A is the first Debye-Hückel constant (0.511 $mol^{-½}\, l^{½}$ at 25°C with water as the solvent), z_i is the valency of ion i, å is the ion-size parameter (3.0 for NO_3^-), B is the second Debye-Hückel constant (0.328 $mol^{-½}\, l^{½}\, Å^{-1}$ at 25°C, water as the solvent) and I is the ionic strength of the medium (M), calculated by:

$$I = 0.5\,(\Sigma\, c_x\, z_x^2) \qquad (3)$$

where c_x is the concentration of any ion in the solution (M) and z_x the valency. When an ion-selective microelectrode containing an ion-selective membrane in its tip comes into contact with an external solution, movement of the ion of interest from the solution into the membrane establishes an electrical potential (electromotive force, EMF, or electrode voltage) across the membrane. If all other potential differences in the circuit are constant, the EMF (in millivolts, mV) will be a function of the ion activity gradient across the membrane (Ammann, 1986) and, at steady state, will be described by the Nernst equation:

$$EMF = E_o + s \log_{10} a_i \qquad (4)$$

where E_o is the electrode reference potential (mV) and s is the Nernstian slope (mV), defined as follows:

$$s = 2.303\ (R\ T/z_i\ F) \qquad (5)$$

where R is the gas constant (8.31441 J K^{-1} mol^{-1}), T is the absolute temperature (K) and F is the Faraday constant (96487 C mol^{-1}). In practice, ion-selective microelectrodes rarely respond as predicted by the Nernst equation, especially at low activities of the measured ion. Ion-selective sensors do not show exclusive selectivity for a particular ion and most measurements are made in solutions where more than one ion is present. The additional contributions to the measured EMF due to the presence of interfering ions must be accounted for (Miller, 1994). The EMF in such conditions is described by a modification of the Nernst equation, the Nicolsky-Eisenman equation:

$$EMF = E_o + s \log_{10} [a_i + \sum K_{ij}^{pot} (a_j)^{zi/zj}] \qquad (6)$$

where K_{ij}^{pot} is the potentiometric selectivity factor ("selectivity coefficient") of the electrode for the ion i with respect to the interfering ion j, a_j is the activity of ion j (M), z_j is the valency of ion j and E_o (mV) is determined as follows:

$$E_o = E_i^o + E_R + E_D \qquad (7)$$

where E_i^o is the constant potential difference (PD) between the internal filling solution and the membrane, E_R is the sum of the constant PDs between the metallic leads of the circuit and the electrolytes of the reference and membrane electrode, and E_D is the liquid-junction PD between the reference electrolyte and the sample solution. E_i^o and E_R are constant for an individual electrode, E_D is variable and sample dependent (Ammann, 1986).

The properties of ion-selective microelectrodes are usually described in terms of the slope, selectivity coefficient, detection limit and response time. Equations (4) and (5) predict that an electrode selective for a monovalent ion should show a log-linear relationship between ion activity and EMF, with a calibration slope of 59.2 mV

(at 25 °C) per decade change in activity. In practice, such ideal linear response only occurs over a limited range. A comparison of the slope of the linear section of a response curve to the theoretical value can be used to characterise electrode function. For a monovalent ion, a useful slope has been defined as between 50 and 60mV (Fluka, 1996).

The selectivity coefficient (see Equation (6)) is a measure of the preference of the sensor for the detected ion over an interfering ion and is thus one of the most important characteristics of an ion-selective microelectrode (Miller, 1994).

The detection limit of an ion-selective microelectrode has been practically defined as the activity at the point of intersection of the two asymptotes of the Nicolsky-Eisenman response curve (Buck and Lindner, 1994). It represents the lowest ion activity that can be detected with confidence (Figure A.1).

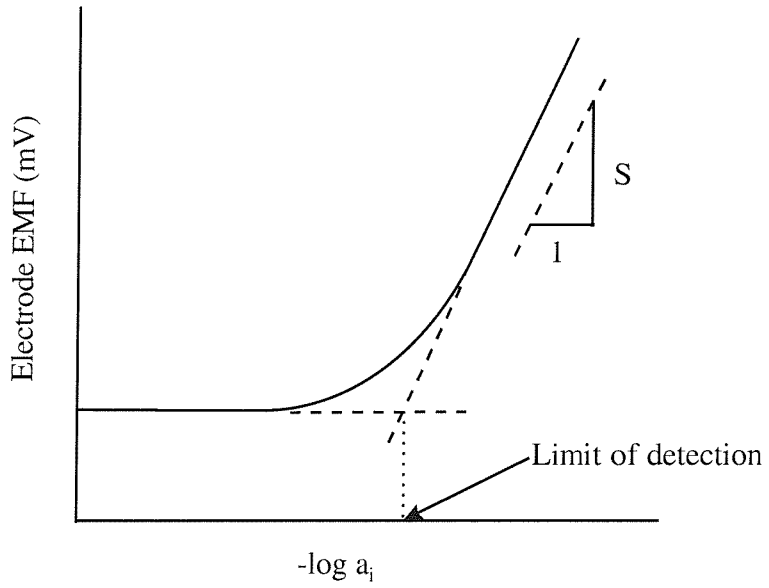

Figure A. 1 Schematic representation of an ideal ion-selective microelectrode calibration curve. The slope is the change in EMF per decade change in activity of the ion, i; the detection limit is the intersection of the two asymptotes of the Nicolsky-Eisenman response curve.

The values of the slope, detection limit, and selectivity coefficient are important parameters in characterising an ion-selective microelectrode. A fourth characteristic that defines microelectrode function is the response time. Response time is defined Buck and Lindner (1994), as the time that elapses between an ISE cell

contacting a sample solution and the first instant at which the EMF/time slope becomes equal to a limiting value selected on the basis of experimental or accuracy requirements. Response time is governed by many factors, including tip geometry, membrane composition and electrical resistance (Miller, 1994).

A typical ion-selective membrane contains: a small percentage of the ion-selective molecule, sensor or exchanger, the membrane matrix, a plasticiser and possibly other additives to improve various qualities of the membrane.

Anion-selective microelectrodes generally use lipophilic quaternary ammonium or phosphonium salts as mobile anion exchange sites to sense anion activity (Ammann, 1986). The lipophilic quaternary ammonium salt tridodecylmethylammonium nitrate (MTDDA.NO_3, $[CH_3(CH_2)_{11}]_3NCH_3.NO_3$) was identified as a nitrate sensor by Wegmann *et al.* (1984). The MTDDA.NO_3 sensor was the basis for the development of nitrate-selective microelectrodes for intracellular use in plant cells by Miller and Zhen (1991). These microelectrodes showed a log-linear response from 0.1 to 100 mM (pNO_3 4 to 1) nitrate with a typical slope of 55.6 mV per decade change in nitrate concentration, a typical example shown in Figure A.2. The only physiologically significant interfering anion was chloride; the lower limit of nitrate detection was 0.5 mM in the presence of 100 mM chloride, therefore this interference would not be important in most physiological situations. The response time of these electrodes was typically under one min.

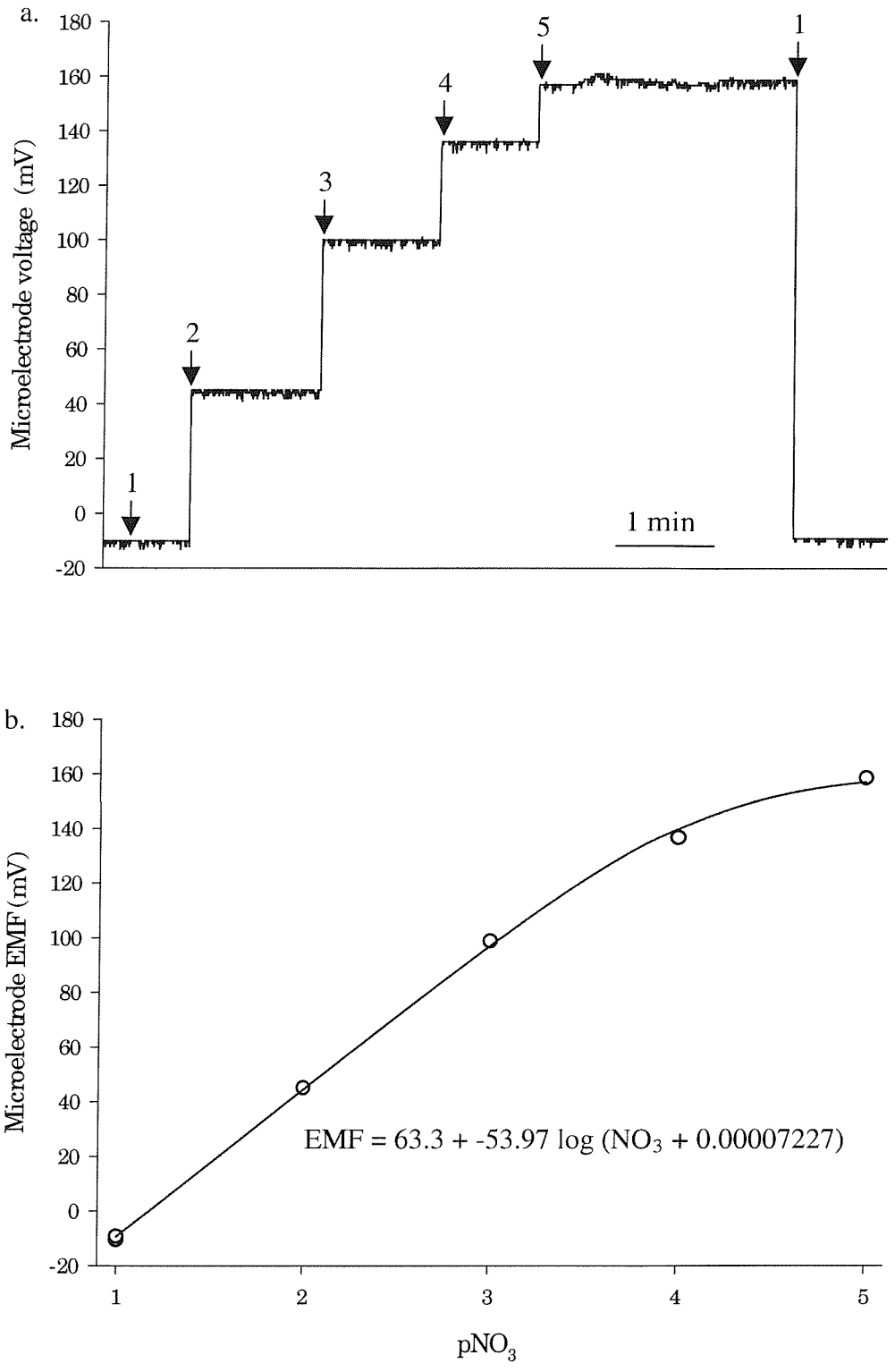

Figure A. 2 a. Nitrate-selective microelectrode barrel EMF response to calibration solutions (Table 2.2, Miller and Zhen, 1991), numbers indicate pNO_3 ($-\log_{10}$ [NO_3^- activity]) value of the solution. b. Mean microelectrode response to each solution versus pNO_3; curve fitted to the Nicolsky-Eisenman equation (equation shown).

When an ion-selective microelectrode is inserted into a plant cell, the measured voltage reflects both the local ion activity and the cell membrane potential. A measurement of membrane potential is thus necessary to correct for the effect of this voltage. This may be achieved using two single-barrelled microelectrodes or a double-barrelled microelectrode (Figure A.3).

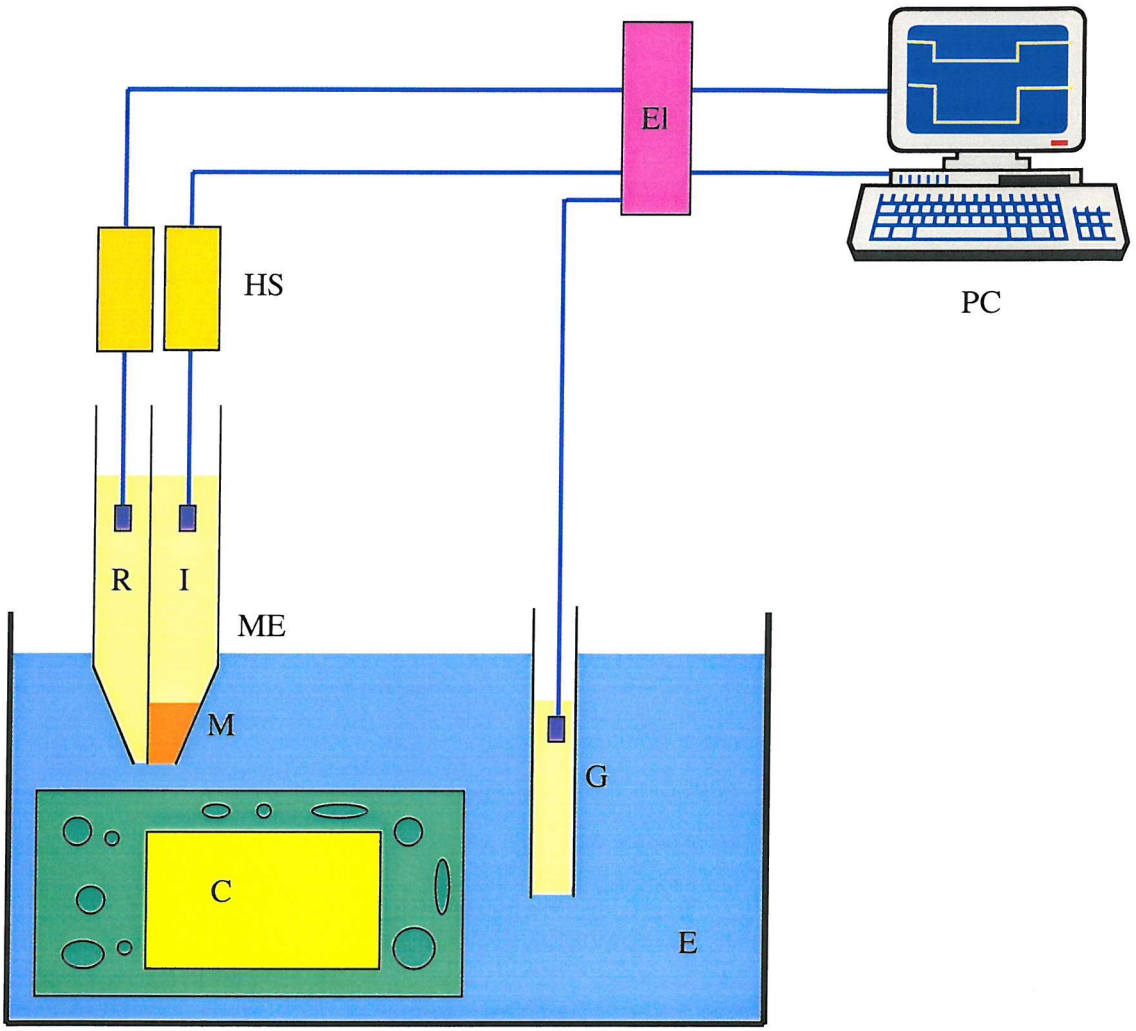

Figure A. 3 Diagram of a double-barrelled ion-selective microelectrode (ME). The tip of barrel I contains an ion-selective membrane (M). Barrel R records the membrane potential of the impaled cell (C). Barrels I and R are connected to a high-impedance electrometer (El) via headstage (HS) amplifiers. The circuit is completed by a ground electrode (G) in the external solution (E).

The output of the membrane potential-sensing barrel (the reference, barrel B in Figure A-3) is subtracted from the output of the ion-sensing barrel (I). Output voltages are measured against a ground electrode in the external solution. Ion activity is determined by referring the output of the ion-sensing microelectrode (after subtraction of membrane potential) to suitable Nicolsky-Eisenman calibration curves.

REFERENCES

Åberg B. (1947) On the mechanism of the toxic action of chorates and some related substances upon young wheat plants. *Journal of the Royal Agricultural College of Sweden*, **15**, 37-107.

Aflalo C. (1991) Biologically localised firefly luciferase: a tool to study cellular processes. *International Review of Cytology*, **130**, 269-323.

Ammann D. (1986) *Ion-Selective Microelectrodes - Principles, Design and Applications.* Springer-Verlag, Berlin.

Aslam M. & Huffaker R.C. (1989) Role of nitrate and nitrite in the induction of nitrite reductase in leaves of barley seedlings. *Plant Physiology*, **91**, 1152-1156.

Aslam M., Travis R. L. & Huffaker R.C. (1992) Comparative kinetics and reciprocal inhibition of nitrate and nitrite uptake in roots of uninduced and induced barley (*Hordeum vulgare* L.) seedlings. *Plant Physiology*, **99**, 1124-1133.

Aslam M., Travis R. L. & Rains D. (1996) Evidence for substrate induction of a nitrate efflux system in barley roots. *Plant Physiology*, **112**, 167-175

Athwal G.S., Huber Y. & Huber S.C. (1998) Phosphorylated nitrate reductase and 14-3-3 proteins: site of interaction, effects of ions, and evidence for an AMP-binding site on 14-3-3 proteins. *Plant Physiology*, **118**, 1041-1038.

Bachmann M., McMichael R.W., Huber J.L., Kaiser W.M. & Huber S.C. (1995) Partial purification and characterization of a calcium-dependent protein kinase and an inhibitor protein required for the activation of spinach leaf nitrate reductase. *Plant Physiology*, **108**, 1083-1091.

Bachmann M., Shiraishi N., Campbell W.H., Yoo B.C., Harmon A.C. & Huber S.C. (1996) Identification of Ser-543 as the major regulatory phosphorylation site in spinach leaf nitrate reductase. *Plant Cell*, **8**, 505-517.

Back E., Dunne W., Schneiderbauer A., de Framond A., Rastogi R. & Rothstein S.J. (1991) Isolation of the spinach nitrite reductase gene promoter which confers nitrate inducibility on GUS gene expression in transgenic tobacco. *Plant Molecular Biology*, **17**, 9-18.

Beffagna N., Romai G., Meraviglia G. & Pallini S. (1997) Effects of abscisic acid and

cytoplasmic pH on potassium and chloride efflux in *Arabidopsis thaliana* seedlings. *Plant Cell Physiology*, **38**, 503-510.

Barclay G.F., Peterson C.A. & Tyree M.T. (1982) Transport of fluorescein in trichomes of *Lycopersicon-esculentum*. *Canadian Journal of Botany*, **60**, 397-402.

Barnes W.M. (1990) Variable patterns of expression of luciferase in transgenic tobacco leaves. *Proceedings of the National Academy of Sciences of the United States of America*, **87**, 9183-9187.

Bechtold N., Ellis J. & Pelletier G. (1993) *In planta Agrobacterium* mediated gene transfer by infiltration of adult *Arabidopsis thaliana* plants. *Comptes Rendus de l'Academie des Sciences Serie III: Sciences de la Vie*, **316**, 1194-1199.

Bevan M. (1984) *Agrobacterium* vectors for plant transformation. *Nucleic Acids Research*, **12**, 8711-8721.

Bevan M., Flavell R.B. & Chilton M.-D. (1983) A chimaeric antibiotic resistance gene as a selectable marker for plant cell transformation. *Nature*, **304**, 184-187.

Bligny R., Gout E., Kaiser W.M., Heber U., Walker D. & Douce R. (1997) pH regulation in acid stressed leaves of pea plants grown in the presence of nitrate or ammonium salts: studies involving ^{31}P-NMR spectroscopy and chlorophyll flourescence. *Biochimica et Biophysica Acta*, **1320**, 142-152.

Blom-Zandstra M., Koot H.T.M., van Hattum J. & Vogelzang S.A. (1995) Isolation of protoplasts for patch-clamp experiments: an improved method requiring minimal amounts of adult leaf or root tissue form monocotyledonous or dicotyledonous plants. *Protoplasma*, **185**, 1-6.

Blom-Zandstra M., Koot H.T.M., van Hattum J. & Vogelzang S.A. (1997) Transient light-induced changes in ion channel and proton pump activities in the plasma membrane of tobacco mesophyll protoplasts. *Journal of Experimental Botany*, **48**, 1623-1630.

Blumwald E., Aharon G.S. & Apse M.P. (2000) Sodium transport in plant cells. *Biochimica et Biophysica Acta*, **1465**, 140-151.

Botrel A., Magne C. & Kaiser W.M. (1996) Nitrate reduction, nitrite reduction and ammonium assimilation in barley roots in response to anoxia. *Plant Physiology and Biochemistry*, **34**, 645-652.

Bowman J. (1994) *Arabidopsis. An Atlas of Morphology and Development*. Springer-

Verlag, Berlin Heidelberg New York.

Bowsher C.G., Long D.M., Oaks A. & Rothstein S.J. (1991) Effect of light/dark cycles on expression of nitrate assimilatory genes in maize shoots and roots. *Plant Physiology*, **95**, 281-285.

Braaksma F.J. & Feenstra W.J. (1982) Nitrate reduction in the wildtype and a nitrate reductase deficient mutant of *Arabidopsis thaliana*. *Physiologia Plantarum*, **54**, 351-360.

Britto D. T., Glass A.D.M., Kronzucker H.J. & Siddiqi M.Y. (2001) Cytosolic concentrations and transmembrane fluxes of NH_4^+/NH_3. An evaluation of recent proposals. *Plant Physiology*, **125**, 523-526.

Britto D.T. & Kronzucker H.J. (2001) Constancy of nitrogen turnover kinetics in the plant cell: insights into the integration of subcellular N fluxes. *Planta*, **213**, 175-181.

Brownlee C. (1987) Microelectrode techniques and plant cells. In: *Microelectrode Techniques - The Plymouth Workshop Handbook* (eds N.B. Standen, P.T.A. Gray, & M.J. Whitaker), pp. 187-198. The Company of Biologists Limited, Cambridge.

Buck R.P. & Lindner E. (1994) Recommendations for nomenclature of ion-selective electrodes. IUPAC recommendations 1994. *Pure and Applied Chemistry*, **66**, 2527-2543.

Buschmann C., Langsdorf G. & Lichtenthaler H.K. (2000) Imaging of the blue, green and red fluorescence emission of plants: an overview. *Photosynthetica*, **38**, 483-491.

Bush D.S. (1995) Calcium regulation and its role in signalling. *Annual Reviews of Plant Physiology and Plant Molecular Biology*, **46**, 95-122.

Caboche M. & Rouze P. (1990) Nitrate reductase: a target for molecular and cellular studies in higher plants (review). *Trends in Genetics*, **6**, 187-192.

Champigny M.L. & Foyer C. (1992) Nitrate activation of cytosolic protein kinases diverts photosynthetic carbon from sucrose to amino acid biosynthesis. *Plant Physiology*, **100**, 7-12.

Champigny M.L., Brauer M., Bismuth E., Manh C.T., Siegl G., van Quy L. & Stitt M. (1992) The short-term effect of NO_3^- and NH_3 assimilation on surcose synthesis in leaves. *Journal of Plant Physiology*, **139**, 361-368.

Champigny M.L., van Quy L., Valadier M.H. & Moyse A. (1991) Short-term effects

of nitrate on CO_2 photoassimilation and sucrose synthesis in wheat leaves. *Comptes Rendus de l'Academie des Sciences Serie III: Sciences de la Vie*, **312**, 469-476.

Chao P., Ammann D., Oesch U., Simon W. & Lang F. (1988) Extra- and intracellular hydrogen ion-selective microelectrode based on neutral carriers with extended pH response range in acid media. *Pflugers Archiv*, **411**, 216-219.

Cheng C.-L., Acedo G.N., Cristinsin M. & Conkling M.A. (1992) Sucrose mimics the light induction of *Arabidopsis* nitrate reductase gene transcription. *Proceedings of the National Academy of Sciences of the United States of America*, **89**, 1861-1864.

Cheng C.-L., Acedo G.N., Dewdney J., Goodman H.M. & Conkling M.A. (1991) Differential expression of the two *Arabidopsis* nitrate reductase genes. *Plant Physiology*, **96**, 275-279.

Cheng C.L., Dewdney J., Kleinhofs A. & Goodman H.M. (1989) Cloning and nitrate induction of nitrate reductase mRNA. *Proceedings of the National Academy of Sciences of the United States of America*, **83**, 6825-6828.

Cheng C.-L., Dewdney J., Nam H., Den Boer B.G.W. & Goodman H.M. (1988) A new locus (*NIA1*) in *Arabidopsis thaliana* encoding nitrate reductase. *EMBO Journal*, **7**, 3309-3314.

Chilton M.P., Drummond M.H., Merlo D.J., Sciaky D., Montoya A., Gordon M.P. & Nester E.W. (1977) Stable incorporation of plasmid DNA into higher plant cells : the molecular basis of crown gall tumorigenesis. *Cell*, **11**, 263-271.

Choi Y.E., Harada E., Wada M., Tsuboi H., Morita Y., Kusano T. & Sano H. (2001) Detoxification of cadmium in tobacco plants: formation and active excretion of crystals containing cadmium and calcium through trichomes. *Planta*, **213**, 45-50.

Coleman J.O.D., Blake-Kalff M.M.A. & Davis T.G.E. (1997) Detoxification of xenobiotics by plants: chemical modification and vacuolar compartmentation. *Trends in Plant Science*, **2**, 144-151.

Cork R.J. (1986) Problems with the application of quin-2-AM to measure cytoplasmic free calcium in plant cells. *Plant, Cell and Environment*, **9**, 157-161.

Crawford N.M. & Campbell W.H. (1990) Fertile fields. *The Plant Cell*, **2**, 829-835.

Crawford N.M. & Glass A.D.M. (1998) Molecular and physiological aspects of nitrate uptake in plants. *Trends in Plant Science*, **3**, 389-395.

Crawford N.M. (1992) Study of chlorate resistant mutants of Arabidopsis: insights into nitrate assimilation and ion metabolism of plants. In: *Genetic Engineering Principles and Methods* (eds J.K. Setlow & A. Hollander), pp. 89-98. Plenum Press, New York.

Crawford N.M. (1995) Nitrate: nutrient and signal for plant growth. *Plant Cell*, **7**, 859-868.

Crawford N.M., Kahn M.L., Leustrek T & Long S.R. (2000) Nitrogen and Sulfur. In: *Biochemistry and Molecular Biology of Plants*. (eds Buchanan R.B., Gruissem W. & Jones R.L.) pp. 786-849. The American Society of Plant Physiologists, Courier Companies Inc., Waldorf.

Crete P., Caboche M. & Meyer C. (1997) Nitrite reductase expression is regulated at the post-transcriptional level by nitrogen source in *Nicotiana plumbaginifolia* and *Arabidopsis thaliana. Plant Journal*, **11**, 625-634.

Cuin T.A., Miller A.J., Laurie S.A. & Leigh R.A. (1999) Nitrate interference with potassium-selective microelectrodes. *Journal of Experimental Botany*, **50**, 1709-1712.

Daniel-Vedele F. & Caboche M. (1996) Molecular analysis of nitrate assimilation in higher plants. *Comptes Rendus de l'Academie des Sciences Serie III: Sciences de la Vie*, **319**, 961-968.

Daniel-Vedele F., Filleur S. & Caboche M. (1998) Nitrate transport: a key step in nitrate assimilation. *Current Opinion in Plant Biology*, **1**, 235-239.

De Luca M. (1976) Firefly luciferase. *Advances in Enzymology*, **44**, 37-68.

De Wet J.R., Wood K.V., De Luca M., Helinski D.R. & Subramani S. (1987) Firefly luciferase gene: structure and expression in mammalian cells. *Molecular and Cellular Biology*, **7**, 725-737.

De Wet J.R., Wood K.V., Helinski D.R. & De Luca M. (1985) Cloning of firefly luciferase cDNA and the expression of active luciferase in *Escherichia coli. Proceedings of the National Academy of Sciences of the United States of America*, **82**, 7870-7873.

Deng M.D., Moureaux T. & Caboche M. (1989) Tungstate, a molybdate analog inactivating nitrate reductase, deregulates the expression of the nitrate reductase structural gene. *Plant Physiology*, **91**, 304-309.

Deng M.-D., Moureaux T., Cherel I., Boutin J.-P. & Caboche M. (1991) Effects of nitrogen metabolites on the regulation and circadian expression of tobacco

nitrate reductase. *Plant Physiology and Biochemistry*, **29**, 237-247.

Desfeux C., Clough S.J. & Bent A.F. (2000) Female reproductive tissues are the primary target of *Agrobacterium*-mediated transformation by the *Arabidopsis* floral-dip method. *Plant Physiology*, **123**, 895-904.

Dixon D.P., Cummins I., Cole D.J. & Edwards R. (1998) Glutathione-mediated detoxification systems in plants. *Current Opinion in Plant Biology*, **1**, 258-266.

Dorbe M.-F., Truong H.-N., Crété P. & Daniel-Vedele F. (1998) Deletion analysis of the tobacco *Nii1* promoter in *Arabidopsis thaliana*. *Plant Science*, **139**, 71-82.

Douglas P., Morrice N. & Mackintosh C. (1995) Identification of a regulatory phosphorylation site in the hinge I region of nitrate reductase form spinach (*Spinacia oleracea*) leaves. *FEBS Letters*, **377**, 113-117.

Douglas P., Pigaglio E., Ferrer A., Halford N.G. & Mackintosh C. (1997) Three spinach leaf nitrate reductase and 3-hydroxy-3-methylglutarly-CoA reductase kinases that are regulated by reversible protein phosphorylation and/or Ca^{2+} ions. *Biochemistry Journal*, **325**, 101-109.

Drew M.C. (1973) Nutrient supply and the growth of the seminal root system in barley. I. The effect of nitrate concentration on the growth of axes and laterals. *Journal of Experimental Botany*, **24**, 1189-1202.

Dzuibany C., Haupt S., Fock H., Beihler K., Migge K. & Becker T.W. (1998) Regulation of nitrate reductase transcript levels by glutamine accumulating in the leaves of a ferredoxin-dependent glutamate synthase mutant of *Arabidopsis thaliana*, and by glutamine provided to the roots. *Planta*, **206**, 515-522.

Elzenga J.T.M., Prins H.B.A. & van Volkenburgh E. (1995) Light-induced membrane potential changes of epidermal and mesophyll cells in growing leaves of *Pisum sativum*. *Planta*, **197**, 127-134.

Entwistle A. & Nobel M. (1994) Optimising the performance of confocal laser scanning microscopes over the full field of view. *Journal of Microscopy*, **175**, 238-251.

Entwistle A. (2000) Confocal microscopy: an overview with a biological and fluorescence microscopy bias. *The Quekett Journal of Microscopy*, **38**, 445-456.

Fahn A. (1988) Secretory tissues in vascular plants. *New Phytologist*, **108**, 229-257.

Felle H.H. & Bertl A. (1986) The fabication of H^+-selective liquid-membrane microelectrodes for use in plant cells. *Journal of Experimental Botany*, **37**, 1416-1428.

Felle H.H. (1987) Proton transport and pH control in *Sinapis alba* root hairs. A study carried out with double-barreled pH-microelectrodes. *Journal of Experimental Botany*, **38**, 340-354.

Felle H.H. (1988) Short-term pH regulation in plants. *Physiologia Plantarum*, **74**, 583-593.

Felle H.H. (1993) Ion-selective microelectrodes: their use and importance in modern plant cell biology. *Botanica Acta*, **106**, 5-12.

Felle H.H., Kondorosi E., Kondorosi A. & Schultze M. (1996) Rapid alkalinization in alfalfa root hairs in response to rhizobial lipochitooligosaccaride signals. *Plant Journal*, **10**, 295-301.

Ferrari T.E., Yoder O.C. & Filner P. (1973) Anaerobic nitrite production by plant cells and tissues. Evidence for two nitrate pools. *Plant Physiology*, **51**, 423-431.

Fluka (1996) *Selectophore. Ionophores. Membranes. Mini ISE.* Fluka Chemie AG, Buchs.

Forde B.G. & Clarkson D.T. (1999) Nitrate and ammonium nutrition in plants: physiological and molecular perspectives. *Advances in Botanical Research*, **30**, 1-90.

Forde B.G. (2000) Nitrate transporters in plants: structure, function and regulation. *Biochimica et Biophysica Acta*, **1465**, 219-235.

Fricker M.D., Tester M. & Gilroy S. (1993) Fluorescence and luminescence techniques to probe ion activities in living plant cells. In: *Fluorescent and Luminescent Probes for Biological Activity* (ed W.T. Mason), pp. 360-377. Academic Press, London.

Fujii S., Shimmen T. & Tazawa M. (1978) Light-induced changes in the membrane potential of *Spirogyra*. *Plant Cell Physiology*, **19**, 573-590.

Galangau F., Daniel-Vedele F., Maureaux T., Dorbe M.F., Leydecker M.D. & Caboche M.T. (1988) Expression of nitrate reductase genes from tomato in relation to light-dark regimes and nitrate supply. *Plant Physiology*, **88**, 383-388.

Geiger M., Walch-Liu P., Engels C., Harnecker J., Schulze E.-D., Ludewig F.,

Sonnewald U., Scheible W.-R. & Stitt M. (1998) Enhanced carbon dioxide leads to a modified diurnal rhythm of nitrate reductase activity in older plants, and a large stimulation of nitrate reductase activity and higher levels of amino acids in young tobacco plants. *Plant, Cell and Environment*, **21**, 253-268.

Geisler M., Axelsen K.B., Harper J.F. & Palmgren M.G. (2000) Molecular aspects of higher plant P-type Ca^{2+}-ATPases. *Biochimica et Biophysica Acta*, **1465**, 52-78.

Gerhardt R., Stitt M. & Heldt H.W. (1987) Subcellular metabolite levels in spinach leaves. *Plant Physiology*, **83**, 399-407.

Gilbeaut D.M., Hulett J., Cramer G.R. & Seemann J.R. (1997) Maximal biomass of *Arabidopsis thaliana* using a simple, low maintenance hydroponic method and favourable environmental conditions. *Plant Physiology*, **115**, 317-319.

Gilliam M.B., Sherman M.P., Griscavage J.M. & Ignarro L.J. (1993) A spectrophotometric assay for nitrate using NADPH oxidation by *Aspergillus* nitrate reductase. *Analytical Biochemistry*, **212**, 359-365.

Glabb J. & Kaiser W.M. (1993) Rapid modulation of nitrate reductase in pea roots. *Planta*, **191**, 173-179.

Glabb J. & Kaiser W.M. (1995) Inactivation of nitrate reductase involves NR protein phosphorylation and subsequent binding of an inhibitor protein. *Planta*, **195**, 514-518.

Glabb J. & Kaiser W.M. (1996) The protein kinase, protein phosphatase and inhibitor protein of nitrate reductase are ubiquitous in higher plants and independent of nitrate reductase expression and turnover. *Planta*, **199**, 57-63.

Glass A.D.M. & Siddiqi M.Y. (1995) Nitrogen absorption by plant roots. In: *Nitrogen Nutrition in Higher Plants* (eds H.S. Srivastava & R.P. Singh), pp. 21-56. Associated Publishing Co., New Delhi.

Glass A.D.M., Shaff J.E. & Kochian L.V. (1992) Studies of the uptake of nitrate in barley. IV. Electrophysiology. *Plant Physiology*, **99**, 456-463.

Gould S.J., Keller G.A. & Subramani S. (1987) Identification of a peroxisomal targeting signal at the carboxy terminus of firefly luciferase. *Journal of Cell Biology*, **105**, 2923-2931.

Gould S.J., Keller G.A., Hosken N., Wilkinson J. & Subramani S. (1989) A conserved tri-peptide sorts proteins into peroxisomes. *Journal of Cell Biology*, **108**, 1657-1664.

Grouzis J.-P., Pouliquin P., Rigand J., Grignon C. & Gibrat R. (1997) *In vitro* study of passive nitrate transport by native and reconstituted plasma membrane vesicles from corn root cells. *Biochimica et Biophysica Acta*, **1325**, 1169-1180.

Guern J., Mathieu Y., Thomine S., Jouanneau J.P. & Beloeil J.C. (1992) Plant cells counteract cytoplasmic pH changes but likely use these pH changes as secondary messages in signal perception. *Current Topics in Plant Biochemistry and Physiology*, **11**, 249-269.

Guilley H., Dudley R.K., Jonard G., Balazs E. & Richards K.E. (1982) Transcription of cauliflower mosaic virus DNA: detection of promoter sequences and characterisation of transcripts. *Cell*, **30**, 763-773.

Gutierrez-Alcala G., Gotor C., Meyer A.J., Fricker M.D., Vega J.M. & Romero L.C. (2000) Glutathione biosynthesis in *Arabidopsis* trichomes cells. *Proceedings of the National Academy of Sciences of the United States of America*, **97**, 11108-11113.

Halliwell J.V. & Whitaker M.J. (1987) Using microelectrodes. In: *Microelectrode Techniques - The Plymouth Workshop Handbook* (eds N.B. Standen, P.T.A. Gray, & M.J. Whitaker), pp. 1-12. The Company of Biologists Limited, Cambridge.

Hansen U.-P., Dau H., Vanselow K.H., Fisahn J., Stein S. & Kolbowski J. (1989) Thylakoid and plasma fluxes. In: *Plant Membrane Transport: The Current Position* (eds J. Dainty, M.I. DeMichelis, E. Marre, & F. Rasa-Caldogno), pp. 345-351. Elsevier, Amsterdam.

Hansen U.-P., Kolbowski J. & Dau H. (1987) Relationship between photosynthesis and plasmalemma transport. *Journal of Experimental Botany*, **38**, 1965-1981.

Hansen U.-P., Moldaenke C., Tabrizi H. & Ramm D. (1993) The effect of transthylakoid proton uptake on cytosolic pH and the imbalance of ATP and NADPH/H^+ production as measured by CO_2- and light-induced depolarisation of the plasmalemma. *Plant Cell Physiology*, **34**, 681-695.

Hanstein S. & Felle H.H. (1999) The influence of atmospheric NH_3 on the apoplastic pH of green leaves: a non-invasive approach with pH-sensitive microelectrodes. *New Phytologist*, **143**, 333-338.

Haugland R.P. (1999) *Handbook of Fluorescent Probes and Research Chemicals.* (6 ed.). Molecular Probes, Eugene.

Heimer Y.M., Wray J.L. & Filner P. (1969) The effect of tungstate on nitrate

assimilation in higher plant tissues. *Plant Physiology*, **44**, 1197-1199.

Hendrich R., I F.U. & Fernandez J.M. (1986) Patch clamp studies of ion transport in isolated plant vacuoles. *FEBS Letters*, **204**, 228-232.

Hendrich R., Kurkdijian A., Guern J. & Flugge U.I. (1989) Compartitive studies on the electrical properties of the H^+ translocating ATPase and pyrophosphatase of the vacuolar -lysosomal compartment. *EMBO Journal*, **8**, 2835-2841.

Hepler P.K. & Gunning B.E.S. (1998) Confocal fluorescence microscopy of plant cells. *Protoplasma*, **201**, 121-157.

Herrera-Estrella A., van Montagu M. & Wang K. (1990) A bacterial peptide acting as a plant nuclear targeting signal: The amino-terminal portion of *Agrobacterium* VirD2 protein directs a β-galactosidase fusion protein into tobacco nuclei. *Proceedings of the National Academy of Sciences of the United States of America*, **87**, 9534-9537.

Hoagland D.R. & Arnon D.I. (1950) The water culture method for growing plants without soil. *California Agricultural Experimental Station Circular*, **347**, 1-32.

Hoekema A., Hirsch P.R., Hooykaas P.J.J. & Schilperoort R.A. (1983) A binary plant vector strategy based on separation of *vir*- and T-region of the *Agrobacterium tumefaciens* Ti-plasmid. *Nature*, **303**, 179-180.

Hoff T., Truong H.N. & Caboche M. (1994) The use of mutants and transgenic plants to study nitrate assimilation. *Plant, Cell and Environment*, **17**, 489-506.

Hooper C.E., Ansorge R.E. & Rusbrooke J.Q. (1994) Low-light imaging technology in the life sciences. *Journal of Bioluminescence and Chemoluminescence*, **9**, 113-122.

Huber J.L., Huber S.C., Campbell W.H. & Redinbaugh M.G. (1992) Reversible light/dark modulation of spinach leaf nitrate reductase activity involves protein phosphorylation. *Archives of Biochemistry and Biophysics*, **296**, 58-65.

Huber S.C. & Kaiser W.M. (1996) 5-aminoimidazole-4-carboxamide riboside activates nitrate reductase in darkened spinach and pea leaves. *Physiologica Plantarium*, **98**, 833-837.

Huppe H.C. & Turpin D.H. (1994) Integration of carbon and nitrogen metabolism in plant and algal cells. *Annual Reviews of Plant Physiology and Plant Molecular Biology*, **45**, 577-607.

Hutzler P.K., Fischbach R., Heller W., Jungblut T.P., Reuber S., Schmitz R., Veit M., Weissenbock G. & Schnitzler J.-P. (1998) Tissue localization of phenolic

compounds in plants by confocal laser scanning microscopy. *Journal of Experimental Botany*, **49**, 953-965.

Hwang C.-F., Lin Y., D'Souza T. & Cheng C.-L. (1997) Sequences necessary for nitrate-dependent transcription of *Arabidopsis* nitrate reductase genes. *Plant Physiology*, **113**, 853-862.

Imsande J. & Touraine B. (1994) N-demand and the regulation of nitrate uptake. *Plant Physiology*, **105**, 3-7.

Ingemarsson B., Oscarson P., af Ugglas M. & Larsson C.-M. (1987) Nitrogen utilisation in *Lemna* III. Short-term effects of ammonium on nitrate uptake and nitrate reduction. *Plant Physiology*, **85**, 865-867.

Johannes E., Ermolayeva E. & Sanders D. (1997) Red light-induced membrane potential transients in the moss *Physcomitrella patens*: ion channel interaction in phytochrome signalling. *Journal of Experimental Botany*, **48**, 599-608.

Johnson C.H., Knight M.R., Kondo T., Masson P., Sedbrook J., Haley A. & Trewavas A.J. (1995) Circadian oscillations of cytosolic and chloroplastic free calcium in plants. *Science*, **269**, 1863-1865.

Kaiser W.M. & Brendle-Behnisch E. (1991) Rapid modulation of spinach leaf nitrate reductase activity by photosynthesis I. Modulation *in vivo* by CO_2 availability. *Plant Physiology*, **96**, 363-367.

Kaiser W.M. & Brendle-Behnisch E. (1995) Acid-base modulation of nitrate reductase in leaf tissues. *Planta*, **196**, 1-6.

Kaiser W.M. & Forster J. (1989) Low CO_2 prevents nitrate reduction in leaves. *Plant Physiology*, **91**, 970-974.

Kaiser W.M. & Huber S.C. (1994) Modulation of nitrate reductase *in vivo* and *in vitro*: effects of protein phosphatase inhibitors, free Mg^{2+} and 5'-AMP. *Planta*, **193**, 358-364.

Kaiser W.M. & Spill D. (1991) Rapid modulation of spinach leaf nitrate reductase by photosynthesis II. *In vitro* modulation by ATP and AMP. *Plant Physiology*, **96**, 368-375.

Kaiser W.M., Kandlbinder A., Stoimenova M. & Glabb J. (2000) Discrepancy between nitrate reduction rates in intact leaves and nitrate reductase activity in leaf extracts: what limits nitrate reduction *in situ*? *Planta*, **210**, 801-807.

Kaiser W.M., Spill D. & Brendle-Behnisch E. (1992) Adenine nucleotides are apparently involved in the light-dark modulation of spinach-leaf nitrate

reductase. *Planta*, **186**, 236-240.

Kaiser W.M., Weiner H. & Huber S.C. (1999) Nitrate reductase in higher plants: A case study for transduction of environmental stimuli into control of catalytic activity. *Physiologica Plantarum*, **105**, 385-390.

Kanayama Y., Kimura K., Nakamura Y. & Ike T. (1999) Purification and characterisation of nitrate reductase from nodule cytosol of soybean plants. *Physiologica Plantarum,* **105**, 396-401.

Karley A.J., Leigh R.A. & Sanders D. (2001) Differential ion accumulation and ion fluxes in the mesophyll and epidermis of barley. *Plant Physiology*, **122**, 835-844.

Katavic V., Haughn G.W., Reed D., Martin M. & Kunst L. (1994) *In planta* transformation of *Arabidopsis thaliana. Molecular and General Genetics*, **245**, 363-370.

Kay R., Chan A., Daly M. & McPherson J. (1987) Duplication of CaMV 35S promoter sequences creates a strong enhancer for plant genes. *Science*, **236**, 1299-1302.

King B.J., Siddiqi M.Y., Ruth T.J., Warner R.L. & Glass A.D.M. (1993) Feedback regulation of nitrate influx in barley roots by nitrate, nitrite and ammonium. *Plant Physiology*, **102**, 1279-1286.

Klein D., Morcuende R., Stitt M. & Krapp A. (2000) Regulation of nitrate reductase expression in leaves by nitrate and nitrogen metabolism is completely overridden when sugars fall below a critical level. *Plant, Cell and Environment*, **23**, 863-871.

Kleinhofs A. & Warner R.L. (1990) Advances in nitrate assimilation. In: *The Biochemistry of Plants - Intermediary Nitrogen Metabolism.*, pp. 89-120.

Koncz C. & Schell J. (1986) The promoter of TL-DNA gene 5 controls the tissue-specific expression of chimeric genes carried by a novel type of *Agrobacterium* binary vector. *Molecular and General Genetics*, **204**, 383-396.

Kramer V., K Lahners K., Back E., Privalle L. & Rothstein S. (1989) Transient accumulation of nitrite reductase mRNA in maize following the addition of nitrate. *Plant Physiology*, **90**, 1214-1220.

Krapp A., Fraisier V., Scheible W.-R., Quesada A., Gojon A. & Stitt M. (1998) Expression studies of *Nrt2:1Np,* a putative high affinity nitrate transporter: evidence for its role in nitrate uptake. *Plant Journal*, **6**, 723-732.

Kronzucker H.J., Glass A.D.M. & Siddiqi M.Y. (1999a) Inhibition of nitrate uptake by ammonium in barley. Analysis of component fluxes. *Plant Physiology*, **120**, 283-291.

Kronzucker H.J., Siddiqi M.Y, Glass A.D.M. & Kirk G.J.D. (1999b) Nitrate-ammonium synergism in rice. A subcellular flux analysis. *Plant Physiology*, **119**, 1041-1045.

Kronzucker H.J., Glass A.D.M. & Siddiqi M.Y. (1995) Nitrate induction in spruce: an approach using compartmental analysis. *Planta*, **196**, 683-690.

Kurkdjian A. & Guern J. (1989) Intracellular pH: measurement and importance in cell activity. *Annual Review of Plant Physiology and Plant Molecular Biology*, **40**, 271-303.

Laibach F. (1943) *Arabidopsis thaliana* (L.) Heynh. als Objekt fur genetische und entwicklungsphysiologische Untersuchungen. *Botanisches Archiv*, **44**, 439-455.

Lee R.B. & Clarkson D.T. (1986) Nitrogen-13 studies of nitrate fluxes in barley roots. I. Compartmental analysis from measurements of ^{13}N efflux. *Journal of Experimental Botany*, **37**, 1753-1767.

Lejay L., Tillard P., Lepetit M., Olive F.D., Filleur S., Daniel-Vedele F. & Gojon A. (1999) Molecular and functional regulaton of two NO_3^- uptake systems by N- and C-status of *Arabidopsis* plants. *Plant Journal*, **18**, 509-519.

Li X.-Z. & Oaks A. (1993) Induction and turnover of nitrate reductase in *Zea mays* Influence of NO_3^-. *Plant Physiology*, **102**, 1251-1257.

Liakopoulos G., Stavrianakou S. & Karabourniotis G. (2001) Analysis of epicuticular phenolics of *Prunus persica* and *Olea europaea* leaves: evidence for the chemical origin of the UV-induced blue fluorescence of stomata. *Annals of Botany*, **87**, 641-648.

Lillo C. (1994) Light regulation of nitrate reductase in green leaves of higher plants. *Physiologica Plantarum*, **90**, 616-620.

Lin Y., Hwang C.F., Brown J.B. & Cheng C.L. (1994) 5' proximal regions of *Arabidopsis* nitrate reductase genes direct nitrate-induced transcription in transgenic tobacco. *Plant Physiology*, **106**, 477-484.

Liu K.-H., Huang C.-H. & Tsay Y.-F. (1999) *CHL1* is a dual-affinity nitrate transporter of *Arabidopsis* involved in multiple phases of nitrate uptake. *Plant Cell*, **11**, 865-874.

Llopis J., McCaffery J.M., Miyawaki A., Farquhar M. & Tsien R.Y. (1998) Measurement of cytosolic, mitochondrial and golgi pH in single living cells with green fluorescent proteins. *Proceedings of the National Academy of Sciences of the United States of America*, **95**, 6803-6808.

Lohaus G., Pennewiss K., Sattelmacher B., Hussmann M. & Mühling K.H. (2001) Is the infiltration-centrifugation technique appropriate for the isolation of apoplastic fluid? A critical evalution with different plant species. *Physiologia Plantarum*, **111**, 457-465.

Lüttge U. & Higinbotham N. (1979) *Transport in Plants*. Springer-Verlag, New York.

MacKintosh C. & Meek S.E.M. (2001) Regulation of plant NR activity by reversible phosphorylation, 14-3-3 proteins and proteolysis. *Cellular and Molecular Life Sciences*, **58**, 205-214.

Mackintosh C. (1992) Regulation of spinach-leaf nitrate reductase by reversible phosphorylation. *Biochimica et Biophysica Acta*, **1137**, 121-126.

Mackintosh C. (1998) Regulation of cytosolic enzymes in primary metabolism by reversible protein phosphorylation. *Current Opinion in Plant Sciences*, **1**, 224-229.

Mackintosh C., Douglas P. & Lillo C. (1995) Identfication of a protein that inhibits the phosphorylated form of nitrate reductase from spinach (*Spinacia oleracea*) leaves. *Plant Physiology*, **107**, 451-457.

Maeshima M. (2000) Vacuolar H^+-pyrophosphatase. *Biochimica et Biophysica Acta*, **1465**, 37-51.

Malhó R., Read N.D., Pais M.S. & Trewavas A.J. (1994) Role of cytosolic free calcium in the reorientation of pollen tube growth. *Plant Journal*, **5**, 331-341.

Maniatis T., Fritsch E.F. & Sambrook J. (1982) *Molecular Cloning. A Laboratory Manual*. Cold Spring Harbor Laboratory, New York.

Marrè M.T., Albergoni F.G., Moroni A. & Marrè E. (1989) Light-induced activation of electrogenic H^+ extrusion and K^+ uptake in *Elodea densa* depends on photosynthesis and is mediated by the plasma membrane H^+-ATPase. *Journal of Experimental Botany*, **40**, 343-352.

Marschner H. (1995) *Mineral Nutrition of Higher Plants*. (2nd ed.). Academic Press, London.

Martinoia E., Heck U. & Wiemken A. (1981) Vacuoles as storage compartments for nitrate in barley leaves. *Nature*, **289**, 292-294.

Martinoia E., Schramm M.J., Flugge U.I. & Kaiser G. (1987) Intracellular distribution of organic and inorganic anions in mesophyll cells: transport mechanisms in the tonoplast. In: *Plant Vacuoles - Their Importance to Solute Compartmentation in Cells and Their Applications in Plant Biotechnology* (ed B. Marin), pp. 407-416. Plenum Press, New York.

Martinoia E., Schramm M.J., Kaiser G., Kaiser W.M. & Heber U. (1986) Transport of anions in isolated barley vacuoles. I. Permeability to anions and evidence for a Cl^- uptake system. *Plant Physiology*, **80**, 895-901.

Matt P., Geiger M., Walch-Liu P., Engels C., Krapp A. & Stitt M. (2001) The immediate cause of the diurnal changes of nitrogen metabolism in leaves of nitrate-replete tobacco: a major imbalance between the rate of nitrate reduction and the rates of nitrate uptake and ammonium metabolism during the first part of the light period. *Plant, Cell and Environment*, **24**, 117-190.

Matt P., Schurr U., Klein D., Krapp A. & Stitt M. (1998) Growth of tobacco in short-day conditions leads to high starch, low sugars, altered diurnal changes in the *Nia* transcript and low nitrate reductase activity, and inhibition of amino acid synthesis. *Planta*, **207**, 27-41.

McAinsh A.R., Webb A.A.R., Taylor J.E. & Hetherington A.M. (1995) Stimulation induced oscillations in guard cell cytosolic free calcium. *Plant Cell*, **7**, 1207-1219.

McClure P.R., Kochian L.V., Spanswick R.M. & Shaff J.E. (1990) Evidence for cotransport of nitrate and protons in maize roots. II. Measurement of NO_3^- and H^+ fluxes with ion-selective microelectrodes. *Plant Physiology*, **93**, 290-294.

Meharg A.A. & Blatt M.R. (1995) NO_3^- transport across the plasma membrane of *Arabidopsis thaliana* root hairs: kinetic control by pH and membrane voltage. *Journal of Membrane Biology*, **145**, 49-66.

Melzer J.M., Kleinhofs A. & Warner R.L. (1989) Nitrate reductase regulation: effects of nitrate and light on nitrate reductase mRNA accumulation. *Molecular and General Genetics*, **217**, 341-346.

Mendel R. (1997) Molybdenum cofactor of higher plants: biosynthesis and molecular biology. *Planta*, **203**, 399-405.

Mendel R.R. & Schwarz G. (1999) Molybdoenzymes and molybdenum cofactor in plants. *Critical Reviews In Plant Sciences*, **18**, 33-69.

Meyer C. & Stitt M. (2001) Nitrate reduction and signalling. In: *Plant Nutrition* (eds

P.J. Lea & J.-F. Morot-Gaudry), pp. 37-60. Springer-Verlag, Berlin Heidelberg New York.

Michelet B. & Chua N.-H. (1996) Improvement of *Arabidopsis* mutant screens based on luciferase imaging *in planta*. *Plant Molecular Biology Reporter*, **14**, 320-329.

Millar A.J., Short S.R., Chua N.-H. & Kay S.A. (1992) A novel circadian phenotype based on firefly luciferase expression in transgenic plants. *Plant Cell*, **4**, 1075-1087.

Miller A.J. & Sanders D. (1987) Depletion of cytosolic free calcium induced by photosynthesis. *Nature*, **326**, 397-400.

Miller A.J. & Smith S.J. (1992) The mechanism of nitrate transport across the tonoplast of barley root cells. *Planta*, **187**, 554-557.

Miller A.J. & Smith S.J. (1996) Nitrate transport and compartmentation in cereal root cells. *Journal of Experimental Botany*, **47**, 843-854.

Miller A.J. & Zhen R.-G. (1991) Measurements of intracellular nitrate concentrations in *Chara* using nitrate-selective microelectrodes. *Planta*, **187**, 47-52.

Miller A.J. (1994) Ion-selective microelectrodes. In: *Plant Cell Biology - A Practical Approach.* (eds N. Harris & K.J. Oparka), pp. 329. IRL Press, Oxford.

Miller A.J., Cookson S.J., Smith S.J. & Wells D.M. (2001) The use of microelectrodes to investigate compartmentation and the transport of metabolized inorganic ions in plants. *Journal of Experimental Botany*, **52**, 1-9.

Moorhead G., Douglas P., Morrice N., Scarabel M., Aitken A. & MacKintosh C. (1996) Phosphorylated nitrate reductase from spinach leaves is inhibited by 14-3-3 proteins and activated by fusiccocin. *Current Biology*, **96**, 1104-1113.

Morcuende R., Krapp A., Hurry V. & Stitt M. (1998) Sucrose-feeding leads to increased rates of nitrate assimilation, increased rates of 2-oxoglutarate synthesis, and increased synthesis of a wide spectrum of amino acids in tobacco leaves. *Planta*, **206**, 394-409.

Morsomme P. & Boutry M. (2000) The plant plasma membrane H^+-ATPase: structure, function and regulation. *Biochimica et Biophysica Acta*, **1465**, 1-16.

Mudge S.R., Lewis-Henderson W.R. & Birch R.G. (1996) Comparison of *Vibrio* and firefly luciferases as reporter gene systems for use in bacteria and plants. *Australian Journal of Plant Physiology*, **23**, 75-83.

Mühling K.H. & Sattelmacher B. (1995) Apoplastic ion concentrations of intact

leaves of field bean (*Vicia faba* L.) as influenced by ammonium and nitrate nutrition. *Journal of Plant Physiology*, **147**, 81-86.

Müller C., Scheible W.-R., Stitt M. & Krapp A. (2001) Influence of malate and 2-oxoglutarate on the *Nia* transcript level and nitrate reductase activity in tobacco leaves. *Plant, Cell and Environment*, **24**, 191-203.

Navarro M.T., Prieto R., Fernandez E. & Galvan A. (1996) Constitutive expression of nitrate reductase changes the regulation of nitrate and nitrite transporters in *Chlamydomonas reinhardtii*. *Plant Journal*, **9**, 819-827.

Neininger A., Kronenberger J. & Mohr H. (1992) Coaction of light, nitrate and a plastidic factor in controlling nitrite-reductase gene expression in tobacco. *Planta*, **187**, 381-387.

Odell J.T., Nagy F. & Chua N.-H. (1985) Identification of DNA sequences required for activity of the cauliflower mosaic virus 35S promoter. *Nature*, **313**, 810-812.

Ow D.W., Wood K.V., De Luca M., De Wet J.R., Helinski D.R. & Howell S.H. (1986) Transient and stable expression of the firefly luciferase gene in plant cells and transgenic plants. *Science*, **234**, 856-859.

Pallaghy J.E. & Lüttge U. (1970) Light-induced H^+-ion fluxes and bioelectric phenomena in mesophyll cells of *Atriplex spongiosa*. *Zeitschrift fur Pflanzenphysiologie*, **62**, 417-425.

Pandey S., Tiwari S.B., Upadhyaya K.C. & Sopory K.S. (2000) Calcium signalling: linking environmental signals to cellular functions. *Critical Reviews in Plant Sciences*, **19**, 291-318.

Parton R.M., Fischer, S., Malhó R., Papasouliotis O., Jelitto T.C., Leonard T. & Read N. D. (1997) Pronounced cytoplasmic pH gradients are not required for tip growth in plant and fungal cells. *Journal of Cell Science*, **110**, 1187-1198.

Plieth C., Sattelmacher B. & Knight M.R. (2000) Ammonium uptake and cellular alkalisation in roots of *Arabidopsis thaliana*: the involvement of cytoplasmic calcium. *Physiologica Plantarum*, **110**, 518-523.

Pollock C.J. & Housley T.L. (1985) Light-induced increase in sucrose-phosphate synthase activity in leaves of *Lolium temulentum*. *Annals of Botany*, **55**, 593-596.

Pouteau S., Cherel I., Vaucheret H. & Caboche M. (1989) Nitrate reductase mRNA regulation in *Nicotiana plumbaginifolia* nitrate reductase-deficient mutants.

Plant Cell, **1**, 1111-1120.

Preiss J., Ball K., Smith-White B., Inglesias A., Kakefuda G. & Li L. (1991) Starch biosynthesis and its regulation. *Biochemistry Society Transactions*, **19**, 539-547.

Prins H.B.A., Harper J.R. & Higinbotham N. (1980) Membrane potentials of *Vallisneria* leaf cells and their relation to photosynthesis. *Plant Physiology*, **65**, 1-5.

Prins H.B.A., Snel J.F.H., Zanstra P.E. & Helder R.J. (1982) The mechanism of bicarbonate assimilation by the polar leaves of *Potamogeton* and *Elodea*: CO_2 concentrations at the leaf surface. *Plant, Cell and Environment*, **5**, 207-214.

Quick W.P., Schurr U., Fichtner K., Schulze E.-D., Rodermel S.-R., Bogorad L. & Stitt M. (1991) The impact of decreased Rubisco on photosynthesis, growth, allocation and storage in tobacco plants which have been transformed with antisense *rbcS*. *Plant Journal*, **1**, 51-58.

Quick W.P., Siegl G., Neuhaus E., Feil R. & Stitt M. (1989) Short-term water stress leads to a stimulation of sucrose synthesis by activating sucrose-phosphate synthase. *Planta*, **177**, 535-546.

Rastogi R., Back E., Schneiderbauer A., Bowsher C.G., Moffatt B. & Rothstein S.J. (1993) A 330 bp region of the spinach nitrite reductase gene promoter directs nitrate-inducible tissue-specific expression in transgenic tobacco. *Plant Journal*, **4**, 317-326.

Rastogi R., Bate N.J., Sivasanker S. & Rothstein S.J. (1997) Footprinting of the spinach nitrite reductase gene promoter reveals the preservation of nitrate regulatory elements between fungi and higher plants. *Plant Molecular Biology*, **34**, 465-476.

Ratajczak R. (2000) Structure, function and regulation of the plant vacuolar H^+-translocating ATPase. *Biochimica et Biophysica Acta*, **1465**, 17-36.

Read N.D., Allan W.T.G., Knight H., Knight M.R., Malhó R., Russell A., Shacklock P.S. & Trewavas A.J. (1992) Imaging and measurement of cytosolic free calcium in plant and fungal cells. *Journal of Microscopy*, **166**, 57-86.

Reid R.J. & Smith F.A. (1988) Measurements of cytoplasmic pH of *Chara corallina* using double-barrelled pH microelectrodes. *Journal of Experimental Botany*, **39**, 1421-1432.

Ricard B., Couee I., Raymond P., Salio P.H., St. Ges V. & Pradet A. (1994) Plant

metabolism under hypoxia and anoxia. *Plant Physiology and Biochemistry*, **32**, 1-10.

Riens B. & Heldt H.W. (1992) Decrease of nitrate reductase activity in spinach leaves during a light-dark transition. *Plant Physiology*, **98**, 573-577.

Riggs C.D. & Chrispeels M.J. (1987) Luciferase reporter gene cassettes for plant gene expression studies. *Nucleic Acids Research*, **15**, 8115.

Rodriguez E., Healy P.L. & Mehta I. (1984) *Biology and Chemistry of Plant Trichomes*. Plenum Press, New York.

Rodriguez-Sotres R. & Munos-Clares R.A. (1987) Short-term regulation of maize leaf phosphoenolpyruvate carboxylase by light. *Journal of Plant Physiology*, **128**, 361-369.

Roos A. & Boron W.F. (1981) Intracellular pH. *Physiological Reviews*, **61**, 296-434.

Roos W. (2000) Ion mapping in plant cells - methods and applications in signal transduction research. *Planta*, **210**, 347-370.

Rothstein S.J. & Sivasanker S. (1999) Nitrate inducibility of gene expression using the nitrite reductase gene promoter. In: *Inducible Gene Expression* (ed P.H.S. Reynolds). CAB International, Wallingford.

Rouby M.B., González C.A. & Kenis J.D. (1998) Substrates regulate the phosphorylation status of nitrate reductase. *Physiologica Plantarum*, **102**, 547-552.

Ruffy T.W., Huber S.C. & Volk R.J. (1988) Alternations in leaf carbohydrate metabolism in response to nitrogen stress. *Plant Physiology*, **88**, 725-730.

Salanoubat M. & Ha D.B.D. (1993) Analysis of the petunia nitrate reductase apoenzyme-encoding gene: a first step for sequence modification analysis. *Gene*, **128**, 147-154.

Sanders D. & Miller A.J. (1986) Measurement of cytosolic calcium activity using ion-selective microelectrodes. In: *Molecular and Cellular Aspects of Calcium in Plant Development* (ed A.J. Trewavas), pp. 149-163. Plenum Press, London.

Sattelmacher B. (2001) The apoplast and its significance for plant mineral nutrition. *New Phytologist*, **149**, 167-192.

Sattelmacher B., Muhling K.H. & Pennewi K. (1998) The apoplast - its significance for the nutrition of higher plants. *Zeitschrift fur Pflanzeneurnahrung und Bodenkunde*, **161**, 485-498.

Savchenko G., Wiese C., Neimanis S., Hendrich R. & Heber U. (2000) pH regulation

in apoplastic and cytoplasmic cell comparments of leaves. *Planta*, **211**, 246-255.

Scheible W.-R., González-Fontes A., Lauerer M., Müller-Röber B., Caboche M. & Stitt M. (1997a) Nitrate acts as a signal to induce organic acid metabolism and repress starch metabolism in tobacco. *Plant Cell*, **9**, 783-798.

Scheible W.-R., González-Fontes A., Morcuende R., Lauerer M., Geiger M., Glabb J., Gojon A., Schulze E.-D. & Stitt M. (1997b) Tobacco mutants with a decreased number of functional *nia* genes compensate by modifying the diurnal regulation of transcription, post-translational modification and turnover of nitrate reductase. *Planta*, **203**, 304-319.

Scheible W.-R., Krapp A. & Stitt M. (2000) Reciprocal diurnal changes of phospho*enol*pyruvate carboxylase expression and cytosolic pyruvate kinase, citrate synthase and NADP-isocitrate dehydrogenase expression regulate organic acid metabolism during nitrate assimilation in tobacco leaves. *Plant, Cell and Environment*, **23**, 1155-1167.

Scheible W.R., Lauerer M., Schulze E.D., Caboche M. & Stitt M. (1997c) Accumulation of nitrate in the shoot acts as a signal to regulate shoot-root allocation in tobacco. *Plant Journal*, **11**, 671-691.

Schneider M., Ow D.W. & Howell S.H. (1990) The *in vivo* pattern of firefly luciferase expression in transgenic plants. *Plant Molecular Biology*, **14**, 935-947.

Schuster C. & Mohr H. (1990) Appearance of nitrite-reductase mRNA in mustard seedlings cotyledons is regulated by phytochrome. *Planta*, **181**, 327-334.

Scott A.C. & Allen N.S. (1999) Changes in cytosolic pH within *Arabidopsis* root columella cells play a key role in the early signalling pathway for root gravitropism. *Plant Physiology*, **121**, 1291-1298.

Seith B., Schuster C. & Mohr H. (1991) Coaction of light, nitrate and a plastidic factor in controlling nitrite reductase gene expression in spinach. *Planta*, **184**, 74-80.

Seith B., Sherman A., Wray J.L. & Mohr H. (1994) Photocontrol of nitrite reductase gene expression in the barley seedling (*Hordeum vulgare* L.). *Planta*, **192**, 110-117.

Shabala S. & Newman I. (1999) Light-induced changes in hydrogen, calcium, potassium, and chloride ion fluxes and concentrations from the mesophyll and

epidermal tissues of bean leaves. Understanding the ionic basis of light-induced bioelectrogenesis. *Plant Physiology*, **119**, 1115-1124.

Shacklock P.S., Read N.D. & Trewavas A.J. (1992) Cytosolic free calcium mediates red light-induced photomorphogenesis. *Nature*, **358**, 753-755.

Shaner D.L. & Boyer J.S. (1976a) Nitrate reductase activity in maize (*Zea mays* L.) leaves. I. Regulation by nitrate flux. *Plant Physiology*, **58**, 499-504.

Shaner D.L. & Boyer J.S. (1976b) Nitrate reductase activity in maize (*Zea mays* L.) leaves. II. Regulation by nitrate flux at low leaf water potential. *Plant Physiology*, **58**, 505-509.

Siddiqi M.Y., Glass A.D.M. & Ruth T.J. (1991) Studies of the uptake of nitrate in barley. III. Compartmentation of NO_3^-. *Journal of Experimental Botany*, **42**, 1455-1463.

Siebrecht S., Mack G. & Tischner R. (1995) Function and contribution of the root tip in the induction of NO_3^- uptake along the barley root axis. *Journal of Experimental Botany*, **292**, 1669-1676.

Sivasanker S., Rastogi R., Jackman L., Oaks A. & Rothstein S. (1998) Analysis of *cis*-acting DNA elements mediating induction and repression of the spinach nitrite reductase gene. *Planta*, **201**, 66-71.

Sivasanker S., Rothstein S.J. & Oaks A. (1997) Regulation of the accumulation and reduction of nitrate by nitrogen and carbon metabolites in *Zea mays* L. seedlings. *Plant Physiology*, **114**, 583-589.

Smith R.D. & Walker J. (1996) Plant protein phosphatases. *Annual Reviews of Plant Physiology and Plant Molecular Biology*, **47**, 101-125.

Solomon P.S. & Oliver R.P. (2001) The nitrogen content of the tomato leaf apoplast increases during infection by *Cladosporium fulvum*. *Planta*, **213**, 241-249.

Solomonson L.P. & Barber M.J. (1990) Assimilatory nitrate reductase: functional properties and regulation. *Annual Reviews of Plant Physiology and Plant Molecular Biology*, **41**, 225-253.

Spalding E.P., Slayman C.L., Goldsmith M.H.M., Gradmann D. & Bertl A. (1992) Ion channels in *Arabidopsis* plasma membrane. Transport characteristics and involvement in light-induced voltage changes. *Plant Physiology*, **99**, 96-102.

St. Ges V., Roby C., Bligny R., Pradet A. & Douce C. (1991) Kinetic studies on the variations of cytoplasmic pH, nucleotide triphosphatase (^{31}P-NMP) and lactate transitions in maize root tips. *European Journal of Biochemistry*, **200**, 477-

482.

Stachel S.E., Timmerman B. & Zambryski P. (1986) Generation of single-stranded T-DNA molecules during the initial stages of T-DNA transfer from *Agrobacterium tumefaciens* to plant cells. *Nature*, **322**, 706-711.

Stahlberg R., von Volkenburgh E. & Cleland R.E. (2000) Chlorophyll is not the primary photoreceptor for the stimulation of P-type H^+ pump and growth in vareigated leaves of *Coleus x hybridus*. *Planta*, **212**, 1-8.

Steingröver E., Ratering P. & Siesling J. (1986) Daily changes in uptake, reduction and storage of nitrate in spinach grown at low light intensity. *Physiologia Plantarum*, **66**, 550-556.

Stitt M. & Feil R. (1999) Lateral root frequency decreases when nitrate accumulates in tobacco transformants with low nitrate reductase activity: consequences for the regulation of biomass partitioning between the shoots and root. *Plant and Soil*, **215**, 143-153.

Stitt M. & Krapp A. (1999) The interaction between elevated carbon dioxide and nitrogen nutrition: the physiological and molecular background. *Plant, Cell and Environment*, **22**, 583-621.

Stitt M. (1999) Nitrate regulation of metabolism and growth. *Current Opinion in Plant Biology*, **2**, 178-186.

Stitt M., Lilley R.M. & Heldt H.W. (1982) Adenine nucleotide levels in the cytosol, chloroplast and mitochondria of wheat leaf protoplasts. *Plant Physiology*, **70**, 971-977.

Stitt M., Wilke I., Feil R. & Heldt H.W. (1988) Course control of sucrose-phosphate synthase in leaves: alternations of the kinetic properties in response to the rate of photosynthesis and the accumulation of sucrose. *Planta*, **174**, 217-230.

Strater T. & Hachtel W. (2000) Identification of light- and nitrate-responsive regions of the nitrate reductase promoter of birch. *Plant Science*, **150**, 153-161.

Su W., Huber S.C. & Crawford N.M. (1996) Identification *in vitro* of a post-translational regulatory site in the hinge-1 region of *Arabidopsis* nitrate reductase. *The Plant Cell*, **8**, 519-527.

Swanson S.J. & Jones R.L. (1996) Gibberellic acid induces vacuolar acidification in barley aleurone. *Plant Cell*, **8**, 2211-2221.

Szymanski D.B., Lloyd A.M. & Marks M.D. (2000) Progress in molecular genetic analysis of trichome initiation and morphogenesis in *Arabidopsis*. *Trends in*

Plant Science, **5**, 214-219.

Tanaka T., Ida S., Irifune K., Oeda K. & Morikawa H. (1994) Nucleotide sequence of a gene for nitrite reductase from *Arabidopsis thaliana*. *DNA Sequence*, **5**, 57-61.

Tang P.S. & Wu H.Y. (1957) Adaptative formation of nitrate reductase in rice seedlings. *Nature*, **179**, 1355-1356.

Tazawa T., Shimmen T. & Mimura T. (1986) Spectrum of light-induced membrane hyperpolarization in *Egeria densa*. *Plant Cell Physiology*, **27**, 163-168.

Temple S.J., Vance C.P. & Gantt J.S. (1998) Glutamate synthase and nitrogen assimilation. *Trends in Plant Science*, **2**, 51-56.

Teyker R.H., Jackson W.A., Volk R.J. & Moll R.H. (1988) Exogenous $^{15}NO_3^-$ influx and endogenous $^{15}NO_3^-$ efflux by two maize (*Zea mays* L.) inbreds during nitrogen deprivation. *Plant Physiology*, **86**, 778-781.

The *Arabidopsis* Genome Initiative (2000) Analysis of the genome sequence of the flowering plant *Arabidopsis thaliana*. *Nature*, **408**, 796-815.

Theissen G., Kim J.T. & Saedler H. (1996) Classification and phylogeny of the MADS-box multigene family suggest defined roles of MADS-box gene subfamilies in the morphological evolution of eukaryotes. *Journal of Molecular Biology*, **43**, 484-516.

Tillard P., Passama L. & Gojon A. (1998) Are phloem amino acids involved in the shoot to root control of nitrate uptake in *Ricinus communis* plants? *Journal of Experimental Botany*, **49**, 1371-1379.

Touraine B., Daniel-Vedele F. & Forde B.G. (2001) Nitrate uptake and its regulation. In: *Plant Nutrition* (eds P.J. Lea & J.-F. Morot-Gaudry), pp. 1-36. Springer-Verlag, Berlin Heidelberg New York.

Trewavas A.J. (1983) Nitrate as a plant hormone. In: *British Plant Growth Regulator Group Monograph 9* (ed M.B. Jackson), pp. 97-110. British Plant Growth Regulator Group, Oxford.

Trewavas A.J. (2000) Signal perception and transduction. In: *Biochemistry and Molecular Biology of Plants*. (eds Buchanan R.B., Gruissem W. & Jones R.L.) pp. 930-987. The American Society of Plant Physiologists, Courier Companies Inc., Waldorf.

Turpin D.H., Weger H.G. & Huppe H.C. (1997) Interactions between photosynthesis, respiration and nitrogen assimilation. In *Plant Metabolism*. (eds Dennis D.T.,

Turpin D.H., Lefebrre D.D. & Layzell P.B.) pp. 509-524. Longman, London.

Ullrich C.I. & Novacky A.J. (1990) Extra- and intracellular pH and membrane potential changes induced by K^+, C^{l-},$H_2PO_4^-$, and NO_3^- uptake and fusicoccin in root hairs of *Limnobium stoloniferum*. *Plant Physiology*, **94**, 1561-1567.

van der Leij M., Smith S.J. & Miller A.J. (1998) Remobilisation of vacuolar stored nitrate in barley roots. *Planta*, **205**, 64-72.

van Quy L., Lamaze T. & Champigny M.L. (1991) Short-term effects of nitrate on sucrose synthesis in wheat leaves. *Planta*, **185**, 53-57.

Vaucheret H., Chabaud M., Kronenberger J. & Caboche M. (1990) Functional complementation of tobacco and *Nicotiana plumbaginifolia* nitrate reductase deficient mutants by transformation with the wild-type alleles of the tobacco structural genes. *Molecular and General Genetics*, **220**, 468-474.

Vaughn K.C. & Campbell W.H. (1988) Immunogold localisation of nitrate reductase in maize leaves. *Plant Physiology*, **88**, 1354-1357.

Vidmar J.J., Zhuo D., Siddiqi M.Y., Schjoerring J.K., Touraine B. & Glass A.D.M. (2000) Regulation of high-affinity nitrate transporter genes and high-affinity nitrate influx by nitrogen pools in roots of barley. *Plant Physiology*, **123**, 307-318.

Vincentz M., Moureaux T., Leydecker M.T., Vaucheret H. & Caboche M. (1993) Regulation of nitrate and nitrite reductase expression in *Nicotiana plumbaginifolia* leaves by nitrogen and carbon metabolites. *Plant Journal*, **3**, 315-324.

Vredenberg W.J. & Tonk W.J.M. (1975) On the steady-state electrical potential difference across the thylakoid membranes of chloroplasts in illuminated plant cells. *Biochimica et Biophysica Acta*, **387**, 580-587.

Wagner G.J. (1991) Secreting glandular trichomes: more than just hairs. *Plant Physiology*, **96**, 675-679.

Walden R., Fritze K., Hayashi H., Miklashevichs E., Harling H. & Schell J. (1994) Activation tagging: a means of isolating genes implicated as playing a role in plant growth and development. *Plant Molecular Biology*, **26**, 1521-1528.

Walker D.J., Smith S.J. & Miller A.J. (1995) Simultaneous measurement of intracellular pH and K^+ or NO_3^- in barley root-cells using triple-barreled, ion-selective microelectrodes. *Plant Physiology*, **108**, 743-751.

Wang R., Guegler K., LaBrie S.T. & Crawford N.M. (2000) Genomic analysis of a

nutrient response in *Arabidopsis* reveals diverse expression patterns and novel metabolic and potential regulatory genes induced by nitrate. *Plant Cell*, **12**, 1491-1509.

Wegmann D., Weiss H., Ammann D., Morf W.E., Pretsch E., Sugahara K. & Simon W. (1984) Anion-selective liquid membrane electrodes based on lipophillic quaternary ammonium compounds. *Mikrochimica Acta*, **III**, 1-16.

Weiner H. & Kaiser W.M. (1999) 14-3-3 proteins control proteolysis of nitrate reductase in spinach leaves. *FEBS Letters*, **455**, 75-78.

Wilkinson J.Q. & Crawford N.M. (1991) Identification of the *Arabidopsis CHL3* gene as the nitrate reductase structural gene *NIA2*. *Plant Cell*, **3**, 461-471.

Wilkinson J.Q. & Crawford N.M. (1993) Identification and characterization of a chlorate-resistant mutant of *Arabidopsis thaliana* with mutations in both nitrate reductase structural genes *NIA1* and *NIA2*. *Molecular and General Genetics*, **239**, 289-297.

Williams D.A., Cody S.H. & Dubbin P.N. (1993) Introducting and calibrating fluorescent probes in cells and organelles. In: *Fluorescent and Luminescent Probes for Biological Activity* (ed W.T. Mason), pp. 321-334. Academic Press, London.

Williams L.E. & Miller A.J. (2001) Transporters responsible for the uptake and partitioning of nitrogenous solutes. *Annual Reviews of Plant Physiology and Plant Molecular Biology*, **52**, 659-688.

Worrel A.C., Bruneau J.-M., Summerfelt K. & Voelker T.A. (1991) Expression of a maize sucrose phosphate synthase in tomato alters leaf carbohydrate partitioning. *Plant Cell*, **3**, 1121-1130.

Wray J. (1989) Molecular biology, genetics and regulation of nitrite reduction in higher plants. *Physiologica Plantarum*, **89**, 607-612.

Wray J. & Kinghorn J. (1989) *Molecular and Genetic Aspects of Nitrate Assimilation*. Oxford Science Publications, Oxford.

Yin Z.-H., Neimanis S., Wagner U. & Heber U. (1990) Light-dependent pH changes in leaves of C_3 plants. *Planta*, **182**, 244-252.

Yu Q., Tang C. & Kuo J. (2000) A critical review on methods to measure apoplastic pH in plants. *Plant and Soil*, **219**, 29-40.

Yu X., Sukumaran S. & Marton L. (1998) Differential expression of the *Arabidopsis Nia1* and *Nia2* genes. *Plant Physiology*, **116**, 1091-1096.

Zaenen I., van Larebeke N., Teuchy H., van Montagu M. & Schell J. (1974) Supercoiled circular DNA in crown-gall inducing *Agrobacterium* strains. *Journal of Molecular Biology*, **86**, 109-127.

Zhang H. & Forde B.G. (1998) An *Arabidopsis* MADS box gene that controls nutrient-induced changes in root architecture. *Science*, **279**, 407-409.

Zhang H., Jennings A., Barlow P.W. & Forde B.G. (1999) Dual pathways for regulation of root branching by nitrate. *Proceedings of the National Academy of Sciences of the United States of America*, **96**, 6529-6534.

Zhen R.G., Koyro H.W., Leigh R.A., Tomos A.D. & Miller A.J. (1991) Compartmental nitrate concentrations in barley root cells measured with nitrate-selective microelectrodes and by single cell sap sampling. *Planta*, **185**, 356-361.

Zhuo D.G., Okamoto M., Vidmar J.J. & Glass A.D.M. (1999) Regulation of a putative high-affinity nitrate transporter (*Nrt2;1At*) in roots of *Arabidopsis thaliana*. *Plant Journal*, **17**, 563-568.

Zimmermann S., Ehrhardt T., Plesch G. & Muller-Rober B. (1999) Ion channels in plant signalling. *Cellular and Molecular Life Sciences*, **55**, 183-203.